Universität Rostock

Traditio et Innovatio

Investigation of the Light-induced Copper-catalyzed Allylic Alkynylation – Exploration of Conditions, Substrates and Reaction Mechanism

Dissertation

Zur Erlangung des akademischen Grades

Doctor rerum naturalium **(Dr. rer. nat.)**

der Mathematisch-Naturwissenschaftlichen Fakultät

der Universität Rostock

Vorgelegt von Paul Ewald Bernhard Hünemörder,

geboren am 26.06.1995 in Rostock (Deutschland)

Rostock, den 17.03.23

https://doi.org/10.18453/rosdok_id00004395

Gutachter:

PD Dr. habil. Esteban Mejía, Rostock, Leibniz-Institut für Katalyse

Prof. Dr. Shoubhik Das, University of Antwerp, Department of Chemistry

Datum der Einreichung: 17.03.2023

Datum der Verteidigung: 27.06.2023

If I have seen further, it is by standing on the shoulder of giants.

Sir Isaac Newton

To Juliana

Eidesstattliche Erklärung

Ich versichere hiermit an Eides statt, dass ich die vorgelegte Dissertation selbständig, ohne fremde Hilfe und ohne Benutzung anderer als die in der Arbeit angegebenen Hilfsmittel angefertigt habe.

Alle Stellen, die wörtlich oder sinngemäß aus veröffentlichen und nicht veröffentlichen Quellen entnommen wurden, sind als solche in der Arbeit kenntlich gemacht.

Rostock, den 17.03.23

_____

Paul Ewald Bernhard Hünemörder

Die vorliegende Dissertation wurde vom 01.10.2019 bis zum 01.03.2023 am Leibniz-Institut für Katalyse e.V. unter Anleitung von PD Dr. habil Esteban Mejía erstellt.

Danksagung

Primero y ante todo, quisiera agradecer al Dr. habil. Esteban Mejía por abrirme las puertas de su grupo durante mi tesis de pregrado y por brindarme, en estos seis años, todas las oportunidades para desarrollarme como científico y también como persona. Estoy profundamente agradecido por todo lo que pude aprender de contigo, por las historias y las anécdotas a la hora del almuerzo y por motivarme, especialmente durante esta etapa del doctorado ¡Gracias! ¡No solo por ser un formidable jefe, sino también un excelente mentor y amigo!

I would also like to thank the ComBioCat Science Campus of the Leibniz Association and the RoHan DAAD SDG Graduate School for their funding and assistance over the past four years.

I am very grateful for the endless help, I have received from the Analytical Department of LIKAT. Especially, I would like to thank Susann Buchholz, Susanne Schareina and Dr. Marcus Klahn for their irreplaceable help in measuring hundreds of samples. Also, I would like to thank Dr. Anke Spannenberg, for her help in measuring and preparing some of the crystal structures measured in this work. Finally, I would like to thank PD Dr. habil. Wolfgang Baumann, for his help and insight with the measurement of the low-temperature NMR-experiments.

Thank you also to all the people of the Biocatalysis & Polymerchemistry (formerly Chemocatalysis & Polymerchemistry) group in LIKAT. The friendly and warm atmosphere you all provided was one of the reasons, I was set on staying in this group and I can fondly say, that this was one of the best decisions I took. Particularly, I want to thank Dr. Abel Salazar, Felix Unglaube, Niklas Schafhausen and Lea Grefe for the wonderful talks and interesting discussions during or after work, for the beers shared at the harbor and for all the wonderful memories from this time.

In general, I would like to thank everyone, who walked this path with me and joined in every scientific discussion or helped me further in my research.

Ich möchte auch meinen vier Studierenden, Janina Schlapp, Jacqueline Maslack, Leo Gräber und Tim Winkels für ihre außerordentlich tatkräftige Unterstützung im Labor danken. Vielen Dank für all eure Hilfe und die großartigen Gespräche während eurer Zeit hier.

Insbesondere möchte ich meinen Freunden danken, die diese anstrengende Zeit umso erträglicher gemacht haben. Die Vorfreude auf gemeinsame Abende war immer eine gute Motivation, um auch schlechte Wochen vorbeiziehen zu lassen. Ich danke euch von ganzem Herzen.

Ich möchte an dieser Stelle auch Jule danken. Danke dafür, dass ich dich immer an meiner Seite wissen kann und wir alle Höhen und Tiefen gemeinsam bewältigen.

Zum Schluss möchte ich meiner Familie von ganzem Herzen danken. Es ist euch zu verdanken, dass ich heute diese Zeilen schreiben kann. Nur durch eure Unterstützung konnte ich so weit kommen. Danke, für einfach alles.

Abstract

The catalytic allylic substitution is a staple reaction in the synthesis of organic compounds due to its flexibility. Since its introduction by Tsuji and Trost, multiple improvements have been made. However, most of them require the use of expensive and rare noble metals such as Pd or Ir. Recently, our group presented the copper-catalyzed allylic alkynylation. Yet, the underlying mechanism was not understood.

This dissertation reports the investigation of the light-induced copper-catalyzed allylic alkynylation. Through further optimization, a reliable and robust protocol was established. In addition, the improved protocol was subjected to various substrates with varied success. Mechanistic studies were accompanied by spectroscopic investigations with NMR, EPR and CV. Together with insights gathered from the perturbation of reaction conditions a new mechanistic proposal could be presented.

Die katalytische allylische Substitution ist aufgrund ihrer Vielseitigkeit eine fundamentale Reaktion in der Synthese organischer Verbindungen. Seit ihrer Entdeckung durch Tsuji und Trost sind zahlreiche Verbesserungen in der Methodik erreicht worden. Allerdings benötigen derartige Reaktionen häufig teure und seltene Edelmetalle wie Palladium oder Iridium. Kürzlich war unsere Arbeitsgruppe in der Lage, eine kupfer-katalysierte allylische Alkynylierung zu präsentieren. Diese war bis jetzt jedoch mechanistisch unzureichend verstanden.

Die vorliegende Dissertation befasst sich mit der Untersuchung der licht-induzierten kupfer-katalysierten allylischen Alkynylierung. Durch weitergehende Optimierungen wurde ein verlässliches und robustes Protokoll etabliert. Zusätzlich konnten weitere Substrate mit unterschiedlichem Erfolg mit dieser Methode untersucht werden. Mechanistische Studien werden durch spektroskopische Untersuchungen mittels NMR, EPR und CV begleitet. Zusammen mit den Erkenntnissen aus vorhergehen Störungsversuchen wird ein neuer mechanistischer Vorschlag präsentiert.

Abbreviation

ACAC – Acetylacetonate

ArM – Artificial Metalloenzyme

BDE – Bond Dissociation Energy

BHT – 2,6-Di-*tert*-butyl-4-methylphenol

BOX – bisoxazoline

CDC – Cross Dehydrogenative Coupling

Chen – Cyclohexene

CuAAC – Copper-catalyzed Azide-Alkyne-Coupling

Cu-PA – Copper phenylacetylide

DABCO – 1,4-Diazabicyclo[2.2.2]octane

DBP – Dibenzoyl peroxide

DDQ – 2,3-Dichloro-5,6-dicyano-1,4-benzoquinone

dF(CF$_3$)ppy – 2-(2,4-difluorophenyl)-5-(trifluoromethyl)pyridine

DMF – Dimethyl formamide

dmp – 2,9-Dimethyl-1,10-phenanthroline

DMPA – 2,2-Dimethoxy-1,2-diphenylethan-1-one

DMPO – 5,5-dimethyl-pyrroline *N*-oxide

DMSO – Dimethyl sulfoxide

dtbbpy – 4,4′-Di-tert-butyl-2,2′-dipyridyl

ESI-MS – Electrospray ionization – mass spectrometry

Et al – et alii

GC-FID – Gas chromatography – Flame ionization Detector

GC-MS – Gas chromatography – mass spectrometry

HAT – Hydrogen Atom Transfer

HMPA – Hexamethylphosphoramide

ICP-OES – Inductively coupled Plasma – Atomic emission spectroscopy

IR – Infrared

KOtBu – Potassium *tert*-butanolate

LiSPh – Lithium thiophenolate

MeCN – Acetonitrile

NaOAC – Sodium acetate

NMO – 4-methylmorpholine *N*-oxide

NMP – *N*-methyl pyrrolidone

NMR – Nuclear Magnetic Resonance

OTf – trifluoromethanesulfonate

PA – phenylacetylene

SET – Single Electron Transfer

TBAB – tetrabutylammonium bromide

TBD – 1,3,4,6,7,8-Hexahydro-2H-pyrimido[1,2-a]pyrimidine

TBHP – *tert*-butyl hydroperoxide

TEMPO – 2,2,6,6-Tetramethylpiperidin-1-yl)oxyl

Tpy – $1^2,2^2:2^6,3^2$-Terpyridine

xantphos – (9,9-Dimethyl-9H-xanthene-4,5-diyl)bis(diphenylphosphane)

Table of Contents

1. Introduction

The allylic group in organic chemistry describes a functional group with the basic structure of $H_2C=CH-CH_2R$, with R being the rest of the molecule the group is attached to.[1] The word “allyl” is derived from the word *Allium* (latin for leek) and was first described by Theodor Weinheim, who isolated an allylic compound from garlic oil.[2] Besides being found in various molecules occurring in extracts from plants of the allium family (i.e. leeks, garlic, onions etc.), the structural motif of the allyl group can be found in various other natural products such as terpenes and terpenoids, fatty acids or natural rubbers derived from the isoprene building block. Selected examples are represented in Figure 1. This ubiquitous functionality is of great interest, not only for the synthesis of novel compounds but also due to its inherent reactivity.

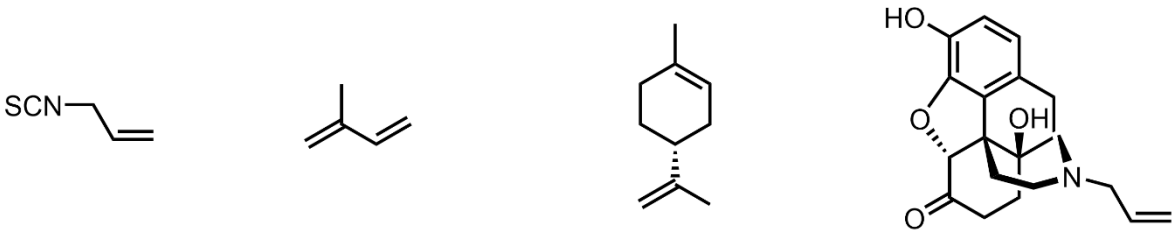

Allyl isothiocyanate Isoprene Limonene Naloxone

Figure 1: Structures of selected examples for molecules containing an allylic function.

Allylic groups are known for their ability to stabilize charges due to resonance of the bonds. Hence, an allylic functionality is capable of stabilizing positive and negative charges as well as radicals.[1] This resonance is depicted in Scheme 1. The ability of the allyl group to stabilize itself makes it an ideal functionality for nucleophilic substitutions. A comparison of the bond dissociation energies for the abstraction of a hydrogen shows a decrease along the series C(sp)-H > $C(sp^2)_{arom}$ > $C(sp^2)_{vinyl}$ > $C(sp^3)_1$ > $C(sp^3)_2$ > $C(sp^3)_3$ >$C(sp^3)_{allylic}$.[3] The cleavage of the hydrogen in alpha position to the double bond is therefore very easy. Furthermore, this also enables the easy substitution of leaving groups on the molecule and makes it a reasonable pathway to achieve a

functionalization of an allylic site. However, such methodologies always require the presence of a good leaving group.

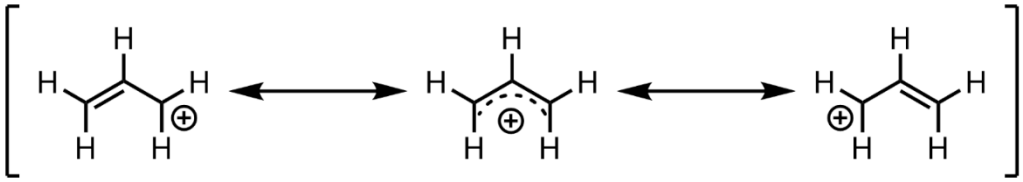

Scheme 1: Resonance structures for an allylic cation and stabilization of the charge through shifts of the double bond.

As an alternative to the stoichiometric pathways for modifying or introducing an allylic group, Tsuji and Trost developed a catalytic pathway as displayed in Scheme 2.[4, 5] Using a functionalized allyl, they were able to introduce a nucleophile with assistance of a palladium catalyst. Initially, the palladium coordinates to the double bond of the functional group in a η^2-mode. The reaction proceeds via an oxidative addition to a η^3-allyl complex of the palladium. The leaving group is then extruded and the allylic group can accept the nucleophile.[6] This first protocol for an allylic substitution set the hallmark for other iterations to come.

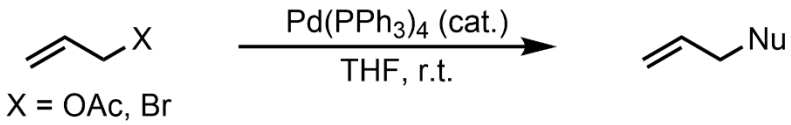

Scheme 2: Tsuji-Trost-Allylation using a Palladium-Catalyst.

Most notably, the advancements of Takeuchi[7] and Helmchen[8] towards branched and asymmetric products stablished the allylic substitution as a versatile method to introduce this group into molecules. Nevertheless, they have a downside, namely the need of very expensive noble metals such as palladium or iridium. As the demand for these metals is rising, their price increases even further. Hence, the need for catalyst from cheaper transition metals arises. One of these arising metals is copper, due to its rich redox chemistry.[9-12] These alternatives will be discussed in detail in later chapters. Moreover, most allylic functionalizations require substrates containing a leaving group.

This diminishes the atom economy due to waste being generated from the leaving group. Optimally, a “green” reaction should minimize waste and allow direct functionalization.[13]

As such, our group has been developing a reaction that kept these key points in mind. Recently, we reported the copper-catalyzed allylic alkynylation of cyclic alkenes with phenylacetylenes under either thermal or light activation.[14, 15] Requiring a sacrificial oxidant in the form of an organic peroxide, the protocol allowed the cross dehydrogenative coupling. Furthermore, it accepted different functional groups very well. This methodology, depicted in Scheme 3, complies with the previously mentioned requirements, presenting an atom-efficient and green reaction. Unfortunately, the underlying mechanism of this reaction has remained elusive so far.

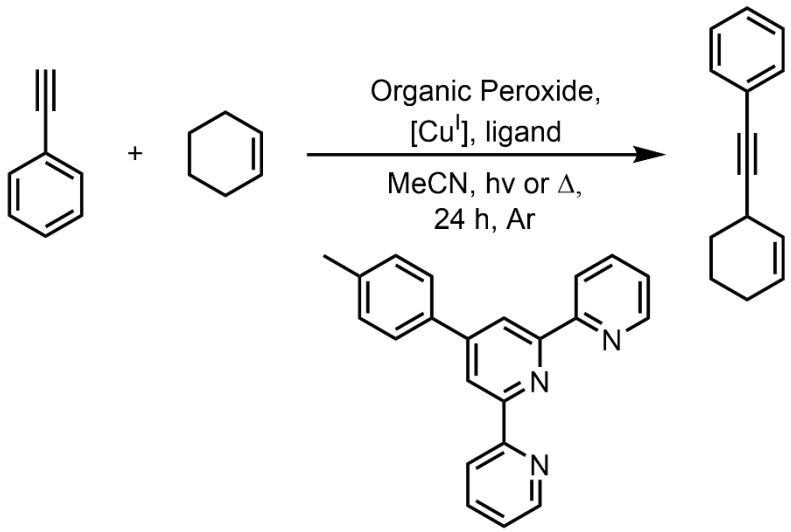

Scheme 3: General Reaction Scheme for Allylic Alkynylation reported by Mejía *et al.*[14, 15]

1.1. Scope of this work

The aim of this work is the further optimization of the copper-catalyzed alkynylation reaction and the elucidation of the underlying mechanism. It is focused on clarifying the reactions steps necessary to accomplish the reaction. This would allow further refinement and optimization of the reaction. Ultimately, clarifying the mechanism might allow the development of asymmetric transformations.

Chapter 2 focusses on further steps to optimize the reaction and investigate its behavior to changes. Herein, reaction conditions and used reagents are varied and evaluated based on the results. Emphasis will be put on increasing the reaction yield as well as decreasing the reaction time. Furthermore, perturbations of the reaction conditions will be tested, and the results evaluated towards their influence on the mechanism.

With an optimized protocol, the reaction will be tested for other substrates in Chapter 3. Especially the use of other allylic substrates will be discussed, including more intricate structural motifs and testing the robustness of the reaction. In addition to this, the new protocol will be compared to the results of the previous publications.

Lastly, Chapter 4 will deal with the elucidation of the mechanism. The reaction will be investigated with NMR, EPR and CV methods. Furthermore, isolation of intermediate species will be presented. From this, conclusions of the mechanism will be drawn with regards to existing models in literature. Lastly, kinetic investigation of the reaction will be conducted. At the end of the chapter a new mechanistic proposal will be presented, incorporating the information gathered in previous chapters.

The results of this work give insight to this very complex system and show a novel selective reactivity of a copper-complex with organic peroxide.

1.2. Copper-catalyzed C-C coupling reactions

Reactions that enable the formation of C-C bonds have been established in synthetic chemistry as the standard for most functionalizations. The interest in new methods constantly involves new reactions and optimization. Methodologies are most commonly optimized towards incorporating unfunctionalized substrates, working under mild conditions with benign compounds, as well as increasing tolerance and selectivity. However, most of these reactions rely on noble metals such as palladium, rhodium, or iridium. However, these metals are highly toxic and due to their scarcity and increasing demand, they are very expensive. Preferably, these metals are replaced with cheaper, more abundant and less toxic alternatives such as early transition metals.[16] One such alternative is copper. Copper belongs to the group of coinage metals like silver and gold and is, compared to the other two, highly abundant on earth.[17] Besides, copper is also a common metal found in living organism as part of metalloenzymes.[18] This makes

copper an ideal choice for a benign and renewable catalyst. Regarding its redox properties, copper can take on oxidation states from 0 to +4 and therefore covers a rich redox chemistry. While it possesses the capability of single electron transfer (SET) reaction, it can also undergo two-electron oxidative addition and reductive elimination processes. The properties of copper catalysts can be fine-tuned with different ligands and their reactions can be thermally activated or photocatalyzed. The manifold of the resulting C-C cross-coupling reactions will be focus of the following chapters.

1.2.1. Coupling of Pre-functionalized Substrates

The most established type of coupling reactions requires the use of pre-functionalized substrates. These reactions have been widely used and the methodology can be found in many prominent examples such as the Suzuki-Miyaura, Heck, Hiyama or Stille-reaction. A wide variety of these reactions have a copper-catalyzed variant. One of the oldest of such examples is the Rosemund-von Braun reaction.[19-21] This reaction allows the cyanation of aryl halides to synthesize nitriles. However, the protocol usually requires a large excess of copper(I) cyanide and high temperatures. Hence, a more efficient protocol was needed. Such method was developed by the Buchwald group in 2003.[22] The reaction could proceed at lower temperatures more efficiently, when an *in-situ* Finkelstein reaction was conducted to exchange the halide. Furthermore, the use of an inexpensive diamine ligand and the replacement of the cyanide source with sodium cyanide increased the reactivity even more and lead to very good conversion of various aromatic and heteroaromatic substrates to the corresponding nitriles. The optimized reaction conditions are depicted in Scheme 4. Circumventing the problem of requiring the more reactive aryl iodides, this methodology elegantly performs the synthesis of these *in-situ*. Still, the reaction has the downside of requiring high temperature and the use of very toxic sodium cyanide.

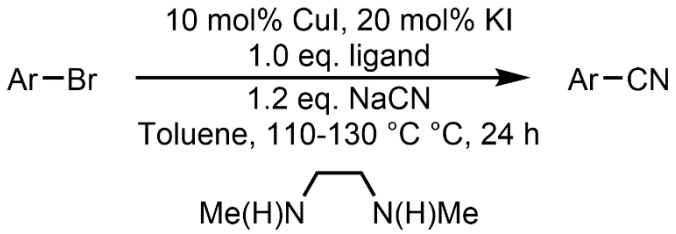

Scheme 4: Rosemund-von Braun cyanation with a modified protocol by the Buchwald group.[22]

The Hurtley reaction is an Ullmann-type condensation of C-H acidic compounds with aryl halides.[23] Similarly to the above mentioned reaction, it is limited by the use of aryl iodides as substrates due to the lower reactivity of other halides. Nevertheless, it was one of the first examples showing the applicability of copper as catalyst for cross-coupling reactions. Modern iterations of the Hurtley reaction perform the coupling of malonates with aryl iodides at room temperature with increased yields using 2-picolinic acid as an assisting ligand.[24] The reaction performed in general very well and accepts various substrates in good to excellent yields. The group of Ma *et al.* reported the coupling of aryl iodides with C-H acidic compounds using *L*-Proline as ligand.[25] They could prove the robustness of the reaction employing various substrates as well as the use of aryl bromides. The first enantioselective version of this coupling was presented by the same group.[26] Adapting the conditions from the previous reaction, they exchanged the proline for *trans*-4-Hydroxy-*L*-proline. At reduced temperatures of about -45 °C they generated selectively the desired product. Their reported protocol (represented in Scheme 5) was able to achieve ee's of about 93 % with yields between 70 and 85 % in several examples. This milestone did not only represent the first enantioselective Hurtley-reaction but is also the first instance of an Ullmann-type reaction at very low temperature. While it still requires a very high loading of catalyst and ligand, it demonstrates very well the capabilities of modern copper-catalysts.

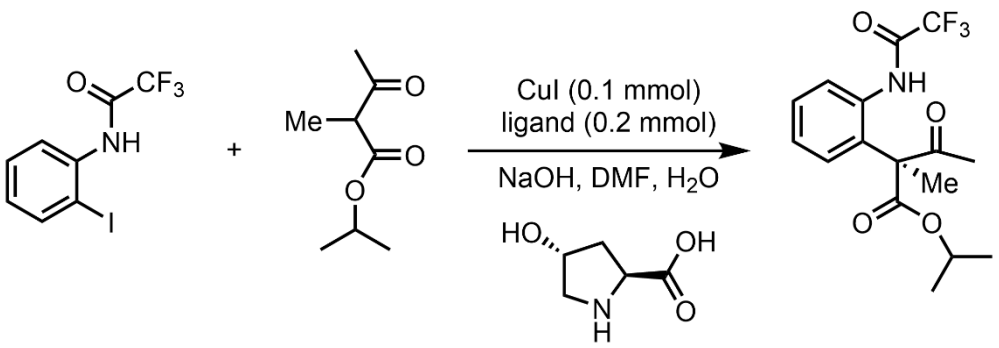

Scheme 5: Enantioselective Hurtley reaction assisted by a chiral proline ligand.[26]

Grignard reagents haven been a staple in organic chemistry for the formation of C-C bonds. However, their reactivity can be severely lacking in the case of some substrates. Kochi *et al*. could already show in 1971 the use of copper-catalysts to perform cross-coupling reaction between Grignard reagents and organic halides.[27] Since then, multiple improvements to this methodologies have been reported in literature. Notably, one of the earlier reports in this area, was able to replace the organic halides with sulfonates, although only primary sulfonates proved to be effective.[28] Commonly, these methods use the cheap and widely available copper(I) iodide as a catalyst in the reaction. Interestingly, reports also showed the applicability of Li_2CuCl_4 as a catalyst, which is in situ reduced by an excess amount of Grignard.[29] In later applications, this copper complex became essential,[30] and could be used in several protocols for the synthesis of intricate molecules.[31-33] Remarkably, another copper halide, copper(I) bromide, shows also good activity even in small quantities of 1 mol%.[34] The reactivity of CuBr can be tuned even further, as shown in the coupling of α,ω-dibromoalkanes, by Oku *et al*.[35] The reactivity of the coupling could be increased with the addition of hexamethylphosphoramide (HMPA). Thus, this is an excellent example for the increase in reactivity of copper complexes by tuning the coordination sphere of the metal center. However, the use of HMPA is regarded as highly critical due to the compound being highly carcinogenic. A more reliable and benign protocol includes the use of [CuBr-LiSPh-LiBr-THF] as a catalytic system in the synthesis of metacylcophanes.[36] With an optimized protocol the authors were even able to reduce the amount of Grignard reagent needed to just one equivalent, whereas commonly an excess is needed. The use of copper-catalyst in the coupling of allylic substrates and Grignard especially grew in popularity. However, the literature to this topic will be discussed in Chapter 1.4. A massive downside to the above-mentioned methods, is the restricted use of Grignard

reagents in the presence of carbonyl groups. The yield of reactions under such conditions drops significantly and side reactions in form of alkylations of the carbonyl group are facilitated. In this regard, Jézéquel *et al*. presented an easy work-around to this problem. They found that the additions of *N*-methyl pyrrolidone (NMP) greatly increases the chemoselectivity of the reaction towards the desired alkylation.[37] The addition of up to nine equivalents of NMP even helped with the reaction of sluggishly reacting alkyl bromides and -iodides.

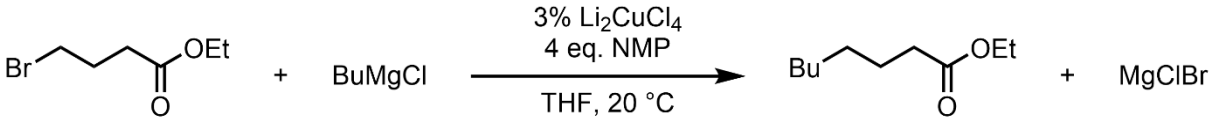

Scheme 6: Selected example for the NMP-assisted Copper-catalyzed alkylation with Grignard reagents.[37]

Besides their application with organomagnesium compounds, the use of copper for Suzuki-like coupling reactions with organoboron compounds was explored briefly. The Rothenberg group investigated the use of copper and copper/noble metal nanoclusters for Suzuki cross-coupling reactions.[38] The sole copper-catalyst showed reactivity for the reaction. However, it was outperformed by the Cu/Pd nanocluster. Expanding on this, Ho *et al*. explored the coupling of aryl boronic acids with hypervalent iodine compounds and were also able to show a carbonylative pathway under these conditions.[39] Only a few years later, a DABCO-assisted copper-catalyzed Suzuki coupling was published in literature.[40] The authors showed the coupling of several vinyl and aryl halides with arylboronic acids with moderate to good yields. Unfortunately, less reactive substrates required a higher loading of the catalyst. These methodologies show the applicability of copper catalysts to well-known protocols and prove, that copper is capable of a similar reactivity to palladium. Ultimately however, palladium-catalyzed protocols remain superior in terms of selectivity, scope and applicability.

A widely applied method in the copper-catalyzed C-C coupling reactions, is the introduction of a trifluoromethyl-group (-CF_3) into a molecule.[41] The trifluoromethylation has gained especial importance in the synthesis of drugs and is a reoccurring structural motif in many modern pharmaceuticals.[42] However, selective fluorination of methyl groups is quite challenging, making the trifluoromethylation the protocol of choice for the selective introduction of fluorine into a molecule. In the copper-catalyzed reaction,

the formation of $CuCF_3$ is considered the key-step. The first reports on the trifluoromethylation of aryl halides by McLoughlin[43] and Kobayashi[44], have been followed by a variety of further reports to improve this methodology. The first isolated and structurally well-defined [$CuCF_3$] complexes showed activity towards the reaction and could transfer the trifluoromethyl group to aryl halides but required the use of stoichiometric amounts of copper complex.[45-47] The first catalytic use of copper complexes in this reaction was reported by Wu *et al*. in 1989.[48] The authors were able to perform the reaction with only 12 mol% of CuI and using methyl fluorosulphonyldifluoroacetate as a fluorinating agent (see Scheme 7). They could successfully transfer the trifluoromethyl group in various examples.

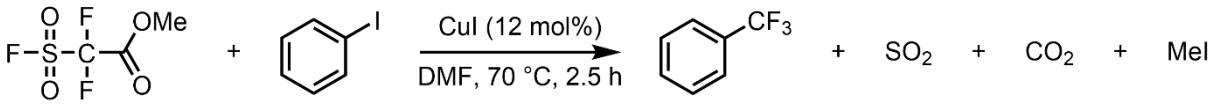

Scheme 7: Selected example for the copper-catalyzed trifluoromethylation of Aryl halides.[48]

Hartwig *et al*. reported the functionalization of aryl halides to aryldifluoroamides starting from the corresponding α-silyldifluoroamide under copper catalysis.[49] The trifluormethylation of aryl halides is mostly limited by the availability of reactive aryl iodides or aryl bromides. In order to overcome this challenges, multiple groups have put effort into this research in order to develop catalytic methods. After showing the first copper-mediated trifluoromethylation of aryl boronic acids in 2010,[50] the group of Qing was able to present a catalytic version of this reaction two years later.[51] Through reaction engineering, they showed that careful dosing of the reagents to the reaction was key to allow the transformation. Besides, Shen *et al*. found the applicability of Togni's Reagent as a source for an electrophilic trifluoromethyl group to functional aryl boronic acids.[52] Delightfully, Sanford *et al*. could show the first dual catalytic approach to the reaction in 2012.[53] They combined the photocatalytic generation via a ruthenium catalyst of a trifluoromethyl radical from CF_3I[54] with the copper cross-coupling chemistry. This method (see Scheme 8) excellently combined two methodologies to generate various products with acceptable to excellent yields under comparably mild conditions.

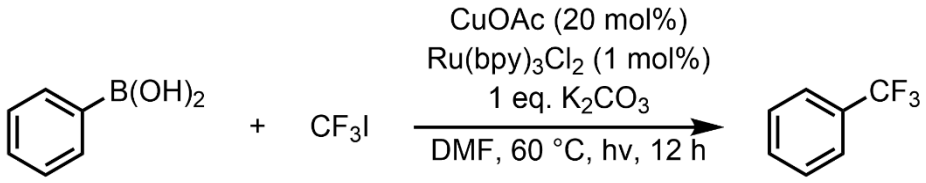

Scheme 8: Dual-Catalytic Trifluoromethylation of aryl boronic acids using CF_3I.[54]

Another widely known methodology in the field of copper-catalyzed cross-coupling reactions of pre-functionalized substrates, is the Sonogashira reaction.[55] It is known as a dual catalytic protocol between palladium and copper in order to couple aryl halides with acetylenes, exploiting the formation of acetylenic cuprates. However, Chapter 1.3 will focus more in depth on the specific interaction between copper and acetylenes.

1.2.2. Cross-Dehydrogenative-Coupling (CDC) Reactions

According to the principles of Green Chemistry by Paul Anastas,[13] the use of sacrificial reagents, protecting groups or leaving groups should be drastically reduced in order to minimize waste and the ecological impact of chemical synthesis. However, many C-C coupling reactions require the presence of a functional group to work. Hence, the use of unfunctionalized or non-derivatized substrates would be ideal, as these would generate a minimum in waste. Such methodology is the cross-dehydrogenative-coupling (CDC) reaction, which can directly transform simple starting materials into complex molecules. Hence, only C-H bonds and oxidative conditions are required.

The furnishing of $C(sp^3)$-$C(sp^3)$ bonds is one challenge of this chemistry. In regard to the copper-catalyzed C-C coupling reactions, the group of Li could show many dehydrogenative couplings. Initially, they showed the dehydrogenative Nitro-Mannich reaction of substrates with an adjacent nitrogen atom.[56] They facilitated the coupling of multiple 1,2,3,4-tetrahydrosioquinolines as well as alkyl-protected anilines with copper(I)-bromide as a catalyst and up to 1.2 eq. of TBHP as an oxidant. This report can be set as the first copper-catalyzed CDC reaction. To increase the generality of this protocol, they envisioned the use of other substrates as well, and could prove the facile coupling of C-H acidic substrates to the isoquinoline. Especially, the use of malonates proved to be successful for obtaining good to excellent yields with various substitution

patterns on the isoquinoline or malonate.[57] In a similar fashion, the group was able to couple malononitrile to the same substrate again, although now with an excess of the nitrile required.[57] The authors proposed the generation of an iminium cation during the reaction, either via hydrogen abstraction and consequent single electron transfer (SET), or first by SET followed hydrogen abstractions. The proposal was later confirmed by Klussmann *et al*.[58, 59] as they could isolate a cuprate coordinated by the iminium salt of the isoquinoline. Eager to further exploit the reactivity of the copper-catalyzed CDC, the group then presented the coupling of malonates with cyclic alkenes such as cyclohexene in the allylic position of the double bond.[60] Although the reaction required cobalt as another catalyst, they could completely forego the need for palladium, which would normally be required in similar Tsuji-Trost-Allylations. With eight different examples in C-H acidic substrates, they could prove the generality of the reaction protocol. A selected example is shown in Scheme 9.

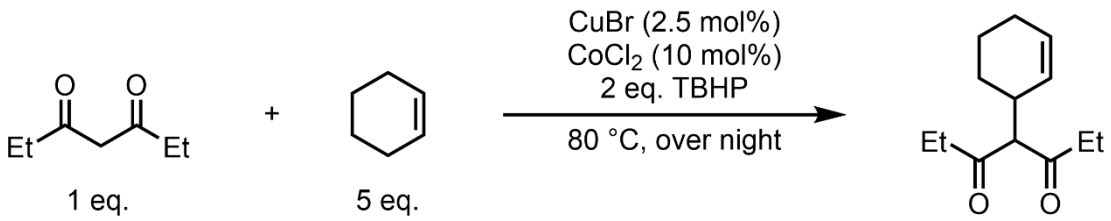

Scheme 9: Selected Example for the CDC of malonates with cyclic alkenes.[60]

In another dual catalytic approach, the group could present the CDC reaction of malonates to a carbon atom adjacent to an oxygen like isochroman.[61] In contrast to the previously reported reactions, a mixture of a copper catalyst and indium catalyst was employed to furnish the desired product. Further on, instead of an organic peroxide, 2,3-dichloro-5,6-dicyanobenzoquinone (DDQ) was used as an oxidant. In absence of the former, no reaction was observed. Similarly, no product was formed when the reaction was performed with copper as the sole catalyst. Again, the group could prove the robustness of the protocol obtaining various products with different substitution patterns. Lastly, the group managed to improve the initial Nitro-Mannich reaction even further by performing it under aerobic conditions in water (see Scheme 10).[62]

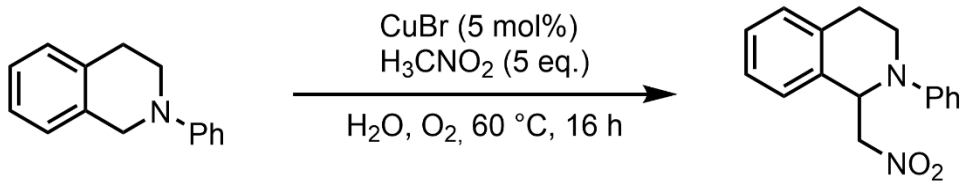

Scheme 10: Copper-Catalyzed CDC Nitro-Mannich reaction in water using oxygen.[62]

This facile and elegant procedure completely neglects the need for harmful or toxic oxidants like organic peroxides and instead allows a transformation under green conditions. Supposedly, the reaction follows a similar mechanism as reported before with an iminium ion as the intermediate species. The methods of the Li group enabled many other methodologies that either complimented the existing protocols or introduced new reactivities based on the same catalytic cycle. As such, Powell *et al*. reported the first dehydrogenative coupling of benzylic substrates with copper.[63] As in the previous reports, they could easily achieve the coupling with malonates. However, they had to add bathocuproine as a ligand to achieve the desired reactivity. Another interesting variation of the reaction was developed by Zhang *et al*., who performed the coupling of ethers to styrene and other vinylarenes.[64] The reaction leads to the formation of a terminal C(sp^3)-C(sp^3) bond and consequent oxidation of the benzylic position of the arene. This activation mode has so far been unprecedented in copper catalysis. Furthermore, the reaction did not proceed to the ketone if there was no TBHP present or if the reaction was conducted under inert atmosphere. However, when up to six equivalents of TBHP were used under inert atmosphere, the product was obtained in 58 % yield. The use of other radical starters or oxidant did not yield the product, but the use of radical scavengers inhibited the reaction. The protocol was robust towards different electronic situations on the arene and overall, the products were obtained in acceptable yields. This reaction protocol could recently be optimized to incorporate linear ethers,[65] and indoles in a three component reaction.[66] In resemblance to the trifluoromethylation (*vide supra*), the groups of Lieu,[67] Wang,[68] and Buchwald,[69] presented separately said functionalization of unactivated alkenes. In all reports, the reactions proceeded smoothly with a simple copper catalyst and without an oxidant. However, these reactions cannot be considered CDC reactions, strictly speaking, as they all require the use of a CF_3-Donor with a leaving group.

The asymmetric formation of C-C bonds remains a great challenge in C-H activation chemistry. Regarding the copper-catalyzed variety, a few reports have been successful especially with the use of chiral ligands. The first enantioselective CDC reaction was reported by Gong *et al*. in 2010 for the coupling of 1,3-dicarbonyls with 3-indolylmethyl in the presence of a chiral ligand.[70] They decided on the use of DDQ as oxidant at low temperatures (see Scheme 11). Their reported protocol also showed very good tolerance towards different substituents as well as other carbonyl species like diketones. Overall, they obtained the desired products in excellent yields (72-99 %) and good ee's (86-96 %) with a scope of eighteen different products. Their mechanistic investigations show the involvement of DDQ in the abstraction of the C-H acidic proton of the diketone. Intermediary, the indolyl moiety forms an iminium cation which is then attacked by the anion to afford the desired product. Using a similar protocol, the group of Wang achieved the coupling of 1,3-dicarbonyl with various amino acids.[71]

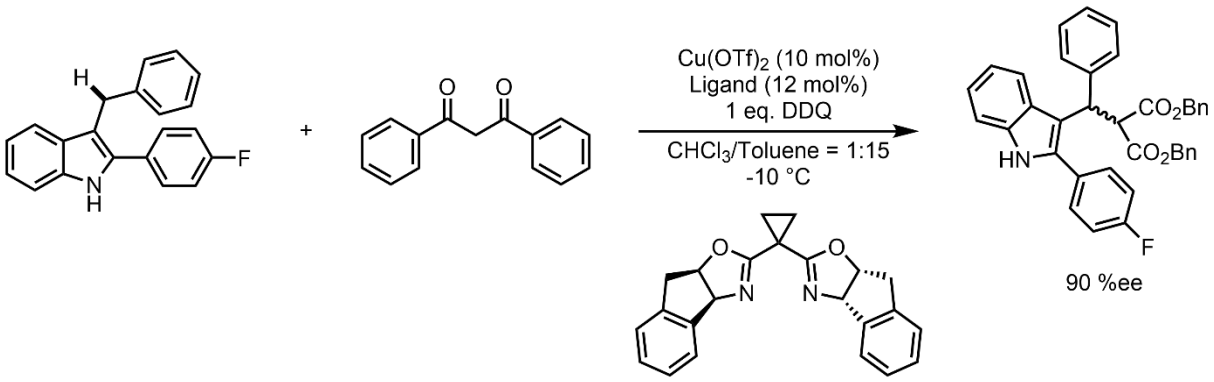

Scheme 11: Selected example of an enantioselective copper-catalyzed CDC reaction.[70]

Scheidt *et al*. used an intramolecular CDC reaction to couple a diketone to a carbon adjacent to an ether functionality.[72] This reaction would be extremely challenging under the conditions used above due to the necessity of forming a highly reactive oxocarbenium ion. Their optimized conditions make use of another bisoxazoline (BOX) ligand as well as DDQ, and a base, at -70 °C. Under these conditions they were able to present the formation of 21 different products with acceptable to good yields and very good ee's. In order to replace the DDQ, they also explored the use of photoredox conditions. While they were able to afford the product, no enantioselectivity could be induced. In a more recent report, the group of Liu showed an intramolecular asymmetric

cyclopropanation involving a radical coupling mechanism.[73] With great effort, they established the reaction conditions with which an enantioselective reaction was observed. In contrast to the other reports, they used hypervalent iodine compounds. Furthermore, the protocol requires the use of a bipyridine ligand for the copper as well as a chiral pyrrolidine additive. With these conditions they achieved excellent conversions and very good enantioselectivities. These reports prove the capability of copper catalysis to operate in an enantioselective fashion. Recent examples report oxidative cascades for the synthesis of natural products like (-)-Suaveoline.[74]

In recent years, the use of copper catalyst for photoactivated or photocatalyzed reactions has increased. As such, also the use of these catalysts for the cross dehydrogenative formation of C-C bonds has found application. Che *et al*. performed the cross coupling of tetrahydroisoquinolines and nitroalkanes in a classic Nitro-Mannich reaction using a copper photocatalyst.[75] In order to increase the lifetime of the transient excited copper species, they synthesized a novel zwitterionic phenantroline and diphosphine-carborane complex. They could show, as a proof of principle, the formation of the desired product under irradiation with light above 420 nm under aerobic conditions. Furthermore, they could also apply the protocol to a broad substrate palette with good success. One year later, the group of Bissember reported the coupling of anilines with phenylmaleinimides using a copper photocatalysis.[76] They found that their reaction required two equivalents of trifluoroacetic acetic under optimized conditions (see Scheme 12). If the acid is left out or the reaction is run in the dark, only traces of product are observed. With their optimized conditions in hand, they could provide a broad substrate scope. Interestingly, in their efforts to replace the TFA they found all other Brønstedt acids or Lewis acids to be ineffective. Mechanistically, they propose the excitation of the copper complex and oxidative quenching under aerobic conditions to a copper(II) complex, which then is reduced by a SET from the nitrogen of the aniline. Simultaneously, the amide is protonated by the acid and the radical attacks the alkene to furnish another radical species. This undergoes intramolecular cyclization and oxidative quenching of the radical would lead to the tetrahydroisoquinoline.

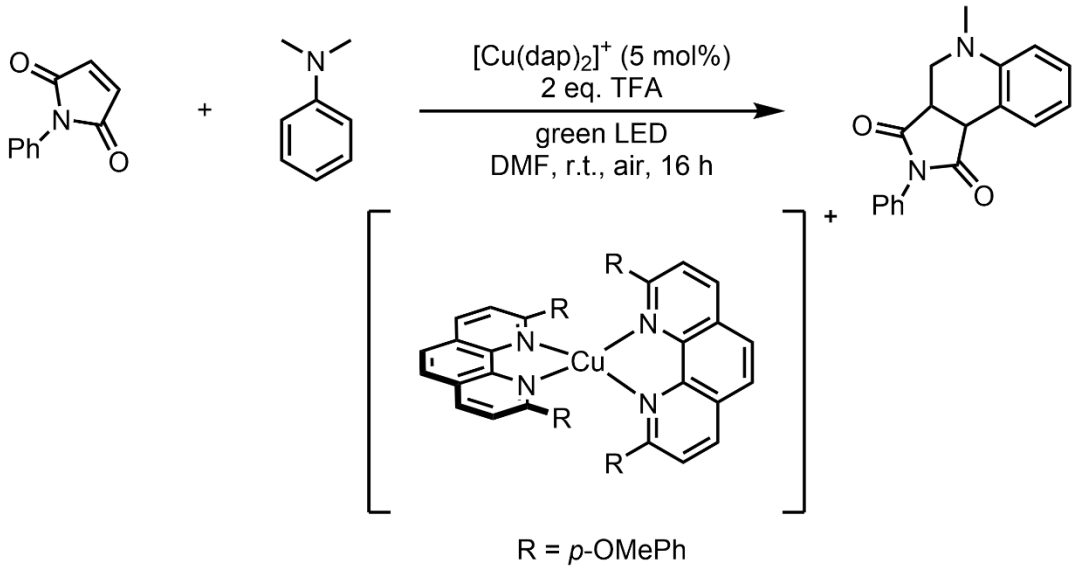

Scheme 12: Exemplary reaction for the copper-based, photocatalyzed formation of substituted tetrahydroisoquinolines.[76]

The coupling of C(sp^3)-C(sp^2) can be furnished in a similar fashion to the above-mentioned protocols. Again, the first to investigate this reaction was the group of Li, who published the first copper-catalyzed oxidative C-H coupling of tetrahydroisoquinolines with aryl boronic acids.[77] In resemblance to the previous protocols, this functionalization proceeded under oxidative conditions. However, strictly speaking, it is not a true CDC reaction as it requires a leaving group. Later, the group of Huang reported one of the first couplings of two unfunctionalized substrates under copper catalysis.[78] The protocol required the use of an organic peroxide to achieve oxidative conditions. This was improved upon by Zhang *et al*., who achieved the same reaction by only using pure oxygen or air. Under these conditions, they could perform coupling reaction with a *N*,*N*-dimethylaniline and *N*-heteroarenes. With a simple setup, they were able to synthesize over twenty different products. Mechanistically, the reaction follows a similar pathway to the other reported coupling with dimethylaniline (*vide supra*) via oxidation of the nitrogen and subsequent coordination to the copper center. Adding to this, Mihovilovic *et al*. realized the coupling of indoles to tetrahydroisoquinolines. Moreover, they also achieved the functionalization of unprotected isoquinolines with very good yields (see Scheme 13).[79] In this manner, the group of Chandrasekharam performed the coupling of indoles with tetrahydroquinolines under mild conditions in water with just air as the oxidant.[80]

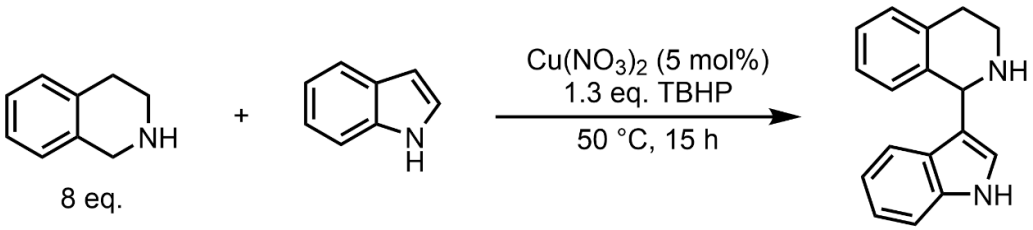

Scheme 13: Indolation of unprotected 1,2,3,4-Tetrahydroisoquinoline in a CDC reaction.[79]

The Ugi-type assembly of tertiary amines, nitriles and carboxylic acids towards α-amino imides has been reported by Xie *et al*. as a novel method in the copper-catalyzed CDC.[81] The reaction proceeded under very mild conditions only requiring TBHP as an oxidant. From this, a broad variety of products was synthesized, which proved the applicability of this protocol. In 2009, the Kündig's group reported the synthesis of oxindoles, replacing with stoichiometric amounts of copper the former palladium catalyst.[82] In 2010, the Taylor's group presented the catalytic intramolecular cross-dehydrogenative coupling of anilides.[83] The reaction could be conducted under air in a few hours, yielding oxindoles in very high yields. However, it required high temperatures (165 °C) to forego the need for a base. Recently, Zhao *et al.* reported the synthesis of cycloalkyl benzo[*b*]phosphole oxides from unactivated cycloalkanes.[84] They obtained their desired products in up to 90 % yield, requiring 140 °C and di-*tert*-butyl peroxide (see Scheme 14). Based on their experimental finds, they proposed a radical mechanism with the C-H bond cleavage of the cycloalkane as the rate limiting step. Further on, Le *et al.* investigated the cross dehydrogenative coupling of *N*-arylglycine esters with 2-arylimidazo[1,2-*a*]pyridines under very mild conditions. The reaction could be carried out under air, without the need for a more reactive oxidant. In general, the method could successfully transform multiple substrates to the desired product with very good yields. Similar to many other reactions discussed here, the addition of 2,2,6,6-tetramethylpiperidin-1-yloxy (TEMPO) lead to complete inhibition of the reaction.

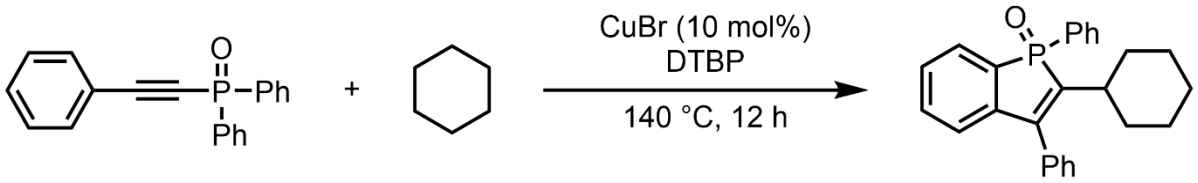

Scheme 14: Synthesis of cyclohexyl benzo[*b*]phosphole oxides under C-H activating Copper catalysis.[84]

The Patureau group reported the *ortho*-aminomethylation of phenols enabled by a copper(II)/peroxide system.[85] Under optimized conditions, the reaction proceeded with 10 mol% of copper catalyst at 80 °C and di-*tert*-butyl peroxide. The authors could show the generality of the reaction protocol with various substrates. Interestingly, their mechanistic investigations showed a dependence of the reaction on a radical mechanism. A straightforward protocol for the formation of all-carbon triaryl quarternary centers from benzofurans with indoles, thiophenes, quinolines and carbazoles was reported by Kambe *et al.* in 2019.[86] They applied the method to a broad variety of substrates using $K_2S_2O_8$ and copper(I). Mechanistically, they propose the formation of Cu(I), Cu(II) and Cu(III) species during the catalytic cycle. A three component-tandem approach for the synthesis of 1,3-oxazines with methanol as a C1-synthon was reported by Baruah *et al*.[87] The coupling proceeds from unprotected 1,2,3,4-tetrahydroisoquinoline and 2-naphtol in methanol with a simple copper(II) catalyst and TBHP in water as shown in Scheme 15. Chang *et al*. reported the alkylation of polyfluoroarenes in 2020 under copper-catalysis using hydrocarbons as the alkyl source.[88] After optimization, they could synthesize a vast library of different products using a copper catalyst with a ketiminate ligand as well as an organic peroxide as oxidant. In addition, they could show the application of their method to the synthesis of precursors for drugs Lidoflazine, Indatraline and Nafenopin.

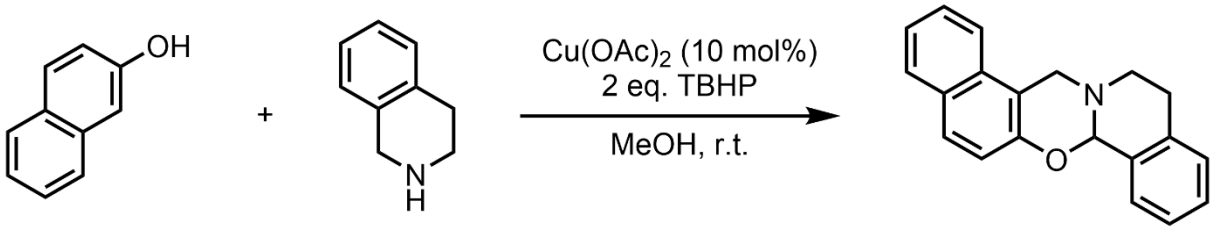

Scheme 15: Tandem multi-component synthesis of 1,3-oxazines in a cross-dehydrogenative fashion.[87]

Although not as present in literature as the other two areas, the coupling between two C(sp^2) bonds is still of interest. Kozlowski *et al*. did mechanistic studies on the coupling of biaryls under oxidative conditions in resemblance to the activity of natural copper-containing enzymes.[89] In another report, the group of Wang showed a one-pot synthesis of pyrrolo [2,1-*a*] isoquinolines as part of a cascade reaction.[90] The reaction proceeds through an oxidation of the isoquinoline and consequent [3+2] cycloaddition which cascades under the oxidative conditions to the desired pyrrolo isoquinolines. This facile method furnishes the desired products at only 50 °C and tolerates the use of various substituents on the substrates. In 2017 the group of Singh synthesized pyrrole-annulated heterocycles within a site-selective dehydrogenative cross-coupling with silver salts as oxidant (see Scheme 16).[91] Initially during their optimization of the reaction, they tested the intramolecular coupling of pyrrole-3-carbaldehyde-azole.

However, in their initial tests the homocoupling of the substrates proved to be the major byproduct. Using a mixture of 4-methylmorpholine *N*-oxide (NMO) and tetrabutylammonium bromide (TBAB), they could suppress the formation of the homocoupling in an acceptable manner. The overall yield however remained moderate (58 %) even under optimized conditions. Nevertheless, they could obtain the coupling product in various instances for derivatized substrates.

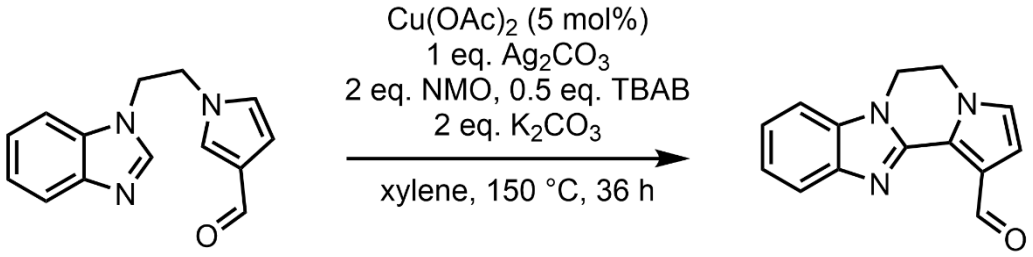

Scheme 16: Intramolecular annulation to pyrrole-annulated heterocycles.[91]

Another facile protocol was published by Pandit *et al*, for the coupling of benzoxazine-2-ones with indoles.[92] The reaction proceeded under aerobic conditions at 60 °C in tetrahydrofuran. With their method, they achieved the synthesis of cephalandole A. Even less prevalent than the cross dehydrogenative formation of C(sp^2)-C(sp^2) bonds in literature are methods for furnishing C(sp)-C(sp^3) under cross dehydrogenative

copper-catalyzed conditions. The earliest report in this area, was set again by Li *et al.* who showed the synthesis of propargylic amines from tertiary amines and phenylacetylene.[93] In similarity to their other reports, they used *tert*-butyl hydroperoxide as an oxidant. The reaction proceeded smoothly, and various different products were obtained. In addition, they managed to show an enantioselective version of this reaction, coupling the phenylacetylene and tetrahydrosioquinolines shortly after.[94] To achieve this, they made use of a chiral Py-BOX ligand for the copper (see Scheme 17). Although, this reaction proceeded only with moderate ee's, it marks the first enantioselective catalytic method for the generation of chiral tetrahydroisoquinolines from acetylenes and the isoquinoline.

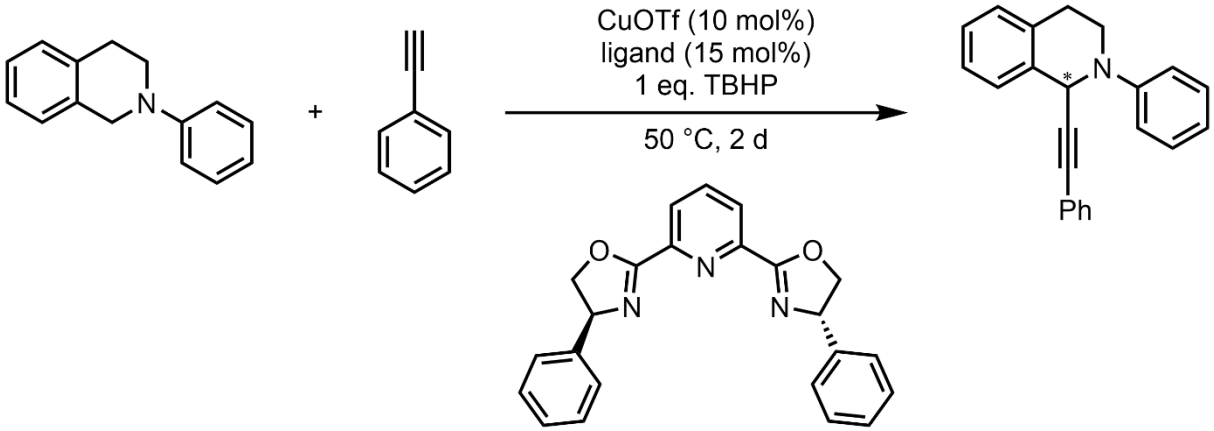

Scheme 17: Enantioselective Alkynylation of tetrahydroisoquinolines under CDC conditions.[94]

In 2008, the group of Zhao modified the protocol of the Li group by replacing the TBHP with *N*-bromosuccinimide.[95] Using this, they achieved the transformation of several aromatic and aliphatic acetylenes. In a very impressive photoredox reaction, the group of Hwang achieved the coupling of terminal alkynes, alcohols and arylamines to propargylic amines under cross dehydrogenative conditions.[96] The reaction was facilitated by a mixture of *N*-methylaniline, phenylacetylene and methanol under irradiation with blue LEDs and in presence of copper(I) chloride and benzoquinone as an oxidant. The authors screened multiple substrates and proved the robustness of the protocol. Interestingly, during their mechanistic investigation, they proposed the initial formation of copper acetylide and consequent photo irradiation to an excited species which can undergo SET reactions. Jain and co-workers were able to improve the reactivity of the

coupling between terminal alkynes and *N,N*-dimethyl anilines by introducing a sulfur or selenium-based ligand to the catalytic system.[97] In 2018 and 2019 the group of Mejía *et al*. reported the cross dehydrogenative coupling of phenylacetylenes with cyclic alkenes.[14, 15] They could show a facile transformation of the substrates, under either thermal, or photocatalytic conditions. The reaction proceeded via a copper(I) complex with a terpyridyl ligand. In both cases the presence of an organic peroxide is required (see Scheme 18). The authors could show the generality of the protocol by applying it to various substrates. The products were synthesized in good up to excellent yields.

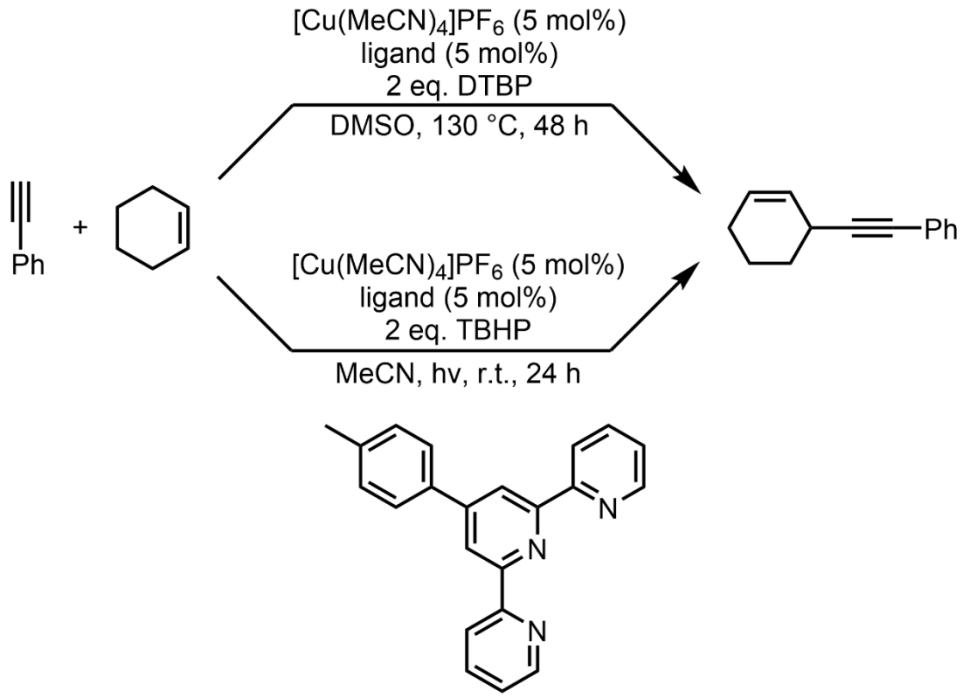

Scheme 18: Cross dehydrogenative alkynylation of cyclic alkenes via copper catalysis under thermal, or photocatalytic conditions.[14, 15]

1.3. Copper Acetylides and their use in coupling reactions

The Glaser coupling is an important functionalization in organic chemistry involving copper acetylides as necessary synthons. First described by Carl Glaser in 1869, he reported the copper catalyzed coupling of acetylenes, obtaining 1,3-diynes under oxidative conditions.[98, 99] Treatment of phenylacetylene with cuprous chloride, ammonium hydroxide in ethanol afforded the copper phenylacetylide as a yellow precipitate. When

treated with oxygen, this reagent afforded the acetylene homocoupling product. The original method of Glaser however, failed to see a wider application in synthetic chemistry. This is mostly attributed to the need of isolation of the potentially explosive copper phenylacetylide. This chemistry remained nearly dormant until 1956, when Eglington and Galbraith found that copper(II) and pyridine were able to facilitate the oxidative coupling of acetylenes.[100, 101] However, this protocol required stoichiometric amounts of copper(II). Later in 1962, Hay found the positive effects of nitrogen-containing ligands on the original Glaser coupling.[102] The use of *N*,*N*,*N*',*N*'-tetramethylethylenediamine as a ligand increased the solubility of the copper acetylides drastically and therefore ruled out the necessity of the isolation. The protocol has since then been named Glaser-Hay-reaction. Still, this method was limited to the homocoupling reaction. Simultaneously, Cadiot and Chodkiewicz developed the heterocoupling of acetylenes in 1957.[103, 104] In order to achieve this, the copper acetylide was firstly synthesized under inert conditions and then treated with an alkyne halide. These methods have seen several iterations over the years and have been applied for the synthesis of macrocylces, of natural products, oligo- and polymers and even in the production of opto-electronic materials.[105-109] As such, the group of Bäuerle presented the synthesis of thiophene based macrocycles in 2000 under modified Glaser-Eglinton conditions (see Scheme 19), which these days are often used as building blocks for organic light emitting diodes (OLED).[110]

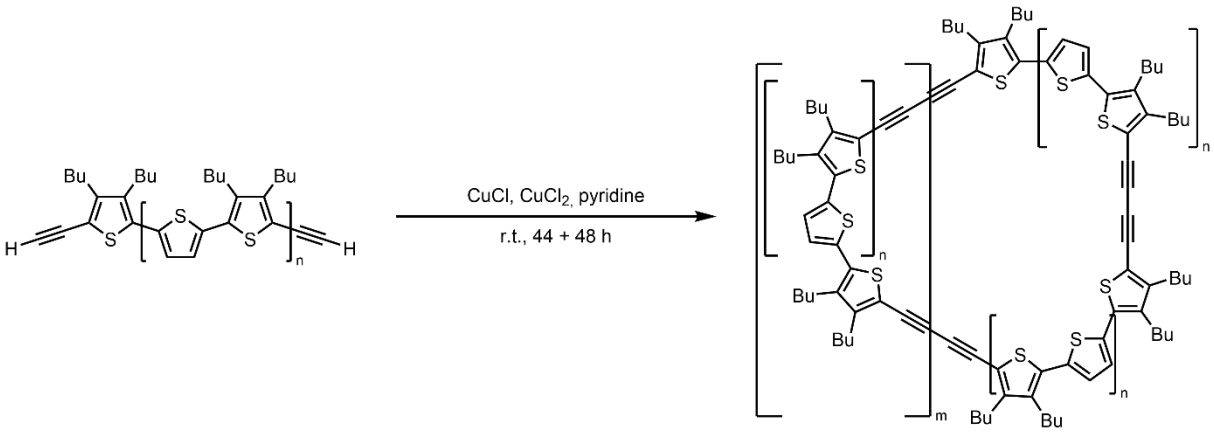

Scheme 19: Synthesis of macrocyclic thiophene-diacetylene moieties under modified Glaser-Eglinton-conditions.[110]

While its applications and uses in literature have been numerous, the discussion of the underlying mechanism is still ongoing. The earliest proposal by Salkind *et al*. involves the formation of an alkynyl radical by oxidation via copper(II) and consequent radical coupling.[111] The Bohlmann group reported the formation of a dimeric copper(II)-acetylene complex via π-bond coordination. The information towards this mechanistic proposal was gained from kinetic measurements.[112] Nielsen *et al*. proposed the formation of a copper(II)-alkyne complex, which undergoes a disproportionate step to form copper(III). After subsequent transmetallation, a dialkynyl copper(III) complex is formed, which yields the product through a reductive elimination.[113] The different mechanistic proposals are presented in Scheme 20.

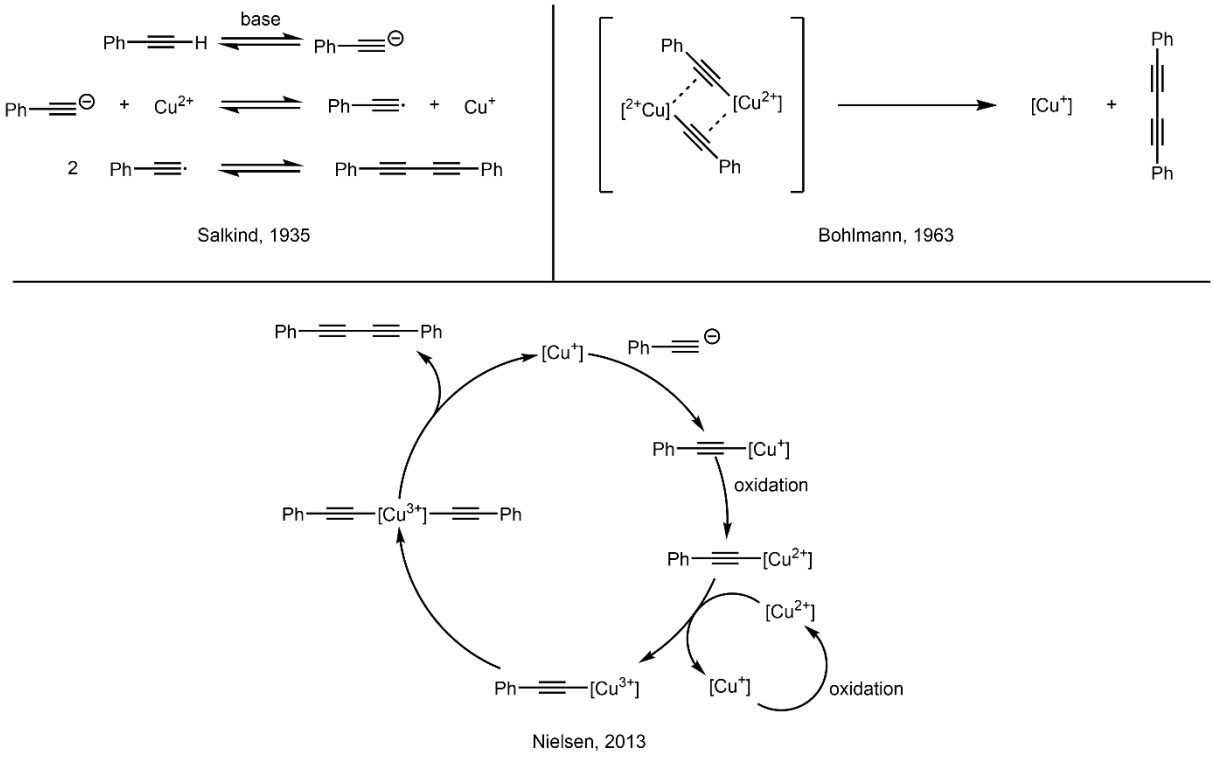

Scheme 20: Different mechanistical proposals for the Glaser coupling reaction.

The use of copper acetylides is not limited to the Glaser-type reaction. The well-known Sonogashira-coupling is a C-C coupling reaction co-catalyzed by copper and palladium to introduce alkynes to aryl or vinyl halides.[55] The copper co-catalyst plays an important role in activating the acetylenes and then transferring the moiety to the palladium catalyst for the cross-coupling. Due to the inherent formation of the cuprate, the Glaser homocoupling is the most prominent side reaction occurring in the Sonogashira

catalytic cycle. The reaction has enormous synthetic capabilities and has received numerous improvements over the years.

Another well-known and practiced application of copper-acetylenes are the azide-alkyne-click-reactions. These were described by Barry Sharpless as “near-perfect” reactions, that enable facile and robust transformation of chemicals into their respective products with high yields and little to no by-products.[114] The original click reaction, the copper-catalyzed-alkyne-azyde-coupling (CuAAC) to form triazoles was independently reported by Sharpless[115] and Meldal[116] in 2002. Together with Bertozzi, who reported the use of copper-free click chemistry for the *in vivo* imaging of biomolecules in living cells,[117] Sharpless was awarded the Noble prize in Chemistry in 2022. Besides, the CuAAC has seen many applications in research revolving around the modification of DNA,[118] reactions in living organisms,[119] carbohydrates,[120] drug-delivery systems,[121] and other medicinal applications,[122] and even efforts for copper-free reactions.[123] Thus, it is to no surprise that this reaction still counts as one of the most important methodologies in synthetic chemistry.

While the CuAAC, Sonogashira reaction and even the Glaser coupling still see a wide application, the use of acetylides as direct coupling partners for other reactions is only scarcely reported. Unfortunately, their use as a nucleophile is limited by their lack of reactivity. At the same time, the synthesis of unreactive organocuprates is very facile and despite their organometallic nature they are not sensitive towards water or oxygen. A comprehensive overview for the oxidative alkynylation of ynamides, trifluoromethyl groups, phosphonates and aryl groups has been made by Evano *et al*. who focused on establishing these acetylides as synthons.[124] They achieved the reported alkynylations under very mild conditions using just oxygen as oxidant. Unfortunately, these reactions require still quantitative amounts of copper. In an important publication, Warren and co-workers extended the mechanistic understanding of copper-acetylides and their reactivity in 2020.[125] They were able to isolate and crystalize a discrete copper(II)-acetylide-complex, which normally occur as polymeric materials.[126] They diligently investigated the reaction of this complex with C(sp), C(sp^2) and C(sp^3) substrates, both experimentally and theoretically, to find suitable mechanistical proposals. The results are depicted in Scheme 21. In regards of the C-C homocoupling between two acetylides or the coupling of acetylides with nucleophiles, the authors suggest a redox disproportionation step, in which a copper(III) complex is formed. These complexes are

susceptible to a quick elimination of the product under formation of the coupling product and reduction of the copper(III) to copper(I). Interestingly, this proposal supports the findings of Vilhelmsen *et al* shown above.[113] At the same time, the authors also suggest the formation of a copper(III) intermediate in the radical capture mechanism which can form the coupling product in a facile reductive elimination as well.

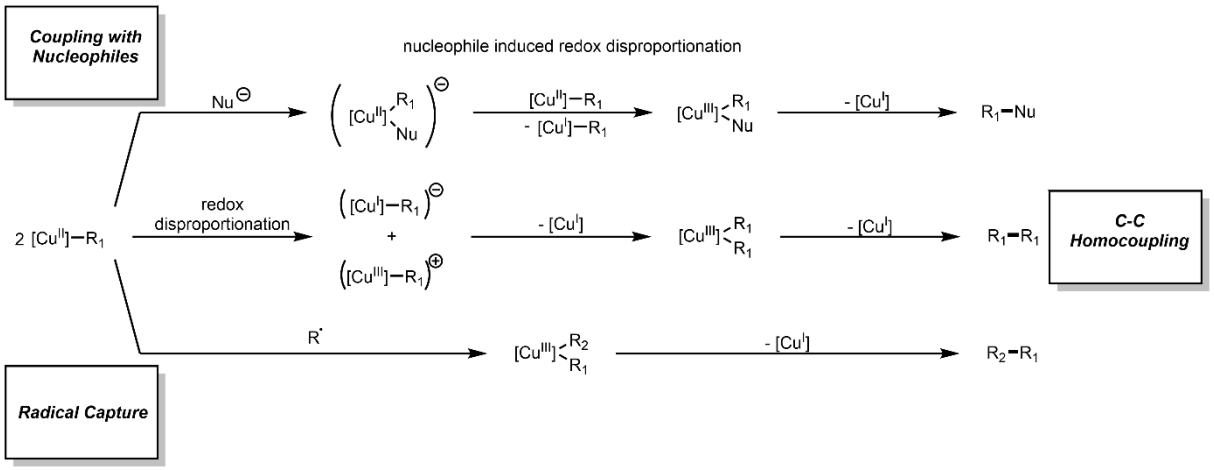

Scheme 21: Proposed mechanism for the functionalization of copper acetylides.[125]

A different approach to the alkynylation methodologies investigated by the Warren group, has been taken by Lalic *et al*. in using photocatalysis to activate the unreactive acetylides for the coupling of alkyl iodides.[127] The seminal work to this approach was laid out by Hwang and co-workers, who introduced a palladium-free Sonogashira reaction with photocatalysis as a driving force.[128] Under irradiation, the reaction is not dependent on the presence of an oxidant. The authors, furthermore, showed the necessity of a ligand for the reaction. Surprisingly, 4,4',4''-tri-tert-butyl-2,2':6',2''-terpyridine proved to be superior in comparison to py-BOX ligands or phenanthrolines. During optimization of the reaction, they also found that irradiation with blue light, the metal, and the ligand are necessary. Especially the use of iodides was required to obtain a reasonable yield. Subsequently, the authors proved that this concept can be applied to various structural motifs and showed a broad substrate scope. This was further expanded by Lie *et al.* who recently reported enantioselective, decarboxylative alkylations.[129] In general, the use of acetylenic cuprates has seen great improvement over the years, as they are key-intermediates in important synthetic protocols. Continued

research on these compounds has led to impressive reactions. It is only reasonable to expect even more reactions in the future using acetylides as building blocks.

1.4. Modifications at allylic sites

Allylation reactions and the modification at allylic sites are one of the most important C-C bond formations, as the allyl group itself provides a useful handle for further functionalizations. Since the introduction of the Tsuji-Trost allylations (*vide infra*), the method has received many improvements over the years. Due to the flexibility and concurrent coordination modes of the allylic group, the modification is versatile and by the variation of the system the selectivity can be drastically changed. Most of the reported methods in literature, employ a transition-metal-based catalyst. At the same time however, most of these protocols require pre-functionalized allylic groups. As described in the previous chapters, the ideal evolution of these reactions is to achieve a direct dehydrogenative allylation. With the adoption of light-activated protocols to the toolkit of modern chemists, also photocatalyzed allylation have found their way into literature. Starting from the early beginnings of the allylation up to the state-of-the-art advances, this chapter will provide a brief overview over current thermal and photoactivated allylation reactions.

1.4.1. Thermally-activated catalyzed Substitutions

Derived from the standard palladium-catalyzed Tsuji-Trost-Allylation, there is a consensus on the reaction mechanism (Scheme 22). The palladium center coordinates to the double bond of the alkene forming a η^2-complex. Following the ionization of the substrate through extrusion of the leaving group. Subsequently, the palladium can change its coordination mode again and a η^3 complex is formed, stabilizing the intermediary allylic cation. In this state, a nucleophile can attack each side of allylic moiety. After decomplexation the product is obtained and the complex regained to restart the catalytic cycle anew.[130]

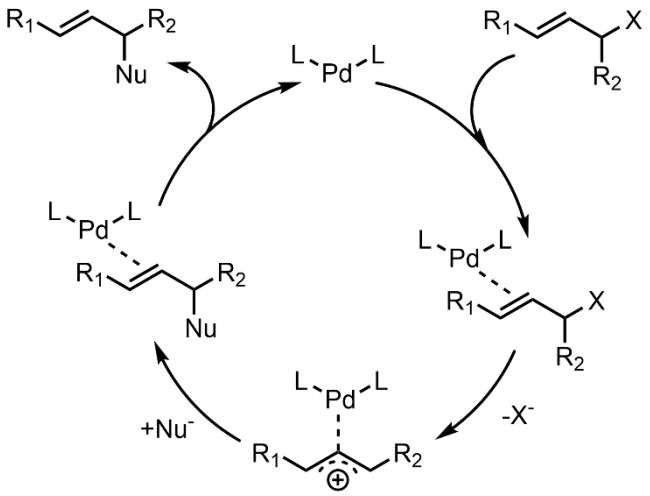

Scheme 22: Mechanism of the palladium-catalyzed Tsuji-Trost-Allylation.[130]

From the classic protocol many more iterations followed, especially including pre-functionalized allylic moieties, commonly carboxylates and halides. The nucleophilic partners include, but are not limited to, stannanes, silanes, zinc reagents, and boranes.[6, 131] One of the more important applications of this method is for asymmetric allylation reactions. Thus the development of chiral ligands for enantioselective transition metal catalyzed reactions is still relevant and research has been focused on finding cheaper and more effective ligands.[132] One example for an enantioselective allylation was presented by Trost and coworkers in 2005.[133] They investigated the allylation of ketones from allyl enol carbonates as described in Scheme 23. This reaction is especially challenging due to the problem of racemization in the presence of most catalysts. However, the authors were able to present a few examples with very good yields and excellent enantioselectivities.

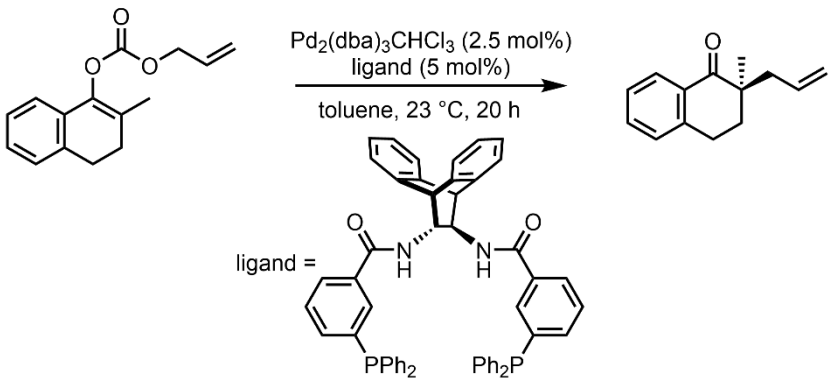

Scheme 23: Palladium-catalyzed, enantioselective allylation of ketones.[133]

Besides the use of the precious metals, palladium and iridium,[7, 8, 134-136], more easily available transition metals have been employed over the last few years. Reports of allylation reactions with iron,[137-139] molybdenum,[140-143] or tungsten,[144] can be found. Copper-catalyzed varieties can also be found in literature. One important work in this area has been made by Miura and co-workers.[145] They report the direct C-H allylation using cinnamyl phosphates (see Scheme 24). The reaction proceeds without the need for an external oxidant in presence of a simple copper-phenanthroline complex.

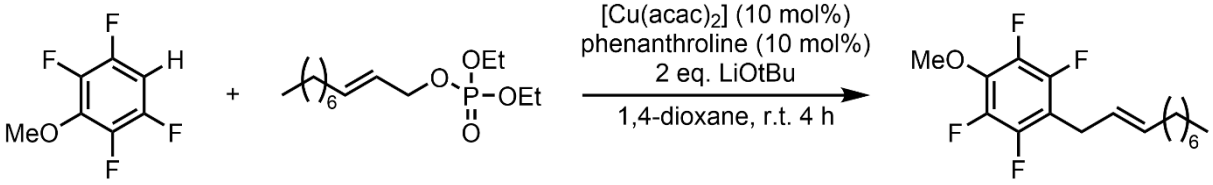

Scheme 24: Copper-catalyzed C(sp^2)-allylation of electron deficient arenes.[145]

Unfortunately, the reaction requires the use of electron-deficient arenes to forego the need for very reactive oxidants. At the same time, the reaction proceeds with very high stereoselectivity, retaining the *E/Z* configuration. The mechanism is proposed to proceed through a η^3-coordination of the copper to the allylic position. Feringa *et al.* also reported the asymmetric synthesis of chiral allylic esters in 2006.[146] Analogous to other copper-catalyzed cross-couplings (*vide supra*), this reaction requires the use of highly reactive carbon nucleophiles like Grignard reagents (see Scheme 25). In this specific reaction, a chiral phosphine ligand was used to attain enantioselectivity at low temperatures. Altogether, the protocol tolerated various substrates and excellent selectivity was reported.

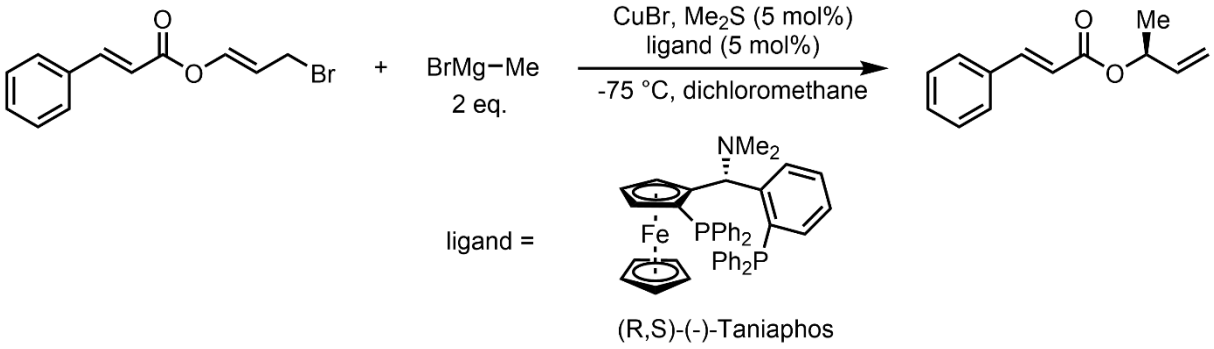

Scheme 25: Asymmetric Synthesis of chiral allylic esters with Grignard-reagents.[146]

More and more protocols allow C-H derivatization of at least one of the substrates, cutting down on the potential waste. However, in common allylation reactions true CDC modes are still rare. C-H allylations including one pre-functionalized substrate are numerous and well investigated.[147] In general, the activation of the allylic group proceeds through the extrusion of a leaving group. These can be, but are not limited to, acetates, carbonates, phosphates, pivalates, silanes or halides. The list of potential substrates is ever increasing and presents a wide toolbox of possible allylic moieties and catalysts to choose from.

1.4.2. Photocatalytic Allylic Substitutions

The harnessing of light for chemical reactions has gained significant interest over the past years.[148, 149] The use of light to activate a reaction provides novel catalytic pathways, which are inaccessible under thermal conditions, and allows milder and greener transformations.[150] Hence, this subchapter will discuss a few highlights of the past years in research for the photocatalyzed allylation reactions.

In general, the scope of this research can be divided into single-catalyst reactions and dual (or synergistic) catalytic approaches. Both are divided into the use of solely transition metals,[151] organic dyes,[152] or both.[153] Concerning the transition metals, ruthenium and iridium complexes have been established as the most productive photocatalysts or photosensitizers. Unfortunately, the constantly rising demand for these metals and their high price make them unattractive for chemical synthesis. Fortunately, many authors report the successful use of cheaper transition metals for these applications.[154]

One of the first reports of photocatalytic allylations was reported by Reiser in 2012, using a copper photocatalyst.[155] He used a modified phenanthroline ligand (see Scheme 26) in order to increase the lifetime of the excited copper species. The reaction required the use of visible light in the range of 530 nm. Under these conditions the authors managed to transfer the allylic group in 17 examples with very good yields. However, this protocol requires the use of highly toxic organotin compounds. This original protocol was later modified by Ollivier *et al*. exchanging both the anisole moieties at the ligand for phenyl.[156] In their protocol, the allylation via a tosylated allyl group with diphenyliodonium reagents was tested. Their system showed similar proficiency to an iridium based photocatalyst. Mechanistically, the authors propose the formation of an aryl based radical from the iodonium reagent through the excited photocatalyst. Reiser and co-workers later presented another photocatalyzed reaction through an iridium-based photosensitizer.[157] On their search for substrates suitable for the cyclisation reaction in the coupling of α-bromochalcones with alkenes, they accidently found the formation of the allylic coupling products in some cases. In the case of cyclohexene or allyl bromides as coupling partners, the allylated chalcones were observed as major products.

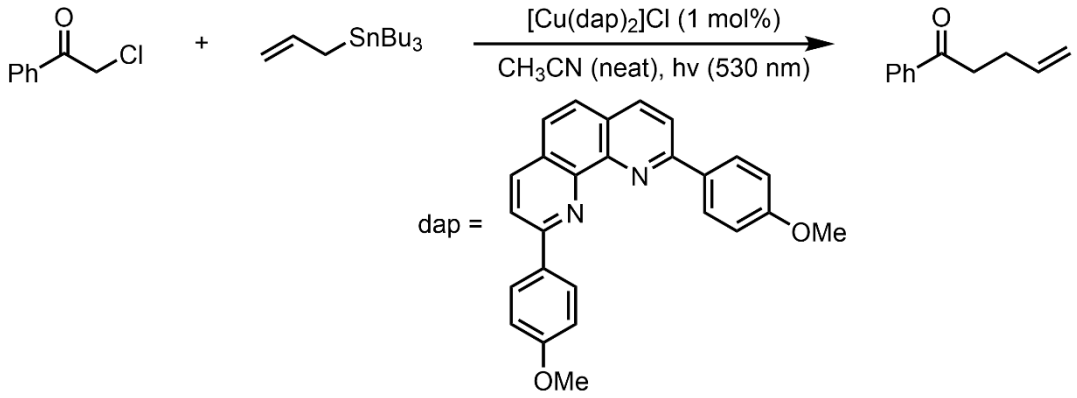

Scheme 26: $Cu(dap)_2$ photocatalyzed allylation using allyl stannanes.[155]

Reports in literature so far required the presence of a leaving group at least for one of the substrates. True cross dehydrogenative protocols were, to the best of our knowledge, unprecedented until the publication of Mejía *et al*. which was discussed earlier in this work (*vide supra*). In this context, it was the first true photocatalyzed CDC allylation of alkynes using copper.

Zhou and co-workers could show the coupling of C(sp^3)-H with allylic substrates under photoredox conditions using an organic photosensitizer (see Scheme 27).[158] The reaction was tested with a mesityl-acridinium dye under blue light irradiation. This very facile protocol proceeded under very mild conditions. The authors also report an impressive library of substrates tested, showing an excellent applicability and tolerance towards different functional groups. The reaction was further improved in a "stop-flow" reactor with increased yield and reduced reaction time. Lastly, they also showed the synthesis of several building blocks for pharmacological substances.

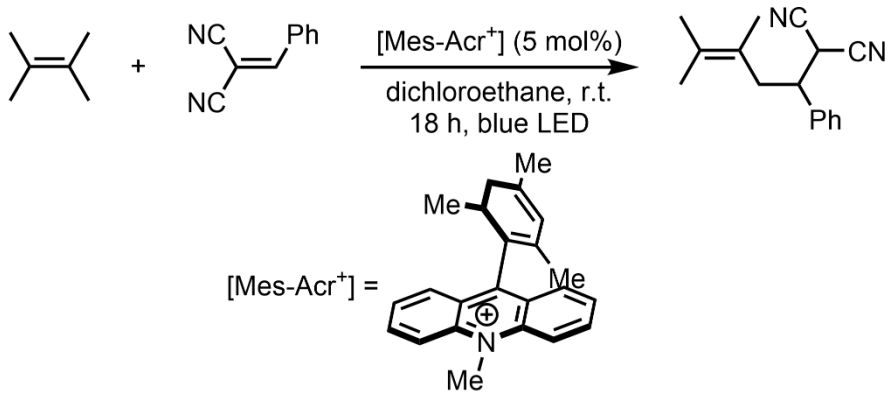

Scheme 27: Allylation of electron-deficient substrates via organic photosensitizer.[158]

Recently, the group of Alemán showed a chromoselective allylation reaction of indoles, pyrroles, amine and alcohols.[159] The reaction of these substrates was either selective towards the *Z*- or the *E*-Isomer depending on the wavelength used (see Scheme 28 for an example). In presence of the phenothiazine and under irradiation at 365 nm the isomerization is driven towards the *Z*-isomer. On the contrary, when the racemate is irradiated at 420 nm, there is nearly complete isomerization towards the *E*-isomer. In presence of the phenoxazine catalyst, still 80 % of the *E*-isomer is formed.

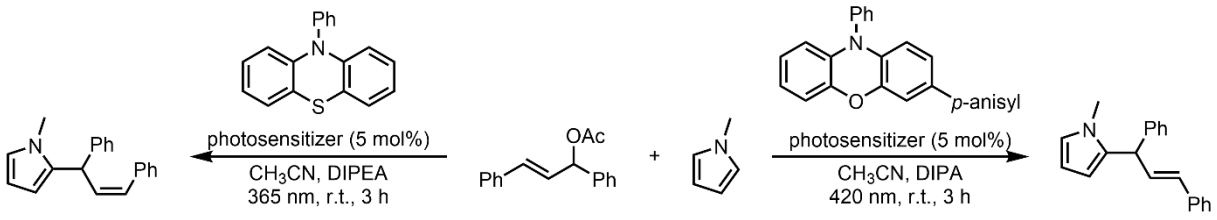

Scheme 28: Exemplary, chromoselective allylation of *N*-methyl pyrrole.[159]

Mechanistically, the authors could show the formation of an intermediary cation via trapping experiment with O^{18}-labeled water. The generation of such cation facilitates a simple Friedel-Crafts-Reaction with the other substrate. With the help of laser flash photolysis experiments they could also show, that the reaction does not proceed through a radical step.

Along with the "traditional" ways of harnessing light for chemical reactions, the use of the so-called *dual catalytic* or *synergistic* systems has been developed. In these systems, upon absorption of light, an excited photosensitizer reacts either through single-electron-transfer (SET) or hydrogen-atom-abstraction (HAT) with a co-catalyst or substrate to form an activated species.[160] The seminal work for the application of this method to allylation reactions has been laid out by MacMillan and co-workers.[161] They employed a combination of an iridium photosensitizer with a thiol-based organocatalyst (see Scheme 29).

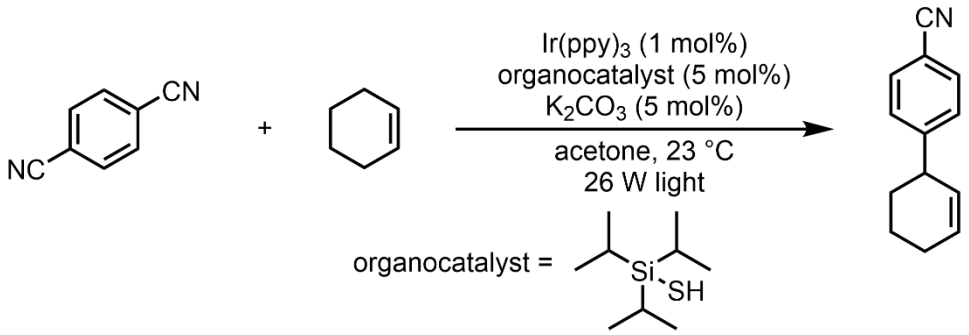

Scheme 29: Dual-catalytic allylation of aryl nitriles.[161]

The reaction proceeds formidably with various aromatic as well as allylic substrates and tolerates very well various functional groups. As such, the protocol is very versatile and application towards more intricate substrates were successful. Through their mechanistic investigations, they found that the photosensitizer proceeds by reductive quenching after irradiation with the nitrile to form a persistent radical. The then oxidized photosensitizer is reduced by a SET with the organocatalyst, which forms a thiyl radical. This radical performs a HAT reaction on the alkene which consequently engages in a radical-radical-coupling with the arene radical to form the desired product.

2. Optimization of the Reaction Protocol

Recently, Mejía *et. al.* reported the copper-catalyzed allylic alkynylation under thermal and light-promoted conditions, as described in Scheme 30. They were able to convert cyclic alkenes with phenylacetylene to the C-C coupling product cyclohex-2-en-1-ylethynyl)benzene (**3A**). The protocol was able to achieve an overall yield of 70 % in both thermal and light-promoted approaches. Additionally, the reaction required a total time of 24 h to achieve these yields. The authors also reported the applicability of the method to various functionalized alkenes as well as with different alkynes. However, the reaction showed problems in reproducibility. The conditions also promoted the homocoupling of the phenylacetylene leading to the formation of 1,4-diphenylbutadiyne (**3B**) as the main side product (later referred to as the Glaser-Product).[98, 99] This limited the efficiency of the reaction greatly.

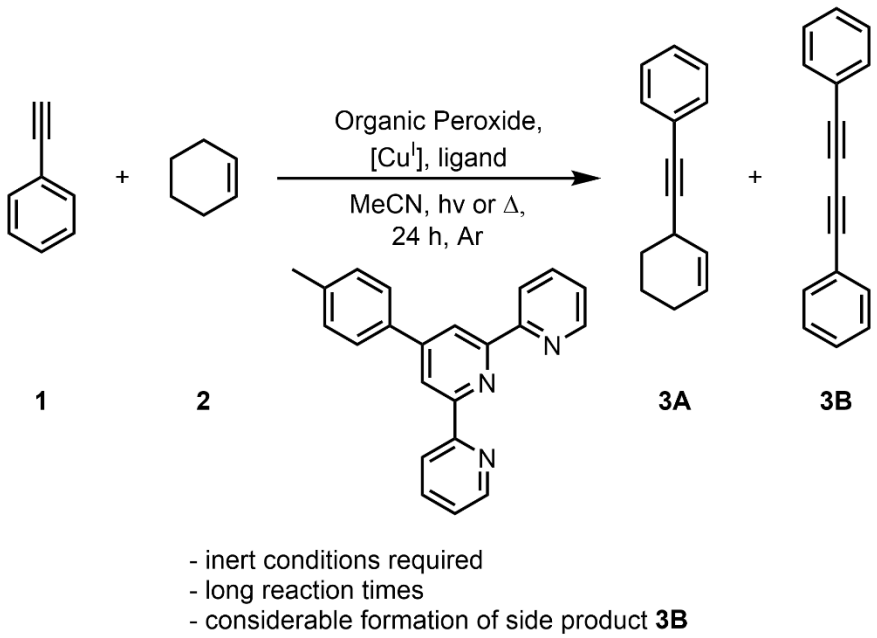

Scheme 30: General reaction protocol for the alkynylation of cyclohexene.[14, 15]

Hence, optimization of the method was set as a priority to allow a more reliable protocol. This will then further enable the screening of intricate substrates or even allow enantioselective transformations. Moreover, variation of the reaction conditions could give valuable information for the reaction mechanism. As the spectroscopic

investigation of the mechanism proved to be rather complex, systematic changes of the reaction conditions were made to gain insight of the intermediates. The following chapter reports about the efforts undertaken towards an optimized reaction protocol. To this purpose, multiple variations on the reaction conditions were tested, using the reaction yield as evaluation parameter. Variations of the reaction conditions were made bearing in mind the principles of 'Green Chemistry'.[13] Further, conditions of similar reaction types in literature were tested to gain knowledge about possible similarities.

2.1. Preliminary Optimization of Reaction Conditions

In order to assess the possible perturbations caused by different reagents, optimized conditions had to be found. Firstly, general necessary conditions were established by changing the ratio of different reagents in solution. In the reported protocol an Asahi Spectra Xenon Light Source 300 W Max-303 was used (340-700 nm, max 300 W). In contrast to this, the light was exchanged for two 390 nm Kessil LED's (max 52 W) which improved reproducibility and output of the reaction greatly. In addition to this, the ligand was exchanged for 4,4′,4″-tri-*tert*-butyl-2,2′:6′,2″-terpyridine **L0** due to its higher solubility in acetonitrile. The results of the first trial runs are presented in Table 1. The first experiments, represented by Entry 2 to 3, show a dependency of the reaction on the used copper-salt, ligand, as well as peroxide. No formation of product **3A** could be observed in the absence of the former. Following this, efforts were undertaken to reduce the amount of copper. It was reduced from 0.05 to 0.025 and 0.0125 mmol respectively. Both reactions showed a slight increase in yield compared to the benchmark reaction. Altering the amount of the reactants was detrimental to the overall yield (Entry 7 to Entry 11). Stoichiometric amounts of reagents and catalyst lead to the formation of Glaser-Product **3B** but only traces of product **3A** (Entry 7). Entry 8 and 9 show a great dependency on an excess of cyclohexene (**1**). Equivalent amounts of cyclohexene and phenylacetylene (**2**) bring the reaction to a complete halt, while 10 equivalents still allow a transformation for up to 71 % of product. This is also shown by Entry 10 and 11. Increasing the amount of phenylacetylene compared to cyclohexene is detrimental to the formation of the product **3A** and instead leads to the formation of the Glaser-Coupling product **3B**.

Table 1: Results of the preliminary Reaction Optimization.

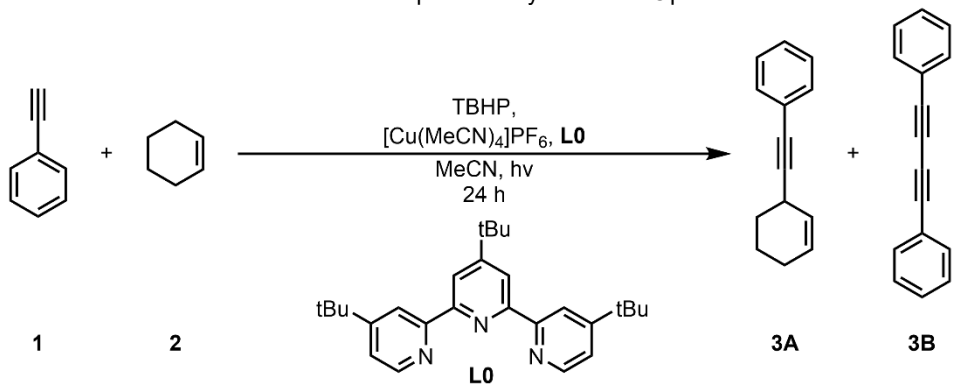

Entry	1 [mmol]	2 [mmol]	TBHP [mmol]	$[Cu(MeCN)_4]PF_6$ [mmol]	L0 [mmol]	Yield of product 3A[a]
1[b]	9.6	0.5	0.959	0.024	0.024	70 %
2	10	0.5	0	0.05	0.05	0 %
3	10	0.5	1	0.05	0	0 %
4	10	0.5	1	0	0.05	0 %
5[c]	10	0.5	1	0.025	0.025	86 %
6[c]	10	0.5	1	0.0125	0.0125	77 %
7	0.5	0.5	0.5	0.05	0.05	traces[d]
8	0.5	0.5	1	0.05	0.05	0 %[d]
9	5	0.5	1	0.05	0.05	71 %
10	0.5	1	1	0.05	0.05	0 %[d]
11	0.5	5	1	0.05	0.05	0 %[d]
12	10	0.5	0.5	0.05	0.05	77 %
13	10	0.5	0.25	0.05	0.05	46 %
14	10	0.5	2.5	0.05	0.05	>99 %
15	10	0.5	1	0.05	0.1	>99 %
16[c,e]	0.5	0.5	1	0.05	0.05	0 %
17[f]	10	0.5	1	0.05	0.05	>99 %
18	**10**	**0.5**	**1**	**0.05**	**0.05**	**>99 % (98 %)**

Standard Reaction Conditions: 10 mmol Cyclohexene, 0.5 mmol Phenylacetylene, 1 mmol *tert*-Butyl Hydroperoxide solution (5-6 M in decane), 0.05 mmol $[Cu(MeCN)_4]PF_6$, 0.05 mmol 4,4′,4″-Tri-tert-butyl-2,2′:6′,2″-terpyridine, 1 ml MeCN, 390 nm, 24 h, 30 °C.
[a] The Yield was determined via GC-MS and is the average of two separate Experiments.
[b] Conditions as mentioned by Mejía *et al.*[15] Ligand: 4′-(4-Methylphenyl)-2,2′:6′,2″-terpyridine.
[c] To avoid overheating issues, the lights were cycled between 5 min on at 100 % intensity and 10 min off at 0 % for 24 h
[d] The Glaser-Product **3B** was observed as the main side product.
[e] The Volume of Acetonitrile was increased to 5 ml
[f] The reaction was conducted under oxygen atmosphere after the addition of the Peroxide.
Isolated yield in parenthesis.

The amount of peroxide seems to be directly correlated to the efficiency of the reaction as suggested by Entry 12 to Entry 14. Reducing the amount of peroxide to less than two equivalents lead to a reduction in yield, while further increases lead to a quantitative formation of **3A**. In Entry 15 the amount of ligand was doubled to assess its influence on the yield. The preliminary result show quantitative conversion of the educt to the product **3A** in presence of two equivalents of ligand. The role of the ligand will be further discussed in following chapters. As the reported reaction required an excess of cyclohexene, efforts were undertaken to use equivalent amounts of educts. However, when the amount of cyclohexene is lowered, and the overall volume is increased no reaction takes place (see Entry 16), thus suggesting that an excess of cyclohexene is necessary. In addition to this, the susceptibility of the reaction to oxygen exposure was tested. The initial protocol required strict inert conditions. However, preliminary experiments showed no influence of the presence of oxygen on the reaction outcome*. Lastly, from the information gathered from these experiments, an improved protocol has been established as shown in Entry 17. Following the initial experiments, further optimization of the reaction time was conducted. The results are presented in Table 2. The time of irradiation was varied from 2.5 h to 48 h in total. Surprisingly, the reaction showed higher efficiency than expected. As seen in Entry 1, the reaction already reaches a high yield after only 2.5 h. In addition to this, the reaction reaches nearly complete conversion after 4 h and no more educt is detected after 6 h. This indicates that a shortening of reaction time under the new setup is feasible. Besides, for Entry 1 to Entry 3 the formation of another compound was observed that completely disappears again after 24 h. Through GC-MS analysis, this compound was identified as 3-(*tert*-butylperoxy)cyclohex-1-ene (**1A**).[162] The corresponding mass-spectrum can be seen in Figure 2.

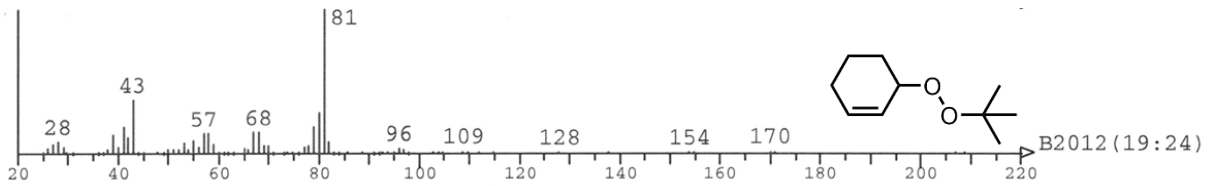

Figure 2: ESI-MS of the 3-(*tert*-butylperoxy)cyclohex-1-ene (**1A**).

* The headspace of the reaction vial was flushed with oxygen after the addition of all reagents.

The formation of this compound has been observed before by Salavati *et al.* using heterogeneous transition metal catalysts.[163] Further increases of irradiation time do not show any influence on the yield of the desired product (**3A**). This indicates that the product is stable enough under the reaction conditions and no degradation can be observed. However, longer reaction times promote side reactions of the cyclohexene. Oxidation of the allylic position was observed leading to the formation of cyclohex-2-en-1-ol (**1B**) and cyclohex-2-en-1-one (**1C**) (see Scheme 31) *. Similar to the compound above, these molecules have been reported as oxidation products from the reaction of cyclohexene with peroxides under transition metal catalysis.[164, 165]

Table 2: Variation of Irradiation Time.

Entry	Reaction time [h]	Time of irradiation [h]	Yield of product 3A[a]
1	2.5	2.5	83 %
2	4	4	97 %
3	6	6	>99 %
4	16	16	>99 %
5	36	36	>99 %
6	48	48	>99 %
7	24	6	83 %
8[b]	24	6	87 %
9	24	0	46 %

Standard Reaction Conditions: 10 mmol Cyclohexene, 0.5 mmol Phenylacetylene, 1 mmol *tert*-Butyl Hydroperoxide solution (5-6 M in decane), 0.05 mmol $[Cu(MeCN)_4]PF_6$, 0.05 mmol 4,4′,4″-Tri-tert-butyl-2,2′:6′,2″-terpyridine, 1 ml MeCN, 390 nm, 24 h, 30 °C.
[a] The Yield was determined via GC-MS and is the average of two separate Experiments.
[b] The light was cycled between 5 min on at 100 % intensity and 10 min off at 0 % for 24 h

* For the GC/MS analysis of the Cyclohex-2-en-1-ol and Cyclohex-2-en-1-one please refer to the Appendix.

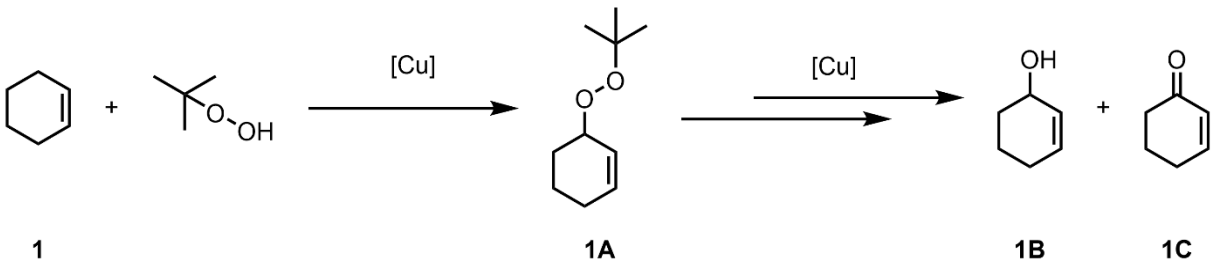

Scheme 31: Copper-Catalyzed Peroxidation and consequent degradation of Cyclohexene with TBHP.[166]

Gade *et al.* reported the formation of the alkylperoxy-species (**1A**) under Copper(I) catalysis and propose a subsequent degradation to the alcohol (**1B**) and ketone (**1C**) as displayed in Scheme 31.[166] To elucidate whether the formation of these products is promoted by the heat produced by the lamps, two additional experiments were performed which can be seen in Entry 7 and Entry 8. The reaction was irradiated for a total amount of 6 hours and analyzed after 24 hours have passed in total. Entry 7 shows the outcome for a reaction which was irradiated continuously for 6 h while in Entry 8 the light source was turned on and shut off in defined intervals. Both entries lead to roughly the same amount of product (**3A**) at the end. Unfortunately, in both cases the reactions underperformed in comparison to Entry 3 which showed a quantitative conversion. Lastly, the reaction was conducted in the complete dark at room temperature as seen in Entry 9. Even under these conditions a conversion was observed and the product (**3A**) was formed in 46 % yield. This confirms that the reaction can be achieved thermally, alas, with lower yield.[14] More intricate investigations to elucidate the promiscuity towards different activation sources are reported down below.

2.2. Variation of the Catalytic System

Following the general optimization route, our interest shifted towards the effect of the reactants in the catalytic system. We wondered, if we could achieve even shorter reaction times or better yields with different ligands, copper precursors or peroxides. The initial experiments showed a lowered conversion at room temperature. So, we set out to test different light sources and heat to investigate its effect on the reaction. Firstly, we focused on finding the optimal ligand for the reaction. The Terpyridine scaffold already showed very good activity in the reaction. However, it is rather expensive and their modification is not straightforward. Additionally, investigations of the expected, *in-*

situ generated copper(I)-terpyridine complex (as seen in Figure 3 **A**) proved to be difficult due to insolubility of the formed product. Crystallization attempts were also futile. Various authors reported about the nature of analogous copper-terpyridine complexes "polymeric".[167, 168] Accordingly, a possible variation of this multimetallic complexe is shown in Figure 3 **B**. Noticeably, one terpyridine moiety is able to coordinate two copper-center.

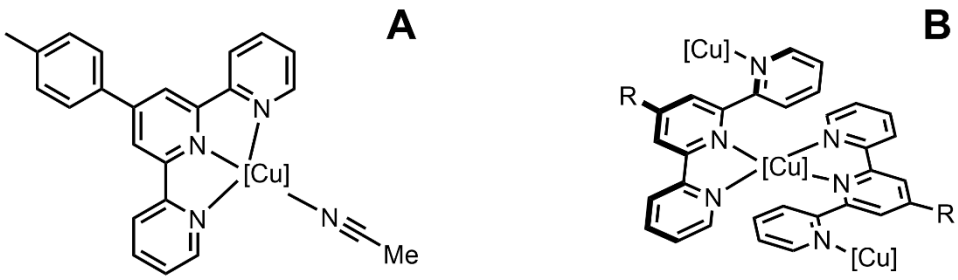

Figure 3: **A**: Copper(I)-Terpyridine-Complex and suggested structures. **B**: Possible polymeric copper complex.

Moreover, Copper(I) is reported to mostly prefer tetrahedral or linear coordination geometries,[169] while the terpyridine moiety generally enforces a square-planar or octahedral coordination with all three nitrogen atoms in the same plane.[170, 171] This missmatch of coordination geometries leads to a variety of struggles in the determination of an exact molecular structure. Further investigations on the molecular structure of the complex can be found in Chapter 4.1. First experiments were focused on different nitrogen-based ligands ranging from structurally easy pyridines to more complex pincer ligands, showing a great dependency on the ligand scaffold. These results are depicted in Figure 4.

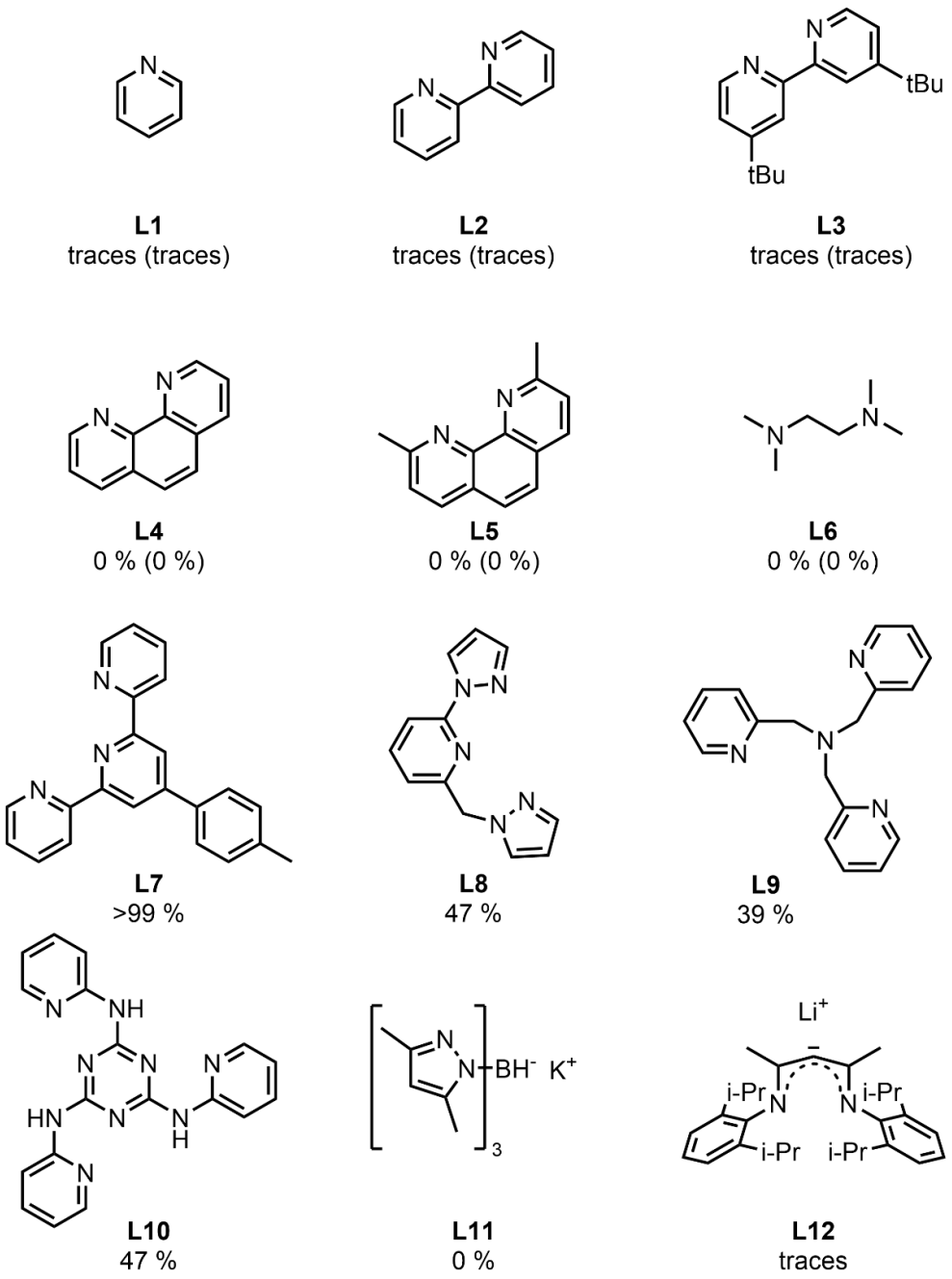

Figure 4: Results of the Screening of various Nitrogen-based ligands. Yields are determined via GC. Depicted in parenthesis are yields with two equivalents of ligand to copper. 370 nm were used for Ligand **L8**.

In general, mono- and bidentate ligands such as pyridines and bipyridines were detrimental for the formation of the desired reaction product **3A**. However, these ligands excelled at the formation of the Glaser-product **3B**. Increasing the amount of ligand to two equivalents (compared to copper) was not fruitful. In contrast to that, the use of tridentate ligands was more successful. The benchmark ligand (**L7**) performed exceptionally, and led to overall quantitative conversion. In comparison to **L0** the solubility is

however remarkably low in the solvent of our choice. Other Pincer ligands, that have been reported to form complexes with copper were tested as well,[125, 172-176] giving only yields of 39-47 % of **3A**. Ionic ligands **11** and **12** inhibited the reaction nearly completely.

In general, the following conclusions can be derived from the tested array of ligands:

- Mono- and bidentate Nitrogen-based ligands do not promote the desired reaction and instead allow the Glaser coupling.
- Tridentate Nitrogen-based ligands have a positive influence on the reaction outcome.
- Terpyridines achieve the highest yields in all test reactions.

Based on these results, further tests were designed to evaluate the dependency of the reaction on the terpyridine. Firstly, it was assumed that the reaction required a copper center coordinated by three nitrogen atoms. Hence, the terpyridine was replaced by a mixture of a bipyridine and pyridine, as depicted in Scheme 32.

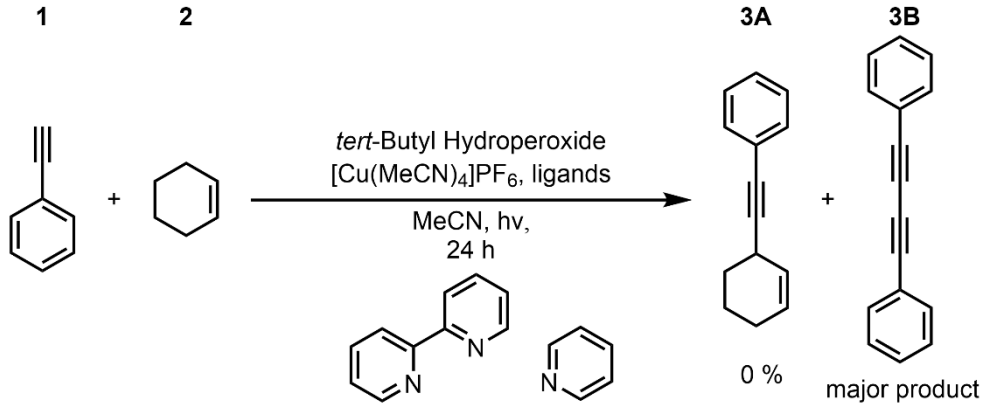

Scheme 32: Replacement of the Terpyridine ligand with Bipyridine and Pyridine.

Surprisingly, the reaction did not yield any product **3A** but instead promoted the formation of the Glaser Product **3B** . This suggests the necessity on a more rigid ligand structure such as the terpyridine. Furthermore, the aromatic system of the terpyridine ligand could have an influence on the reactivity. Jones *et al.* report the possible involvement of the terpyridine ligand in nickel-catalyzed alkyl-alkyl-cross-coupling reaction.[177] They describe the terpyridine as a non-innocent and redox-active ligand and crucial for the reaction. Similar to the results reported here, other nitrogen-based

ligands did not result in any improved reactivity. This was later confirmed by Ciszewski *et al.*, stating the ligand sphere plays a much more important role in the reaction than metal center does.[178] Unfortunately, these results still did not give an answer to the nature of the coordination of the ligand to the copper. It was therefore decided to modify the terpyridine ligand and exchange one pyridine ring with a benzene ring, resulting in 6-phenyl-2,2'-bipyridine. This ligand could potentially coordinate via its two nitrogen atoms and also provide a delocalized π-System. The result of it is depicted in Scheme 33.

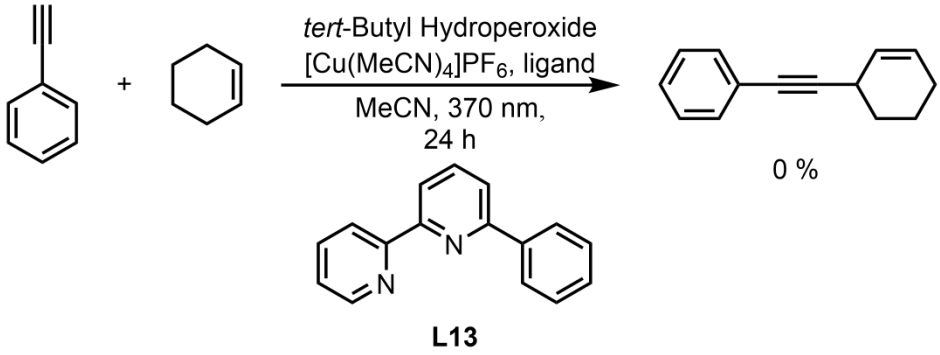

Scheme 33: Test reaction of the ligand 6-Phenyl-2,2'-bipyridine (**L13**).

Similar to the previous reaction, no conversion to the desired product **3A** was observed, as no reaction took place. Both experiments imply that the terpyridine moiety is necessary for the reaction to succeed. A more detailed investigation of the catalyst properties and characteristics can be found in Chapter 4.1.

Lastly, efforts were undertaken to replace the Ligands with commonly available Phosphines and Phosphine oxides or -sulfides as can be seen in Figure 5. The trend continued in these experiments and no conversion of the educts to the desired product **3A** was achieved. However, no tridentate phosphorous-based ligands were screened.

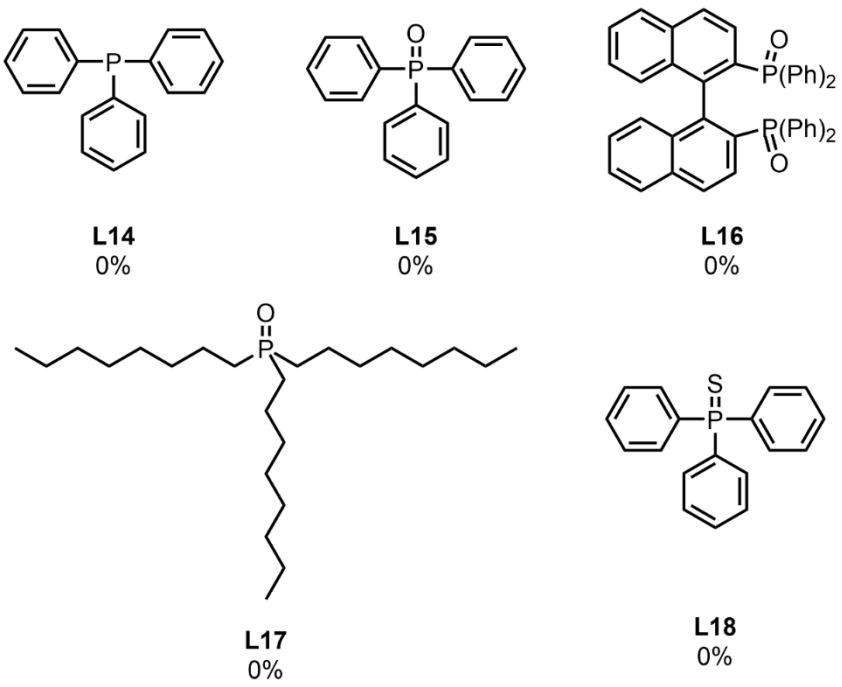

Figure 5: Screening of various Phosphorous-based ligands. Yields are determined via GC. For **L14** and **L15** four equivalents of Ligand compared to Copper were used.

The investigations of different copper precursors was of special interest, as multiple sources state a promiscuity of copper to catalyze reactions in +1 as well as +2 oxidation state.[179-181] In order to elucidate whether this is also applicable to our reaction, a variety of copper salts have been screened. The results of these experiments are summarized in Table 3. Both Cu(I) and Cu(II) complexes promote the reaction. However, with Cu(II) the reaction is rather sluggish and the yields drop significantly. The best yield was achieved with $Cu_2(OH)_2CO_3$ with 19 %, followed by $Cu(OTf)_2$ and $CuCl_2$. No reaction was observed with $Cu(acac)_2$ or copper(II) phtalocyanine. Surprisingly, CuO lead to the formation of a small amount of product which has not been observed when Cu_2O is used. Interestingly, there is only a marginal difference between the various anions for Cu(II). In contrast to that, the anion seems to play an important role for the Cu(I) precursors.

Table 3: Screening of various Copper sources.

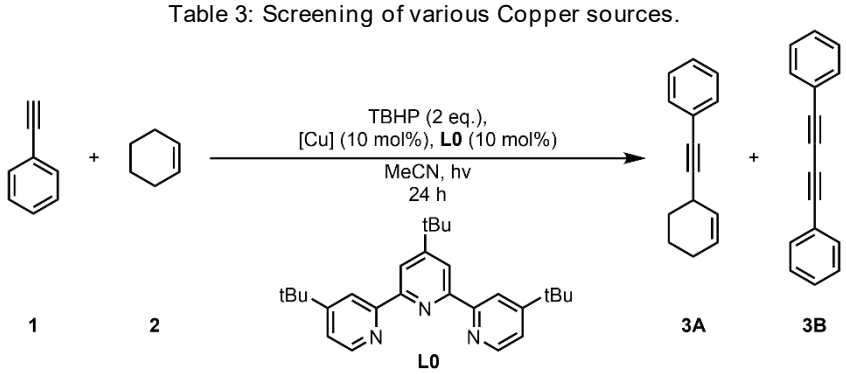

Entry	Copper Precursor	Yield of product 3A[a]
1	CuCl	34 %
2	CuBr	55 %
3	CuI	70 %
4	Cu(I)-acetate	29 %
5	Cu_2O	0 %
6	$[Cu(MeCN)_4]BF_4$	84 %
7	$Cu_2(OH)_2CO_3$	19 %
8	$CuCl_2$	14 %
9	CuO	7 %
10[b]	Cu(II)(acac)	0 %
11	$Cu(OTf)_2$	15 %
12	Cu(II)(phtalocyanine)	0 %
13[c]	Cu(II)(phtalocyanine)	0 %

Standard Reaction Conditions: 10 mmol Cyclohexene, 0.5 mmol Phenylacetylene, 1 mmol *tert*-Butyl Hydroperoxide solution (5-6 M in decane), 0.05 mmol Copper Precursor , 0.05 mmol 4,4′,4″-Tri-tert-butyl-2,2′:6′,2″-terpyridine, 1 ml MeCN, 390 nm, 24 h, 30 °C
[a] The Yield was determined via GC-MS and is the average of two separate Experiments.
[b] The reaction was irradiated with 370 nm.
[c] No ligand was used.

As it can be seen in Entries 1 to 3, the Cu(I) halides perform better as they move down the periodic group. The yield of the product **3A** increases from 34 % with the chloride salt to 70 % with the iodide salt. This could be reasoned with stronger coulomb interactions of smaller halogen ions. As the ionic radius is increasing with the heavier halogens, the charge of the ion is more diffuse. Hence the interaction of the anion with the Cu(I) cation is less prominent. This could be an indication of possible ionic

interactions during the reaction, in which a strongly coordinating anion would act competitively with a substrate or intermediate. The same effect has been observed in the case of CuOAc and $[Cu(MeCN)_4]BF_4$. The tetrafluoroborate anion is known for its weakly coordinating properties.[182] On the contrary, the acetate is rather strongly coordinating and therefore shows lowered reactivity. In general, the reaction shows better performance with copper(I) salts. The anion plays an important role in the catalysis. Stronger coordinating anions inhibit the reaction while weakly coordinating ions promote it.

As shown in the initial experiments (*vide supra)*, the peroxide is crucial for the transformation to take place. In both reports of Mejía *et al*. organic peroxides had to be used to promote the reaction.[14, 15] However, it was unclear, if the reaction is promoted via a radical pathways or other unknown mechanisms. A broad variety of radical starters was tested to assess on this. The results of this screenings are shown in Table 4.

Surprisingly, no reaction was observed in Entry 1 to 4 with common available radical starters, such as 2,2-dimethoxy-2-phenylacetophenone (DMAP), which are used for photoactivated radical polymerization.[183] Also triethylborane ($B(Et)_3$), which promotes radical reactions after activation with oxygen,[184] did not enable the reaction. However, as seen in Entry 5 to 9 peroxides could promote the reaction leading to formation of the product **3A** with varying efficiency. The lowest yield was achieved with aqueous hydrogen peroxide. Unfortunately, the easier to handle and store hydrogen peroxide/urea adduct did not show any reactivity. In comparison, the hydroperoxides as well as dialkyl peroxides reacted all with considerable yields (56-99 %).

Table 4: Screening Results of different Radical Starters.

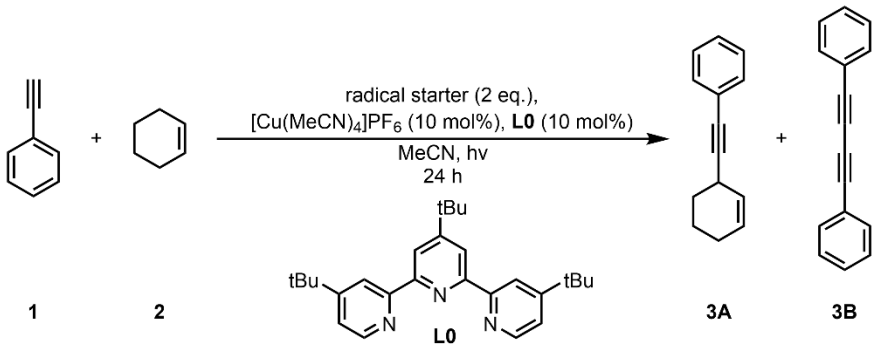

Entry	Radical Starter	Yield of product 3A[a]
1	DMPA	0 %
2[b]	$B(Et)_3$	0 %
3	$K_2S_2O_8$	0 %
4[c]	Oxygen	0 %
5	Di-*tert*-butyl peroxide	56 %
6	Cumyl hydroperoxide[d]	59 %
7	Dicumyl peroxide	74 %
8	Dibenzoyl peroxide	>99 %
9	H_2O_2 [e]	24 %
10	H_2O_2 / Urea	0 %

Standard Reaction Conditions: 10 mmol Cyclohexene, 0.5 mmol Phenylacetylene, 1 mmol radical starter, 0.05 mmol $[Cu(MeCN)_4]PF_6$, 0.05 mmol 4,4′,4″-Tri-tert-butyl-2,2′:6′,2″-terpyridine, 1 ml MeCN, 390 nm, 24 h, 30 °C.
[a] The Yield was determined via GC-MS and is the average of two separate Experiments.
[b] Air was added to the reaction via a syringe after all reagents were added.
[c] Oxygen was bubbled through via a needle for 15 min.
[d] 80 % in Cumene
[e] 35 % in water

To evaluate the reactivity these peroxides, the Bond Dissociation Energy (BDE) of the O-O bond was considered. The BDE is the energy required for the homolytic cleavage (Table 5). Interestingly, there is no apparent correlation between the O-O BDE and the yield of the desired product in this case. Hydrogen peroxide, which has the highest BDE and is the most reactive shows the lowest yield. Furthermore, the most effective peroxides TBHP and DBP show no exceptional BDE compared to the rest of the array. This suggests a more complex interaction between the peroxide and the catalyst. The homolytic cleavage of the O-O bond might not be a necessary step in the reaction

mechanism, or is not rate-determining. A deeper investigation of this will be subject of Chapter 4.2.

Table 5: O-O Bond Dissociation Energies of Peroxides used in these experiments.

Entry	Peroxide	Yield of product 3A	BDE [kcal mol^{-1}]
1	Dibenzoyl peroxide	>99 %	41.1[185]
2	Dicumyl peroxide	74 %	34.3[186]
3	Cumyl hydroperoxide	59 %	45.01[185]
4	Di-*tert*-butyl peroxide	56 %	38.9[187]
5	H_2O_2	24 %	51.1[187]
6	*tert*-Butyl hydroperoxide	>99 %	44.1[187]

Previous reports on this reaction mostly use acetonitrile as a solvent, as it showed the best overall performance. However, acetonitrile is known to be able to coordinate to the copper center. A series of solvents ranging from polar to non-polar were tested to assess the influence of a coordinating solvent on the reaction. The results are displayed in Table 6 from estimated most polar solvent to most non-polar solvent, based on the dielectric constant of the solvent.

Table 6: Results of the Solvent Screening sorted from most polar to most non-polar Solvent.

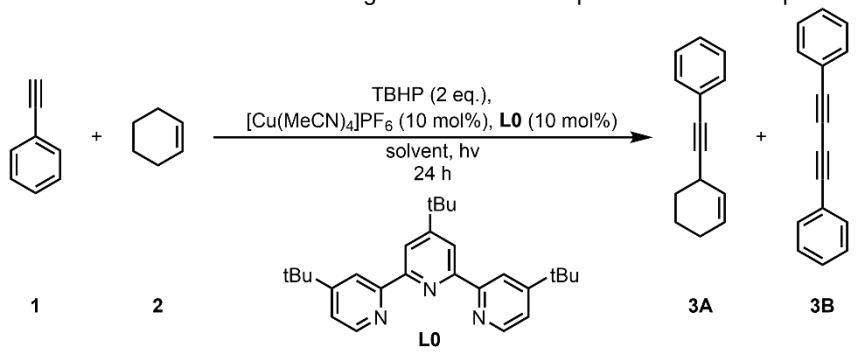

Entry	Solvent	Yield of product 3A[a]	ε_r (25 °C)[188-190]
1	Water	0 %	78
2	Dimethyl sulfoxide	89 %	47
3	Dimethyl formamide	88 %	37
4	Acetonitrile	>99 %	36.6
5	Methanol	>99 %	33
6	N-methyl-2-pyrrolidone	79 %	32.2
7	2-Propanol	40 %	20.3
8	Dichloromethane	43 %	8.9
9	Tetrahydrofuran	traces	7.6
10	Chlorobenzene	0 %	5.6
11	Toluene	0 %	2.4
12	Tetrachloromethane	traces	2.24
13	Heptane	0 %	1.88

Standard Reaction Conditions: 10 mmol Cyclohexene, 0.5 mmol Phenylacetylene, 1 mmol *tert*-Butyl Hydroperoxide solution (5-6 M in decane), 0.05 mmol $[Cu(MeCN)_4]PF_6$, 0.05 mmol 4,4′,4″-Tri-tert-butyl-2,2′:6′,2″-terpyridine, 1 ml Solvent, 390 nm, 24 h, 30 °C. All solvent were degassed via Freeze-Pump-Thaw-method beforehand.
[a] The Yield was determined via GC-MS and is the average of two separate Experiments.

Non-polar solvents seem to generally inhibit the reaction. In contrast, polar solvents are generally good accepted and yields between 40% and 99 % are achieved. The most efficient solvent besides acetonitrile was methanol, leading to quantitative formation of the product **3A**. The higher alcohol 2-propanol, on the other hand, seems to be detrimental for the reaction. Furthermore, solvents like dimethyl sulfoxide (DMSO), dimethyl formamide (DMF) and *N*-methyl-2-pyrrolidone (NMP) are well accepted by the reaction and lead to high yields of the product **3A**. Interestingly, all these solvents

are known for their ability to coordinate to transition metals.[191-193] This suggests that the reaction benefits from the solvent acting as an auxiliary coordinating moiety. Dichloromethane, a non-coordinating solvent of lower polarity, showed reduced activity of the transformation. Besides, water showed no activity whatsoever and completely inhibited the reaction. We found that dissolution of the ligand and the complex in the same solvent poses the biggest issue. For instance, if the ligand is only soluble in minute amounts (like in water) the complex is not formed. To conclude, the reactivity depends highly on the polarity of the solvent and its ability to coordinate copper. Non-polar and non-coordinating solvents completely shut down all reactivity.

The results reported in Chapter 2.1 suggest already a promiscuity of the reaction towards different sources of activation (i.e. heat or light) similarly to the reports of Mejía *et al*.[14, 15] Hence, we had great interest in finding out the exact nature of this activation. Thus, different monochromatic light sources and temperatures were screened. The results can be found in Table 7. Entry 1 to Entry 4 focused on testing different light sources without changing the setup. Furthermore, the intensity of these sources is tunable. Interestingly, the reaction behaves similarly to the standard condition for all other wavelengths set to 100 % (between 43 and 52 W). High yields are achieved in all cases. In contrast to that, at the lowest setting of 25 % Intensity (between 10.75 and 13 W) the yield drops considerably. At 390 nm a decreased yield of 39 % was observed. At 370 nm this decrease in yield was smaller (96%) and for 440 nm there was no discernable difference to the standard conditions. This could hint towards a light active species that has an absorption maximum in this region. Further investigations on this are done in Chapter 4.1. Replacing the monochromatic light sources with a simple LED strip also shows a relatively effective conversion. However, the LED strip heats up considerably during the reaction. Activation of the reaction with heat was successful as well, leading the desired product with 70 % at 40 °C and nearly quantitative at 80 °C. This proves that the reaction can be conducted with a similar setup under light irradiation, as well as under elevated temperature.

Table 7: Screening for the influence of various Activation sources and results.

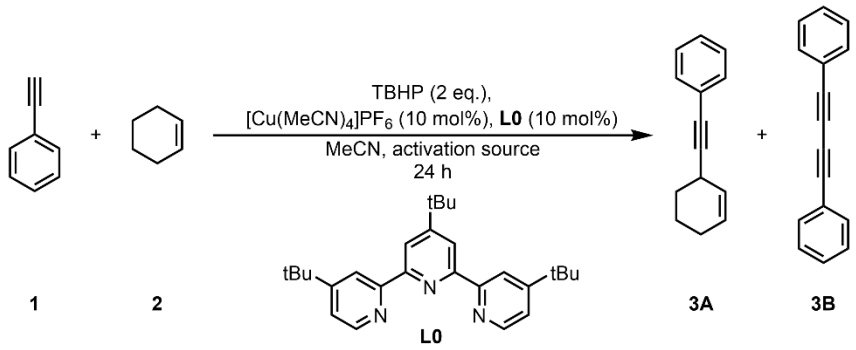

Entry	Activation source	Yield of product 3A[a]
1[b]	LED 390 nm at 13 W (30 °C)	39 %
2[b]	LED 440 nm at 45 W (30 °C)	>99 %
3[b]	LED 440 nm at 11.25 W (30 °C)	96 %
4[b]	LED 370 nm at 43 W (30 °C)	96 %
5[b]	LED 370 nm at 10.75 W (30 °C)	76 %
6[c]	LED Strip (60 °C)	78 %
7[d]	no light, 40 °C	70 %
8[d]	no light, 80 °C	96 %

Standard Reaction Conditions: 10 mmol Cyclohexene, 0.5 mmol Phenylacetylene, 1 mmol *tert*-Butyl Hydroperoxide solution (5-6 M in decane), 0.05 mmol $[Cu(MeCN)_4]PF_6$, 0.05 mmol 4,4′,4″-Tri-tert-butyl-2,2′:6′,2″-terpyridine, 1 ml MeCN, 390 nm, 24 h.
[a] The Yield was determined via GC-MS and is the average of two separate experiments.
[b] KESSIL Science PRL160 LEDs were used with the reported wavelength and intensity set to the corresponding option.
[c] A standard commercially available blue LED strip was used.
[d] The reaction was conducted in a 10 ml Pressure tube in an oil bath.

2.3. Influence of Additives on the reaction

The previous chapter showed the susceptibility of the reaction to changes in the conditions. Still, we wondered if the addition of other reagents to the reaction would help to accelerate it or give some insights to better understand it.

As reported by Mejía *et al.*[14, 15] the reaction proceeds either under thermal conditions, as well as under light irradiation. Thus, different photosensitizers were tested as additives in this reaction and the results are displayed in Table 8. The reaction took place

in all cases with relatively good yields and high selectivity, although no improvement was observed. Importantly, the used excitation wavelength (390nm) was not the most suitable for most of the tested photosensitizers,[194-197] except for Thioxanthone.[198].

Table 8: Screening results of various Photosensitizers as additives.

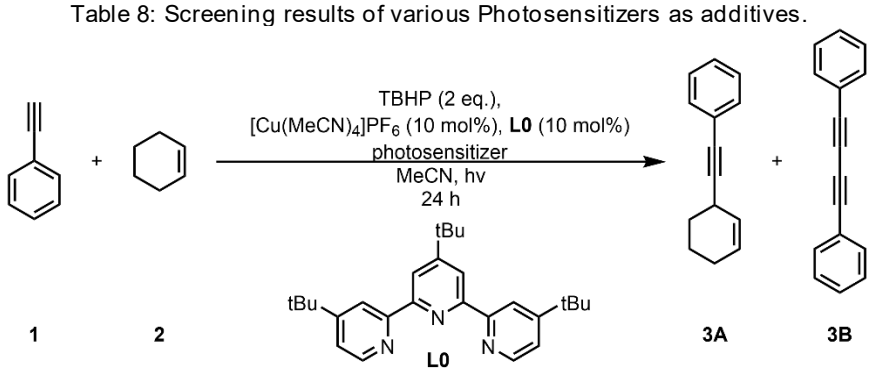

Entry	Photosensitizer	Yield of product 3A[a]
1	$(Ir[dF(CF_3)ppy]_2(dtbbpy))PF_6$	85 %
2	2,4,6-Triphenyl-pyrylium-tetrafluoroborate	65 %
3	$[Ru(bpz)_3][PF_6]_2$	84 %
4[b]	Cu(dmp)(xanthphos)	78 %
5[b]	Thioxanthone	76 %

Standard Reaction Conditions: 10 mmol Cyclohexene, 0.5 mmol Phenylacetylene, 1 mmol *tert*-Butyl Hydroperoxide solution (5-6 M in decane), 0.05 mmol $[Cu(MeCN)_4]PF_6$, 0.05 mmol 4,4′,4″-Tri-tert-butyl-2,2′:6′,2″-terpyridine, 0.01 mmol of Photosensitizer, 1 ml MeCN, 390 nm, 24 h, 30 °C.
[a] The Yield was determined via GC-MS and is the average of two separate Experiments.
[b] 0.1 mmol of Photosensitizer was used.

The acetylenic proton is relatively acidic (pK_A = 28.7),[199] allowing deprotonation by strong bases to form reactive carbanions. This reactivity was exploited by Glaser, who converted phenylacetylenes to 1,4-diphenylbutadiyne using a base and copper catalyst.[98, 99] Later modified by Hay to allow an easier reaction setup,[102] the protocol became the standard for the homocoupling of acetylenes. Motivated by this, we set out to assess the effect of different bases on the reaction. The results are presented in Table 9 with the different bases sorted according to their pK_B Value. Strong bases like KOH, TBD or KOtBu (Entry 1 to Entry 3) are detrimental for the reactivity. The reaction does not yield any product in these cases. However, analytics showed the presence of major amounts of Glaser Coupling product **3B**. Similarly, the addition of potassium phosphate (Entry 4) lowers the yield to 57 %. In contrast to that, copper(II) phosphate

seems to have little to no influence on the reaction yield. Arguably, the addition of a stoichiometric amount of copper could increase the output of the reaction and therefore the influence of the base might be negligible.

Table 9: Results of Screening various bases sorted by their pK_B value.

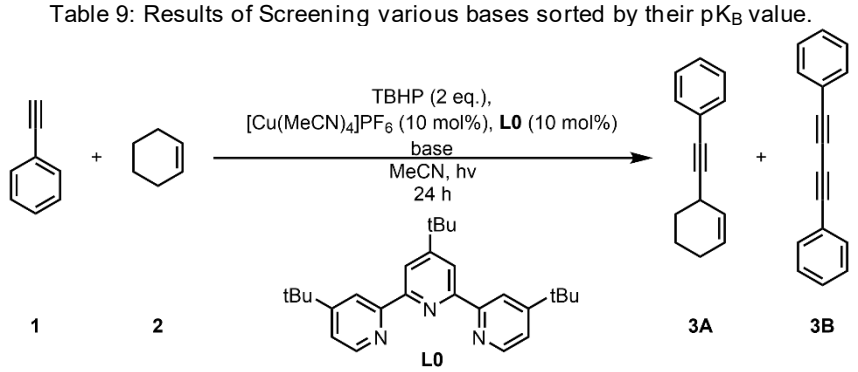

Entry	Base	Yield of product 3A[a]	pK_B Value[b]
1	Potassium *tert*-butoxide	0 %	-18.2[200, 201]
2[c]	1,5,7-Triazabicyclo[4.4.0]dec-5-en	0 %	-12.2[202]
3	KOH	0 %	-1.74[203]
4[c]	K_3PO_4	57 %	1.68[200]
5[c]	$Cu_3(PO_4)_2$	>99 %	1.68[200]
6	Na_2CO_3	90 %	3.7[203]
7	K_2CO_3	89 %	3.7[203]
8[c]	Cs_2CO_3	0 %	3.7[203]
9	$NaHCO_3$	95 %	7.6[203]
10[c]	NaOAc	45 %	9.2[203]

Standard Reaction Conditions: 10 mmol Cyclohexene, 0.5 mmol Phenylacetylene, 1 mmol *tert*-Butyl Hydroperoxide solution (5-6 M in decane), 0.05 mmol $[Cu(MeCN)_4]PF_6$, 0.05 mmol 4,4′,4″-Tri-tert-butyl-2,2′:6′,2″-terpyridine, 1 mmol of base, 1 ml MeCN, 390 nm, 24 h, 30 °C.
[a] The Yield was determined via GC-MS and is the average of two separate Experiments.
[b] The pK_B Value was calculated from the reported pK_A Value ($pK_B = 14 - pK_A$).
[c] The reaction was irradiated with 370 nm.

Interestingly, weaker bases such as carbonates and hydrogen carbonates seem to only have minimal influence on the reactivity as the yield of product **3A** stays between 89 % and 95 %. This trend is however not observed with cesium carbonate, which completely shuts down the reaction. This is puzzling, as there is no clear trend visible.

The solubility of these carbonates increases with higher homologues.[204-206] However, this trend does not explain the drastic change in reactivity from potassium to cesium. As of now, an explanation to this remains elusive. Lastly, sodium acetate (Entry 10), the weakest base in these trials, shows a detrimental effect on the reaction by lowering the yield to around 45 %. In short, strong bases promote the Glaser Coupling of the acetylenes towards **3B**, effectively shutting down the desired reactivity. Weaker bases have a negligible effect, although in most cases a slight reduction in reactivity is observable. Therefore, the addition of bases to the reaction is not beneficial.

Questioning the underlying mechanism of this transformation, we considered using additives inspired by reports in literature. The resulting experiments and effects on the yield are displayed in Table 10.

Table 10: Screening of different additives and the corresponding results.

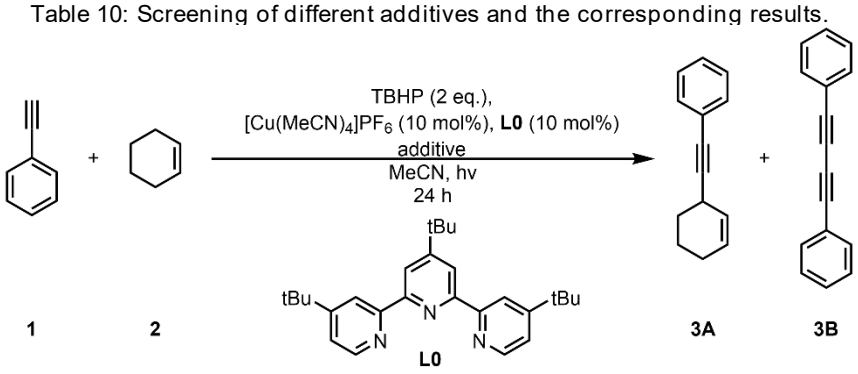

Entry	Additive	Yield of product 3A[a]
1[b]	2,2,2-Trifluoroethanol	99 %
2[c]	Boronic Acid	68 %
3[c, d]	1-*N*-Methylpyrole	34 %
4[c, d]	Aluminium chloride	0 %
5[c]	Iron(III) chloride	0 %
6[b]	n-Decane	97 %
7[c]	Sodium Chloride	56 %

Standard Reaction Conditions: 10 mmol Cyclohexene, 0.5 mmol Phenylacetylene, 1 mmol *tert*-Butyl Hydroperoxide solution (5-6 M in decane), 0.05 mmol $[Cu(MeCN)_4]PF_6$, 0.05 mmol 4,4′,4″-Tri-tert-butyl-2,2′:6′,2″-terpyridine, 1 ml MeCN, 390 nm, 24 h, 30 °C
[a] The Yield was determined via GC-MS and is the average of two separate Experiments.
[b] 1 ml was added to the Standard reaction setup
[c] 1 mmol was added to the Standard reaction setup
[d] The reaction was irradiated at 370 nm.

Stahl *et al*. used 2,2,2-trifluoroethanol (TFE) as a solvent in nickel-catalyzed methylations of benzylic bonds using di-*tert*-butyl peroxide.[207] They found, that the addition of TFE improved the formation of methyl radicals. Inspired by this, trials with this compound as an additive in equal volumetric amounts were conducted. This however, showed no effect on the reaction, as the yield remained high. Additionally, they also reported that the addition of boronic acid is beneficial for their reaction in promoting the formation of methyl radicals. In our case, the addition of this reagent lead to lower yields. The addition 1-*N*-methylpyrrole to the reaction could help stabilize intermediates by coordinating to the metal center during the reaction[208]. This was not observed during our tests. There, the compound led to a general inhibition and increased formation of the Glaser coupling product **3B**. We also suspected that the influence of Lewis' Acids might be beneficial for the reactivity as activation of the peroxides by the former has been reported in literature.[209, 210] The addition of aluminium chloride and iron(III) chloride (Entry 4 and Entry 5) completely inhibited the reaction. No product could be identified from these experiments. As the employed *tert*-butyl hydroperoxide is only available as a solution in decane, we wanted to make sure that the alkane has no influence on the reaction. Entry 6 shows that there is only a slight effect on the yield, suggesting that decane is not involved in the reaction, as expected. Lastly, the results of precatalyst screening (*vide supra*) suggest an influence of the anion accompanying the copper complex on the overall yield. Therefore, we hypothesized that the addition of a strong anion such as chloride should have a noticeable effect on the yield. Indeed, this was confirmed with the experiment in Entry 7. The addition of 1 mmol of sodium chloride led to a decrease in yield to 56 %.

2.4. Summary

- The reported reaction protocol was optimized (Figure 6) by systematic changes on the reaction conditions, reagents, and additives. We achieved quantitative conversion of cyclohexene and phenylacetylene to cyclohex-2-en-1-ylethynyl)benzene (**3A**) in 5 h at 35 °C using monochromatic light (390 nm). The protocol is reproducible.

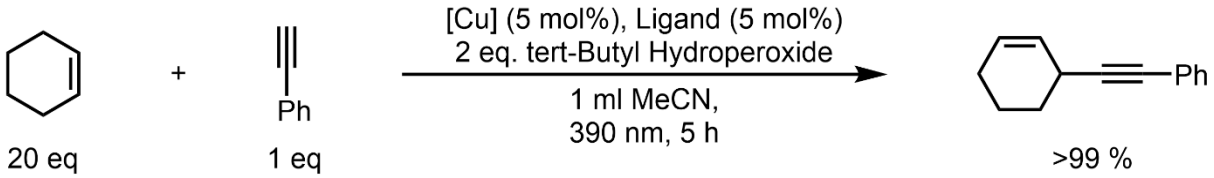

Figure 6: Optimized Reaction conditions for the Copper-catalyzed Allylic Alkynylation.

- The original stoichiometric ratios of reactants (20 eq. cyclohexene, 1 eq. phenylacetylene, 2 eq. TBHP) are key to the success of the reaction.
- The transformation can be conducted either under irradiation with blue light or by heating up to 80 °C with comparable yields.
- The anion of the copper source is important for its reactivity. Strongly coordinating anions are detrimental while weakly binding anions are favorable for the coupling reaction.
- Both copper(I) and copper(II) complexes are able to catalyze the reaction. However, copper(II) only shows low conversions.
- The presence of the terpyridine ligand is necessary for the quantitative conversion. In general, the reaction only accepts tridentate ligands. A specific interaction of the terpyridine in the reaction is proposed.
- Common radical starters do not promote the reaction. Only in the presence of peroxides the desired product is obtained. The reaction tolerates both bisalkyl- as well as hydroperoxides.
- None of the tested additives showed to be beneficial for the reaction.

3. Application of the Improved Reaction Protocol to novel Substrates

With a modified and optimized reaction protocol, we envisioned to expand the scope of possible substrates beyond the structural motifs tested in previous reports.[14, 15] These mostly focused on the variation of substituents on the aromatic ring of the phenylacetylene in order to assess electronic effects of the substrate on the reaction. However, the cyclohexene was barely modified. Expanding the substrate scope would allow to incorporate more intricate structural motifs which then could be used for further functionalization.

Several compounds found in nature contain the cyclohexene structural motif. They are especially found in terpenes and terpenoids, a class of molecules derived from isoprene, or 2-methyl-1,3-butadiene,[211] that can be found in various natural products. Because of their complex molecular structures, terpenes and terpenoids are especially interesting substrates. A late-stage functionalization of these molecules could therefore be very useful. In contrast to that, the use of more sophisticated acetylenes could lead to applications in organic conducting materials. These are only a few examples of possible uses for this methodology.

3.1. Alkynylation of cyclic Alkenes

A variety of different cyclic alkenes containing an allylic CH or CH_2 group were tested as substrates in the reaction. These reactions were mostly conducted via thermal activation at 80 °C in pressure vials, as this was operationally simpler than the photoactivated methodology. Nevertheless, some of the substrates were tested using the modified photoactivation.

In general, the reaction showed drastic differences in yields depending on the substrate's bulkiness and substituents. Elaborate substitutions on the ring were mostly detrimental to the reactivity, while general modifications of the carbon backbone were tolerated. The results are shown in Figure 7.

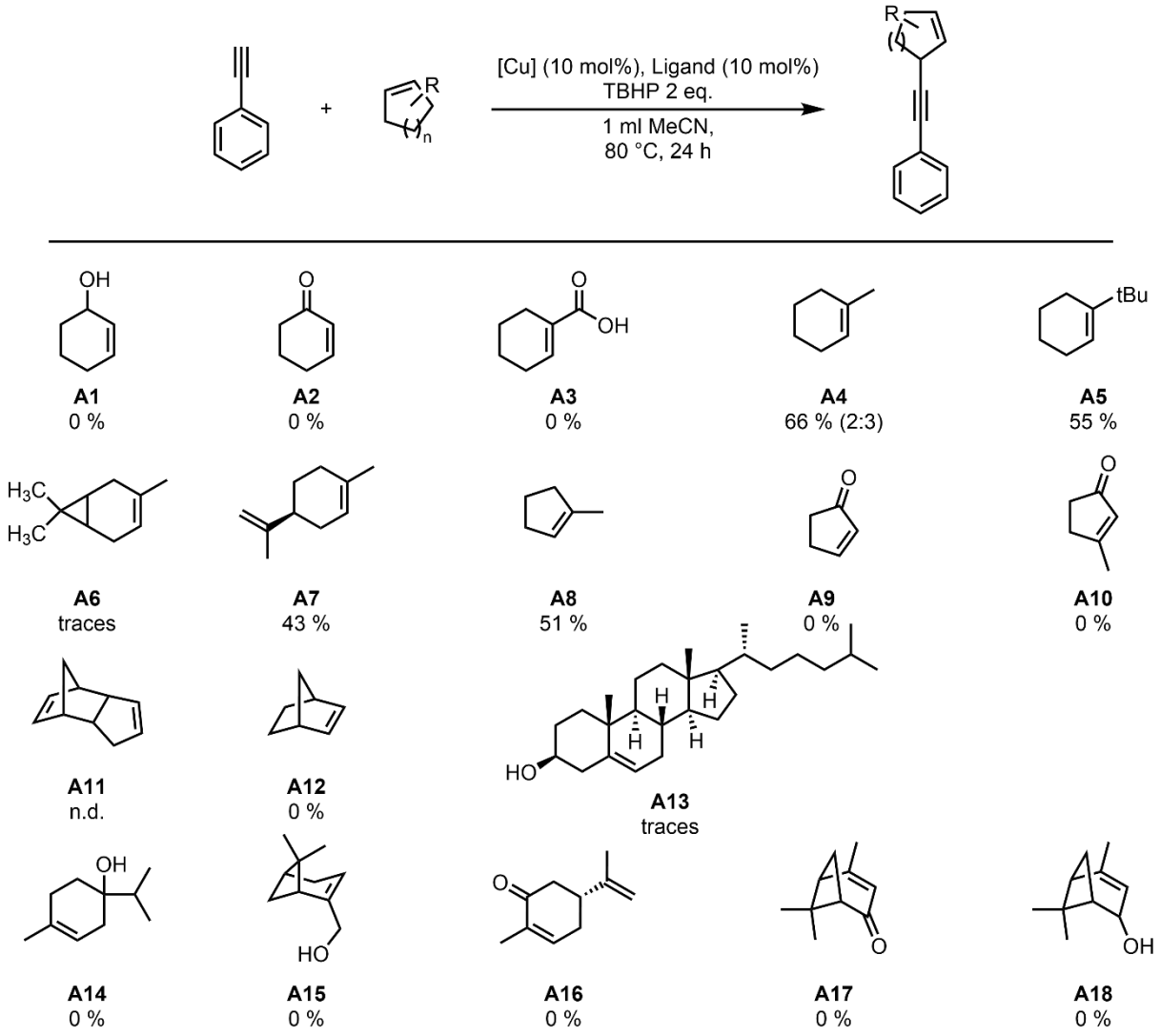

Figure 7: Screening results of new cyclic Alkenes and Cyclohexene derivatives.

Surprisingly, the reaction showed striking sensitivity towards any oxygen functionality as seen in Entries **A1** to **A3**. In all cases, the reaction was completely inhibited, and no reaction product could be observed. These results were also confirmed with the cyclopentene derivative **A9** and **A10**, as well as **A14** to **A18**. In every case an oxygen-containing functionality is present in the molecule and no traces of the desired product are observed. Similar observations were made during the screening (*vide supra*) using copper(I) acetyl acetonate as a precursor. Seemingly, coordination of the oxygen-containing functions to the copper inhibits further reactivity. On the contrary, a complete inhibition was not observed when alcohols were used as solvents (*vide supra*). At this point, we assume a strong coordination of the oxygen to the copper-metal, deactivating the catalyst in the process. While the exact nature of this interaction was not investigated further, other substrates mostly displayed extension of the carbon-frame of the

cyclohexene as seen in Entry **A4** to **A8**. For these substrates mostly acceptable yields were achieved. The 1-methylcyclohex-1-ene (**A4**) led to the alkynylation product to achieve an overall yield of 66 %. Interestingly, two regioisomers were observed in each of the allylic positions yielding a mixture of ((2-methylcyclohex-2-en-1-yl)ethynyl)benzene and ((3-methylcyclohex-2-en-1-yl)ethynyl)benzene in a ratio of 3:2. In contrast to that, 1-(tert-butyl)cyclohex-1-ene (**A5**) only produced one isomer with a total yield of 55 %, suggesting a steric protection due to the *tert*-butyl group. Isolation of the reaction product from substrate **A6** was not possible. However, a product with the desired mass was detected in GC-MS and HR-EI-MS as well. Entry **A7** and **A8** lead to the formation of a single regioisomer in 43 % and 51 % respectively. The reaction of dicyclopentadiene (**A11**) led to a plethora of various products which could not be separated and characterized. It can be assumed, that under the present conditions the substrate undergoes a Retro Diels-Alder reaction to cyclopentadiene, which can react further. While a full structural characterization of such a product was not possible, the presence of one alkynylation product was shown with EI-MS. The reaction of **A12** did not lead to the formation of any product. Similarly, to the Entries **A16**, **A17** and **A18** the allylic positions are obscured by a bridged carbon atom. This enforces a tetrahedral geometry on the carbon atom, making it impossible to assume a trigonal planar geometry as a carbocation or carbon-centered radical. Most surprisingly, the reaction with cholesterol (**A13**) afforded the desired product although only in trace amounts (see Appendix). This indicates that the alkynylation of more complex allylic substrates might be possible with further optimization. However, so far only modification of molecules with no heteroatomic functional groups were feasible and afforded the desired product.

Regarding the experiments under light irradiation, the substrates **A4**, **A10** and **A17** were chosen for the trials. The reactions were irradiated at 390 nm at room temperature. The results are listed in Figure 8.

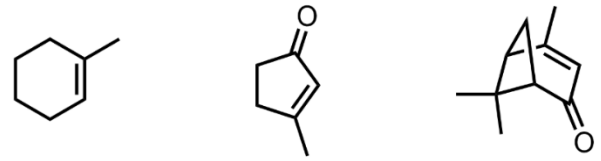

A4
95 % (2:3)

A10
0 %

A17
0 %

Figure 8: Results of the photoactivated conversion of new cyclic Alkenes.

In general, the results of the thermal activation could be confirmed. Substrate **A4** did yield the desired product while the substrates **A10** and **A17** did not react to any product. Most interestingly, the substrate **A4** showed a drastically increased yield from 66 % up to 95 % while the ratio between the different regioisomers remains the same. This indicates that the use of photocatalytic conditions provides a benefit to the yield. In contrast to that, it will not facilitate the transformation of demanding substrates, nor increase the selectivity.

3.2. Substitution of the Alkyne

The previous results showed that the reaction was very selective towards functionalization of cyclic alkenes. Based on the results of Mejía *et al.* we investigated the functionalization of different acetylenes as well.[15] The reactions were conducted in a similar fashion to the previous experiments.

To test the tolerance of the reaction towards new substrates, different acetylenes with various functional groups, heterocycles and carbon chains of various lengths were tested. The results of these screening reactions are presented in Figure 9. To our delight, every tested substrate yielded the desired products. However, it must be noted, that alkynes **B3** to **B5** as well as **B8** to **B10** could not be obtained as clean products. Purification via column chromatography did not yield pure products. Further efforts to purify these were either not successful or led to decomposition of the resulting products. Hence, no yield could be reported.

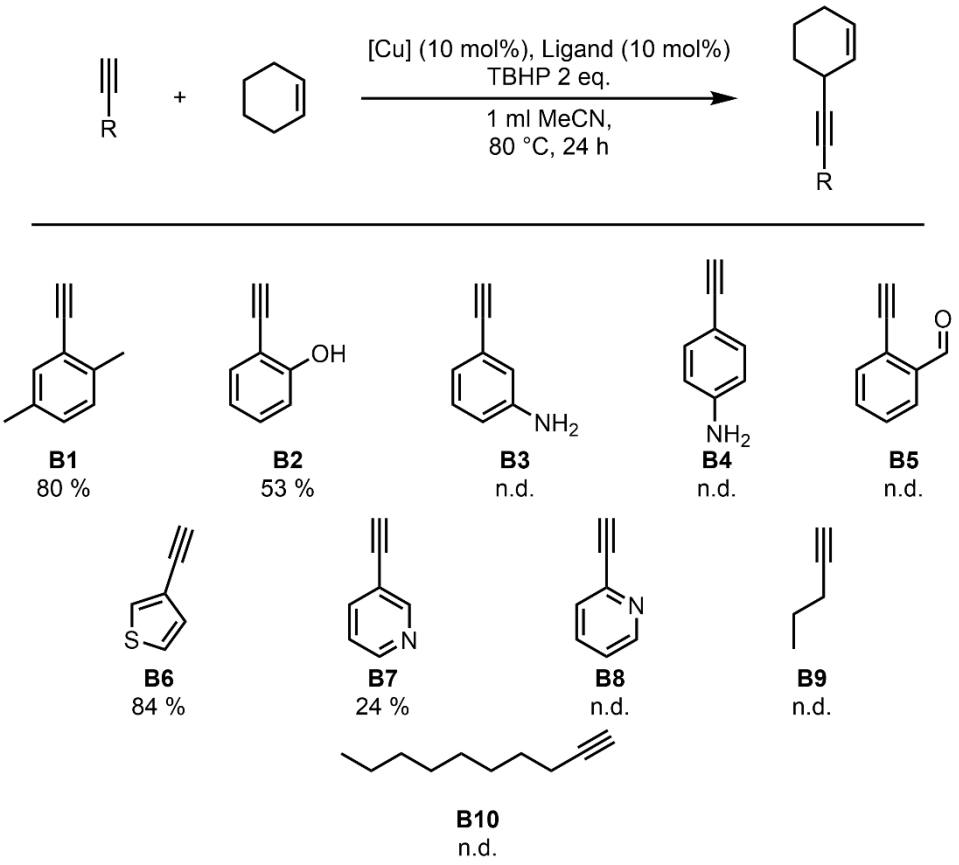

Figure 9: Screening results for various new alkynes (n.d.= the yield could not be determined due to persistent impurities).

Nevertheless, it must be noted, that in all cases a reaction product was observed. Intriguingly, in the case of alkynes the presence of oxygen-containing groups on the substrate does not inhibit the reaction. To our delight, also heterocyclic alkynes and linear alkynes were accepted as substrate and yielded the desired products. However, due to the complications in the work-up no comparison between the substrates can be made.

3.3. Screening of allylic and C-H-acidic Substrates

Chapter 3.1 focused mostly on cyclic alkenes. However, other allylic substrates such as several acyclic olefins could be regarded as interesting substrates, as they are useful synthetic building blocks. Furthermore, we hypothesized that C-H-acidic substrates could be activated in a similar fashion. Hence, we decided to employ compounds of

this type that have been reported in literature to undergo C-C coupling.[59, 60, 212] The results of these tests are represented in Figure 10.

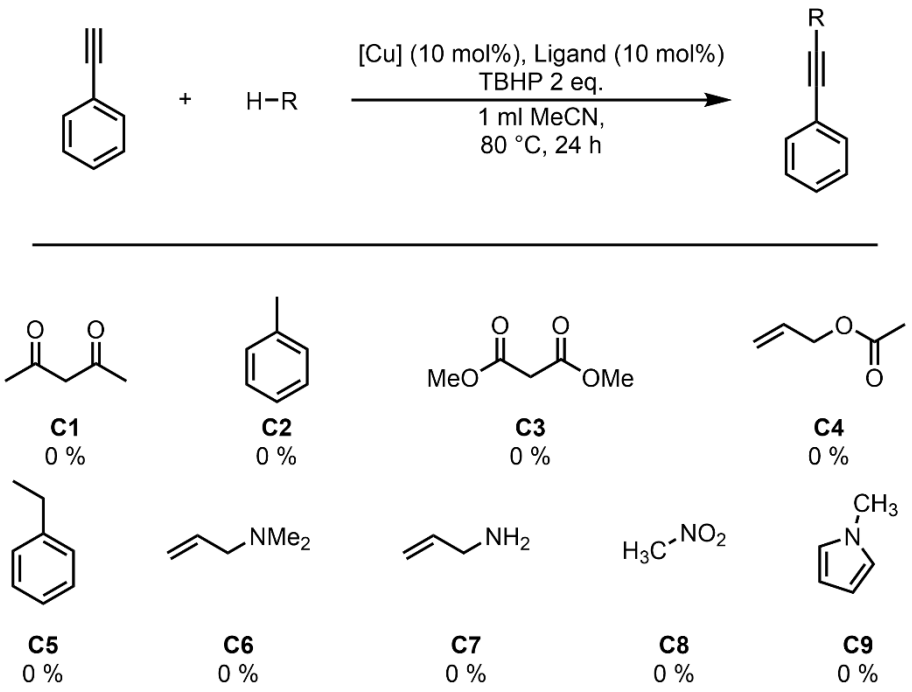

Figure 10: Test reaction of new allylic and C-H-acidic substrates.

Unfortunately, none of the tested substrates lead to any reaction. Interestingly, none of the allylic substrates (**C4**, **C6** and **C8**) showed any conversion either. This could imply, that the reaction is very selective towards the transformation of cyclic alkenes. Alternatively, this observation could be linked to the presence of reactive functional groups. As seen above, the presence of oxygen-containing moieties inhibits the reaction completely. Also, the absence of any reaction product for toluene (**C2**) and ethylbenzene (**C5**) is puzzling considering that their BDE is similar to that of cyclohexene (84.5 kcal·mol^{-1}).[213] This is another indication, that the reactivity of the cyclohexene in the protocol is rather specific. Lastly, the results from Klussmann *et al*. inspired us to test other kinds of substrates (**C1**, **C3**, **C8** and **C9**) in the reaction.[59] Similarly to the other results, no transformation was observed and no product was formed. While this diminishes the applicability of the reaction to other substrates, it allows comparison to other reported mechanisms, like radical coupling, which in view of these results, seems highly unlikely.

3.4. Summary

- The Reaction showed poor compatibility with cyclic alkenes containing oxygenated functional groups. It can be suspected that the coordination of oxygen to the copper center inhibits the reactivity.
- The modification of the carbon “frame” of these cyclic alkenes is accepted by the reaction. However, rigid, tertiary carbon centers do not allow the reaction giving indication towards either a homolytic or heterolytic cleavage of the C-H bond.
- The Reaction is very selective towards the functionalization of the allylic position in cyclic Alkenes. Other commonly used substrates in such radical mediated reaction did not lead to any conversion.

4. Mechanistic Investigations

The elucidation of reaction mechanism is of great interest for any reaction, as it can give valuable information to optimize said reaction or make reaction design easier. In the report of Mejía *et al.* a mechanistic proposal for the oxidative allylic alkynylation was published.[15] It is presented in Scheme 34.

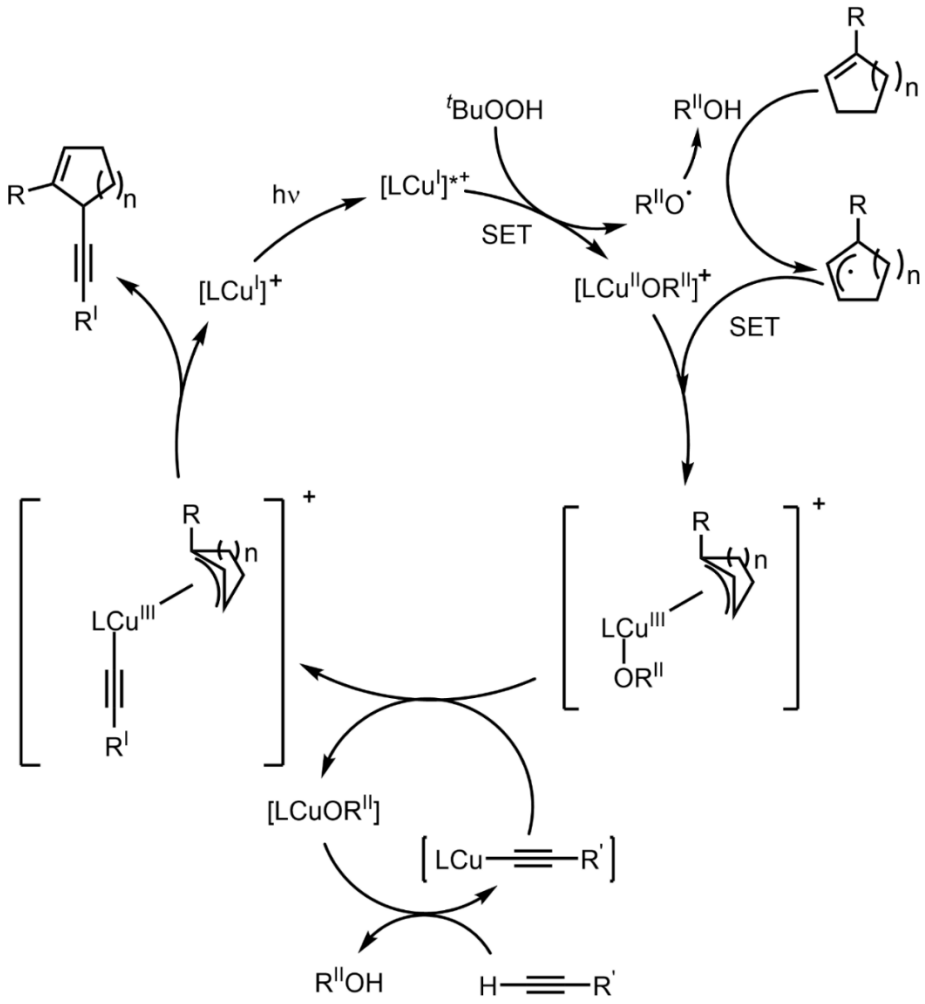

Scheme 34: Mechanistic proposal for the copper-catalyzed allylic alkynylation presented by Mejía *et al.*

They described a single electron transfer (SET) from the hydroperoxide to an excited copper(I) complex, forming a copper(II)-alkoxide and an alkoxy-radical in the process. The radical then undergoes a HAT to abstract the allylic proton of the cyclohexene forming a cyclohexenyl radical. This is followed by another SET on the copper to form a η^2-copper(III)-alkenyl-complex. Simultaneously, another copper atom forms

phenylacetylide cuprate via an acid-base-reaction. Through a transmetallation, a copper(III)-alkenyl-phenylacetylide complex is obtained, which forms the desired coupling product through reductive elimination and regaining the copper(I) catalyst.

In this early mechanistic proposal, a few open questions remain. First, the role of the terpyridine ligand remains unclear. The screening of the various other ligands (*vide supra*) showed a high dependency of the reaction on the terpyridine scaffold. Even structurally identical motifs did not show comparable activity. In most of the reported complexes of terpyridine, it favors the planar (meridional) tridentate coordination geometry.[170, 214] In contrast to that, copper(I) is usually known to prefer a tetrahedral, or in some cases, a linear coordination geometry.[169] This discrepancy between the two different geometries preferred by ligand and metal might enable the metal center to facilitate the desired reaction. Furthermore, terpyridines are known for being "non-innocent" ligands, being able to assist or facilitate redox reaction via electron transfer from the ligand.[214] Moreover, the terpyridine moiety and its metal complexes are known for their photophysical properties.[215] This all makes the terpyridine-copper-complex an essential part of the catalytic system.

Secondly, the interaction of the peroxide and copper is not clear. Over the years, a myriad of proposals for the interaction of copper and *tert*-butyl hydroperoxide have been published.[216-219] While a clear mechanism for the degradation of the peroxide has not been experimentally found, most authors report the cleavage of the hydroperoxide to an alkoxy radical and through subsequent reaction the formation of a peroxyl radical. However, the equilibria of these reactions seem extremely sensitive towards the reaction conditions.

Lastly, it is not clear, how the coupling step of both substrates proceed. So far, a bimetallic activation was proposed but as of now, this has not been proven. Moreover, other reaction intermediates have not been investigated and it remains unclear, how the catalyst interacts with substrates. This includes the generation of different oxidation states of copper during the reaction and activation of both substrates.

4.1. Structural Investigations of the Copper(I)-Complex

Initially, we focused on the elucidation of the catalyst structure. As described before (*vide supra*) the copper(I) ion is not likely to engage in a planar, tridentate coordination

with the terpyridine ligand. Thus, in order to investigate the molecular structure, different analytical methods were chosen. The NMR spectra of the free ligand **L0**, as well as in the presence of Cu(I) (**4**) can be seen in Figure 11. A comprehensive NMR analysis of the complex can be found in the Appendix.

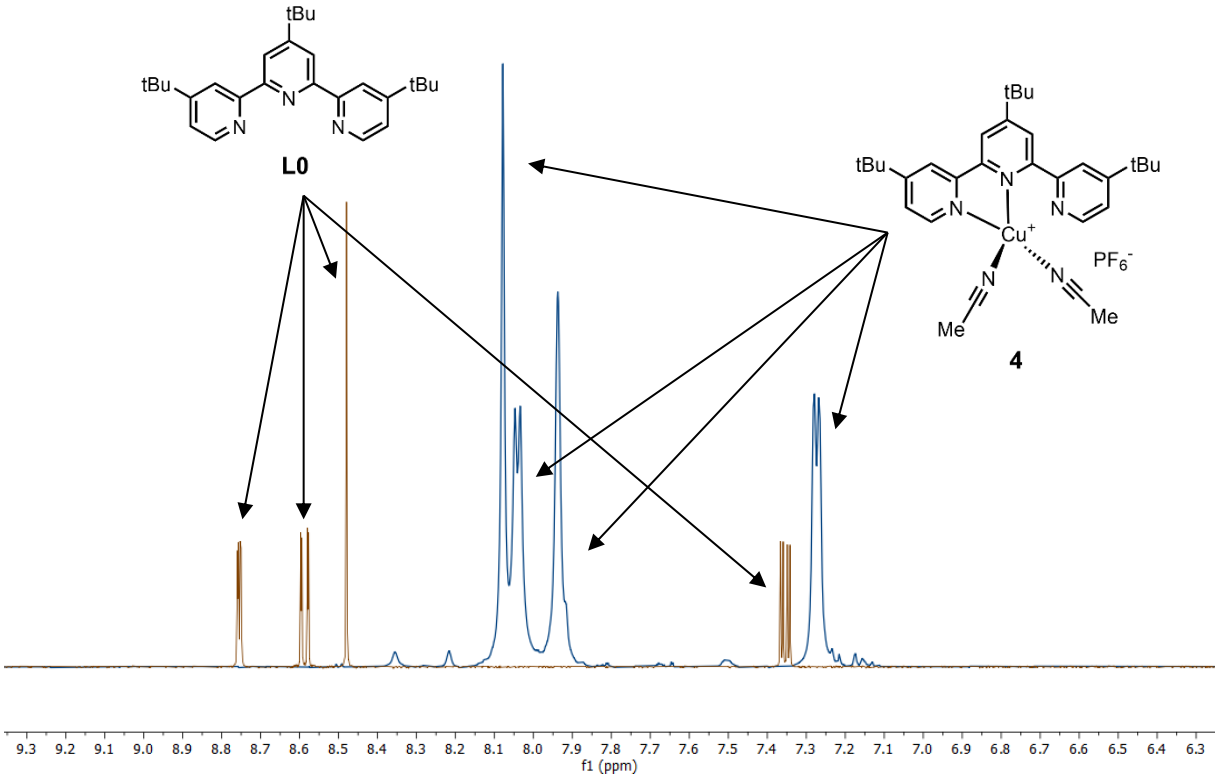

Figure 11: ^{1}H (300 MHz, CD_2Cl_2) NMR spectrum comparison between the ligand with and without Copper(I) salt.

Comparing both spectra, a change of the aromatic signal of the terpyridine is clearly visible. In general, a high-field-shift is visible, indicating a deshielding of the protons due to the distribution of the electron density towards the metal. This shift is around 0.8 ppm, at most. Additionally, a loss of the signals' multiplicity is visible. The signals at 8.75 ppm and 8.59 ppm shift to 8.08 ppm and 8.04 ppm respectively. Both change from two double-doublets to one singlet and one doublet as it can be seen in detail in Figure 12.

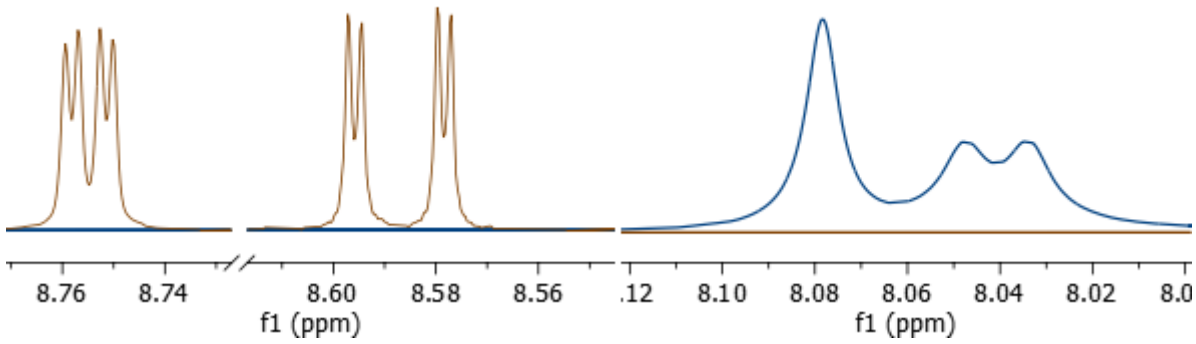

Figure 12: Detailed NMR spectra for the loss of multiplicity upon complexation of copper(I) with terpyridine.

According to reports in literature, the non-coordinated terpyridine occurs in a *trans*, *trans* geometry in solution to avoid repulsion of the nitrogen lone pairs.[214] With the introduction of a metal, the pyridine rings "turn" and slightly distort to afford the coordination of the metal.[220] Assuming that a tridentate coordination to the metal is not feasible, only two pyridine rings of the ligands should coordinate at a time. In solution, the system might be very dynamic, and the ligand will exchange the coordinating rings constantly, with the other two coordination sites occupied by acetonitrile. Such a dynamic system would result in the loss of multiplicity as it can be seen in the spectra. This equilibrium is illustrated in Scheme 35.

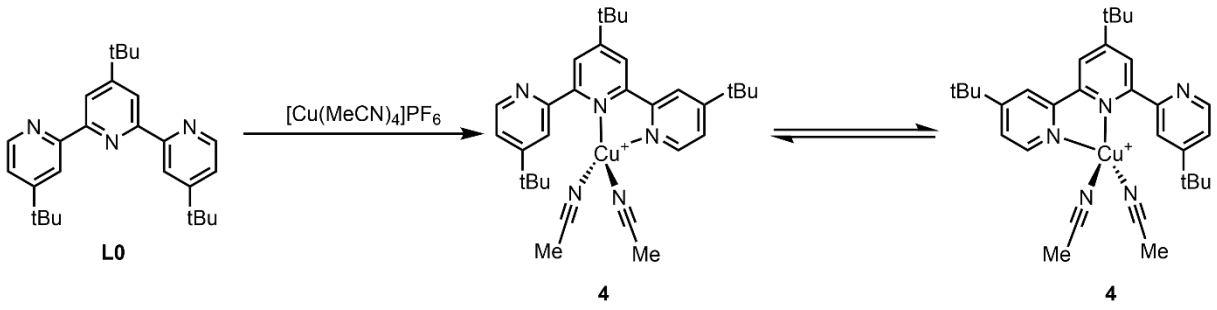

Scheme 35: Illustration of the coordination and change of geometry. The anion was omitted for clarity.

Due to dynamic nature of the coordination of the complex, we decided to investigate its behavior at lower temperatures. Lowering the temperature should slow down the exchange process, making it possible to distinguish between the different states if the exchange equilibrium occurs at lower rate than the NMR timescale. Hence, we

recorded spectra of the complex in deuterated acetonitrile between 297-237 K. The results are illustrated in Figure 13.

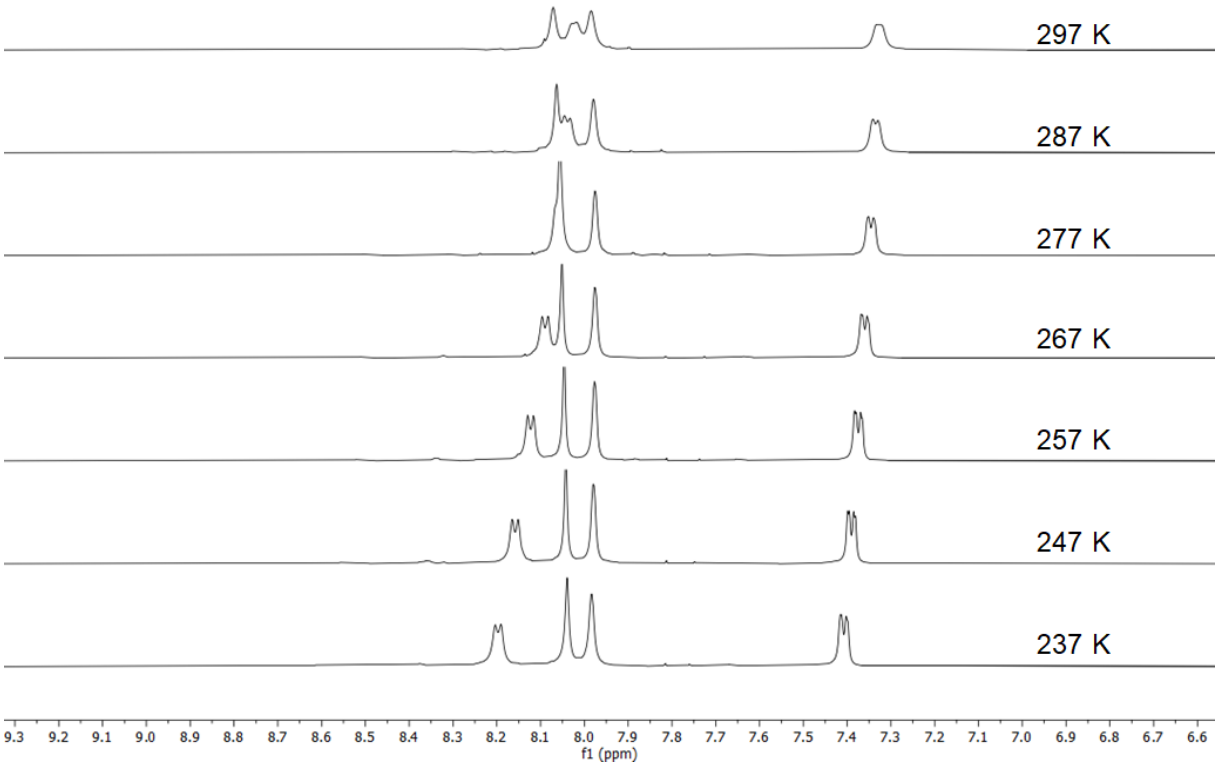

Figure 13: Low-Temperature Dynamic ^{1}H NMR (300 MHz, CD_3CN) Experiments.

In total, the temperature was lowered to around 237 K. Afterwards, the solvent started to solidify, making the measurement impossible. Interestingly, an immediate change is already visible at just 287 K. Both the signal at 8.00 ppm and 7.32 ppm shift slightly and show the recovery of multiplicity. This continues upon further lowering down the temperature to 237 K, at which the signals have shifted to 8.20 ppm and 7.40 ppm respectively. The spectra show a shift of all aromatic signals at lowered temperature, indicating a coordination of all three pyridine rings to the metal center. However, the loss of multiplicity implies a highly dynamic system, in which the coordination of the pyridine rings to the metal center is constantly changing. At lower temperature, the shift of the signals corresponding to the outer rings of the terpyridine suggest that these are subjected to the dynamic change. In contrast, the pyridine ring in the middle remains coordinated to the copper, as confirmed by the singlet at 8.10 ppm. Therefore, the

dynamic equilibrium is determined by the outer pyridine rings and their exchange of coordination with acetonitrile in solution.

Experiments with other solvents or solvent mixtures proved to be ineffective, as the complex degraded in the absence of acetonitrile. Based on this, we hypothesized, that the “free” pyridine ring could eventually engage in the activation of the substrates, acting as internal base towards cyclohexene and phenylacetylene. Therefore, we conducted NMR experiments with equivalent amounts of substrate added to the complex. The addition of *tert*-butyl hydroperoxide is separately discussed in the next chapter. The resulting NMR spectra of the addition of substrates are found below in Figure 14.

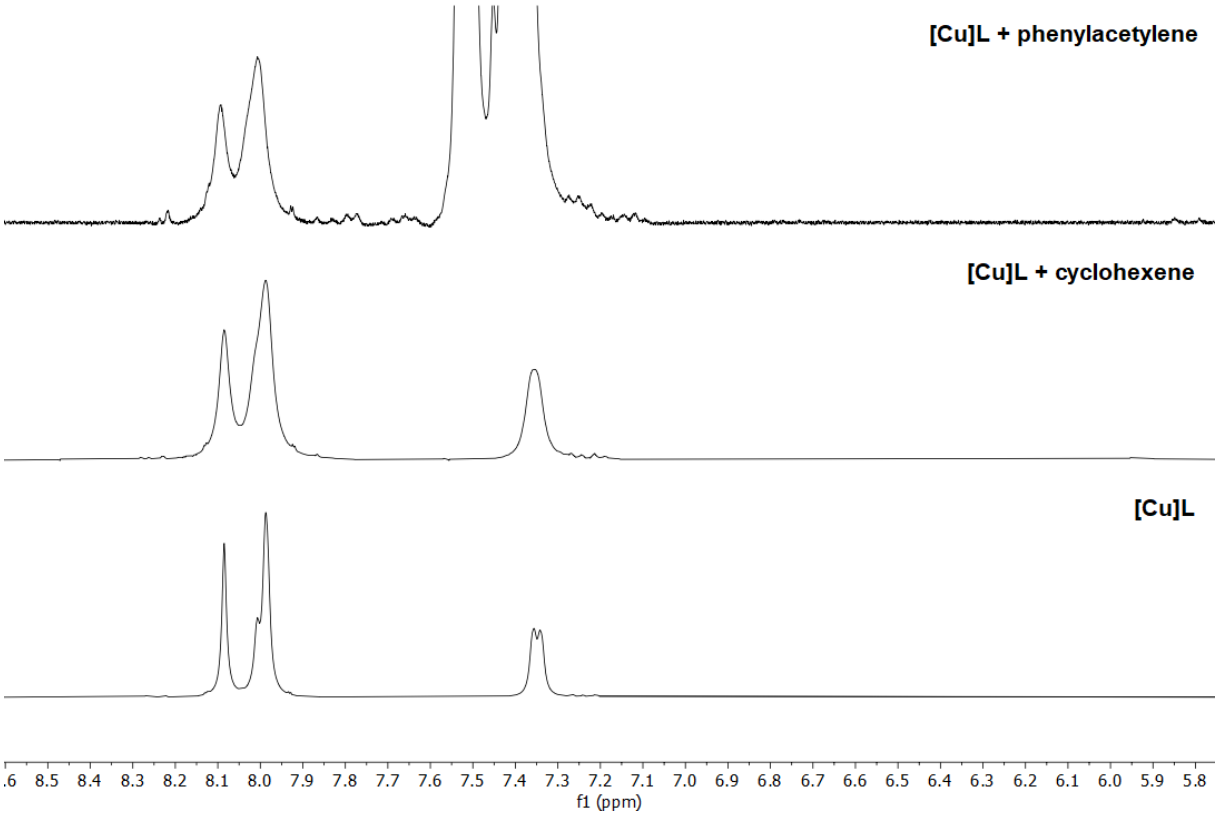

Figure 14: ^{1}H NMR (300 MHz, CD_3CN) spectrum for the addition of substrates to the copper-terpyridine complex. The complex is prepared from 0.1 mmol $[Cu(MeCN)_4]PF_6$ and 0.1 mmol terpyridine in 1 ml deuterated MeCN, Substrates are added as one equivalent to copper.

Interestingly, there is only a minor change upon the addition of the substrates. In both cases a general broadening of the signals is observable, which can be attributed to disturbance of the coordination equilibrium by the added substrates. Furthermore, the signals of phenylacetylene overlap the signal at 7.4 ppm, so the effect is not visible

there. However, during this experiment a change of the solution is visible, as a yellow precipitate is formed in the NMR tube. This clearly indicates that there is no direct interaction of the ligand with both substrates, and similarly, no change of the electronic environment around the copper (such as the coordination of a substrate) is occurring.

4.2. Interaction of the Copper(I)-Complex with the organic Peroxide

At first, we investigated the possible changes in the NMR spectrum of the complex upon reaction with the organic peroxide. Immediately after addition of TBHP to an acetonitrile solution of the Cu(I) complex, a drastic color change (from dark red to green) is visible. The resulting ^{1}H-NMR spectra shows the disappearance of the corresponding signals, and only the water impurity and the residual solvent peak remained visible. It is suspected, that the addition of the strongly oxidizing peroxide leads to the oxidation of the copper(I) to copper(II), which is paramagnetic, thus rendering the analysis by NMR unsuitable. To get more insight into the electronic situation of this new copper complex, we decided to investigate it via EPR spectroscopy. The resulting spectrum is shown in Figure 15. The strong EPR signal confirms the presence of unpaired electrons, probably resulting from the oxidation of copper(I) to copper(II). The signal is extremely complex, so a computer simulation of the spectrum was not successful.

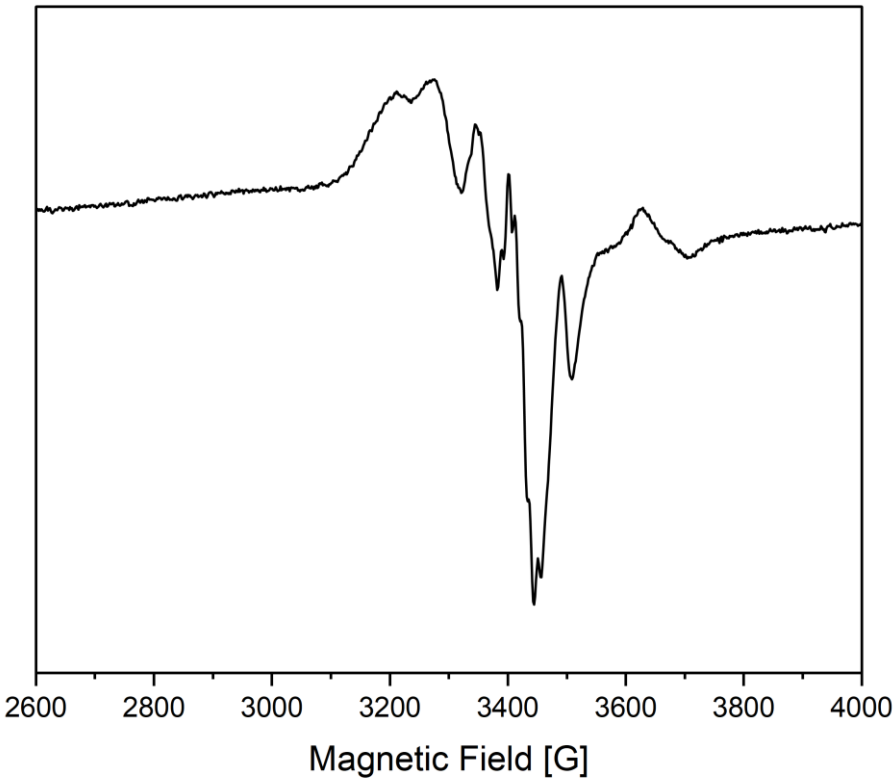

Figure 15: EPR Spectrum of the reaction product between the copper(I)-complex (0.05 mmol) and TBHP (1 mmol) in 1 ml MeCN under exclusion of atmospheric oxygen. Sample was transferred to a microcapillary tube (Hirschmann) to measure.

The interaction of organic peroxides with copper complexes has been amply discussed in literature. In a seminal work, Kharasch *et al.* showed the oxidation of allylic substrates with *tert*-Butyl perbenzoate and cuprous halides.[221] In further reports, they implied the homolytic cleavage of the peroxy-ester to yield two equivalents of the alkoxy-radical, and showed the formation of peroxy-radicals and methyl-radicals from the decomposition of the alkoxy-radical under varying conditions.[207, 222, 223] This makes the characterization of the intermediate species very complex. As Sawyer *et al.* showed, the interaction of copper with peroxides leads to a complex mixture of products, influenced by various factors such as ligand, solvent, and presence of oxygen.[219] The characterization of intermediary states and compounds is even more complicated, as the reaction between the peroxide and copper happens almost instantaneously.

Thus, the resulting spectrum for our compound might contain signals for a diverse variety of radical species. Based on the previously mentioned reports, it is plausible that

during the reaction of the copper complex with the peroxide, a mixture of alkoxy-, peroxy-, hydroxy- and methyl-radicals are forming, as reported by Klussmann *et al*.[59] and illustrated in Scheme 36.

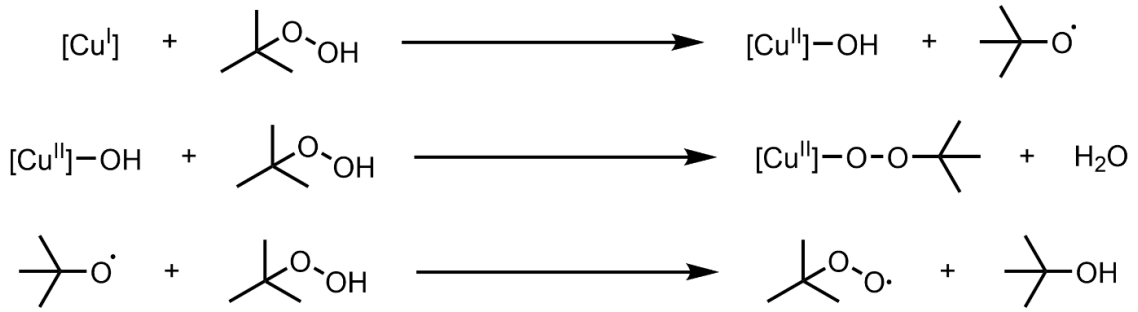

Scheme 36: Possible pathway for the generation of radicals upon reaction of Copper with TBHP.

In the first step, the hydroperoxide is homolytically cleaved to afford the copper(II) hydroxide complex and the alkoxy-radical. The copper(II) hydroxide complex can then react with another molecule of the hydroperoxide in a Haber-Weiss-type mechanism,[224] to afford the copper-peroxide complex and one equivalent of water. Simultaneously, the alkoxy-radical can undergo a Hydrogen Atom Transfer with unreacted hydroperoxide to afford the peroxy-radical.

However, at this point it is not clear which of the possible intermediate is involved in the allylic alkynylation reaction. Additionally, reports in literature also suggest the presence of Copper(III) in these reactions, which increases the complexity of the reaction even further.[225] In order to elucidate the nature of this complex, we decided to conduct radical trapping experiments. These experiments allow to make transient radicals visible on the EPR time scale by forming adducts with a substance like 5,5-dimethyl-1-pyrrolin-N-oxid (DMPO). The resulting spectrum is shown in Figure 16. By comparing literature reports,[226] we could confirm that the measured signals for our reaction agree with the presence of alkoxy and/or peroxy radicals in the mixture. Thus, it is most likely, that the degradation of the peroxide follows the same mechanisms as described above. At this point however, it is still not clear, if these radicals are promoting the coupling reactions or forming as a side product. Importantly, the formation of cyclohex-2-en-1-ol (**1B**), cyclohex-2-en-1-one (**1C**) and 3-(tert-butylperoxy)cyclohex-1-ene (**1A**) was observed under our tested reaction conditions. Assuming the reaction proceeds

via a HAT from the cyclohexene to an intermediate radical, the formation of the alkylperoxy-species of the cyclohexene as a radical recombination product is plausible. This peroxide is then degrading to the alcohol and ketone via a homolytic cleavage of the O-O bond. In contrast to that, Klussmann *et al.* reported such peroxides to be the crucial intermediate in the functionalization of tetrahydroisoquinolines.[59] Further investigations on this are conducted in the following chapter (*vide infra*).

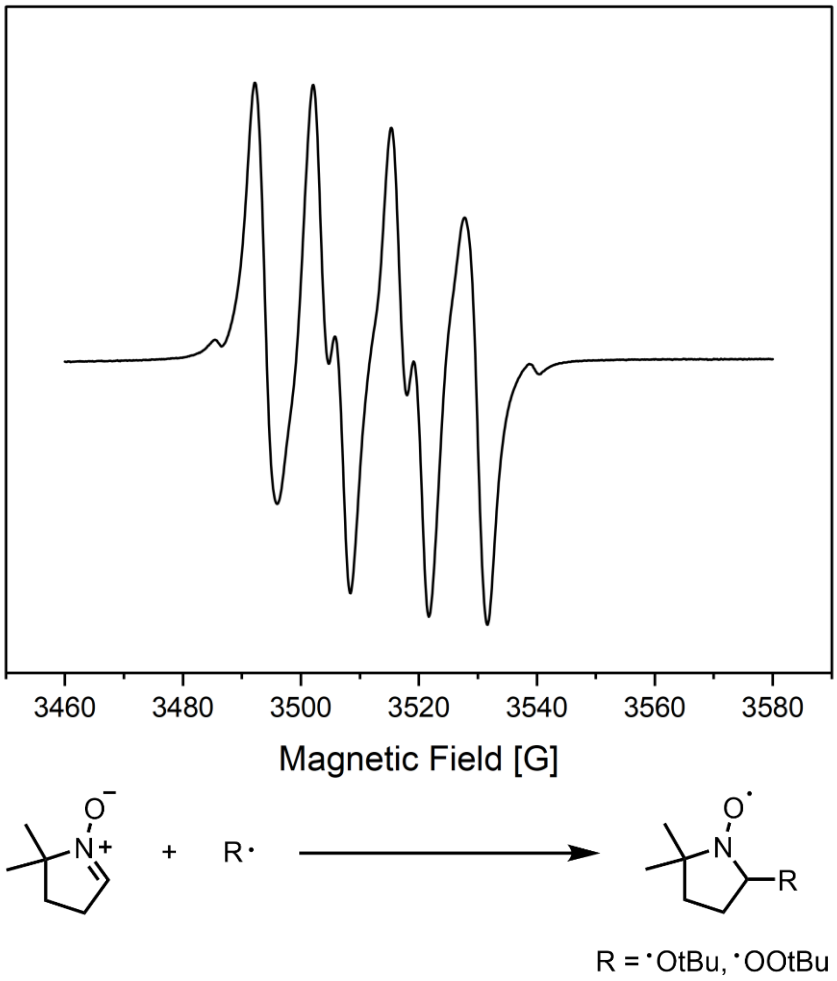

Figure 16: EPR spectrum for the DMPO Spin-Trapping Experiment and Spin Trapping Mechanism for Transient Radicals. 0.05 mmol of the complex in 1 ml MeCN were mixed with 1 mmol of TBHP and 10 µl of DMPO. The sample was then transferred to a microcapillary tube (Hirschmann) and measured.

Based on these results we could see the formation of a new copper(II) complex. However, structural characterization was not possible due to the complexity of the system. Nevertheless, radical trapping experiments showed the presence of peroxy- and alkoxy-radicals inside a solution of the catalyst and peroxide. From this we wondered,

if we could see any interaction of the substrates with this green complex in the EPR spectrum. Thus, further EPR studies were conducted by performing the same experiments as before but adding each of the reagents to the tube separately. The resulting spectra are presented in Figure 17.

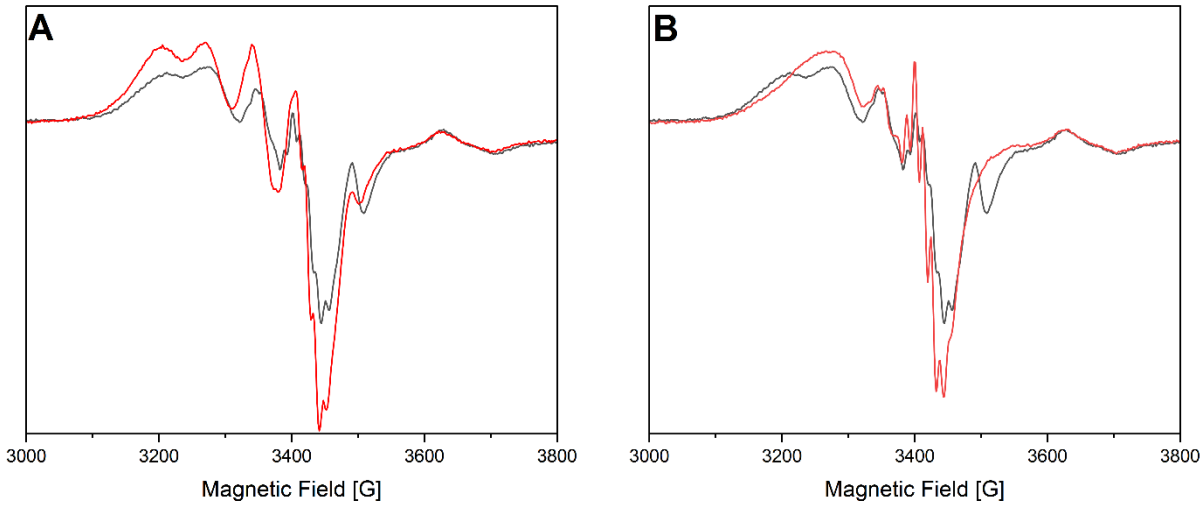

Figure 17: Comparison of the EPR signals of the copper(II) complex (0.05 mmol) alone (black) and upon addition of the substrates (red). Spectrum **A** for the addition of phenylacetylene (0.5 mmol), spectrum **B** for the addition of cyclohexene (0.5 mmol). Samples were taken and directly transferred to a microcapillary tube (Hirschmann) for measuring.

Some changes were observable in the EPR spectra upon mixing. Primarily, the addition of Cyclohexene (Figure 17 **B**) introduced a visible change into the spectrum compared to the spectrum of only the Copper(II) complex (Figure 15). In detail, a loss of the signal at 3500 G is visible. Similarly, the splitting of the signal of 3250 G to a bigger signal is observable, while the signal at 3400 G shows a higher complexity. As discussed before, simulations of these mixtures were not successful. However, literature suggests that a coordination of the olefin to the copper center is possible. This is especially reported for the copper catalyzed allylic amination.[227, 228] Also copper(I) complexes of cyclohexene are known in literature.[229] As the change of the EPR spectra imply a change in the structure of the paramagnetic species, this could indicate a coordination of the cyclohexene to the copper center. In contrast to that, the addition of phenylacetylene to the complex does not induce a change in the EPR spectrum (see Figure 17 **A**). Hence, the paramagnetic copper complex is more likely to form an adduct with cyclohexene than with phenylacetylene. This supports the hypothesis, that the

interaction of the copper complex with the cyclohexene is a crucial step in the catalytic cycle. The proposed intermediates are shown in Scheme 37. Itoh *et al*. showed the formation of a peroxo-complex with copper(II) and reported EPR spectra similar to ours.[230]

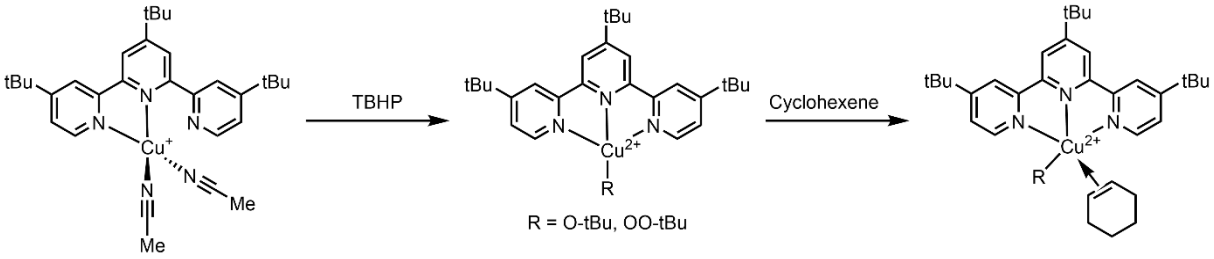

Scheme 37: Proposed formation of the reactive Copper(II)-Peroxide intermediate and subsequent coordination of cyclohexene.

Moreover, we investigated the changes on the EPR signal over time while irradiating the sample. The resulting spectra are presented in Figure 18. The measurement was conducted in a flat cell with a reactant ratio similar to the standard reaction setup. The cell was irradiated over the course of 30 min at 395 nm while a measurement was taken every minute.

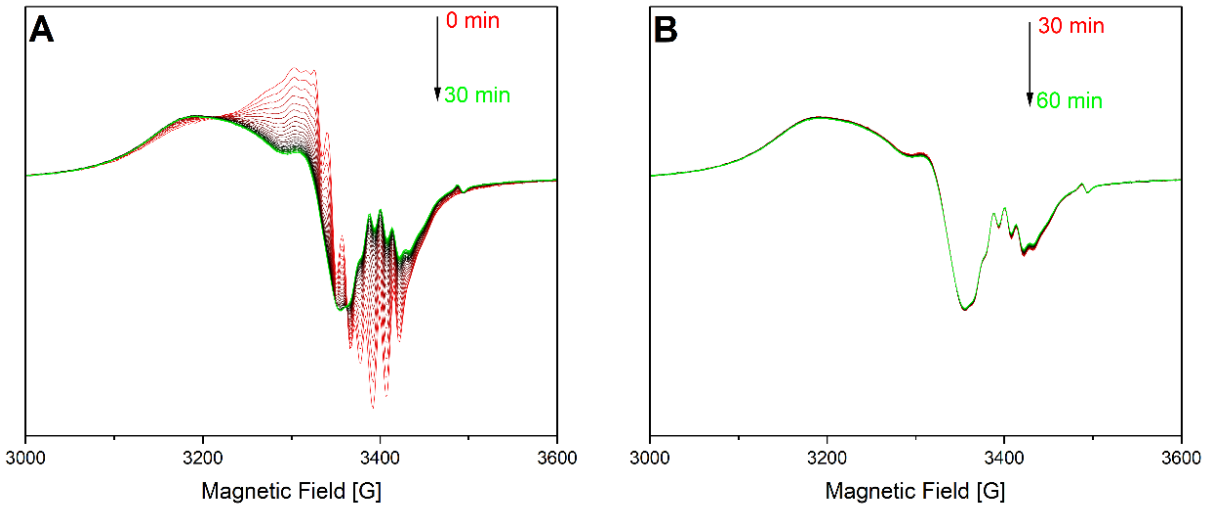

Figure 18: Time-resolved EPR of the irradiated (395 nm) Reaction. **A**: The light was turned on. **B**: The light was turned off. The reaction was conducted in a quartz flat-cell, flushed with argon by adding a sample from a solution of 0.1 mmol copper-complex, 0.1 mmolTBHP, 0.1 mmol cyclohexene and 0.1 mmol phenylacetylene in 1 ml of MeCN.

Afterwards, the light was switched off, and measurements were continued for 30 min. Interestingly, a quick change of the signal is visible during the irradiation, simulating our standard reaction conditions. The signal at 3400 G (Figure 18 **A**) shows an inversion and consequent decrease in intensity, implying a drastic change of the composition of the radical species in the mixture. Our efforts to characterize the species so far were not successful. However, it can be assumed, that the coordination environment of the copper changes. This also confirms that the complex is reactive under irradiation. When the light is switched off, no further change is observed in the signal, as it remains stable over the course of 30 min (Figure 18 **B**). In conclusion, the reaction of the hydroperoxide with copper(I) leads to its fast oxidation to produce an unknown copper(II) complex. It is assumed, that a copper(II)-peroxo or -alkoxy complex is forming. This complex is then able to coordinate cyclohexene to form a new reaction intermediate. When a mixture similar to the reaction conditions is irradiated at 395 nm, a change of the complex is observable, as attested by the change of the EPR spectrum. If the sample is then kept in the dark, no such change is observable, indicating a light-dependent reaction of the complex.

During the course of these experiments we were able to isolate a crystal which had suitable quality to be analyzed via X-Ray diffraction.* The resulting structure of the complex (**CR1**) is depicted in Figure 19. It consists of two atoms of copper(II), each coordinated to a terpyridine, and bridged by two peroxides. Interestingly, a difference in the bond lengths between one copper center and each peroxide is visible. One peroxide is bound to the copper center with a strong covalent interaction, while the other peroxide shows a weaker coordination through one non-bonding electron pair of the terminal oxygen. The sum formula of the compound **CR1** confirms the presence of two anions and two equivalents of acetonitrile per copper center, thus both have Cu(II) character. Interestingly, such complexes are only scarcely found in literature. Similar structural motifs are reported for copper-containing metalloenzymes involved in the activation of dioxygen.[231-234] Enzymes such as hemocyanin can reversibly bind dioxygen in the catalytic pocket and reduce it to water. Depending on the particular class of enzyme, either one, two or multiple copper centers interact with the oxygen to activate

* The compound was crystallized by Leo Gräber during partial fulfillment of his Master Thesis at the University of Rostock; April to August 2022.

it. Interestingly, the reported distances between the copper centers in those metalloenzymes are in a similar range to the distances found in **CR1**.[234]

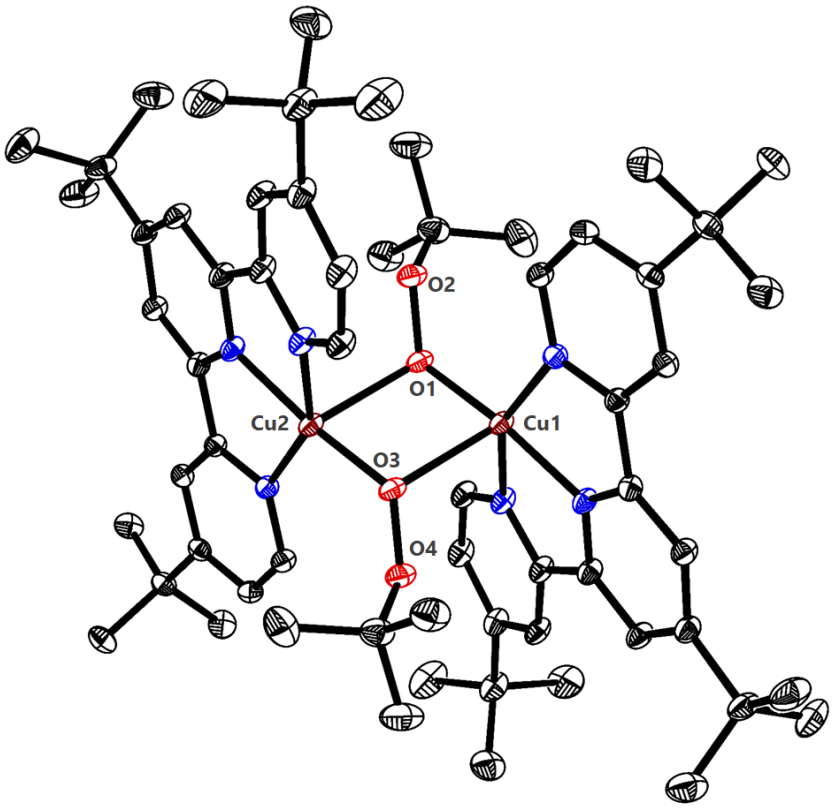

Bond	Distance in Å
Cu2 – O1	2.253(2)
Cu2 – O3	1.886(2)
Cu1 – O1	1.886(2)
Cu1 – O3	2.253(2)
Cu1 – Cu2	3.1019(7)

Figure 19: Single Crystal X-Ray Diffraction Crystal Structure of a Copper(II)-Peroxide complex **CR1**. Displacement ellipsoids correspond to a probability level of 30 %. Anions, H-atoms and co-crystallized solvents were omitted for clarity.

Besides the investigation of natural enzymes, also synthetic "analogues" of enzymes have been studied for the activation of dioxygen. These biomimetic or bioinspired complexes of copper give a deeper insight into the activation. Tolman *et al.* showed the activation of dioxygen with either monometallic or bimetallic copper complexes with the help of tridentate ligands.[235-237] Especially the bimetallic copper-complex bears resemblance to the structure **CR1**. Also, reports about halide-bridged copper-complexes with

similar structures to **CR1** can be found in literature.[238] In a similar fashion to the above mentioned compounds, Tolman *et al.* reported a η^2-peroxo bimetallic complexes with bond lengths comparable to those in complex **CR1**.[239] However, in their case, the peroxo-complex formed as a reaction product between a copper-dioxygen-complex and a phenol derivate. Thus, the structure of **CR1** is, to the best of our knowledge, the first reported peroxo-bridged, bimetallic copper(II) complex synthesized from copper(I) and a hydroperoxide. Currently, it is not clear, if this compound also forms in the catalytic cycle, or is an off-cycle species. It is likely that under reaction conditions such bimetallic complex is not forming due to coordination of acetonitrile.

Further trials to crystallize important intermediates were unsuccessful. However, in some cases the formation of blue-greenish crystals was observed, which could be identified as a homoleptic copper(II) terpyridine complex **CR3**. The crystal structure is shown in Figure 20.

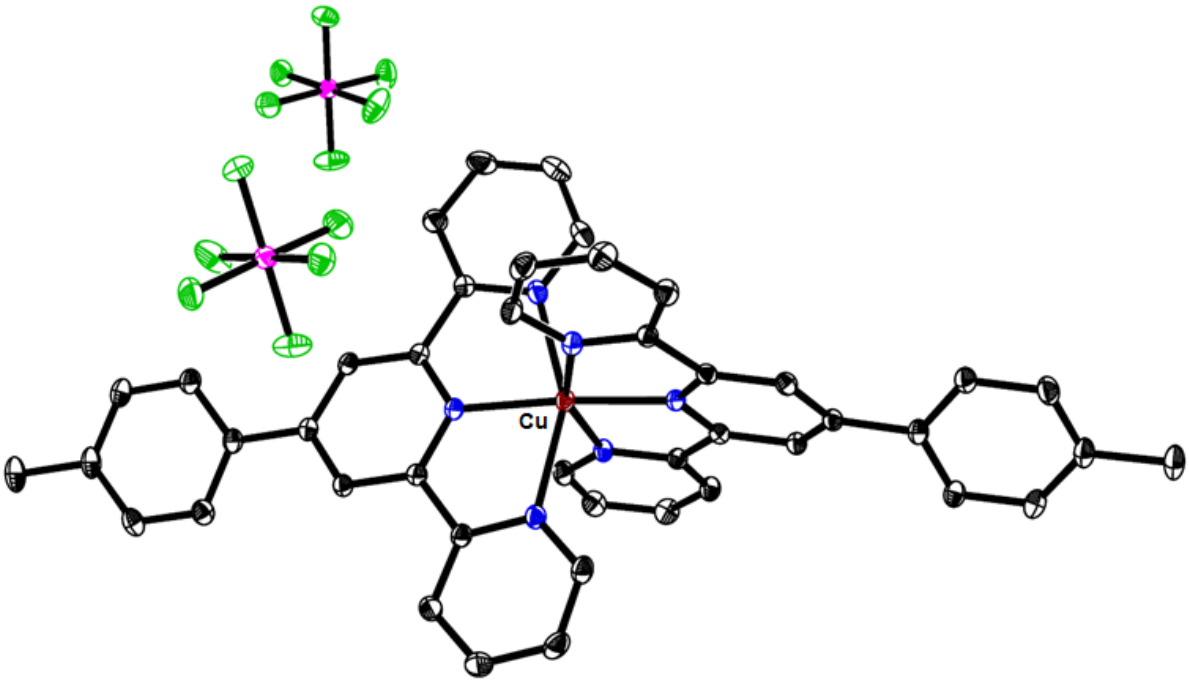

Figure 20: Single Crystal X-Ray Diffraction Crystal Structure Homoleptic complex of Copper(II) and 4-phenyl terpyridine **CR3**. Displacement ellipsoids correspond to a probability level of 30 %. H-atoms and co-crystallized solvents were omitted for clarity.

This complex is formed under reaction conditions if no substrate is present, or if the reaction is not activated. After the immediate oxidation of the copper(I) and possible intermediary formation of the bridged peroxo-complex, one copper center will be coordinated by two terpyridine centers, effectively rendering it unreactive due to the absence of available coordination sites. Therefore, this complex (**CR3**) is most likely a deactivation product of the catalyst.

Additionally, cyclovoltammetric (CV) measurements were conducted to investigate the redox properties of this complex.* The measurements are illustrated in Figure 21. The voltammogram of the copper complex **4** shows a sharp irreversible oxidation which can be assigned to the Cu(I)/Cu(II) redox couple with a voltage of -0.44 V. A second cycle reveals a less intense signal that is shifted to a lower voltage of -0.57 V which could result from passivation of the electrode or limitations in the diffusion. The inhibition of the reoxidation of copper(I)-terpyridine complexes to Cu(II) has also been discussed by Hetterscheid *et al.*, caused by a lack in electron-donating capabilities.[240]

* The measurements were made by Leo Gräber during partial fulfillment of his Master Thesis at the University of Rostock; April to August 2022.

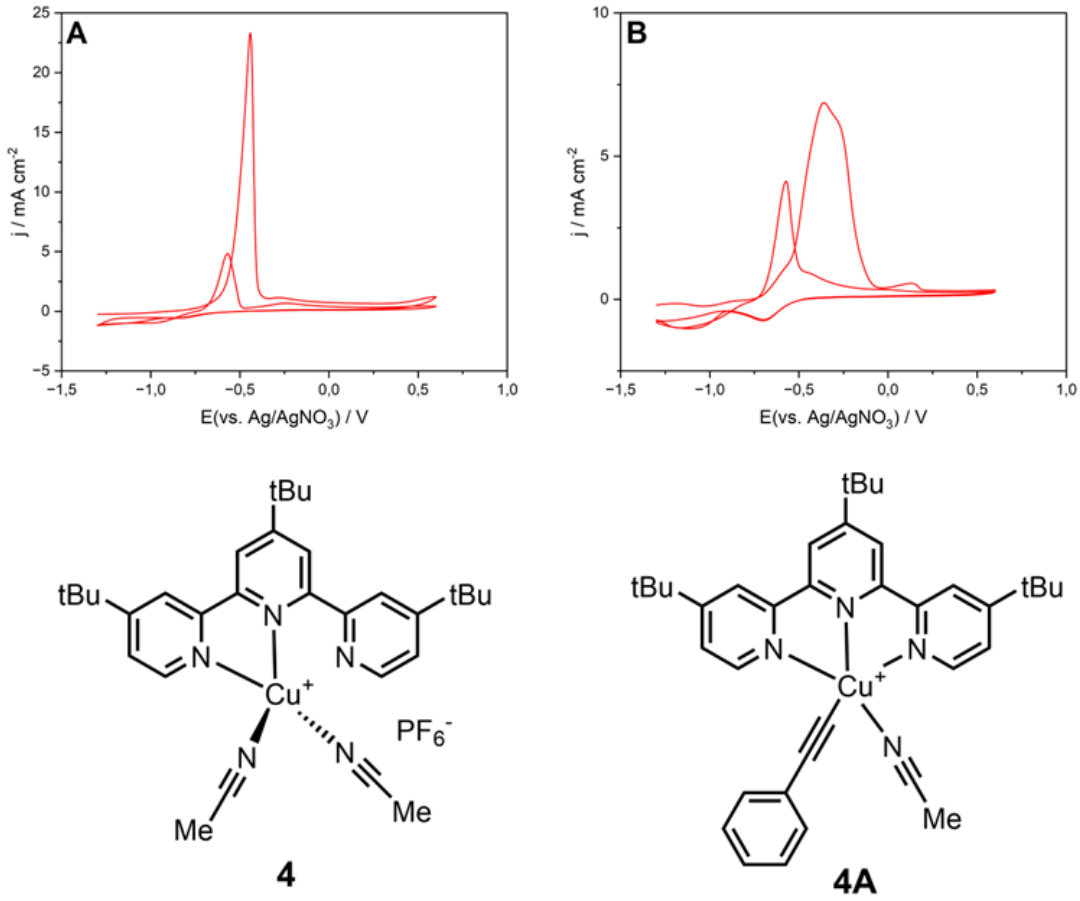

Figure 21: Voltammograms of two cycles between -1.3 V and 0.6 V measured with a scanning rate of 250 mV/s against $Ag/AgNO_3$ and structural suggestions. **A**: Cu(I)-Complex **4**. **B**: Cu(I)-Complex with equimolar Phenylacetylene **4A**.

Next, the redox behavior of the complex **4A** was investigated. After equimolar addition of phenylacetylene to the complex **4**, two oxidative cycles were conducted. A smaller oxidation peak with significantly smaller current density occurs at a slightly higher voltage of -0.36 V. This species could be associated with the copper-phenylacetylene complex **4A** in solution. When a second oxidative cycle is run, a smaller oxidation peak appears at -0.57 V. Interestingly, a small reduction peak at -0.72 V can be seen, which we were not able to attribute to any species. Certainly, it is not the full reduction of the acetylide species due to the significant lowered intensity compared to the oxidation. During the measurement a bright yellow precipitate formed, that could be identified as copper-phenylacetylide. It is possible, that the formation of small quantities of this phenylacetylides cause the reduction signal.

Furthermore, the redox properties of the proposed copper-peroxide complex **4B** were investigated. For this, equal amounts of the catalyst **4** and TBHP were mixed in acetonitrile (Scheme 38).

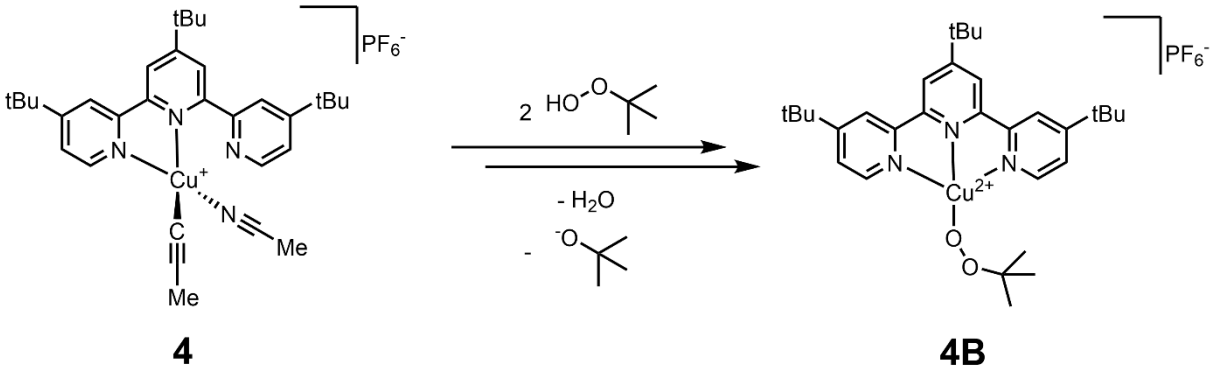

4 **4B**

Scheme 38: Generation of an intermediary copper-peroxide complex.

The results are presented in Figure 22. A different shape of the signal is visible, indicating the formation of another complex. Figure 22**A** and Figure 22**B** show the application of a reductive current to the complex. They reveal an irreversible reduction between -0.4 V and -1.1 V. The signal at around -0.4 V can be attributed to the Cu(I)/Cu(II) redox couple. Smaller saddle points and the broad shoulder suggest the reduction of several other species in this voltage range. Likely, these occur after complete decomposition of the copper-peroxide complex **4B**. Due to the lability of the peroxide, the decomposition of it might initiate various follow-up reactions recorded here. The shoulder at -0.85 V could be related to the oxidation of superoxide into molecular oxygen.[241] In reference to the previously mentioned EPR Spectra, the formation of such a species is likely, and can occur under the reaction conditions. However, the explicit assignment of this signal to a certain oxidation event is difficult due to the overlapping of various signals. Furthermore, oxidative currents were applied to the mixture of TBHP and copper-complex **4**. Firstly, the current was applied between 0 and 1.0 V and the resulting spectra are represented in Figure 22**C** and Figure 22**D**. Interestingly, two clear irreversible oxidation peaks are visible, suggesting a two-step oxidation of the complex. This could be attributed to the oxidation of the copper to a very reactive copper(III). However, the presence of copper(III) in such systems is highly debated.[242,

[243]. It is more likely that the terpyridine ligand undergoes oxidation to form a radical cation, as this has also been reported in literature.[177, 244] Hence, the terpyridine might interact in the reaction as a so-called “non-innocent” ligand, as its redox properties may assist or facilitate the reaction. This hypothesis is also supported by the extraordinary sensitivity of the reaction towards the ligand. A redox-active ligand would also explain unusual oxidation states, which are not realizable by the metal center alone. Further, metal-terpyridine complexes are known for their capabilities to enable electron transfer processes.[245]

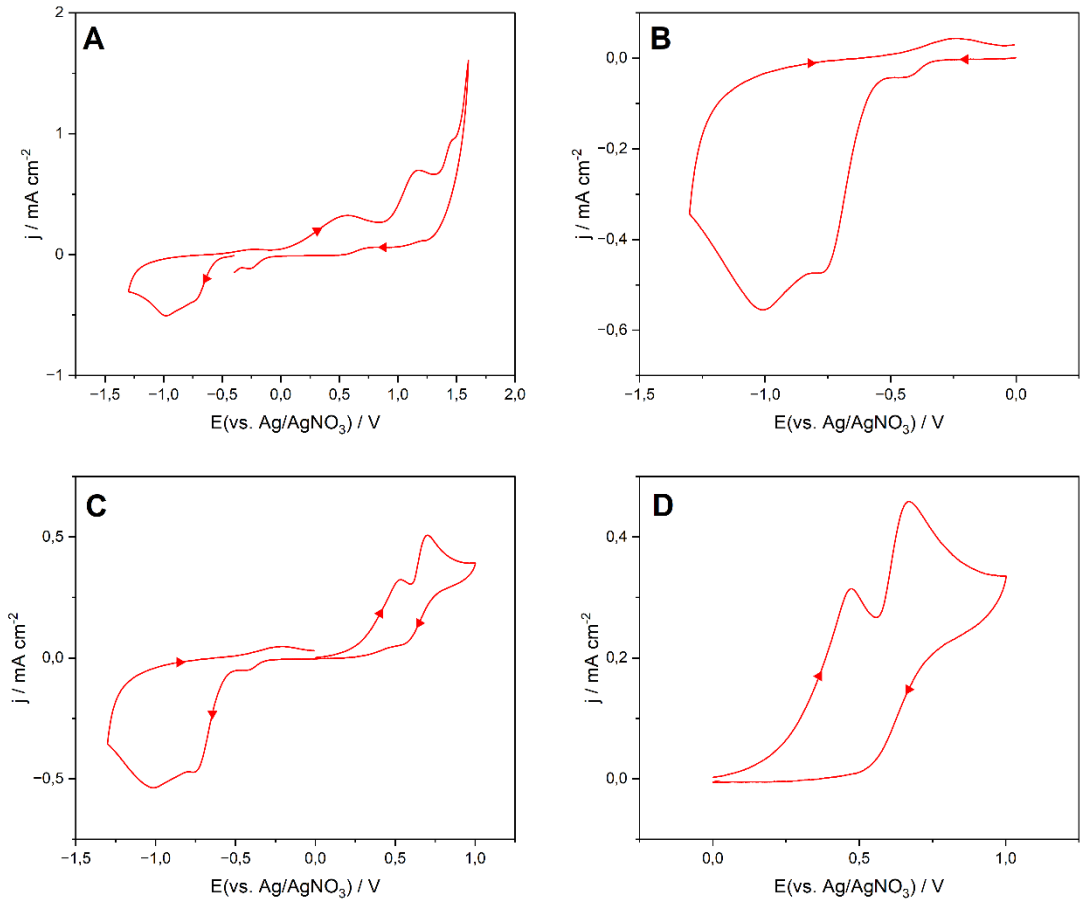

Figure 22: Voltammograms of a Copper-Terpyridine Complex with TBHP in MeCN measured with a scanning rate of 100 mV/s against $Ag/AgNO_3$ starting with the reductive current (A and B) and with oxidative current (C and D)

Having a closer look at the oxidation steps, a relatively low voltage of 0.47 V and 0.67 V for each step is detected. Thus, the oxidation of the complex occurs relatively easy

and, in this case, does not require strong oxidizing agents. Interestingly, when the reduction is performed first a consequent oxidation of the complex is not possible and the oxidation peaks reported above do not appear. In contrast to this, when the oxidation is performed first, the broad reduction shoulder is detected again. This indicates the decomposition of the complex **4B** upon reduction as mentioned before. The peroxide will easily undergo reduction to form more stable species. Furthermore, this suggests, that the oxidation peaks shown in Figure 22**C** and Figure 22**D** can be attributed to the whole complex and not only one component.

4.3. Perturbation of Reaction Conditions and Radical Trapping Experiments

While the spectroscopic investigations gave rise to a better understanding of the initial activation, the concomitant reaction pathway(s) and its mechanism remained unclear. In this section, we investigated the reaction product between the copper-complex and the peroxide as well as the influence of the perturbations to the standard reaction conditions. Lastly, we aimed at clarifying the role of the phenylacetylene in the reaction.

The investigation of radical species is not straightforward, as their lifetimes tend to be rather short. Due to their inherent reactivity, the trapping of such radicals by appropriate scavengers is a feasible strategy to detect this short-lived species. Well-known examples for radical trapping agents are (2,2,6,6-tetramethylpiperidin-1-yl)oxyl (TEMPO), butylated hydroxytoluene (BHT), styrene and ascorbic acid. Thus, we decided to add these compounds to our standard reaction conditions. The results are displayed in Table 11.

Table 11: Addition of Radical Trapping Reagents to Standard Reaction Conditions.*

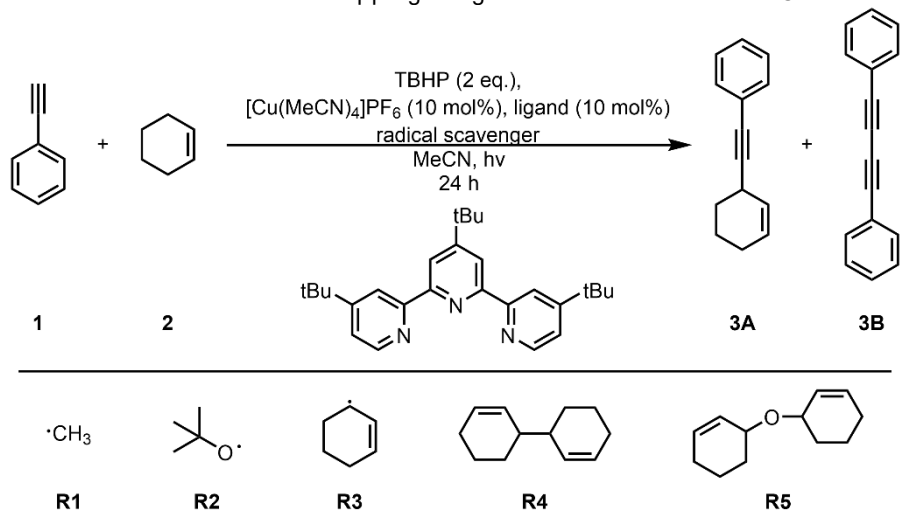

Entry	Radical Trapping agent	Yield of 3A[a]	Observation
1	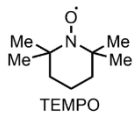 TEMPO	54 %	**R1**
2	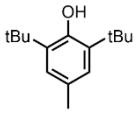 BHT	1 %	**R1**, **R2**, **R3**
3	 Styrene	94 %	no side-products observed
4	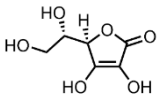 ascorbic acid	< 1 %	**R4** and **R5**

Standard Reaction Conditions: 10 mmol Cyclohexene, 0.5 mmol Phenylacetylene, 1 mmol *tert*-Butyl Hydroperoxide solution (5-6 M in decane), 0.05 mmol $[Cu(MeCN)_4]PF_6$, 0.05 mmol 4,4′,4″-Tri-tert-butyl-2,2′:6′,2″-terpyridine, 1 ml MeCN, 1 mmol of radical trapping agent, 390 nm, 24 h, 30 °C.
[a] The Yield was determined via GC-MS.

Interestingly, different results were obtained from the various trapping agents. The addition of TEMPO to the reaction lead to a noticeable decrease in the yield of the coupling product **3A**. Furthermore, the analysis of the reaction mixture showed the formation of a TEMPO-methyl adduct (see Appendix). This indicates the formation of methyl-radicals (**R1**) in solution. However, no other intermediates were observed. The

* The reactions with BHT, Styrene and Ascorbic Acid were conducted by Leo Gräber during partial fulfillment of his Master Thesis at the University of Rostock; April to August 2022.

cleavage of a methyl-radical from an organic peroxide such as TBHP or DTBP is well known to literature.[207] Hence, it is to no surprise, that such radicals can be trapped. The addition of BHT however, showed a broader scope of possibly transient radical species in solution. BHT is very well known as radical inhibitor and was used in many commercial products.[246] Employed in the reaction, adducts of methyl (**R1**), and tert-butyloxy radicals (**R2**) could be detected. Especially, the formation of alkoxy radicals supports the proposed degradation mechanism of the peroxide during the initial activation. Nevertheless, the presence of peroxyl radical was not detected. To our surprise, also the adduct of cyclohexene (**R3**) and BHT was detected. This implies the presence cyclohexene radicals during the reaction. We decided to investigate the effect of BHT on the reaction more closely, by conducting experiments in different concentrations and adding the radical trap at different reaction times. The results are depicted in Table 12.

Table 12: Addition of BHT to the standard reaction at different points and in different concentrations.

Entry	Equivalents of BHT to phenylacetylene	Yield of 3A[a]	Time of Addition
1	1	44 %	after peroxide
2	1	14 %	before peroxide
3	0.1	97 %	after peroxide
4	0.1	94 %	before peroxide

Standard Reaction Conditions: 10 mmol Cyclohexene, 0.5 mmol Phenylacetylene, 1 mmol *tert*-Butyl Hydroperoxide solution (5-6 M in decane), 0.05 mmol $[Cu(MeCN)_4]PF_6$, 0.05 mmol 4,4′,4″-Tri-tert-butyl-2,2′:6′,2″-terpyridine, 1 ml MeCN, 390 nm, 24 h.
[a] The Yield was determined via GC-MS.

Comparing Entry 1 and 2, a significant change can be detected in the yield of the desired product depending on the point in time the BHT was added to reaction. When BHT is added after addition of peroxide, still a yield of 44 % could be achieved. This implies that only one equivalent of the peroxide was quenched, while the other half is still able to facilitate the reaction. However, when the BHT is added before the peroxide the yield drops significantly, effectively hindering the reaction. Thus again, the results

indicate, that the crucial point of the reaction is the formation of a catalytic species between the copper and peroxide. If the amount of radical inhibitor is lowered to only 0.1 equivalents compared to phenylacetylene, no such significant change is observed. This also shows that the reaction is relatively robust towards small amounts of the radical inhibitor. In regard to the employed styrene, no influence on the reaction and no additional radical coupling products were observed. The addition of ascorbic acid however, led to a strong inhibition of the reaction. Ascorbic acid is a natural antioxidant, occurring in many living beings to protect the organism from oxidation through free radicals.[247] Interestingly, the analysis of the reaction mixture shows the formation of cyclohexene radical coupling products (see Appendix) such as the homocoupling of two cyclohexenes (**R4**) as well as a di-cyclohexene ether (**R5**). This shows the degradation of the oxidant in solution by the ascorbic acid. Nevertheless, the formation of radical species is still possible and leads to different cyclohexene coupling products. The results of these experiments might also indicate that the formation of a radical is not crucial as mentioned also in previous chapters. Thus, the peroxide acts more as a sacrificial oxidant rather than a radical starter.

As the system and the underlying mechanism have been, so far, too complex to analyze via conventional methods, we decided to simplify the substrates. One such simplifications was motivated by the findings of Klussmann *et al.*[59] They proposed the formation of a peroxy-ether on the substrate, that consequently undergoes a nucleophilic substitution to afford the desired products. While we observed similar peroxy-ether of cyclohexene (*vide supra*), the isolation of such intermediates was extremely difficult and dangerous due to the inherent reactivity of peroxides. We therefore decided to introduce a cyclohexene with a good leaving group like a bromide. The result when conducting the experiment with 3-bromocyclohexene is depicted in Table 13. No reaction is observed in absence of the peroxide, neither in the dark, nor under irradiation. However, in presence of the peroxide under irradiation, trace amounts of various coupling products were observed: the desired product **3A**, the glaser-product **3B** and one coupling product with the bromide **P1** still intact. From these results, insights of the mechanism can be obtained. First of all, the presence of the peroxide is absolutely necessary for the reaction to proceed. In absence of the TBHP, no reaction is observed, even when the substrates contain a good leaving group. When the peroxide is added, no regioselectivity is observed. Hence, the reaction does not proceed via

nucleophilic substitution at the cyclohexene. It is therefore unlikely, that our reaction follows a similar pathway to the reaction reported by Klussmann *et al.*

Table 13: Test Experiments for nucleophilic Substitutions *

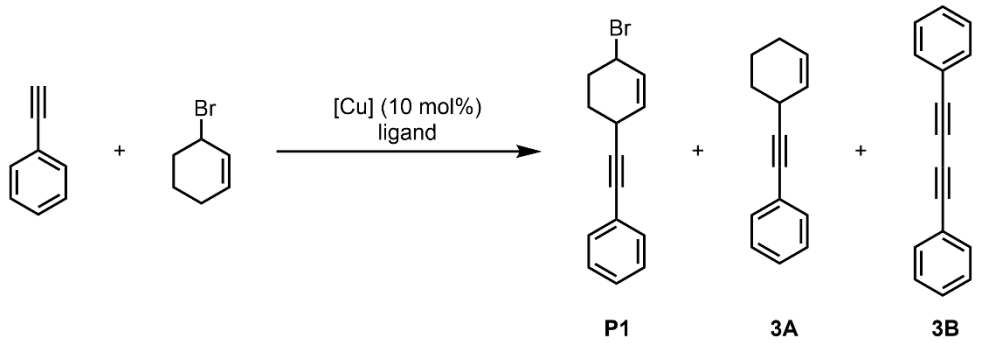

Entry	Remarks	Result
1	no peroxide, hv 390 nm, r.T., 24 h	no reaction
2	no peroxide, dark, r.T., 24 h	no reaction
3	2 eq. TBHP, hv 390 nm, r.T., 24 h	mixture of **P1**, **3A** and **3B**

Standard Reaction Conditions: 10 mmol 3-Bromocyclohexene, 0.5 mmol Phenylacetylene, 1 mmol *tert*-Butyl Hydroperoxide solution (5-6 M in decane), 0.05 mmol $[Cu(MeCN)_4]PF_6$, 0.05 mmol 4,4′,4″-Tri-tert-butyl-2,2′:6′,2″-terpyridine, 1 ml MeCN, 390 nm, 24 h. The Yield was determined via GC-MS.

Lastly, we were interested in investigating the activation of the phenylacetylene. The most important side reaction is the homocoupling of the phenylacetylene, also called the Glaser coupling.[98, 99] While the mechanism of this coupling is not clear yet,[125] all accepted proposals suggest the formation of a copper-phenylacetylide intermediate. This yellow organometallic compound can easily be isolated in a reaction between copper(I) salts and phenylacetylene. As we have observed the formation of Glaser products in the reaction, as well as a yellow precipitate, we proposed the formation of such as phenylacetylide intermediate under our reaction conditions. To assess if this compound is an intermediate of the desired product, we decided to add it directly to the reaction mixture. First, the synthesized copper phenylacetylide **1D** was used as a replacement of the phenylacetylene as can be seen in Scheme 39.

* The final investigations of this subchapter were conducted by Leo Gräber during partial fulfillment of his Master Thesis at the University of Rostock; April to August 2022.

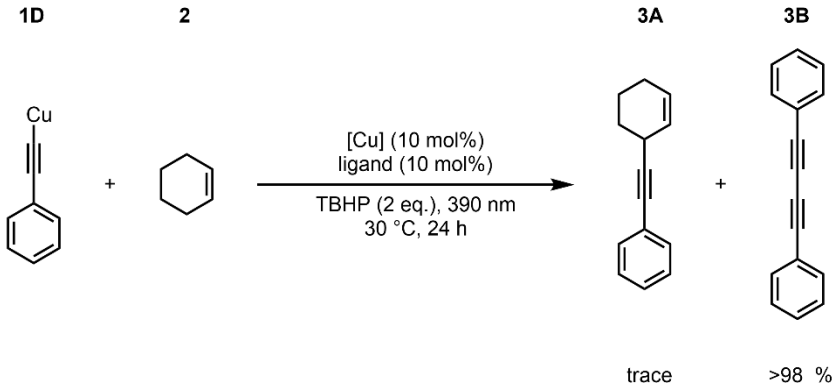

Scheme 39: Standard reaction with Copper-Phenylacetylide as alkyne source. Yields are determined via GC.

The synthesized acetylide **1D** was used in the same quantities as the phenylacetylene, while other conditions were kept according to the standard reaction conditions. As a result, the major coupling product of the reaction is the homo-coupling of the acetylenes **3B**. Only trace amounts of the desired product **3A** have been observed. It is reasonable to assume, that the high concentration of acetylide suppresses the allylic alkynylation.

A similar result to the previous reaction was observed by replacing the copper(I) precursor by the copper acetylide **1D** (Scheme 40). Again, the major product formed is the homo-coupling. In contrast to the previous reaction, the alkynylation product was obtained in 10 %.

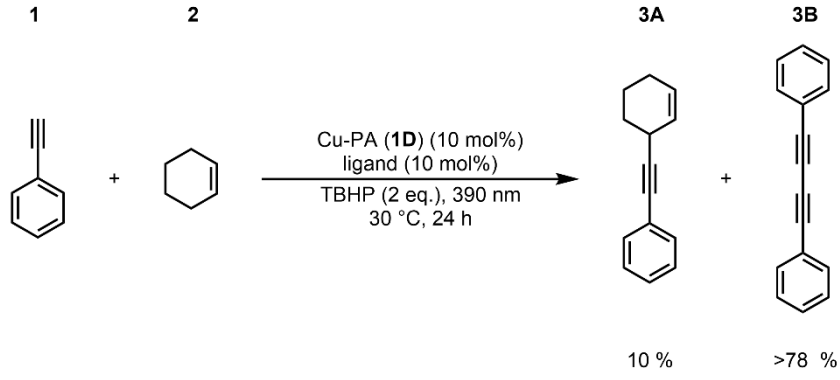

Scheme 40: Standard Reaction with Copper-Phenylacetylide as catalyst precursor. Yields are determined via GC.

Similar to the reported Glaser mechanisms, a bimetallic pathway could be necessary to furnish the desired product.[112, 248] Yet, this type of bimetallic mechanism could not be confirmed for this reaction. In regard to the formation of the acetylide, literature also reports the use of copper-acetylides as photocatalysts or photoinitiators.[249-251]. So far, there has been little to no evidence for the formation of an intermediate complex incorporating this moiety. Therefore, future investigations should be focused on these intermediates.

4.4. Kinetic Investigations

For the kinetic profiling of the photocatalyzed allylic alkynylation we followed both, the consumption of phenylacetylene, and formation of our desired product. The recorded concentration profiles for the reactions under irradiation at 370 nm, and 440 nm are shown in Figure 23.

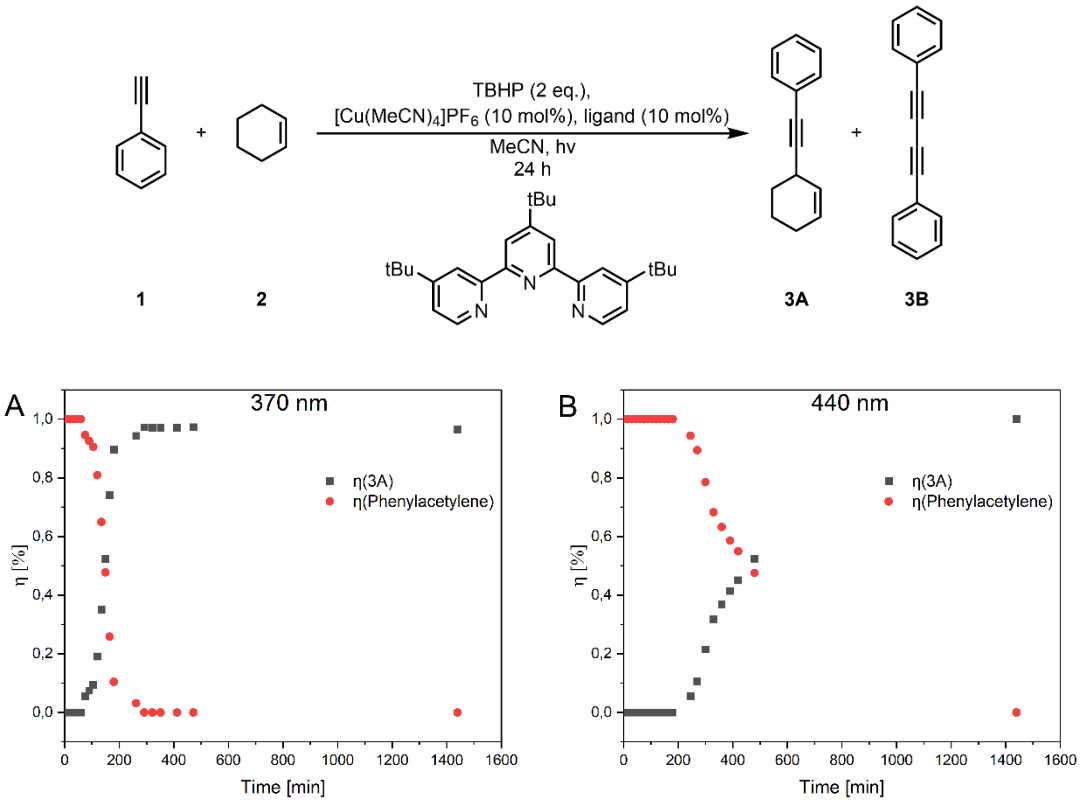

Figure 23: Kinetic Measurements and Graphical Representation for the Reaction under Standard Conditions irradiated at 370 nm (**A**) and 440 nm (**B**) at 25 °C.

Interestingly, two different profiles for the different wavelengths can be observed. In both cases, an induction period is visible, and seems to be dependent on the wavelength, as the reaction at 370 nm starts showing changes at around 60 min, while the reaction at 440 nm starts at around 200 min. The reaction at 440 nm proceeds slower and only reaches about 50 % conversion after 8 h, while reaction at 370 nm reaches nearly full conversion at around 5 h. After 24 h, both reactions show a quantitative conversion. This demonstrates the dependency of the reaction time on the wavelength of the light. The catalytic system likely has a higher absorption at the lower wavelength of 370 nm (see Appendix). Furthermore, the presence of this induction period is interesting considering the mechanism, indicating either the reaction of the pre-catalyst to a catalytically active species or the formation of an intermediate. This suggests that the reaction is not photocatalyzed but photoinitiated. The complexity of these kinetics was confirmed, as common models could not be fitted to the data.

4.5. Proposed Reaction Mechanism

In the previous chapter, different aspects of the underlying mechanism of the light-induced copper-catalyzed allylic alkynylation were discussed. The reaction system proved to be very complex and showed a high variety of possible reaction intermediates. Analysis of the reaction proved to be very extensive as the reaction was either very difficult to analyze, or the rapid formation of various reactive species precluded the use of traditional analytical methods. In total, we were able to define some initial steps of the reaction, and show that this system has a novel reactivity not yet reported in literature. Considering every result from the past three chapters, we were able to propose a new mechanistic scheme which is presented in Scheme 41.

In our experiments, the ligand proved to be irreplaceable to the reaction, allowing a very dynamic interaction in solution with the copper center, exposing a vacant coordination side for the incoming substrate, and leaving an uncoordinated pyridine ring hanging in the proximity of the metal. Upon reaction of the Cu(I) precatalyst **I** with TBHP, the dark red solution turns into a bright green. While the interaction and reactions of copper salts with peroxides are widely discussed in literature, there is no consensus of the exact pathways the reaction takes. Ultimately, the reaction proceeds

nearly instantaneous upon addition of the peroxide and renders its spectroscopic analysis difficult. We propose an initial acid-base interaction of the free pyridine ring at the ligand with the hydroperoxide. Then, the resulting peroxyl-anion coordinates to the copper, where it quickly oxidizes it upon homolytic cleavage of the oxygen-oxygen bond (**II**). Consequently, a *tert*-butoxide radical is expelled from the complex and copper-hydroxide-complex **III** is formed. Eventually, this complex is able to form the dimeric copper-peroxide complex **IV** mentioned previously. The monomeric complex also forms under incorporation of another molecule of TBHP and subsequent elimination of water. Based on our findings from EPR measurements and radical trapping, the formation of complex **V** is also possible. Henceforth, the peroxyl-complex is coordinated by a cyclohexene in a η^2-manner. Such formation of a complex was assumed due to the change in the EPR signal previously. In the following step, complex **VI** then activates the allylic proton of the cyclohexene assisted by either heating or irradiation of the reaction.

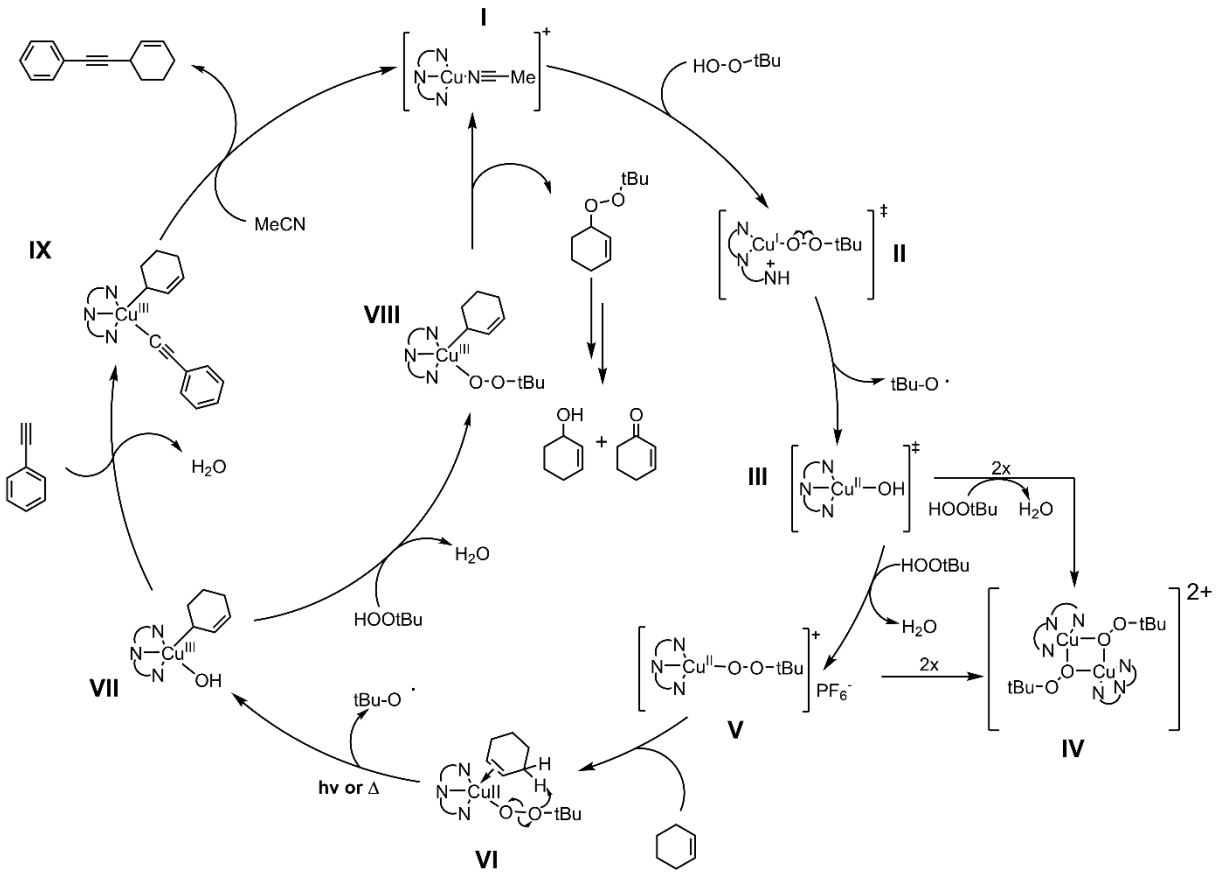

Scheme 41: New mechanistic proposal for the copper-catalyzed allylic alkynylation.

Under elimination of *tert*-butanol an organo-copper(III) complex (**VII**) shall be formed. Nevertheless, the existence of such species in copper-catalyzed carbon-carbon coupling is highly discussed.[242, 243] Certainly, the activation of the phenylacetylene in a similar fashion to the Glaser-Hay coupling seems unlikely, as the previous experiments showed no direct coupling from the phenylacetylide to the desired product. This indicates another mode of activation for the acetylenic proton. It is reasonable to assume, that the ligand and its capability to act as internal base might allow this activation. Ultimately, the exact nature of this intermediary species in our reaction is unknown. Alternatively, the cyclohexene complex **VII** can react with the acetylene via an acid-base-reaction with the hydroxide ligand, forming the copper(III) phenylacetylide **IX**. The reaction is then concluded via a reductive elimination to yield the coupling product and regenerating the copper(I) complex **I**, closing the catalytic cycle.

The cycle can be interrupted by side reactions between the active copper complexes and the cyclohexene as depicted in Scheme 42. The alkoxide radicals **X** can interact with unreacted TBHP to form peroxy radicals **XI**. Simultaneously, alkoxide radicals **X** can also abstract the allylic proton on the cylcohexene. Ultimately, the radicals will be terminated in radical quenching reactions to yield the cyclohexene peroxyether **XIII** and the homocoupling of the cyclohexene **XIV**. Interestingly, the coupled alkoxide **XV** is not observed, indicating that the alkoxy radical is consumed faster than the cyclohexene radical is formed.

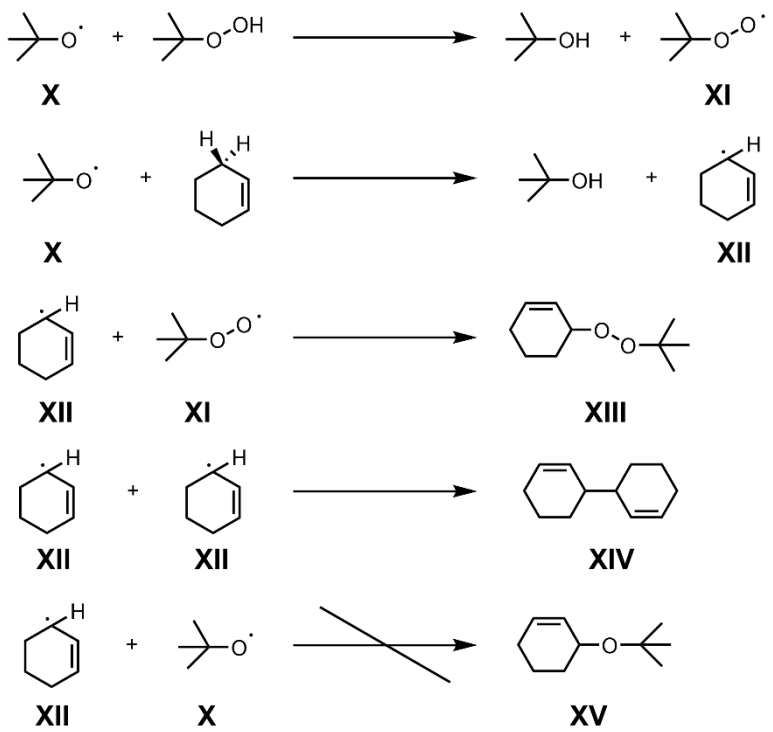

Scheme 42: Formation of cyclohexene-byproducts as off-cycle products.

The peroxyether species **XIII** however, decomposes under the reaction conditions to yield the observed cyclohexene alcohol and ketone. This pathway therefore presents no productive reaction to yield the desired product.

4.6. Summary

- The mechanistic hypothesis published by Mejía and co-workers was disproven and a new mechanism was proposed, including dedicated spectroscopic and experimental work.
- It was shown that the copper(I)-terpyridine complex **I** is a highly dynamic systems, shifting its geometry at room temperature. This dynamic relationship of the ligand and metal center might have drastic influence on the reactivity, even facilitating the reaction.
- The interaction between the peroxide and the copper center is extremely diverse and yields a great range of products. The reactions occur almost immediately upon addition of peroxide to the metal.

- EPR analysis, Spin-trapping and radical quenching experiments show the formation of alkoxide and peroxide radicals in solution. Further analysis suggests the formation of a peroxide complex.
- We could isolate a novel copper(II)-peroxide complex (**CR1**), which has not been reported before. The complex shows a symmetric coordination of two peroxides to two copper centers.
- Cyclovoltammetric measurements suggests that rather than the formation of a copper(III) complex, a redox activity of the ligand is possible. However, such oxidized ligand could not be isolated yet.
- Kinetic measurements and dynamic EPR measurements show a dependency of the reaction time on the light source. Presumably, the catalytically active species shows a higher absorption in the range of 370 to 390 nm.

5. Conclusion and Outlook

The copper-catalyzed allylic alkynylation provides a novel pathway to functionalize relatively unreactive substrates. However, intricate research of the underlying mechanism proved to be difficult due to the complexity of the system. In this work, we were able to present a novel reaction mechanism based on various spectroscopic findings and systematic changes of the reaction conditions.

Chapter 2 showed the sensitivity of the reaction towards the conditions. The terpyridine ligand was found to be crucial for the reaction's success, as well as the use of an organic peroxide. Furthermore, the findings of the chapter implied that the mechanism did not proceed via free radicals as previously proposed. Further, as a conclusion of Chapter 2 a new reaction protocol was presented which allowed an easier handling of the reaction as well as drastically shortened reaction times from 24 h to 5 h. We could level out the strict exclusion from oxygen to just using degassed solvent. Most interestingly, it was found that the reaction requires an excess of cyclohexene to proceed in the desired fashion.

Chapter 3 confirmed the extraordinary selectivity of the reaction again, ruling out allylic substrates, that are acyclic or possess any oxygenated groups. On the other hand, the reaction showed great acceptability of various phenylacetylenes. Therefore, the

interaction of the complex with the cyclohexene must be very specific and probably presents a key-step in the whole reaction.

Chapter 4 confirmed the complexity of the system. An important find in this chapter was the dynamic coordination of the copper by the terpyridine ligand. This coordination mode and the applicability of the ligand as a non-innocent participant in the reaction justifies the key role of the compound in the reaction system. We furthermore could prove the existence of copper-peroxides and copper-alkoxides during the course of the reaction, allowing a non-radical pathway. As a result, a new mechanistic proposal was made.

This new proposal allows a deeper insight in the reaction and potentially helps in further optimizing the conditions. Still, the biggest challenge of the reaction remains the use of hazardous peroxides as well as the excess of cyclohexene. Potentially, the new-gained knowledge can be used to replace the organic peroxide with benign oxidants or even dioxygen. Furthermore, reaction engineering and the use of flow-chemistry will help to mitigate the effects of side-reactions.[252, 253]

Lastly, the use of prochiral substrates such as cyclohexene makes the reaction interesting for the enantioselective formation of products. Approaches towards this could make use of novel ligand systems, that would incorporate the necessary reactivity as well as the possibility for the formation of an asymmetric product. Another approach would be the use of artificial metalloenzymes.[254, 255] This rather novel technology would incorporate the complex into a protein scaffold and optimally use synergistic effects between the scaffold and metal center to afford an enantioselective transformation. Currently, the investigations of these systems are ongoing in our lab.

6. References

1. K. P. C. Vollhardt and N. E. Schore, *Organische Chemie*, John Wiley & Sons, 5 edn., 2011.
2. T. Wertheim, *Justus Liebigs Annalen der Chemie*, 1844, **51**, 289-315.
3. F. Roudesly, J. Oble and G. Poli, *Journal of Molecular Catalysis A: Chemical*, 2017, **426**, 275-296.
4. J. Tsuji, H. Takahashi and M. Morikawa, *Tetrahedron Letters*, 1965, **6**, 4387-4388.
5. B. M. Trost and T. J. Fullerton, *Journal of the American Chemical Society*, 1973, **95**, 292-294.
6. B. M. Trost and D. L. Van Vranken, *Chemical Reviews*, 1996, **96**, 395-422.
7. R. Takeuchi and M. Kashio, *Journal of the American Chemical Society*, 1998, **120**, 8647-8655.
8. B. Bartels and G. Helmchen, *Chemical Communications*, 1999, 741-742.
9. A. Alexakis, J. E. Bäckvall, N. Krause, O. Pàmies and M. Diéguez, *Chemical Reviews*, 2008, **108**, 2796-2823.
10. V. Hornillos, M. Pérez, M. Fañanás-Mastral and B. L. Feringa, *Journal of the American Chemical Society*, 2013, **135**, 2140-2143.
11. A. S. E. Karlström, F. F. Huerta, G. J. Meuzelaar and J.-E. Bäckvall, *Synlett*, 2001, **2001**, 0923-0926.
12. H. Malda, A. W. van Zijl, L. A. Arnold and B. L. Feringa, *Organic Letters*, 2001, **3**, 1169-1171.
13. P. T. Anastas and J. C. Warner, *Green Chemistry: Theory and Practive*, New York, 1998.
14. A. A. Almasalma and E. Mejía, *Chemistry–A European Journal*, 2018, **24**, 12269-12273.
15. A. A. Almasalma and E. Mejía, *Synthesis*, 2019, **51**, A-H.
16. M. Beller, *Chemical Reviews*, 2019, **119**, 2089-2089.
17. R. R. Conry, in *Encyclopedia of Inorganic and Bioinorganic Chemistry*.
18. L. Que and W. B. Tolman, *Nature*, 2008, **455**, 333-340.
19. G. P. Ellis and T. M. Romney-Alexander, *Chemical Reviews*, 1987, **87**, 779-794.
20. J. V. Braun and E. Anton, *Berichte der deutschen chemischen Gesellschaft (A and B Series)*, 1934, **67**, 1051-1056.
21. K. W. Rosenmund and E. Struck, *Berichte der deutschen chemischen Gesellschaft (A and B Series)*, 1919, **52**, 1749-1756.
22. J. Zanon, A. Klapars and S. L. Buchwald, *Journal of the American Chemical Society*, 2003, **125**, 2890-2891.
23. W. R. H. Hurtley, *Journal of the Chemical Society (Resumed)*, 1929, 1870-1873.
24. S. F. Yip, H. Y. Cheung, Z. Zhou and F. Y. Kwong, *Organic Letters*, 2007, **9**, 3469-3472.
25. X. Xie, G. Cai and D. Ma, *Organic Letters*, 2005, **7**, 4693-4695.
26. X. Xie, Y. Chen and D. Ma, *Journal of the American Chemical Society*, 2006, **128**, 16050-16051.
27. M. Tamura and J. Kochi, *Synthesis*, 1971, **1971**, 303-305.
28. G. Fouquet and M. Schlosser, *Angewandte Chemie International Edition in English*, 1974, **13**, 82-83.

29. D. K. Johnson, J. P. Ciavarri, F. T. Ishmael, K. J. Schillinger, T. A. P. van Geel and S. M. Stratton, *Tetrahedron Letters*, 1995, **36**, 8565-8568.
30. J. R. Vyvyan, C. L. Holst, A. J. Johnson and C. M. Schwenk, *The Journal of Organic Chemistry*, 2002, **67**, 2263-2265.
31. M. Seki and K. Mori, *European Journal of Organic Chemistry*, 2001, **2001**, 3797-3809.
32. H. Tamagawa, H. Takikawa and K. Mori, *European Journal of Organic Chemistry*, 1999, **1999**, 973-978.
33. P. T. Baraldi, P. H. G. Zarbin, P. C. Vieira and A. G. Corrêa, *Tetrahedron: Asymmetry*, 2002, **13**, 621-624.
34. R.-J. de Lang, M. J. C. M. van Hooijdonk, L. Brandsma, H. Kramer and W. Seinen, *Tetrahedron*, 1998, **54**, 2953-2966.
35. N. Jun, Y. Noriyuki, H. Yuzuru, U. Eiji, O. Akihiro and O. Akira, *Bulletin of the Chemical Society of Japan*, 1986, **59**, 2035-2037.
36. D. H. Burns, J. D. Miller, H.-K. Chan and M. O. Delaney, *Journal of the American Chemical Society*, 1997, **119**, 2125-2133.
37. G. Cahiez, C. Chaboche and M. Jézéquel, *Tetrahedron*, 2000, **56**, 2733-2737.
38. M. B. Thathagar, J. Beckers and G. Rothenberg, *Journal of the American Chemical Society*, 2002, **124**, 11858-11859.
39. S.-K. Kang, T. Yamaguchi, T.-H. Kim and P.-S. Ho, *The Journal of Organic Chemistry*, 1996, **61**, 9082-9083.
40. J.-H. Li, J.-L. Li, D.-P. Wang, S.-F. Pi, Y.-X. Xie, M.-B. Zhang and X.-C. Hu, *The Journal of Organic Chemistry*, 2007, **72**, 2053-2057.
41. A. A. Almasalma and E. Mejía, *Synthesis*, 2020.
42. C. Alonso, E. Martínez de Marigorta, G. Rubiales and F. Palacios, *Chemical Reviews*, 2015, **115**, 1847-1935.
43. V. C. R. McLoughlin and J. Thrower, *Tetrahedron*, 1969, **25**, 5921-5940.
44. Y. Kobayashi, K. Yamamoto and I. Kumadaki, *Tetrahedron Letters*, 1979, **20**, 4071-4072.
45. O. A. Tomashenko, E. C. Escudero-Adán, M. Martínez Belmonte and V. V. Grushin, *Angewandte Chemie International Edition*, 2011, **50**, 7655-7659.
46. H. Morimoto, T. Tsubogo, N. D. Litvinas and J. F. Hartwig, *Angewandte Chemie International Edition*, 2011, **50**, 3793-3798.
47. G. G. Dubinina, H. Furutachi and D. A. Vicic, *Journal of the American Chemical Society*, 2008, **130**, 8600-8601.
48. Q.-Y. Chen and S.-W. Wu, *Journal of the Chemical Society, Chemical Communications*, 1989, 705-706.
49. S. I. Arlow and J. F. Hartwig, *Angewandte Chemie International Edition*, 2016, **55**, 4567-4572.
50. L. Chu and F.-L. Qing, *Organic Letters*, 2010, **12**, 5060-5063.
51. X. Jiang, L. Chu and F.-L. Qing, *The Journal of Organic Chemistry*, 2012, **77**, 1251-1257.
52. T. Liu and Q. Shen, *Organic Letters*, 2011, **13**, 2342-2345.
53. Y. Ye and M. S. Sanford, *Journal of the American Chemical Society*, 2012, **134**, 9034-9037.
54. D. A. Nagib, M. E. Scott and D. W. C. MacMillan, *Journal of the American Chemical Society*, 2009, **131**, 10875-10877.
55. K. Sonogashira, Y. Tohda and N. Hagihara, *Tetrahedron letters*, 1975, **16**, 4467-4470.
56. Z. Li and C.-J. Li, *Journal of the American Chemical Society*, 2005, **127**, 3672-3673.

57. Z. Li, D. S. Bohle and C.-J. Li, *Proceedings of the National Academy of Sciences*, 2006, **103**, 8928-8933.
58. E. Boess, D. Sureshkumar, A. Sud, C. Wirtz, C. Farès and M. Klussmann, *Journal of the American Chemical Society*, 2011, **133**, 8106-8109.
59. E. Boess, C. Schmitz and M. Klussmann, *Journal of the American Chemical Society*, 2012, **134**, 5317-5325.
60. Z. Li and C.-J. Li, *Journal of the American Chemical Society*, 2006, **128**, 56-57.
61. Y. Zhang and C.-J. Li, *Angewandte Chemie International Edition*, 2006, **45**, 1949-1952.
62. O. Baslé and C.-J. Li, *Green Chemistry*, 2007, **9**, 1047-1050.
63. N. Borduas and D. A. Powell, *The Journal of Organic Chemistry*, 2008, **73**, 7822-7825.
64. K. Cheng, L. Huang and Y. Zhang, *Organic Letters*, 2009, **11**, 2908-2911.
65. R. Su, Y. Li, M.-Y. Min, X.-H. Ouyang, R.-J. Song and J.-H. Li, *Chemical Communications*, 2018, **54**, 13511-13514.
66. Z. Yan, N.-X. Wang, X.-W. Gao, J.-L. Li, Y.-H. Wu, T. Zhang, S.-L. Chen and Y. Xing, *Advanced Synthesis & Catalysis*, 2019, **361**, 1007-1011.
67. J. Xu, Y. Fu, D.-F. Luo, Y.-Y. Jiang, B. Xiao, Z.-J. Liu, T.-J. Gong and L. Liu, *Journal of the American Chemical Society*, 2011, **133**, 15300-15303.
68. X. Wang, Y. Ye, S. Zhang, J. Feng, Y. Xu, Y. Zhang and J. Wang, *Journal of the American Chemical Society*, 2011, **133**, 16410-16413.
69. A. T. Parsons and S. L. Buchwald, *Angewandte Chemie International Edition*, 2011, **50**, 9120-9123.
70. C. Guo, J. Song, S.-W. Luo and L.-Z. Gong, *Angewandte Chemie International Edition*, 2010, **49**, 5558-5562.
71. G. Zhang, Y. Zhang and R. Wang, *Angewandte Chemie International Edition*, 2011, **50**, 10429-10432.
72. A. Lee, R. C. Betori, E. A. Crane and K. A. Scheidt, *Journal of the American Chemical Society*, 2018, **140**, 6212-6216.
73. L. Ye, Q.-S. Gu, Y. Tian, X. Meng, G.-C. Chen and X.-Y. Liu, *Nature Communications*, 2018, **9**, 227.
74. Q. Tan, Z. Yang, D. Jiang, Y. Cheng, J. Yang, S. Xi and M. Zhang, *Angewandte Chemie International Edition*, 2019, **58**, 6420-6424.
75. B. Wang, D. P. Shelar, X.-Z. Han, T.-T. Li, X. Guan, W. Lu, K. Liu, Y. Chen, W.-F. Fu and C.-M. Che, *Chemistry – A European Journal*, 2015, **21**, 1184-1190.
76. T. P. Nicholls, G. E. Constable, J. C. Robertson, M. G. Gardiner and A. C. Bissember, *ACS Catalysis*, 2016, **6**, 451-457.
77. O. Baslé and C.-J. Li, *Organic Letters*, 2008, **10**, 3661-3663.
78. F. Yang, J. Li, J. Xie and Z.-Z. Huang, *Organic Letters*, 2010, **12**, 5214-5217.
79. M. Ghobrial, M. Schnürch and M. D. Mihovilovic, *The Journal of Organic Chemistry*, 2011, **76**, 8781-8793.
80. D. V. Ramana and M. Chandrasekharam, *Advanced Synthesis & Catalysis*, 2018, **360**, 4080-4083.
81. X. Ye, C. Xie, Y. Pan, L. Han and T. Xie, *Organic Letters*, 2010, **12**, 4240-4243.
82. Y.-X. Jia and E. P. Kündig, *Angewandte Chemie International Edition*, 2009, **48**, 1636-1639.
83. J. E. M. N. Klein, A. Perry, D. S. Pugh and R. J. K. Taylor, *Organic Letters*, 2010, **12**, 3446-3449.

84. D. Ma, J. Pan, L. Yin, P. Xu, Y. Gao, Y. Yin and Y. Zhao, *Organic Letters*, 2018, **20**, 3455-3459.
85. C. Yu and F. W. Patureau, *Angewandte Chemie International Edition*, 2018, **57**, 11807-11811.
86. Z. Tang, Z. Liu, Z. Tong, Z. Xu, C.-T. Au, R. Qiu and N. Kambe, *Organic Letters*, 2019, **21**, 5152-5156.
87. P. J. Borpatra, M. L. Deb and P. K. Baruah, *Synlett*, 2018, **29**, 1171-1175.
88. W. Xie, J. Heo, D. Kim and S. Chang, *Journal of the American Chemical Society*, 2020, **142**, 7487-7496.
89. J. B. Hewgley, S. S. Stahl and M. C. Kozlowski, *Journal of the American Chemical Society*, 2008, **130**, 12232-12233.
90. C. Yu, Y. Zhang, S. Zhang, H. Li and W. Wang, *Chemical Communications*, 2011, **47**, 1036-1038.
91. K. N. Tripathi, D. Ray and R. P. Singh, *European Journal of Organic Chemistry*, 2017, **2017**, 5809-5813.
92. R. P. Pandit, J.-J. Shim, S. H. Kim and Y. R. Lee, *RSC Advances*, 2017, **7**, 55288-55295.
93. Z. Li and C.-J. Li, *Journal of the American Chemical Society*, 2004, **126**, 11810-11811.
94. Z. Li and C.-J. Li, *Organic Letters*, 2004, **6**, 4997-4999.
95. M. Niu, Z. Yin, H. Fu, Y. Jiang and Y. Zhao, *The Journal of Organic Chemistry*, 2008, **73**, 3961-3963.
96. A. Sagadevan, V. K. K. Pampana and K. C. Hwang, *Angewandte Chemie International Edition*, 2019, **58**, 3838-3842.
97. S. Gupta, P. Dubey, A. K. Singh and N. Jain, *Dalton Transactions*, 2019, **48**, 10129-10137.
98. C. Glaser, *Berichte der deutschen chemischen Gesellschaft*, 1869, **2**, 422-424.
99. C. Glaser, *Justus Liebigs Annalen der Chemie*, 1870, **154**, 137-171.
100. G. Eglinton and A. R. Galbraith, *Chemistry & Industry* 1956, 737-738.
101. G. Eglinton and A. R. Galbraith, *Journal of the Chemical Society (Resumed)*, 1959, 889-896.
102. A. S. Hay, *The Journal of Organic Chemistry*, 1962, **27**, 3320-3321.
103. P. Cadiot and W. Chodkiewicz, *by Viehe HG, Marcel Dekker, New York*, 1969, 597-648.
104. W. Chodkiewicz, *Ann. Chim. Paris* 1957, 819-869.
105. R. Akhtar and A. F. Zahoor, *Synthetic Communications*, 2020, **50**, 3337-3368.
106. W. Shi and A. Lei, *Tetrahedron Letters*, 2014, **55**, 2763-2772.
107. K. S. Sindhu and G. Anilkumar, *RSC Advances*, 2014, **4**, 27867-27887.
108. A. F. Adeleke, A. P. N. Brown, L.-J. Cheng, K. A. M. Mosleh and C. J. Cordier, *Synthesis*, 2017, **49**, 790-801.
109. P. Siemsen, R. C. Livingston and F. Diederich, *Angewandte Chemie International Edition*, 2000, **39**, 2632-2657.
110. J. Krömer, I. Rios-Carreras, G. Fuhrmann, C. Musch, M. Wunderlin, T. Debaerdemaeker, E. Mena-Osteritz and P. Bäuerle, *Angewandte Chemie International Edition*, 2000, **39**, 3481-3486.
111. J. S. Salkind and B. Fundyler, *Berichte der deutschen chemischen Gesellschaft (A and B Series)*, 1936, **69**, 128-130.
112. F. Bohlmann, H. Schönowsky, E. Inhoffen and G. Grau, *Chemische Berichte*, 1964, **97**, 794-800.

113. M. H. Vilhelmsen, J. Jensen, C. G. Tortzen and M. B. Nielsen, *European Journal of Organic Chemistry*, 2013, **2013**, 701-711.
114. H. C. Kolb and K. B. Sharpless, *Drug Discovery Today*, 2003, **8**, 1128-1137.
115. V. V. Rostovtsev, L. G. Green, V. V. Fokin and K. B. Sharpless, *Angewandte Chemie International Edition*, 2002, **41**, 2596-2599.
116. C. W. Tornøe, C. Christensen and M. Meldal, *The Journal of Organic Chemistry*, 2002, **67**, 3057-3064.
117. J. M. Baskin, J. A. Prescher, S. T. Laughlin, N. J. Agard, P. V. Chang, I. A. Miller, A. Lo, J. A. Codelli and C. R. Bertozzi, *Proceedings of the National Academy of Sciences*, 2007, **104**, 16793-16797.
118. A. H. El-Sagheer and T. Brown, *Chemical Society Reviews*, 2010, **39**, 1388-1405.
119. E. M. Sletten and C. R. Bertozzi, *Accounts of Chemical Research*, 2011, **44**, 666-676.
120. V. K. Tiwari, B. B. Mishra, K. B. Mishra, N. Mishra, A. S. Singh and X. Chen, *Chemical Reviews*, 2016, **116**, 3086-3240.
121. J.-F. Lutz and Z. Zarafshani, *Advanced Drug Delivery Reviews*, 2008, **60**, 958-970.
122. K. Bozorov, J. Zhao and H. A. Aisa, *Bioorganic & Medicinal Chemistry*, 2019, **27**, 3511-3531.
123. S. Neumann, M. Biewend, S. Rana and W. H. Binder, *Macromolecular Rapid Communications*, 2020, **41**, 1900359.
124. G. Evano, K. Jouvin, C. Theunissen, C. Guissart, A. Laouiti, C. Tresse, J. Heimburger, Y. Bouhoute, R. Veillard, M. Lecomte, A. Nitelet, S. Schweizer, N. Blanchard, C. Alayrac and A. C. Gaumont, *Chemical Communications*, 2014, **50**, 10008-10018.
125. A. Bakhoda, O. E. Okoromoba, C. Greene, M. R. Boroujeni, J. A. Bertke and T. H. Warren, *Journal of the American Chemical Society*, 2020, **142**, 18483-18490.
126. E. Zuidema and C. Bolm, *Chemistry – A European Journal*, 2010, **16**, 4181-4185.
127. A. Hazra, M. T. Lee, J. F. Chiu and G. Lalic, *Angewandte Chemie International Edition*, 2018, **57**, 5492-5496.
128. A. Sagadevan and K. C. Hwang, *Advanced Synthesis & Catalysis*, 2012, **354**, 3421-3427.
129. H.-D. Xia, Z.-L. Li, Q.-S. Gu, X.-Y. Dong, J.-H. Fang, X.-Y. Du, L.-L. Wang and X.-Y. Liu, *Angewandte Chemie International Edition*, 2020, **59**, 16926-16932.
130. B. M. Trost and M. L. Crawley, *Chemical Reviews*, 2003, **103**, 2921-2944.
131. B. M. Trost, T. Zhang and J. D. Sieber, *Chemical Science*, 2010, **1**, 427-440.
132. Z. Lu and S. Ma, *Angewandte Chemie International Edition*, 2008, **47**, 258-297.
133. B. M. Trost and J. Xu, *Journal of the American Chemical Society*, 2005, **127**, 2846-2847.
134. B. Bartels, C. García-Yebra, F. Rominger and G. Helmchen, *European Journal of Inorganic Chemistry*, 2002, 2569-2586.
135. B. Bartels, C. García-Yebra and G. Helmchen, *European Journal of Organic Chemistry*, 2003, 1097-1103.
136. W.-B. Liu, C. M. Reeves and B. M. Stoltz, *Journal of the American Chemical Society*, 2013, **135**, 17298-17301.
137. Y. Xu and B. Zhou, *The Journal of Organic Chemistry*, 1987, **52**, 974-977.
138. U. Eberhardt and G. Mattern, *Chemische Berichte*, 1988, **121**, 1531-1534.

139. B. Plietker, *Angewandte Chemie International Edition*, 2006, **45**, 1469-1473.
140. B. M. Trost and I. Hachiya, *Journal of the American Chemical Society*, 1998, **120**, 1104-1105.
141. F. Glorius and A. Pfaltz, *Organic Letters*, 1999, **1**, 141-144.
142. B. M. Trost, K. Dogra, I. Hachiya, T. Emura, D. L. Hughes, S. Krska, R. A. Reamer, M. Palucki, N. Yasuda and P. J. Reider, *Angewandte Chemie International Edition*, 2002, **41**, 1929-1932.
143. O. Belda and C. Moberg, *Accounts of Chemical Research*, 2004, **37**, 159-167.
144. G. C. Lloyd-Jones and A. Pfaltz, *Angewandte Chemie International Edition*, 1995, **34**, 462-464.
145. T. Yao, K. Hirano, T. Satoh and M. Miura, *Angewandte Chemie International Edition*, 2011, **50**, 2990-2994.
146. K. Geurts, S. P. Fletcher and B. L. Feringa, *Journal of the American Chemical Society*, 2006, **128**, 15572-15573.
147. S. Dutta, T. Bhattacharya, D. B. Werz and D. Maiti, *Chem*, 2021, **7**, 555-605.
148. J. K. Matsui, S. B. Lang, D. R. Heitz and G. A. Molander, *ACS Catalysis*, 2017, **7**, 2563-2575.
149. S. E. Braslavsky, *Pure and Applied Chemistry*, 2007, **79**, 293-465.
150. T. P. Yoon, M. A. Ischay and J. Du, *Nature Chemistry*, 2010, **2**, 527-532.
151. J. M. Narayanam and C. R. Stephenson, *Chemical Society Reviews*, 2011, **40**, 102-113.
152. D. A. Nicewicz and T. M. Nguyen, *ACS Catalysis*, 2014, **4**, 355-360.
153. P. Hünemörder and E. Mejía, *Catalysis Science & Technology*, 2020, **10**, 6754-6768.
154. N. Hoffmann, *ChemSusChem*, 2012, **5**, 352-371.
155. M. Pirtsch, S. Paria, T. Matsuno, H. Isobe and O. Reiser, *Chemistry–A European Journal*, 2012, **18**, 7336-7340.
156. A. Baralle, L. Fensterbank, J. P. Goddard and C. Ollivier, *Chemistry–A European Journal*, 2013, **19**, 10809-10813.
157. S. Paria, V. Kais and O. Reiser, *Advanced Synthesis & Catalysis*, 2014, **356**, 2853-2858.
158. R. Zhou, H. Liu, H. Tao, X. Yu and J. Wu, *Chemical Science*, 2017, **8**, 4654-4659.
159. A. M. Martínez-Gualda, R. Cano, L. Marzo, R. Pérez-Ruiz, J. Luis-Barrera, R. Mas-Ballesté, A. Fraile, A. Víctor and J. Alemán, *Nature Communications*, 2019, **10**, 1-10.
160. K. L. Skubi, T. R. Blum and T. P. Yoon, *Chemical reviews*, 2016, **116**, 10035-10074.
161. J. D. Cuthbertson and D. W. MacMillan, *Nature*, 2015, **519**, 74-77.
162. X. Ma, P. Wang, Z. Liu, C. Xin, S. Wang, J. Jia, P. Ma, J. Niu and J. Wang, *Inorganic Chemistry*, 2020, **59**, 8690-8698.
163. M. Salavati-Niasari, M. Shaterian, M. R. Ganjali and P. Norouzi, *Journal of Molecular Catalysis A: Chemical*, 2007, **261**, 147-155.
164. J.-Q. Yu and E. J. Corey, *Organic Letters*, 2002, **4**, 2727-2730.
165. M. Tonigold, Y. Lu, B. Bredenkötter, B. Rieger, S. Bahnmüller, J. Hitzbleck, G. Langstein and D. Volkmer, *Angewandte Chemie International Edition*, 2009, **48**, 7546-7550.
166. Markus B. Meder and Lutz H. Gade, *European Journal of Inorganic Chemistry*, 2004, **2004**, 2716-2722.
167. B. Schoentjes and J.-M. Lehn, *Helvetica Chimica Acta*, 1995, **78**, 1-12.

168. J. M. Lehn, A. Rigault, J. Siegel, J. Harrowfield, B. Chevrier and D. Moras, *Proceedings of the National Academy of Sciences*, 1987, **84**, 2565-2569.
169. E. Riedel and C. Janiak, *Anorganische Chemie*, De Gruyter, Göttingen, 2011.
170. G. Baum, E. C. Constable, D. Fenske, C. E. Housecroft, T. Kulke, M. Neuburger and M. Zehnder, *Journal of the Chemical Society, Dalton Transactions*, 2000, 945-959.
171. C. A. Bessel, R. F. See, D. L. Jameson, M. R. Churchill and K. J. Takeuchi, *Journal of the Chemical Society, Dalton Transactions*, 1992, 3223-3228.
172. M. J. Moure, R. SanMartin and E. Domínguez, *Advanced Synthesis & Catalysis*, 2014, **356**, 2070-2080.
173. N. Zohreh and M. Jahani, *Journal of Molecular Catalysis A: Chemical*, 2017, **426**, 117-129.
174. E. A. Ambundo, M.-V. Deydier, A. J. Grall, N. Aguera-Vega, L. T. Dressel, T. H. Cooper, M. J. Heeg, L. A. Ochrymowycz and D. B. Rorabacher, *Inorganic Chemistry*, 1999, **38**, 4233-4242.
175. V. O. Rodionov, S. I. Presolski, D. Díaz Díaz, V. V. Fokin and M. G. Finn, *Journal of the American Chemical Society*, 2007, **129**, 12705-12712.
176. A. A. C. Braga, F. Maseras, J. Urbano, A. Caballero, M. M. Díaz-Requejo and P. J. Pérez, *Organometallics*, 2006, **25**, 5292-5300.
177. G. D. Jones, J. L. Martin, C. McFarland, O. R. Allen, R. E. Hall, A. D. Haley, R. J. Brandon, T. Konovalova, P. J. Desrochers, P. Pulay and D. A. Vicic, *Journal of the American Chemical Society*, 2006, **128**, 13175-13183.
178. J. T. Ciszewski, D. Y. Mikhaylov, K. V. Holin, M. K. Kadirov, Y. H. Budnikova, O. Sinyashin and D. A. Vicic, *Inorganic Chemistry*, 2011, **50**, 8630-8635.
179. W. Hao and Y. Liu, *Beilstein Journal of Organic Chemistry*, 2015, **11**, 2132-2144.
180. K. W. Shimkin and D. A. Watson, *Beilstein Journal of Organic Chemistry*, 2015, **11**, 2278-2288.
181. J.-P. Wan and Y. Jing, *Beilstein Journal of Organic Chemistry*, 2015, **11**, 2209-2222.
182. M. R. Rosenthal, *Journal of Chemical Education*, 1973, **50**, 331.
183. J. Lalevée and J.-P. Fouassier, *Photopolymerisation initiating systems*, Royal Society of Chemistry, 2018.
184. G. O'Mahony, *Synlett*, 2004, **2004**, 572-573.
185. R. D. Bach and H. B. Schlegel, *The Journal of Physical Chemistry A*, 2020, **124**, 4742-4751.
186. C. Fasciani, C. J. B. Alejo, M. Grenier, J. C. Netto-Ferreira and J. C. Scaiano, *Organic Letters*, 2011, **13**, 204-207.
187. W. Reints, D. A. Pratt, H.-G. Korth and P. Mulder, *The Journal of Physical Chemistry A*, 2000, **104**, 10713-10720.
188. V. J. Barwick, *TrAC Trends in Analytical Chemistry*, 1997, **16**, 293-309.
189. A. A. Maryott and E. R. Smith, *Table of dielectric constants of pure liquids*, US Government Printing Office, 1951.
190. C. Reichardt and T. Welton, *Appendix A. Properites, Purification, and Use of Organic Solvents. In Solvents and Solvent Effects in Organic Chemistry*, John Wiley & Sons, Ltd, 2010.
191. R. D. Willett, G. Pon and C. Nagy, *Inorganic Chemistry*, 2001, **40**, 4342-4352.
192. S. Monge, V. Darcos and D. M. Haddleton, *Journal of Polymer Science Part A: Polymer Chemistry*, 2004, **42**, 6299-6308.
193. W.-Q. Zhang, W.-Y. Zhang, R.-D. Wang, C.-Y. Ren, Q.-Q. Li, Y.-P. Fan, B. Liu, P. Liu and Y.-Y. Wang, *Crystal Growth & Design*, 2017, **17**, 517-526.

194. C. Li, R. Dickson, N. Rockstroh, J. Rabeah, D. B. Cordes, A. M. Z. Slawin, P. Hünemörder, A. Spannenberg, M. Bühl, E. Mejía, E. Zysman-Colman and P. C. J. Kamer, *Catalysis Science & Technology*, 2020, **10**, 7745-7756.
195. M. S. Lowry, J. I. Goldsmith, J. D. Slinker, R. Rohl, R. A. Pascal, G. G. Malliaras and S. Bernhard, *Chemistry of Materials*, 2005, **17**, 5712-5719.
196. E. L. Tyson, Z. L. Niemeyer and T. P. Yoon, *The Journal of Organic Chemistry*, 2014, **79**, 1427-1436.
197. P. Montes-Navajas, L. Teruel, A. Corma and H. Garcia, *Chemistry – A European Journal*, 2008, **14**, 1762-1768.
198. N. S. Allen, F. Catalina, P. N. Green and W. A. Green, *Journal of Photochemistry*, 1987, **36**, 99-112.
199. F. G. Bordwell, G. E. Drucker, N. H. Andersen and A. D. Denniston, *Journal of the American Chemical Society*, 1986, **108**, 7310-7313.
200. Engineering ToolBox - Inorganic Acids and Bases - pKa Values, https://www.engineeringtoolbox.com/pKa-inorganic-acid-base-hydrated-metal-ion-monoprotic-diprotic-triprotic-tetraprotic-d_1950.htm, (accessed 09.09., 2022).
201. W. N. Olmstead, Z. Margolin and F. G. Bordwell, *The Journal of organic chemistry*, 1980, **45**, 3295-3299.
202. C. Sabot, K. A. Kumar, C. Antheaume and C. Mioskowski, *The Journal of Organic Chemistry*, 2007, **72**, 5001-5004.
203. pK_a Values for Organic and Inorganic Bronstedt Acids at 25 °C, https://owl.oit.umass.edu/departments/OrganicChemistry/appendix/pKaTable.html, (accessed 09.09., 2022).
204. GESTIS-Stoffdatenbank - Natriumcarbonat, https://gestis.dguv.de/data?name=490211, (accessed 12.09., 2022).
205. GESTIS-Stoffdatenbank - Kaliumcarbonat, https://gestis.dguv.de/data?name=002070, (accessed 12.09., 2022).
206. Sicherheitsdatenblatt Caesiumcarbonat, https://www.fishersci.de/store/msds?partNumber=10008972&productDescription=5g;%20Kunstoffflasche&countryCode=DE&language=de, (accessed 12.09., 2022).
207. A. Vasilopoulos, S. W. Krska and S. S. Stahl, *Science*, 2021, **372**, 398-403.
208. A. C. Varas, T. Noël, Q. Wang and V. Hessel, *ChemSusChem*, 2012, **5**, 1703-1707.
209. M.-B. Zhou, C.-Y. Wang, R.-J. Song, Y. Liu, W.-T. Wei and J.-H. Li, *Chemical Communications*, 2013, **49**, 10817-10819.
210. Y.-M. Lee, S. Bang, Y. M. Kim, J. Cho, S. Hong, T. Nomura, T. Ogura, O. Troeppner, I. Ivanović-Burmazović, R. Sarangi, S. Fukuzumi and W. Nam, *Chemical Science*, 2013, **4**, 3917-3923.
211. G. P. Moss, P. A. S. Smith and D. Tavernier, *Pure and Applied Chemistry*, 1995, **67**, 1307-1375.
212. Y.-W. Zheng, R. Narobe, K. Donabauer, S. Yakubov and B. König, *ACS Catalysis*, 2020, **10**, 8582-8589.
213. S. L. Khursan, D. A. Mikhailov, V. M. Yanborisov and D. I. Borisov, *Reaction Kinetics and Catalysis Letters*, 1997, **61**, 91-95.
214. C. Wei, Y. He, X. Shi and Z. Song, *Coordination Chemistry Reviews*, 2019, **385**, 1-19.
215. P. Liu, G. Shi and X. Chen, *Frontiers in Chemistry*, 2020, **8**.
216. C. M. Jones and M. J. Burkitt, *Journal of the American Chemical Society*, 2003, **125**, 6946-6954.

217. L. Pecci, G. Montefoschi and D. Cavallini, *Biochemical and Biophysical Research Communications*, 1997, **235**, 264-267.
218. J. K. Kochi, *Tetrahedron*, 1962, **18**, 483-497.
219. A. Sobkowiak, A. Qui, X. Liu, A. Llobet and D. T. Sawyer, *Journal of the American Chemical Society*, 1993, **115**, 609-614.
220. E. C. Constable, in *Advances in Inorganic Chemistry*, ed. H. J. Emeléus, Academic Press, 1986, vol. 30, pp. 69-121.
221. M. Kharasch and G. Sosnovsky, *Journal of the American Chemical Society*, 1958, **80**, 756-756.
222. M. Kharasch and A. Fono, *The Journal of Organic Chemistry*, 1959, **24**, 72-78.
223. M. Kharasch and A. Fono, *The Journal of Organic Chemistry*, 1959, **24**, 606-614.
224. F. Haber and J. Weiss, *Naturwissenschaften*, 1932, **20**, 948-950.
225. B. D. Neisen, N. L. Gagnon, D. Dhar, A. D. Spaeth and W. B. Tolman, *Journal of the American Chemical Society*, 2017, **139**, 10220-10223.
226. D. P. Barr and R. P. Mason, *Journal of Biological Chemistry*, 1995, **270**, 12709-12716.
227. R. S. Srivastava, N. R. Tarver and K. M. Nicholas, *Journal of the American Chemical Society*, 2007, **129**, 15250-15258.
228. G. Lu, R. Y. Liu, Y. Yang, C. Fang, D. S. Lambrecht, S. L. Buchwald and P. Liu, *Journal of the American Chemical Society*, 2017, **139**, 16548-16555.
229. P. J. J. A. Timmermans, A. Mackor, A. L. Spek and B. Kojić-Prodić, *Journal of Organometallic Chemistry*, 1984, **276**, 287-295.
230. T. Tano, M. Z. Ertem, S. Yamaguchi, A. Kunishita, H. Sugimoto, N. Fujieda, T. Ogura, C. J. Cramer and S. Itoh, *Dalton Transactions*, 2011, **40**, 10326-10336.
231. E. I. Solomon, P. Chen, M. Metz, S.-K. Lee and A. E. Palmer, *Angewandte Chemie International Edition*, 2001, **40**, 4570-4590.
232. C. E. Elwell, N. L. Gagnon, B. D. Neisen, D. Dhar, A. D. Spaeth, G. M. Yee and W. B. Tolman, *Chemical Reviews*, 2017, **117**, 2059-2107.
233. S. T. Prigge, B. A. Eipper, R. E. Mains and L. M. Amzel, *Science*, 2004, **304**, 864-867.
234. A. C. Rosenzweig and M. H. Sazinsky, *Current Opinion in Structural Biology*, 2006, **16**, 729-735.
235. D. J. E. Spencer, N. W. Aboelella, A. M. Reynolds, P. L. Holland and W. B. Tolman, *Journal of the American Chemical Society*, 2002, **124**, 2108-2109.
236. N. W. Aboelella, E. A. Lewis, A. M. Reynolds, W. W. Brennessel, C. J. Cramer and W. B. Tolman, *Journal of the American Chemical Society*, 2002, **124**, 10660-10661.
237. S. Mahapatra, J. A. Halfen, E. C. Wilkinson, L. Que, Jr. and W. B. Tolman, *Journal of the American Chemical Society*, 1994, **116**, 9785-9786.
238. F. H. Jardine, L. Rule and A. G. Vohra, *Journal of the Chemical Society A: Inorganic, Physical, Theoretical*, 1970, 238-240.
239. J. A. Halfen, V. G. Young and W. B. Tolman, *Inorganic Chemistry*, 1998, **37**, 2102-2103.
240. N. W. G. Smits, B. van Dijk, I. de Bruin, S. L. T. Groeneveld, M. A. Siegler and D. G. H. Hetterscheid, *Inorganic Chemistry*, 2020, **59**, 16398-16409.
241. T. Lewis, W. Wallace, F. D. Peterson, S. Rafferty and S. Martic, *Electrochemical Science Advances*, 2022, **2**, e2100054.
242. I. M. DiMucci, J. T. Lukens, S. Chatterjee, K. M. Carsch, C. J. Titus, S. J. Lee, D. Nordlund, T. A. Betley, S. N. MacMillan and K. M. Lancaster, *Journal of the American Chemical Society*, 2019, **141**, 18508-18520.

243. S.-J. Li and Y. Lan, *Chemical Communications*, 2020, **56**, 6609-6619.
244. G. B. Shul'pin, Y. N. Kozlov and L. S. Shul'pina, *Catalysts*, 2019, **9**, 1046.
245. R. J. Allenbaugh, A. L. Rheingold and L. H. Doerrer, *Dalton Transactions*, 2009, 1155-1163.
246. W. A. Yehye, N. A. Rahman, A. Ariffin, S. B. Abd Hamid, A. A. Alhadi, F. A. Kadir and M. Yaeghoobi, *European Journal of Medicinal Chemistry*, 2015, **101**, 295-312.
247. D. Njus, P. M. Kelley, Y.-J. Tu and H. B. Schlegel, *Free Radical Biology and Medicine*, 2020, **159**, 37-43.
248. P. W. Seavill, K. B. Holt and J. D. Wilden, *Faraday Discussions*, 2019, **220**, 269-281.
249. A. Sagadevan, V. P. Charpe, A. Ragupathi and K. C. Hwang, *Journal of the American Chemical Society*, 2017, **139**, 2896-2899.
250. A. Sagadevan, A. Ragupathi and K. C. Hwang, *Angewandte Chemie International Edition*, 2015, **54**, 13896-13901.
251. A. Sagadevan, A. Ragupathi, C.-C. Lin, J. R. Hwu and K. C. Hwang, *Green Chemistry*, 2015, **17**, 1113-1119.
252. M. Guidi, P. H. Seeberger and K. Gilmore, *Chemical Society Reviews*, 2020, **49**, 8910-8932.
253. M. Movsisyan, E. I. P. Delbeke, J. K. E. T. Berton, C. Battilocchio, S. V. Ley and C. V. Stevens, *Chemical Society Reviews*, 2016, **45**, 4892-4928.
254. C. M. Thomas and T. R. Ward, *Chemical Society Reviews*, 2005, **34**, 337-346.
255. J. Pierron, C. Malan, M. Creus, J. Gradinaru, I. Hafner, A. Ivanova, A. Sardo and T. R. Ward, *Angewandte Chemie International Edition*, 2008, **47**, 701-705.
256. G. M. Sheldrick, *Acta Crystallographica Section C: Structural Chemistry*, 2015, **71**, 3-8.
257. A. K. Mondal, J. Jover, E. Ruiz and S. Konar, *Chemistry – A European Journal*, 2017, **23**, 12550-12558.
258. M. Stender, R. J. Wright, B. E. Eichler, J. Prust, M. M. Olmstead, H. W. Roesky and P. P. Power, *Journal of the Chemical Society, Dalton Transactions*, 2001, 3465-3469.
259. N. Vogt, A. Sandleben, L. Kletsch, S. Schäfer, M. T. Chin, D. A. Vicic, G. Hörner and A. Klein, *Organometallics*, 2021, **40**, 1776-1785.
260. J. Dai, Z. Li, T. Wang and R. Bai, *Organic & Biomolecular Chemistry*, 2016, **14**, 4382-4386.
261. J.-C. Wang, Y.-H. Hu, G.-J. Chen and Y.-B. Dong, *Chemical Communications*, 2016, **52**, 13116-13119.

A. Appendix

A.1. Experimental Part

A.1.1. Materials

If not mentioned otherwise, reactions were performed using standard Schlenk Techniques. Tetrakisacetonitrile Copper(I) Hexafluorophosphate (97 %, Sigma Aldrich), 4,4′,4″-Tri-tert-butyl-2,2′:6′,2″-terpyridine (95 %, Sigma Aldrich), tert-Butyl Hydroperoxide solution 5-6 M in decane (Sigma Aldrich), Ethynylbenzene (>98 %, TCI), Cyclohexene (inhibitor-free, ReagentPlus®, 99 %, Sigma Aldrich), Naphtalene (99 %, Sigma Aldrich), Pyridine (99.7 %, VWR), 2,2′-Bipyridine (>99 %, TCI), 4,4′-Di-tert.-butyl-2,2′-dipyridyl (>98 % Sigma Aldrich), 1,10-Phenanthroline (≥98 %, Sigma Aldrich), 2,9-Dimethyl-1,10-phenanthroline (≥98 %, Sigma Aldrich), 4′(4-Methylphenyl)-2,2′:6′,2′-terpyridin (98 %, Alfa Aesar), N,N,N′,N′-Tetramethylethylendiamin (99 %, Sigma Aldrich), Potassium hydrotris(3,5-dimethylpyrazol-1-yl)borate (97 %, TCI), Triphenylphosphine (99 %, Acros Organics), Copper(I) chloride (98+ %, Sigma Aldrich), Copper(I) bromide (98 %, Sigma Aldrich), Copper(I) iodide (98 %, Alfa Aesar), Copper(I) acetate (97 %, Sigma Aldrich), Copper(I) oxide (≥99 %, Sigma Aldrich), Tetrakisacetonitrile Copper(I) tetrafluoroborate (>98 %, TCI), Copper Carbonate Hydroxide (>98 % Sigma Aldrich), Copper(II) trifluoromethanesulfonate (>98 %, TCI), Copper(II) phtalocyanine (90 % dye content, Sigma Aldrich), Copper(II) chloride (98 %, Thermo Scientific), Copper(II) oxide (99 %, Sigma Aldrich), Copper(II) acetylacetonate (99.9 % Sigma Aldrich), Copper(II) acetate (98 %, Sigma Aldrich), 2-(tert-Butylperoxy)-2-methylpropane (98 %, Sigma Aldrich), Cumene hydroperoxide (technical grade 80 %, Sigma Aldrich), Dicumyl peroxide (98 %, Sigma Aldrich), Benzoyl peroxide (75 %, remainder water, Sigma Aldrich), Hydrogen peroxide urea (99 %, Sigma Aldrich), Hydrogen peroxide (35 %, aqueous solution, abcr), 2,2-Dimethoxy-2-phenylacetophenone (98 %, TCI), , Potassium pyrosulfate (99 %, Fluka), Triethyl borane (11 % solution in THF, TCI), Acetonitrile (≥99 %, Honeywell), Methanol (≥99.9 %, Fisher Scientific), Dimethyl sulfoxide (≥99.7 % extra dry, Acros), Dichloromethane (≥99 %, Acros), Tetrachloromethane (99.8 %, Acros), Dimethyl formamide (99.8 % extra dry, Acros), Toluene (99.99 %, Acros), Heptane (99.9 %, Fisher Scientific), Chlorobenzene (98 %, Fluka), 2-propanol (99 %, Acros), *N*-Methyl-2-pyrrolidone (99.5 %, Acros), Tetrahydrofuran (99.5 %, Acros), [4,4′-Bis(1,1-dimethylethyl)-2,2′-bipyridine-N1,N1′]bis[3,5-difluoro-2-[5-(trifluoromethyl)-2-pyridinyl-N]phenyl-C]Iridium(III) hexafluorophosphate (Sigma Aldrich),

2,4,6-Triphenylpyrylium tetrafluoroborate (98 %, Sigma Aldrich), Tris(2,2′-bipyrazine-N1,N1′)ruthenium(II) hexafluorophosphate (95 %, Sigma Aldrich), 4,5-Bis(diphenylphosphino)-9,9-dimethylxanthene (98 %, TCI), Thioxanthone (97 %, Sigma Aldrich), Sodium Carbonate (99.5 %, Sigma Aldrich), Sodium Hydrogencarbonate (ch.rein, SCS) Potassium Carbonate (99 %, Fluka), Potassium Hydroxide (98.41 %, Fluka), Potassium Phosphate (95 %, Riedel-de Haën), 1,5,7-Triazabicyclo[4.4.0]dec-5-ene (98 %, Sigma Aldrich), Copper(II) Phosphate (97 %, Sigma Aldrich), Potassium tert-Butoxide (≥98 %, Sigma Aldrich), Sodium Acetate (≥98.5 %, TCI), Caesium Carbonate (99 %, Sigma Aldrich), 2,2,2-Trifluoroethanol (Merck), Decane (>99 %, Sigma Aldrich), Aluminium Chloride (>98 %, Merck), Iron(III) Chloride (>98 %, Merck), 1-Methylimidazole (99 %, abcr) were purchased and used as received. For the synthesis of the ligands, (6-Bromopyridin-2-yl)methanol (95 %, abcr), Methanesulfonyl chloride (98 %, Alfa Aesar), Pyrazole (>98 %, TCI), Sodium Hydride (90 %, Sigma Aldrich), 2-(Chloromethyl)pyridine Hydrochloride (>97 %, TCI), 2-Picolylamine (>98 %, TCI), Cyanuric chloride (99 %, Sigma Aldrich), 2-Aminopyridine (>99 %, TCI), Acetylacetone (>99 %, Sigma Aldrich), 2,6-Diisopropylaniline (>90 %, Alfa Aesar), n-Butyllithium solution (2.5 M in hexane, Sigma Aldrich), 1-[2-Oxo-2-(2-pyridinyl)ethyl]pyridinium iodide (>97 %, TCI), 3-(Dimethylamino)propiophenone hydrochloride (>98 %, TCI) were purchased and used as received.

2-Cyclohexen-1-one (≥95 %, Sigma Aldrich), 1-Cyclohexene-1-carboxylic acid (97 %, Sigma Aldrich), 2-Cyclohexen-1-ol (95 %, Sigma Aldrich), 1-Methyl-1-cyclohexene (97 %, Sigma Aldrich), 1-tert-Butyl-1-cyclohexene (technical 80 %. Sigma Aldrich), 3-Carene (≥90 %, Sigma Aldrich),1-Methylcyclopentene (98 %, Sigma Aldrich), (S)-(−)-Limonene (>95 %, TCI), 2-Cyclopenten-1-one (98 %, Sigma Aldrich), 3-Methyl-2-cyclopenten-1-one (97 %, Sigma Aldrich), Dicyclopentadiene (contains BHT as stabilizer, Sigma Aldrich), 2-Norbornene (>99 %, TCI), Cholesterol (≥99 %, Sigma Aldrich), 2-Ethynyl-1,4-dimethylbenzene (97 %, Sigma Aldrich), 3-Ethynylphenol (>98 %, TCI), 3-Ethynylaniline (≥98 %, Sigma Aldrich), 4-Ethynylaniline (97 %, Sigma Aldrich), 2-Ethynylbenzaldehyde (>95 %, TCI), 1-Pentyne (>98 %, TCI), 1-Decyne (>95 %, TCI), 3-Ethynylthiophene (96 %, Sigma Aldrich), 2-Ethynylpyridine (98 %, Sigma Aldrich), 3-Ethynylpyridine (98 %, Sigma Aldrich), (−)-Terpinen-4-ol (≥95 %, Sigma Aldrich), (1R)-(−)-Myrtenol (95 %, Sigma Aldrich), (R)-(−)-Carvone (98 %, Sigma Aldrich), (1S)-(−)-Verbenone (94 %, Sigma Aldrich), (S)-cis-Verbenol (95 %, Sigma Aldrich), 2,4-Pentanedione (≥99 %, Sigma Aldrich), Ethynylbenzene (>98 %, TCI), Dimethyl malonate

(98 %, Sigma Aldrich), Allylamine (98 %, Sigma Aldrich), Allyl Acetate (>97 %, TCI), N,N-Dimethylallylamine (>98 %, TCI), N-Methylpyrrole (99 %, Sigma Aldrich), Nitromethane (≥95 %, Sigma Aldrich), 2,2,6,6-Tetramethylpiperidine 1-oxyl (98 %, Sigma Aldrich), 3,5-Di-tert-4-butylhydroxytoluene (99 %, Sigma Aldrich), Styrene (>99 %, Sigma Aldrich), Ascorbic acid (99 %, Sigma Aldrich), 3-Bromocyclohexene (90 % technical grade, Sigma Aldrich) were purchased and used without any further purification.

Solvents for moisture or oxygen sensitive compounds and reactions were obtained commercially via Sigma-Aldrich or Acros Organics as dry solvents over mol sieves and under inert gas. Dry and degassed Acetonitrile was obtained from the solvent-purification-system MB-SPS-5 from MBraun and was prior to use degassed again via freeze-pump-thaw-methods. The solvent was stored in Schlenk tubes under Argon.

If not mentioned otherwise, the photoactivated reactions are conducted in a dedicated photoreactor (45 cm wide, 45 cm deep, 45 cm high) made from PVC with a UV-light filter. Into the reactor a ventilator is incorporated to regulate the temperature. Reactions are irradiated with two KESSIL Science PRL 390 nm LED light sources. The lights are placed about 20 cm apart with a light way of about 5 cm to the reaction vessel. For the screening of conditions, six reactions were performed simultaneously by placing them in two rows with three vials facing one light each. The setup is displayed in Figure 24.

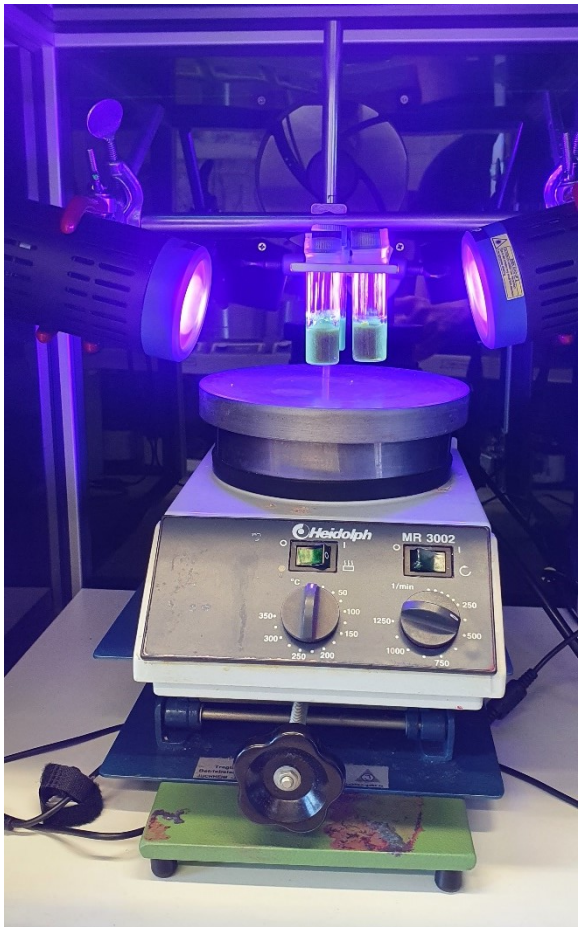

Figure 24: Standard reaction setup incorporating a magnetic stirring plate, two Kessil Science PRL 160 390 nm lights and a fan to regulate temperature. Six reactions can be performed simultaneously. The whole setup is contained in a protected box.

A.1.2. Characterization methods

A.1.2.1. Nuclear Magnetic Resonance Spectroscopy (NMR)

NMR spectra of the samples were measured on Bruker 300 MHz (AV300 or Fourier 300: ^{1}H = 300 MHz, ^{13}C = 75 MHz) or on Bruker 400 MHz (AV400: ^{1}H = 400 MHz, ^{13}C = 101 MHz, ^{19}F = 282 MHz, ^{31}P = 122 MHz) spectrometers. Spectra shifts are reported as δ-values in ppm relative to the deuterated solvent shift(s). Following solvents were used for referencing NMR spectra:

d_1-chloroform (^{1}H = 7.26 ppm, ^{13}C = 77 ppm), d_8-toluene (^{1}H = 2.08, 6.97, 7.01, 7.09 ppm, ^{13}C = 137.48, 128.87, 127.96, 125.13, 20.43 ppm), d_3-acetonitrile (^{1}H = 1.94 ppm, ^{13}C = 1.32, 118.26 ppm), d^2-dichloromethan (^{1}H = 5.32 ppm, ^{13}C = 53.84 ppm), d^6-dimethylsulfoxide (^{1}H = 2.49 ppm, ^{13}C = 7.0 ppm).

The abbreviations used to describe the multiplicity of the spectra peaks are: s (singlet), d (doublet), t (triplet), q (quadruplet), dd (doublet of doublets), dt (doublet of triplets), ddd (doublet of doublets of doublets) and m (multiplet), etc. Coupling constant J is reported in Hertz (Hz).

A.1.2.2. Infrared Spectroscopy (IR)

ATR infrared spectra of the samples were measured on Bruker Alpha-P spectrometer. All samples were measured neat. Liquid samples were measured in a film, while solid samples were pressed directly on to the IR-detector window. Adsorption bands are given in wave numbers (cm^{-1}) and were measured in the range from 400 to 4000 cm^{-1}

A.1.2.3. Mass Spectrometry: Electron spray ionization (ESI), Electron Ionisation (EI)

Samples for mass spectrometry were dissolved in tetrahydrofuran (THF), acetonitrile or dichloromethane depending on the solubility of the sample. Mass spectra were measured on an Agilent 6890/5973 (GC-MS), Agilent 7890/5977 (GC-MS), Agilent 1260/6130 Quadrupol (LC-MS), Agilent 1200/6210 Time-of-Flight (LC-MS). The ratio of mass to charge are indicated, intensities relative to the base peak (I = 100) are written in parentheses. High resolution mass spectra (HRMS) were recorded on Thermo Electron MAT 95-XP (EI) or Agilent 1200/6210 Time-of-Flight (ESI). Electron ionization (EI) spectra were performed at 70 eV using methane as the carrier gas, with time-of-flight (TOF) mass analyzer. Electrospray ionization (ESI) spectra were performed using a time-of-flight (TOF) mass analyzer.

A.1.2.4. Gas chromatography – Flame Ionization Detector (GC-FID)

Gas chromatography was measured on a Hewlett Packard/Agilent GC HP6890 and Agilent GC 7890A equipped with flame ionization detectors. Samples are prepared by taking 50 µl of sample directly from the reaction and 50 µl of an internal standard stock-

solution (0.235 mol·l^{-1} naphthalene in toluene) and adding it to a GC-vial. The sample is then diluted to 1 ml with acetonitrile (HPLC grade).

From this sample, 1 µl is injected into a preheated inlet (260 °C) and led onto the column (Agilent 19091J-413) with a split of 150:1. The oven is ramping up the temperature from 50 °C to 260 °C (8 °C·min^{-1}) and holding it for 5 min, then heating to 280 °C (8 °C·min^{-1}) and holding it for 5 min and lastly heating to 300 °C (8 °C·min^{-1}) and holding for 5 min for a total runtime of 46.25 min. The gas flow is run at a constant 1 ml·min^{-1}. Substances are detected at 320 °C with a hydrogen flow of 40 ml·ml^{-1} inside the FID.

A.1.2.5. Electron Paramagnetic Resonance (EPR) Spectroscopy

EPR measurements were conducted by adding a stock solution of the catalyst in Acetonitrile (c = 0.05 mmol·ml^{-1}) under exclusion of oxygen to a microcapillary glass tube (Hirschmann) and measuring immediately. To this, two equivalents of the peroxide were added and the sample was measured again. Subsequently, one equivalent of phenylacetylene and 20 equivalents of cyclohexene were added to the tube and measured in between. Radical trapping experiments were conducted by repeating the above mentioned steps and adding 10 µl of DMPO (Biotechnik GERBU) to the sample before measuring.

Time-resolved experiments were conducted in a flat-cell, that was flushed with argon prior to use. Equivalent amounts of reagents were added to the reactor, before it was irradiated at 395 nm.

A.1.2.6. Single-Crystal X-Ray Diffraction (XRD)

Crystallographic data were obtained on a Bruker KAPPA APEX II DUO diffractometer. The structure was solved by direct methods and refined by full-matrix least-squares procedures on F2. The SHELXTL[256] software package XP (Bruker AXS) was used for graphical representation. Displacement of ellipsoids are drawn at the 30 % probability.

A.1.2.7. Cyclovoltametry (CV)

All electrochemical investigations were performed at room temperature in 10 ml dried acetonitrile p.A. (VWR) under an argon atmosphere with 0.1 M tetrabutylammonium hexafluorophosphate as conducting salt using an Autolab (PGSTAT 204, METROHM). The solutions were purged with argon and an argon layer was maintained above the solutions during the electrochemical measurements. A glassy carbon disk electrode (d = 2 mm) was used as working electrode, a platinum electrode as the counter electrode and an $Ag/AgNO_3$ sat. in H_2O system as the reference electrode (all electrodes: METROHM). The measurements were performed with 20 µmol compound dissolved in the electrolyte. Differential pulse voltammetry (DPV) was conducted using a scan rate of 10 mV s^{-1}, step potential of 5 mV, modulation potential of 25 mV, modulation time of 0.05 s and interval time of 0.5 s in both oxidative and reductive direction.

A.1.3. Synthetic Protocols

All reactions involving moisture or air sensitive compounds were performed under argon atmosphere using standard Schlenk techniques. Argon was dried by passing it through a column with phosphorous pentoxide on silica (Siccapent). All glassware was oven-dried, evacuated and flushed with argon three times prior to usage. Syringes, needles and other tools were flushed with argon three times before use.

A.1.3.1. Synthesis of (cyclohex-2-en-1-ylethynyl)benzene and characterization of side products.

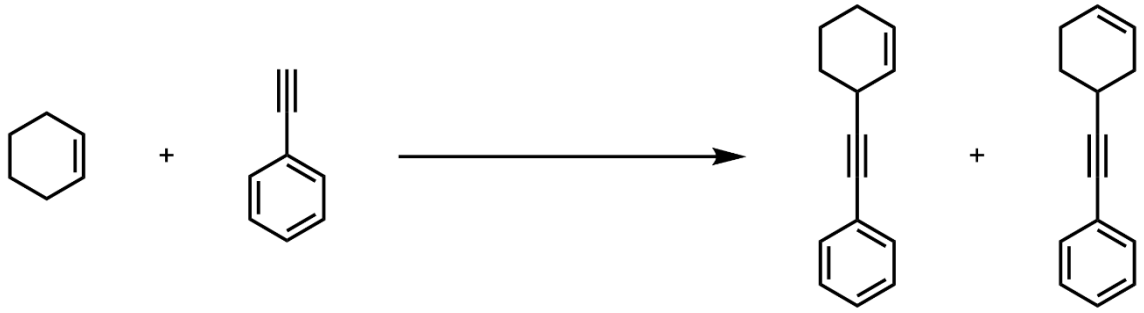

Scheme 43: Standard Reaction for the formation of (cyclohex-2-en-1-ylethynyl)benzene and its side product.

To an 8 ml screw cap vial with a magnetic stirring bar, 18.6 mg (0.05 mmol) of Tetrakisacetonitrile Copper(I) Hexafluorophosphate and 20.1 mg (0.05 mmol) of 4,4′,4″-Tri-tert-butyl-2,2′:6′,2″-terpyridine are added. The vial is then flushed with an Argon stream for 30 s before 1 ml of dry and degassed Acetonitrile is added via a syringe. The solution turns immediately to a dark brown/red. To this solution 181.9 µl (1 mmol) of the tert-Butyl hydroperoxide solution is added via a pipette. Following this, the solution turns green rapidly under sporadic evolution of a gas. Consequently, 51.1 µl (0.5 mmol) of Phenylacetylene and 1 ml (10 mmol) of cyclohexene are added to the vial, while stirring the mixture. The gas phase is then once again flushed with Argon before being sealed with the cap and parafilm. The vials are then placed in a photoreactor box between two lights with a distance of 5 cm each. The reaction is irradiated for 24 h with two Kessil Science PR160L 390 nm LED at 100 % Intensity. Afterwards, the reaction is quenched with 30 ml of water and extracted three times with 50 ml dichloromethane each. The crude product is then purified via Flash Column Chromatography using Pentane. After removing the solvent, (cyclohex-2-en-1-ylethynyl)benzene is obtained as a colorless oil with 89.3 mg (98 %, 0.49 mmol). The analytics were according to literature.[15] After exposition to oxygen, a second product is forming, which was characterized via 2d-NMR and identified as (cyclohex-3-en-1-ylethynyl)benzene.

^{1}H NMR (400 MHz, CD2Cl2) δ = 7.54 – 7.46 (m, 2H), 7.40 – 7.32 (m, 3H), 5.91 – 5.79 (m, 2H), 3.39 (tdd, J = 7.4, 3.0, 2.0 Hz, 1H), 2.18 – 2.03 (m, 3H), 1.99 – 1.84 (m, 2H), 1.74 – 1.64 (m, 1H).

^{13}C NMR (101 MHz, CD2Cl2) δ = 132.94, 131.97, 128.98, 128.68, 128.49, 128.05, 127.45, 124.46, 93.41, 80.69, 29.93, 28.54, 25.18, 21.18.

A.1.3.2. General Procedure for the Screening of Reaction conditions

All Reaction performed while optimizing the standard Reaction protocol were conducted according to this description. Deviations to this protocol are specially noted. To an 8 ml screw cap vial with a magnetic stirring bar, 18.6 mg (0.05 mmol) of Tetrakisacetonitrile Copper(I) Hexafluorophosphate and 20.1 mg (0.05 mmol) of 4,4′,4″-Tri-tert-butyl-2,2′:6′,2″-terpyridine are added. The vial is then flushed with an Argon stream for 30 s before 1 ml of dry and degassed Acetonitrile is added via a syringe. The solution turns immediately to a dark brown/red. To this solution 181.9 µl (1 mmol) of the tert-Butyl hydroperoxide solution is added via a pipette. Following this, the solution turns green rapidly under sporadic evolution of a gas. Consequently, 51.1 µl (0.5 mmol) of Phenylacetylene and 1 ml (10 mmol) of cyclohexene are added to the vial, while stirring the mixture. The gas phase is then once again flushed with Argon before being sealed with the cap and parafilm. The vials are then placed in a photoreactor box and the reaction is irradiated for 24 h with two Kessil Science PR160L 390 nm LED at 100 % Intensity. The reaction is irradiated for 24 h with two Kessil Science PR160L 390 nm LED at 100 % Intensity. After the reaction has finished, the lights are shut off and a sample is taken and analyzed via GC-FID and GC-MS with Naphtalene as an internal Standard. The yield is calculated based on the resulting peak area of the product in reference to the peak area of phenylacetylene and 1,4-Diphenylbutadiyne. An exemplary calculation with calibration curves and chromatogram can be found in Chapter A.1.

A.1.3.3. Synthesis of (6-bromopyridin-2-yl)methyl methanesulfonate

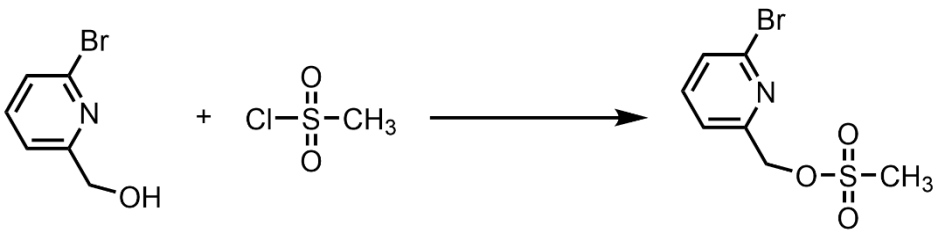

Scheme 44: Synthesis of (6-bromopyridin-2-yl)methyl methanesulfonate

The ligand was synthesized according to a reported protocol.[172] An oven-dried 25 ml Schlenk flask equipped with a magnetic stirring bar is evacuated refilled with Argon three times. To this 5 ml of anhydrous Methylene Chloride are added under argon through a septum with a syringe. Following this, 5 mmol of (6-bromopyridin-2-yl)methanol are added to the flask. The mixture is stirred under Argon and cooled down to 0 °C. Consequently, 11 mmol of Triethyl amine and 13 mmol of Methanesulfonyl chloride is added via syringe under a constant Argon stream to the solution. The resulting yellow mixture is then gradually warmed to room temperature and stirred for additional 15 min before being quenched with 5 ml of water. Subsequently, the reaction mixture is extracted two times with 20 ml of Diethylether. The combined organic phases are washed with a saturated solution of Ammonium chloride and dried with Sodium sulfate. The solvent is then removed under vacuo yielding (6-bromopyridin-2-yl)methyl methanesulfonate 1.217 g (93 %). It is used without any further purification.

A.1.3.4. Synthesis of 2-((1H-pyrazol-1-yl)methyl)-6-(1H-pyrazol-1-yl)pyridine (L8)

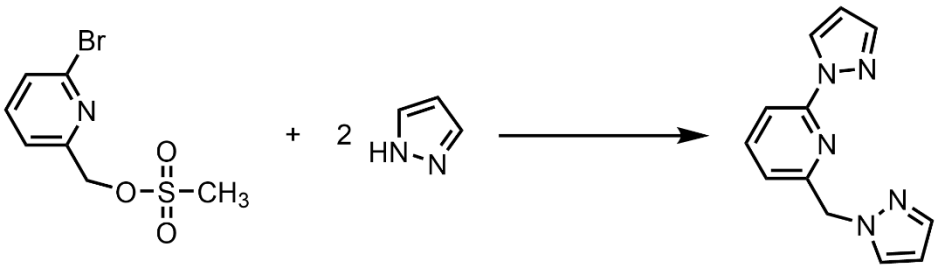

Scheme 45: Synthesis of 2-((1H-pyrazol-1-yl)methyl)-6-(1H-pyrazol-1-yl)pyridine (L8)

An oven-dried 50 ml Schlenk flask equipped with a magnetic stirring bar is evacuated and refilled with Argon three times. To this 12.14 mmol of Sodium hydride is added in a glove box. The flask is then sealed and removed from the glovebox. Consequently, 10 ml of bis(2-methoxyethyl) ether to the solid via a syringe through a septum under constant Argon stream. Following this, 10 mmol of pyrazole suspended in 10 ml of bis(2-methoxyethyl) ether is added dropwise to the mixture via a dropping funnel. This dispersion is then stirred at 70 °C for 90 min before a solution of 4.57 mmol of (6-

bromopyridin-2-yl)methyl methanesulfonate is added slowly to the reaction. The mixture is then heated at 130 °C for 24 h under Argon. After letting it cool to room temperature, 30 ml of water is added to the solution and then extracted three times with Ethyl acetate (10 ml) and consequently dried over sodium sulfate. The crude product is then purified via Flash Column Chromatography using Ethyl Acetate and Heptane (1:1) as eluents. It is then dried under high vacuum for a day to remove traces of solvent. The product is a colorless oil and yielded with 658 mg (63 %, 2.9 mmol). Analytics were according to literature.[172]

^{1}H NMR (300 MHz, CDCl3) δ = 8.45 (dd, J = 2.6, 0.7 Hz, 1H), 7.78 (m, 1H), 7.68 – 7.56 (m, 2H), 7.51 (m, 2H), 6.73 (m, 1H), 6.36 (dd, J = 2.6, 1.7 Hz, 1H), 6.25 (m, 1H), 5.35 (s, 2H).

^{13}C NMR (75 MHz, CDCl3) δ = 155.27, 150.84, 141.98, 139.82, 139.80, 139.53, 130.00, 126.89, 118.68, 111.04, 107.64, 106.09.

MS (ESI-TOF): *m/z* calcd $[M + H]^+$: 226.11; found: 226.1090, *m/z* calcd $[M+Na]^+$: 248.09; found: 248.0911.

A.1.3.5. Synthesis of tris(pyridin-2-ylmethyl)amine (L9)

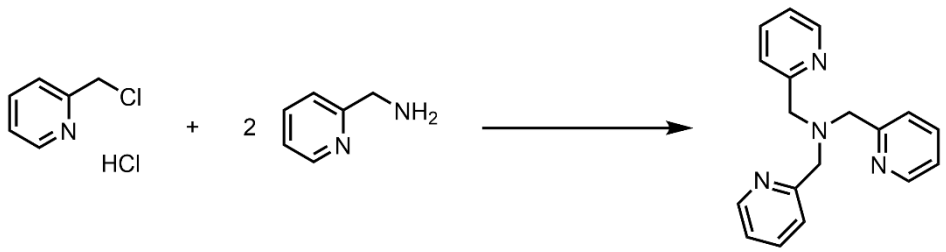

Scheme 46: Synthesis of tris(pyridin-2-ylmethyl)amine (L9)

The ligand was synthesized according to literature procedure.[257] To a 100 ml round-bottomed flask with a magnetic stirrer 20 ml of distilled water is added. To that 46.24 mmol of 2-Picolylchloride is added. Subsequently, 23.12 mmol of 2-(aminomethyl)pyridine is added to the solution. Consequently, 10 ml of 10 M solution of Sodium hydroxide in distilled water is added dropwise slowly while stirring over the course of 2 h. Then, the reaction is heated for 30 min at 70 °C and then cooled to room

temperature. The product is extracted with Chloroform (3x150 ml) and the combined organic phases are dried over Sodium sulfate. The crude product is purified via Flash Column Chromatography with Ethyl Acetate and heptane (1:1). A dark brown solid is obtained with 5.388 g (80 %, 18.56 mmol). Analytics were according to literature.[257]

^{1}H NMR (300 MHz, CD2Cl2) δ = 8.50 (ddd, J = 4.9, 1.8, 1.0 Hz, 3H), 7.72 – 7.56 (m, 6H), 7.14 (ddd, J = 7.3, 4.9, 1.5 Hz, 3H), 3.84 (s, 6H).

^{13}C NMR (75 MHz, CD2Cl2) δ = 160.04, 149.39, 136.58, 123.15, 122.25, 60.53.

MS (ESI-TOF): *m/z* calcd $[M + H]^+$: 291.1609; found: 291.1608.

A.1.3.6. Synthesis of N2,N4,N6-tri(pyridin-2-yl)-1,3,5-triazine-2,4,6-triamine (L10)

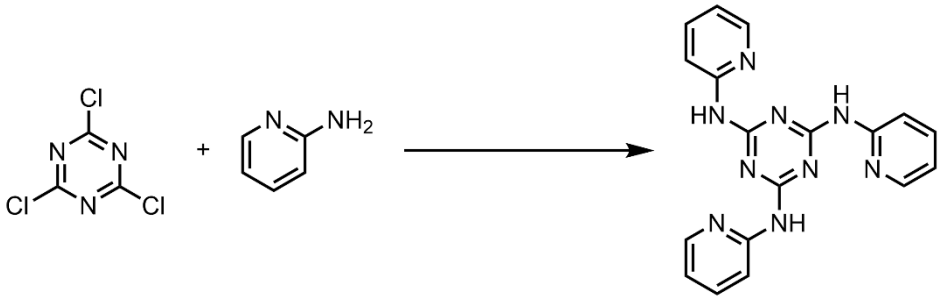

Scheme 47: Synthesis of N2,N4,N6-tri(pyridin-2-yl)-1,3,5-triazine-2,4,6-triamine (L10)

The synthesis was taken from Literature.[173] An oven-dried 50 ml Schlenk flask with a magnetic stirring bar is evacuated and refilled with Argon three times. To this 5 mmol of Cyanuric Chloride are added under an Argon stream. Consequently, 25 ml of N,N-Diisopropylethylamine and 10 ml of dry Acetonitrile are added while cooling the mixture down to -5 °C. Following this, 15 mmol of 2-aminopyridine are added dropwise through a dropping funnel. Subsequently, the mixture is stirred 2 h and then heated to 70 °C for 12 h. After cooling to room temperature, the solvent is removed under vacuo and the bright yellow solid is washed with Ethanol, chloroform and diethylether. After drying it under high vacuum a yellow powder is obtained in 1.658 g (92 %, 4.64 mmol). Analytics were according to the literature.[173]

MS (EI-MS): *m/z* calcd $[M]^+$: 357.14449; found: 357.14360.

A.1.3.7. Synthesis (2E,4E)-N2,N4-bis(2,6-diisopropylphenyl)pentane-2,4-diimine

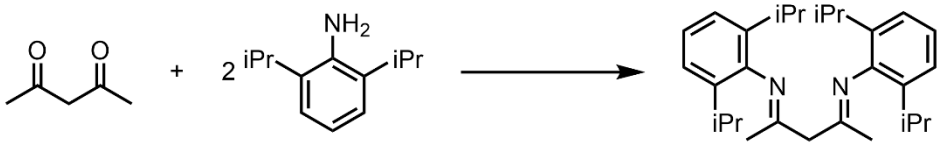

Scheme 48: Synthesis of (2E,4E)-N2,N4-bis(2,6-diisopropylphenyl)pentane-2,4-diimine

The synthesis was conducted according to a procedure reported in literature.[258] To a 500 ml flask 44.45 mmol of 2,4-pentadione, 107.73 mmol of 2,6-diisopropylaniline and 5 ml of Hydrochloric Acid (12 M) are added and stirred with a magnetic stirring bar. The reaction is heated for 3 days under reflux. After letting the mixture cool to room temperature, the solvent is removed under vacuo. The residue is then refluxed in 300 ml of heptane for 1 h. Afterwards, the solid is filtered off and treated with 200 ml of aqueous Sodium carbonate and 300 ml of dichloromethane until the solid dissolves. The organic layer is then separated and dried with magnesium sulfate. Lastly, the supernatant is filtered and the solvent is removed under vacuo. The remaining grey solid is washed with cold (0 °C) methanol and dried under vacuo. A grey solid with 16.348 g (87 %, 39.08 mmol). Analytics were according to reports in literature.[258]

^{1}H NMR (300 MHz, CD2Cl2) δ = 12.05 (s, 1H), 7.12 (s, 6H), 4.91 (s, 1H), 3.12 (h, J = 6.9 Hz, 4H), 1.71 (s, 6H), 1.17 (dd, J = 28.6, 6.9 Hz, 24H).

^{13}C NMR (75 MHz, CD2Cl2) δ = 161.56, 142.94, 141.30, 125.47, 123.35, 93.75, 28.59, 24.46, 23.31, 20.93.

A.1.3.8. Synthesis of lithium (2E,4E)-2,4-bis((2,6-diisopropylphenyl)imino)pentan-3-ide (L12)

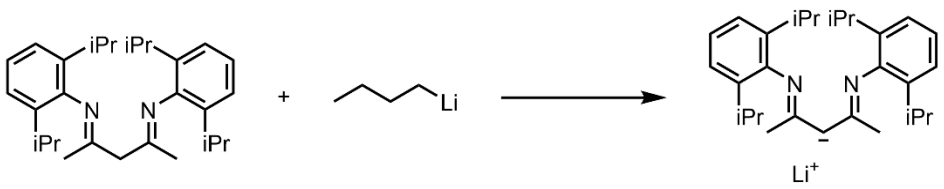

Scheme 49: Synthesis of lithium (2E,4E)-2,4-bis((2,6-diisopropylphenyl)imino)pentan-3-ide (L12)

The procedure was adapted from literature.[258] An oven-dried three-necked round-bottomed flask with a magnetic stirring bar is evacuated and refilled with Argon three times. The flask is equipped with a thermometer and then 19.1 mmol of (2E,4E)-N2,N4-bis(2,6-diisopropylphenyl)pentane-2,4-diimine are added to it under a steady stream of Argon. To this, 60 ml of dry tetrahydrofurane is added. The mixture is cooled to -20 °C with a sodium chloride/ice bath. Then 8 ml of a 2.5 M n-butyl lithium solution in hexane is added dropwise slowly via a syringe through a septum. The mixture is then allowed to slowly heat to room temperature and it is stirred overnight. The following day, the solvent is removed under vacuo until a precipitate is forming. It is redissolved via heating and consequently cooled to -20 °C to obtain colorless crystals in 4.874 g (60 %, 11.48 mmol). Analytics were according to the reports in literature.[258]

^{1}H NMR (300 MHz, C6D6) δ = 7.26 – 7.09 (m, 6H), 5.06 (s, 1H), 3.47 (p, J = 6.9 Hz, 4H), 1.96 (s, 6H), 1.34 (d, J = 6.9 Hz, 12H), 1.26 – 1.22 (d, J = 6.9 Hz, 12H).

^{13}C NMR (75 MHz, C6D6) δ = 163.55, 149.56, 140.90, 123.27, 67.92, 28.13, 24.93, 24.45, 23.53, 23.17.

MS (ESI-TOF): *m/z* calcd $[M + H]^+$: 417.3265; found: 417.3271.

A.1.3.9. Synthesis of 6-phenyl-2,2'-bipyridine (L13)

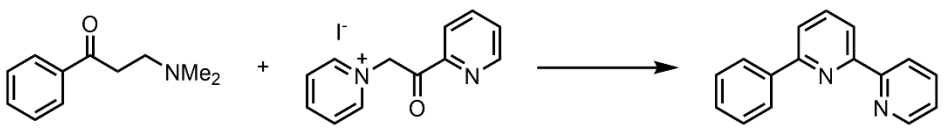

Scheme 50: Synthesis of 6-phenyl-2,2'-bipyridine (L13)

The procedure was adapted from literature.[259] To a 100 ml round-bottomed flask 8 mmol of 1-[2-Oxo-2-(2-pyridyl)ethyl]-pyridinium Iodide and 80 mmol of ammonium acetate are added. Consequently, 20 ml of glacial acetic acid are added to the reaction. To this, 8 mmol of 3-(dimethylamino)propiophenone is added before the mixture is heated to reflux for 22 h. After letting the reaction cool to room temperature the solvent is removed under vacuo. The dark brown oil is then dissolved in 100 ml of distilled water and extracted with 100 ml of chloroform. The crude product is then purified via flash column chromatography with Ethylacetate and Heptane (1:1). After removing the solvent, white crystals are obtained in 1.254 g (68 %, 5.4 mmol). Analytics were according to reports in literature.[259]

^{1}H NMR (300 MHz, CDCl3) δ = 8.70 (ddd, J = 4.8, 1.8, 0.9 Hz, 1H), 8.65 (dt, J = 8.0, 1.1 Hz, 1H), 8.39 (dd, J = 7.7, 1.0 Hz, 1H), 8.20 – 8.12 (m, 2H), 7.93 – 7.74 (m, 3H), 7.56 – 7.41 (m, 3H), 7.32 (ddd, J = 7.5, 4.8, 1.2 Hz, 1H).

^{13}C NMR (75 MHz, CDCl3) δ = 156.54, 156.48, 155.84, 149.17, 139.46, 137.82, 136.98, 129.14, 128.85, 127.06, 123.86, 121.43, 120.41, 119.42.

MS (ESI-TOF): *m/z* calcd $[M + H]^+$: 233.39; found: 233.1082.

A.1.3.10. General Procedure for the testing of new allylic substrates

The test reaction for new allylic substrates were conducted according to the following procedure if not mentioned otherwise. To a 10 ml pressure tube with an olive on the side a magnetic stirring bar is added. Then 18.6 mg (0.05 mmol) of Tetrakisacetonitrile Copper(I) Hexafluorophosphate and 20.1 mg (0.05 mmol) 4,4′,4″-Tri-tert-butyl-2,2′:6′,2″-terpyridine are added to the tube. The setup is then evacuated and flushed with Argon three times. Consequently, 1 ml of dry and degassed Acetonitrile is added upon which the solution turns dark brown/red. Following this, 181.9 µl (1 mmol) of tert-Butyl hydroperoxide is added via a pipette. Subsequently, 51.1 µl (0.5 mmol) of Phenylacetylene and 10 mmol of the allylic substrate are added via a pipette. The reaction is then heated in an oil bath at 80 °C for 24 h while being stirred. Upon completion, the

reaction is cooled to room temperature and then quenched with 25 ml of distilled water. The suspension is then extracted three times with 50 ml of Dichloromethane each. The crude product is then purified via Flash Column Chromatography and analyzed via NMR and ESI-TOF MS.

A.1.3.10.1. 1-methylcyclohex-1-ene (A4)

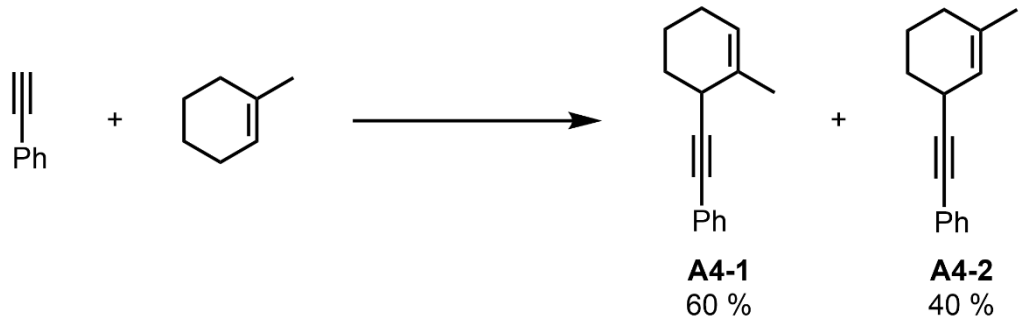

Scheme 51: Synthesis of ((2-methylcyclohex-2-en-1-yl)ethynyl)benzene (**A4-1**) and ((2-methylcyclohex-2-en-1-yl)ethynyl)benzene (**A4-2**).

1-methylcyclohex-1-ene (10 mmol, 961.7 mg) and phenylacetylene (0.5 mmol, 51.1 mg) afforded after separation with pentane a mixture of ((2-methylcyclohex-2-en-1-yl)ethynyl)benzene (**A4-1**) and ((3-methylcyclohex-2-en-1-yl)ethynyl)benzene (**A4-2**) in ratio of 3:2 as a colorless oil. The mixture could not be separated. Total yield: 64.9 mg (66 %, 0.33 mmol). **^{1}H NMR** (300 MHz, CDCl3) δ = 7.48 – 7.40 (m, 2H), 7.33 – 7.25 (m, 3H), 5.48 (dq, J = 3.2, 1.6 Hz, 1H), 3.30 (dtt, J = 7.2, 3.3, 1.6 Hz, 1H), 2.14 – 1.75 (m, 4H), 1.75 – 1.68 (m, 3H), 1.68 – 1.51 (m, 1H). **^{13}C NMR** (75 MHz, CDCl3) δ = 135.45, 131.72, 131.68, 128.27, 128.21, 127.57, 124.11, 121.21, 93.50, 80.16, 29.76, 29.29, 28.40, 23.92, 21.19. **EI-MS**, m/z: 196 $[M\text{-}CH_3]^+$ (100 %), 181 $[C_{14}H_{13}]^+$, 167 $[C_{13}H_{11}]^+$, 153 $[C_{12}H_9]^+$, 128 $[C_{10}H_8]^+$, 115 $[C_9H_7]^+$, 91 $[C_7H_7]^+$, 77 $[C_6H_5]^+$.

A.1.3.10.2. 1-(tert-butyl)cyclohex-1-ene (A5)

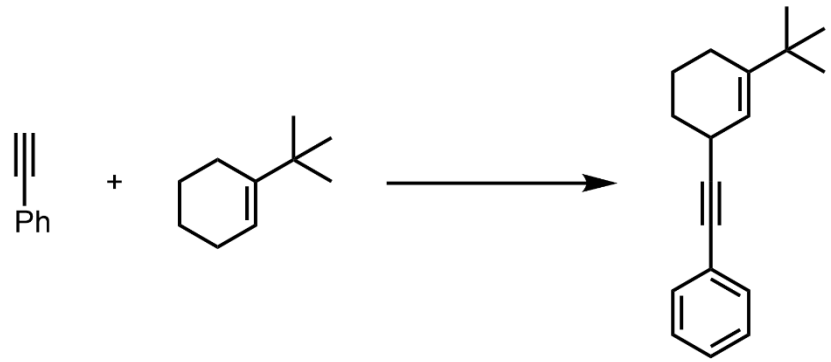

A5-1

Scheme 52: Synthesis of ((3-(tert-butyl)cyclohex-2-en-1-yl)ethynyl)benzene (**A5-1**).

1-(tert-butyl)cyclohex-1-ene (10 mmol, 1382.5 mg) and phenylacetylene (0.5 mmol, 51.1 mg) afforded after separation with pentane ((3-(tert-butyl)cyclohex-2-en-1-yl)ethynyl)benzene (**A5-1**) as a colorless oil. Yield: 66.2 mg (55 %, 0.277 mmol). **^{1}H NMR** (300 MHz, CDCl3) δ = 7.55 – 7.41 (m, 2H), 7.41 – 7.26 (m, 3H), 5.58 – 5.55 (m, 1H), 3.43 – 3.33 (m, 1H), 2.18 – 1.85 (m, 5H), 1.85 – 1.71 (m, 1H), 1.70 – 1.55 (m, 2H), 1.12 (s, 9H). **^{13}C NMR** (75 MHz, CDCl3) δ = 146.66, 131.77, 128.25, 127.57, 117.89, 94.01, 80.05, 35.57, 29.55, 29.17, 29.14, 29.10, 28.81, 25.66, 24.63, 24.30, 23.67, 22.73, 21.95. **EI-MS**, m/z: 238 $[M\text{-}CH_3]^+$, 223 $[C_{17}H_{19}]^+$, 195 $[C_{15}H_{15}]^+$, 181 $[C_{14}H_{13}]^+$ (100 %), 165 $[C_{13}H_{10}]^+$, 152 $[C_{12}H_8]^+$, 141 $[C_{11}H_{10}]^+$, 128 $[C_{10}H_8]^+$, 115 $[C_9H_7]^+$, 91 $[C_7H_7]^+$, 77 $[C_6H_5]^+$.

A.1.3.10.3. (+)-3-Caren (A6)

(+)-3-Caren (10 mmol, 1362.3 mg) and phenylacetylene (0.5 mmol, 51.1 mg) were reacted under standard conditions. After separation with pentane, a colorless oil was obtained. Characterization of the reaction product via NMR spectroscopy was not successful. However, a product with the desired mass was found in the HR-EI-MS (for GC/MS see Appendix). **HR-EI-MS**, *m/z* calcd $[M]^+$: 236.15659; found: 236.155595.

A.1.3.10.4. *S*-Limonene (A7)

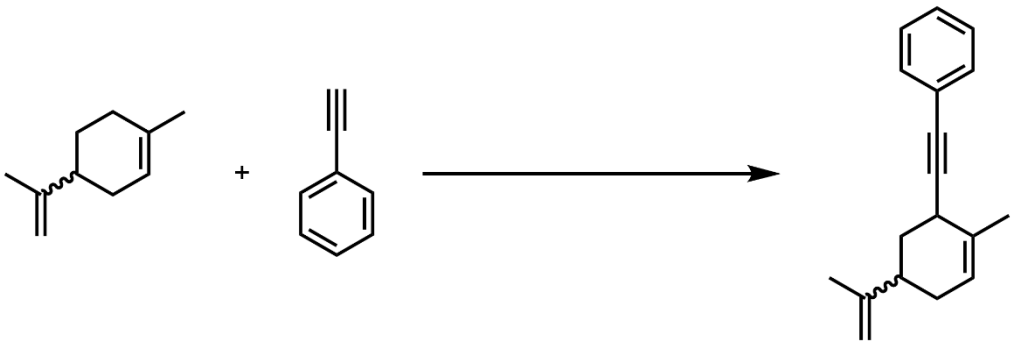

Scheme 53: Synthesis of ((2-methyl-5-(prop-1-en-2-yl)cyclohex-2-en-1-yl)ethynyl)benzene (**A7-1**).

S-Limonene (10 mmol, 1362.4 mg) and phenylacetylene (0.5 mmol, 51.1 mg) afforded after separation with pentane ((2-methyl-5-(prop-1-en-2-yl)cyclohex-2-en-1-yl)ethynyl)benzene (**A7-1**) as a mixture of Enantiomers. Yield: 51.2 mg (43 %, 0.22 mmol). **^{1}H NMR** (300 MHz, CDCl3) δ = 7.45 – 7.31 (m, 2H), 7.31 – 7.18 (m, 3H), 5.56 – 5.32 (m, 1H), 4.87 – 4.80 (m, 1H), 4.78 – 4.64 (m, 1H), 3.20 – 3.12 (m, 1H), 2.58 – 1.86 (m, 2H), 1.86 – 1.61 (m, 6H), 1.61 – 1.33 (m, 1H). **^{13}C NMR** (75 MHz, CDCl3) δ = 149.55, 131.77, 131.72, 128.32, 128.26, 128.21, 127.66, 127.59, 122.72, 108.95, 87.54, 80.98, 47.81, 34.05, 33.44, 32.88, 22.43. **EI-MS**, m/z: 236 $[M\text{-}CH_3]^+$, 221 $[C_{17}H_{18}]^+$, 193 $[C_{15}H_{13}]^+$, 178 $[C_{14}H_{10}]^+$, 167 $[C_{13}H_9]^+$ (100 %), 152 $[C_{12}H_8]^+$, 141 $[C_{11}H_{10}]^+$, 115 $[C_9H_7]^+$, 91 $[C_7H_7]^+$.

A.1.3.10.5. 1-methylcyclopent-1-ene (A8)

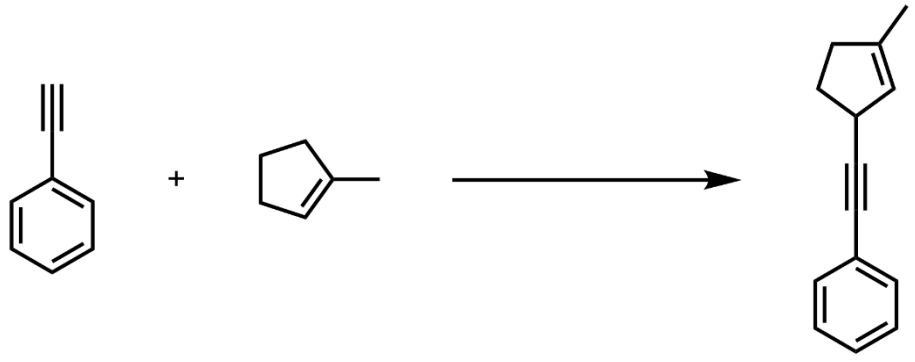

A8-1

Scheme 54: Synthesis of ((3-methylcyclopent-2-en-1-yl)ethynyl)benzene (**A8-1**)

1-methylcyclopent-1-ene (10 mmol, 821.4 mg) and phenylacetylene (0.5 mmol, 51.1 mg) afforded after separation with pentane ((3-methylcyclopent-2-en-1-yl)ethynyl)benzene (**A8-1**). Yield: 46.4 mg (51 %, 0.25 mmol). **^{1}H NMR** (300 MHz, CDCl3) δ = 7.40 – 7.33 (m, 2H), 7.26 – 7.20 (m, 3H), 5.32 (tt, J = 2.1, 1.6 Hz, 1H), 3.72 – 3.62 (m, 1H), 2.45 – 2.17 (m, 3H), 2.09 – 1.94 (m, 1H), 1.74 (ddt, J = 2.1, 1.6, 1.1 Hz, 3H). **^{13}C NMR** (75 MHz, CDCl3) δ = 142.23, 131.71, 128.26, 127.60, 124.95, 36.76, 36.46, 32.56, 16.68. **HR-EI-MS**, *m/z* calcd $[C_{14}H_{14}]^{+}$: 182.10857; found: 182.10900, *m/z* calcd $[C_{14}H_{13}]^{+}$: 181.10127; found: 181.10118.

A.1.3.10.6. Dicyclopentadiene (A11)

Dicyclopentadiene (10 mmol, 1322 mg) and phenylacetylene (0.5 mmol, 51.1 mg) were reacted under standard conditions. After separation with pentane, a colorless oil was obtained. Characterization of the reaction product via NMR spectroscopy was not successful. However, a product with the desired mass was found in the GC-MS (EI) (see Appendix).

A.1.3.10.7. Cholesterol (A13)

Cholesterol (1 mmol, 386 mg) and phenylacetylene (0.05 mmol, 5.1 mg) were reacted with 0.1 mmol of *tert*-Butyl hydroperoxide (9 mg), 0.01 mmol Copper(I)

Hexafluorophosphate (1.9 mg) and 0.01 mmol 4,4′,4″-Tri-tert-butyl-2,2′:6′,2″-terpyridine (2.0 mg) in 1 ml of Acetonitrile according to the general procedure. The workup with pentane did not yield any product. However, traces of the product were observed in the EI-MS (see Appendix).

A.1.3.11. General Procedure for Acetylenic Substrates

The test reaction for new acetylenic substrates were conducted according to the following procedure if not mentioned otherwise. To a 10 ml pressure tube with an olive on the side a magnetic stirring bar is added. Then 18.6 mg (0.05 mmol) of Tetrakisacetonitrile Copper(I) Hexafluorophosphate and 20.1 mg (0.05 mmol) 4,4′,4″-Tri-tert-butyl-2,2′:6′,2″-terpyridine are added to the tube. The setup is then evacuated and flushed with Argon three times. Consequently, 1 ml of dry and degassed Acetonitrile is added upon which the solution turns dark brown/red. Following this, 181.9 µl (1 mmol) of tert-Butyl hydroperoxide is added via a pipette. Subsequently, 0.5 mmol of Acetylenic Substrate and 821.5 mg (10 mmol) of cyclohexene are added via a pipette. The reaction is then heated in an oil bath at 80 °C for 24 h while being stirred. Upon completion, the reaction is cooled to room temperature and then quenched with 25 ml of distilled water. The suspension is then extracted three times with 50 ml of Dichloromethane each. The crude product is then purified via Flash Column Chromatography and analyzed via NMR and ESI-TOF MS.

A.1.3.11.1. 2-ethynyl-1,4-dimethylbenzene (B1)

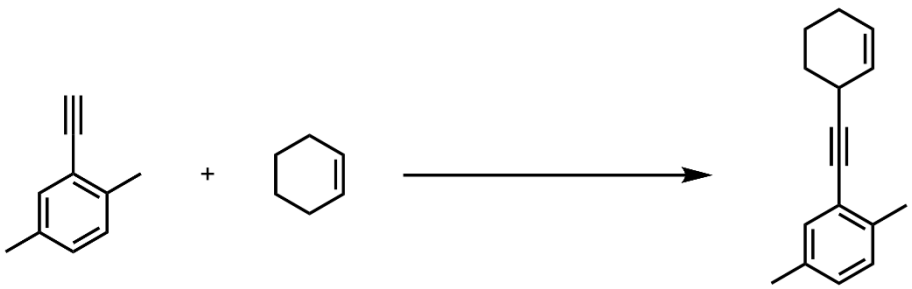

B1-1

Scheme 55: Synthesis of 2-(cyclohex-2-en-1-ylethynyl)-1,4-dimethylbenzene (**B1-1**)

Cyclohexene (10 mmol, 821.5 mg) and 2-ethynyl-1,4-dimethylbenzene (0.5 mmol, 65.1 mg) afforded after separation with pentane 2-(cyclohex-2-en-1-ylethynyl)-1,4-dimethylbenzene (**B1-1**). Yield: 84.4 mg (80 %, 0.4 mmol). Analytics were according to literature.[15] **^{1}H NMR** (300 MHz, CDCl3) δ = 7.28 – 7.18 (m, 2H), 7.16 – 6.93 (m, 3H), 5.83 – 5.71 (m, 1H), 3.43 – 3.29 (m, 1H), 2.43 – 2.35 (m, 3H), 2.34 – 2.21 (m, 3H), 2.13 – 1.54 (m, 6H). **^{13}C NMR** (75 MHz, CDCl3) δ = 136.99, 134.91, 132.40, 132.36, 129.43, 129.39, 129.28, 129.26, 128.53, 128.51, 127.99, 127.42, 123.49, 96.65, 79.51, 78.52, 29.71, 28.29, 24.83, 20.84, 20.76, 20.31.

A.1.3.11.2. 2-ethynylphenol (B2)

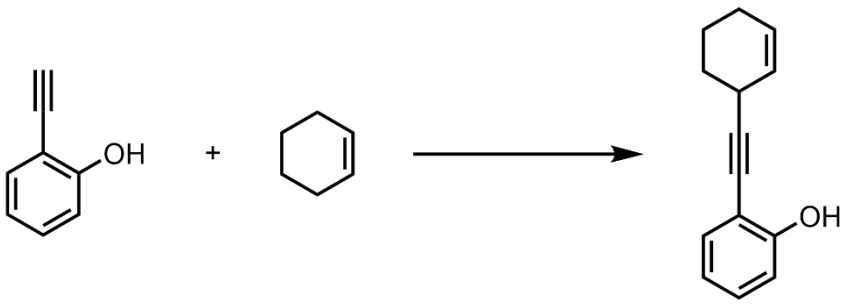

B2-1

Scheme 56: Synthesis of 2-(cyclohex-2-en-1-ylethynyl)phenol (**B2-1**)

Cyclohexene (10 mmol, 821.5 mg) and 2-ethynylphenol (0.5 mmol, 59.1 mg) afforded after separation with ethyl acetate and pentane (1:2) 2-(cyclohex-2-en-1-ylethynyl)phenol (**B2-1**). Yield: 53.5 mg (53 %, 0.26 mmol). Analytics were according to literature.[15] **^{1}H NMR** (300 MHz, CDCl3) δ = 7.20 – 7.08 (m, 1H), 6.99 – 6.93 (m, 1H), 6.90 – 6.87 (m, 1H), 6.79 – 6.73 (m, 1H), 5.81 – 5.74 (m, 1H), 5.74 – 5.68 (m, 1H), 5.68 – 5.67 (m, 0H), 3.33 – 3.23 (m, 1H), 2.13 – 1.91 (m, 3H), 1.91 – 1.68 (m, 2H), 1.68 – 1.50 (m, 1H). **^{13}C NMR** (75 MHz, CDCl3) δ = 155.60, 152.20, 129.50, 128.21, 127.05, 124.20, 118.50, 115.24, 92.98, 80.15, 29.42, 28.08, 24.77, 20.74.

A.1.3.11.3. 3-ethynylaniline (B3)

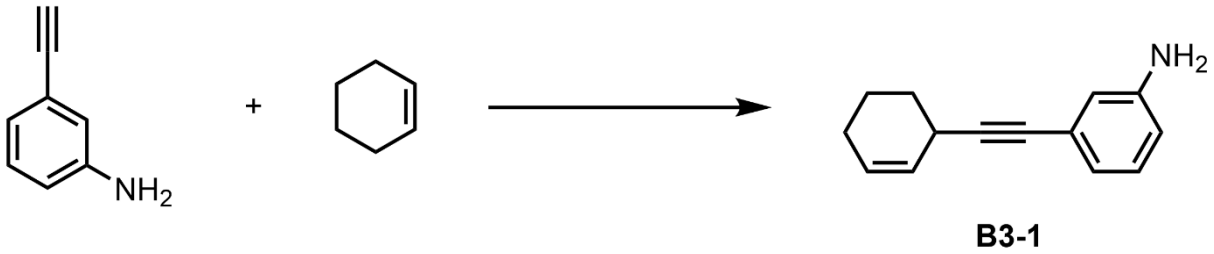

Scheme 57: Synthesis of 3-(cyclohex-2-en-1-ylethynyl)aniline (**B3-1**).

Cyclohexene (10 mmol, 821.5 mg) and 3-ethynylaniline (0.5 mmol, 58.6 mg) afforded 3-(cyclohex-2-en-1-ylethynyl)aniline (**B3-1**). The separation with ethyl acetate and pentane (1:2) was not successful and only a crude mixture was obtained. Further efforts to purify the product did not obtain a clean product. Hence no yield was determined. The crude NMR can be found in the Appendix. Mass of crude product: m = 44.6 mg. **MS (ESI-TOF):** *m/z* calcd $[M + H]^+$: 198.1283; found: 198.1287.

A.1.3.11.4. 4-ethynylaniline (B4)

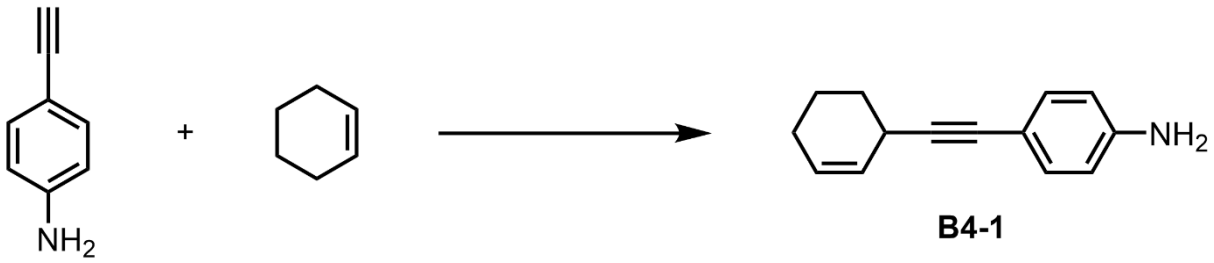

Scheme 58: Synthesis of 4-(cyclohex-2-en-1-ylethynyl)aniline (**B4-1**).

Cyclohexene (10 mmol, 821.5 mg) and 4-ethynylaniline (0.5 mmol, 58.6 mg) afforded 4-(cyclohex-2-en-1-ylethynyl)aniline (**B4-1**). The separation with ethyl acetate and pentane (1:2) was not successful and only a crude mixture was obtained. Further efforts to purify the product did not obtain a clean product. Hence no yield was determined. The crude NMR can be found in the Appendix. Mass of crude product: m = 27.1 mg. **MS (ESI-TOF):** *m/z* calcd $[M + H]^+$: 198.1283; found: 198.1282.

A.1.3.11.5. 2-ethynylbenzaldehyde (B5)

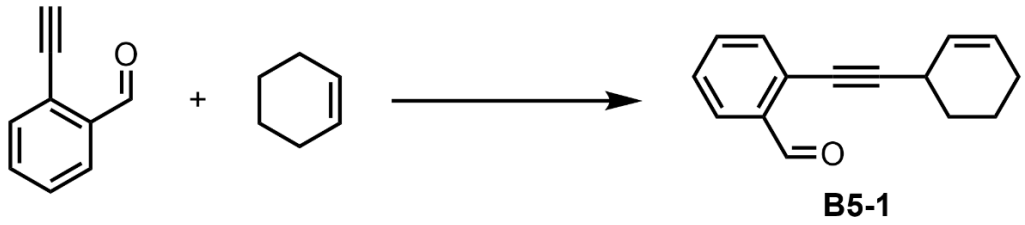

B5-1

Scheme 59: Synthesis of 2-(cyclohex-2-en-1-ylethynyl)benzaldehyde (**B5-1**).

Cyclohexene (10 mmol, 821.5 mg) and 2-ethynylbenzaldehyde (0.5 mmol, 65.1 mg) afforded 2-(cyclohex-2-en-1-ylethynyl)benzaldehyde (**B5-1**). The separation with ethyl acetate and pentane (1:2) was not successful and only a crude mixture was obtained. Further efforts to purify the product did not obtain a clean product. Hence no yield was determined. The crude NMR can be found in the Appendix. Mass of crude product: m = 12.6 mg. **MS (EI-MS):** *m/z* calcd $[M]^+$: 210.10392; found: 210.10349.

A.1.3.11.6. 3-ethynylthiophene (B6)

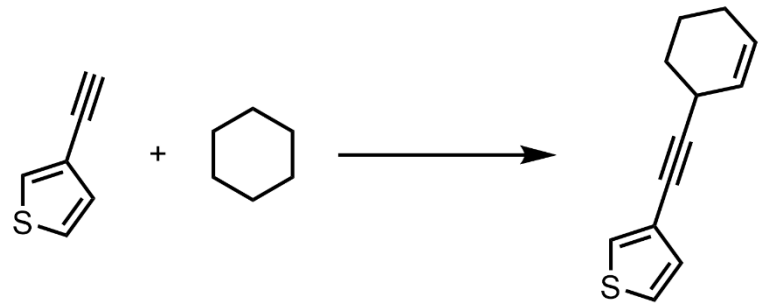

B6-1

Scheme 60: Synthesis of 3-(cyclohex-2-en-1-ylethynyl)thiophene (**B6-1**)

Cyclohexene (10 mmol, 821.5 mg) and 3-ethynylthiophene (0.5 mmol, 54.1 mg) afforded after separation with pentane 3-(cyclohex-2-en-1-ylethynyl)thiophene (**B6-1**). Yield: 38.4 mg (71 %, 0.355 mmol). Analytics were according to literature.[15] **^{1}H NMR**

(300 MHz, CDCl3) δ = 7.38 – 7.33 (m, 1H), 7.25 – 7.20 (m, 1H), 7.08 (dd, J = 5.0, 1.2 Hz, 1H), 5.78 (dtd, J = 9.9, 3.3, 1.9 Hz, 1H), 5.75 – 5.64 (m, 1H), 3.35 – 3.16 (m, 1H), 2.12 – 1.51 (m, 6H). **^{13}C NMR** (75 MHz, CDCl3) δ = 130.20, 128.25, 127.85, 127.08, 125.05, 92.47, 75.44, 29.46, 28.12, 24.80, 20.78. **MS (ESI-TOF):** *m/z* calcd $[M + H]^+$: 188.06529; found: 188.06542.

A.1.3.11.7. 3-ethynylpyridine (B7)

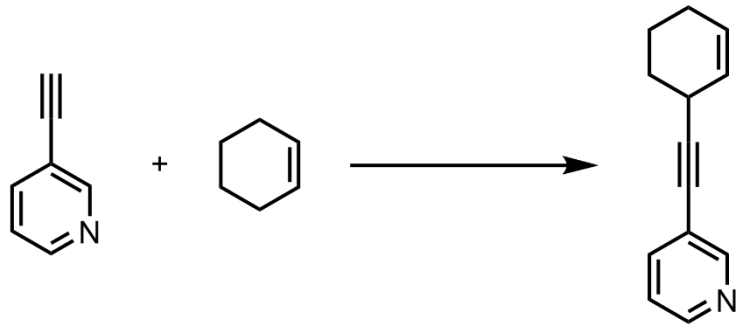

B7-1

Scheme 61: Synthesis of 3-(cyclohex-2-en-1-ylethynyl)pyridine (**B7-1**)

Cyclohexene (10 mmol, 821.5 mg) and 3-ethynylpyridine (0.5 mmol, 51.6 mg) afforded after separation with ethyl acetate and pentane (1:9) 3-(cyclohex-2-en-1-ylethynyl)pyridine (**B7-1**). Yield: 22.6 mg (24 %, 0.12 mmol). **^{1}H NMR** (300 MHz, CDCl3) δ = 8.60 (dt, J = 2.2, 1.1 Hz, 1H), 8.45 (dd, J = 4.9, 1.7 Hz, 1H), 7.70 – 7.60 (m, 1H), 7.22 – 7.14 (m, 1H), 5.78 (dtd, J = 10.5, 3.5, 2.0 Hz, 1H), 5.68 (ddt, J = 9.9, 3.6, 2.0 Hz, 1H), 3.33 – 3.24 (m, 1H), 2.07 – 1.91 (m, 2H), 1.90 – 1.70 (m, 2H), 1.70 – 1.50 (m, 2H). **^{13}C NMR** (75 MHz, CDCl3) δ = 152.36, 147.93, 138.63, 128.55, 126.49, 122.95, 121.14, 96.58, 29.23, 28.10, 24.69, 20.64. **MS (ESI-TOF):** *m/z* calcd $[M + H]^+$: 184.1126; found: 184.1131.

A.1.3.11.8. 2-ethynylpyridine (B8)

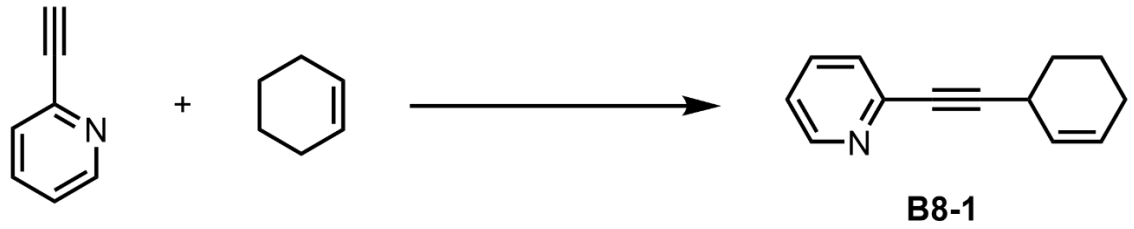

Scheme 62: Synthesis of 2-(cyclohex-2-en-1-ylethynyl)pyridine (**B8-1**).

Cyclohexene (10 mmol, 821.5 mg) and 2-ethynylpyridine (0.5 mmol, 51.6 mg) afforded 2-(cyclohex-2-en-1-ylethynyl)pyridine (**B8-1**). The separation with ethyl acetate and pentane (1:2) was not successful and only a crude mixture was obtained. Further efforts to purify the product did not obtain a clean product. Hence no yield was determined. The crude NMR can be found in the Appendix. Mass of crude product: m = 100.2 mg. **MS (ESI-TOF):** *m/z* calcd $[M + H]^+$: 184.1126; found: 184.1129.

A.1.3.11.9. pent-1-yne (B9)

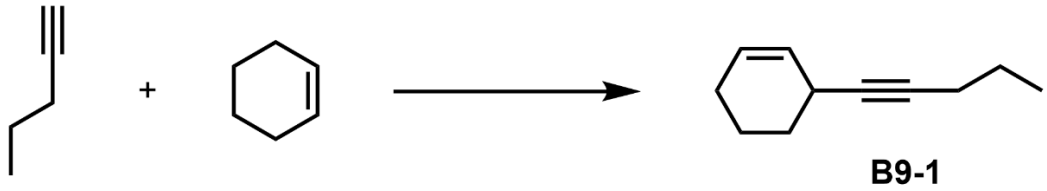

Scheme 63: Synthesis of 3-(pent-1-yn-1-yl)cyclohex-1-ene (**B9-1**).

Cyclohexene (10 mmol, 821.5 mg) and pent-1-yne (0.5 mmol, 34.1 mg) afforded 3-(pent-1-yn-1-yl)cyclohex-1-ene (**B9-1**). The separation with pentane was not successful and only a crude mixture was obtained. Further efforts to purify the product did not obtain a clean product. Extensive drying under vacuum led to decomposition. Hence no yield was determined. The crude NMR can be found in the Appendix. Mass of crude product: m = 34.1 mg. **MS (EI-MS):** *m/z* calcd $[M]^+$: 147.11683; found: 147.11698.

A.1.3.11.10. dec-1-yne (B10)

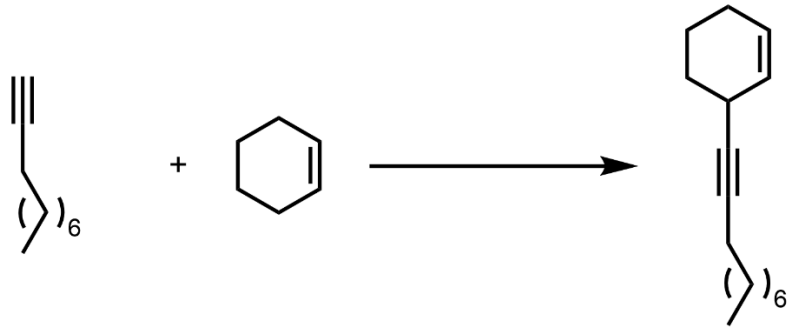

B10-1

Scheme 64: Synthesis of 3-(dec-1-yn-1-yl)cyclohex-1-ene (**B10-1**).

Cyclohexene (10 mmol, 821.5 mg) and dec-1-yne (0.5 mmol, 69.1 mg) afforded 3-(dec-1-yn-1-yl)cyclohex-1-ene (**B10-1**). The separation with pentane was not successful and only a crude mixture was obtained. Further efforts to purify the product did not obtain a clean product. Hence no yield was determined. The crude NMR and GC-MS can be found in the Appendix. Mass of crude product: m = 38 mg. **MS (EI-MS):** *m/z* calcd $[M]^+$: 217.19508; found: 217.19488.

A.1.3.12. General Procedure for other allylic or C-H acidic Substrates.

The test reaction for other allylic or C-H acidic substrates were conducted according to the following procedure. A 10 ml pressure tube equipped with a magnetic stirring bar is evacuated and refilled with Argon for a total amount of three times. To this tube 18.6 mg (0.05 mmol) of Tetrakisacetonitrile Copper(I) Hexafluorophosphate and 20.1 mg (0.05 mmol) 4,4′,4″-Tri-tert-butyl-2,2′:6′,2″-terpyridine are added. The tube is then evacuated again and flushed with Argon. Consequently, the solids are dissolved in 1 ml of dry and degassed Acetonitrile. Following this, 181.9 µl (1 mmol) of tert-Butyl hydroperoxide is added via a pipette. Subsequently, 51.1 µl (0.5 mmol) Phenylacetylene and 10 mmol of substrate are added to the reaction. The setup is then heated in an oil bath at 80 °C for 24 h while being stirred. Upon completion, the reaction is cooled to room temperature and the reaction is analyzed via GC/MS.

A.1.3.13. General Procedure for the synthesis of the Terpyridine-Copper(I) complex

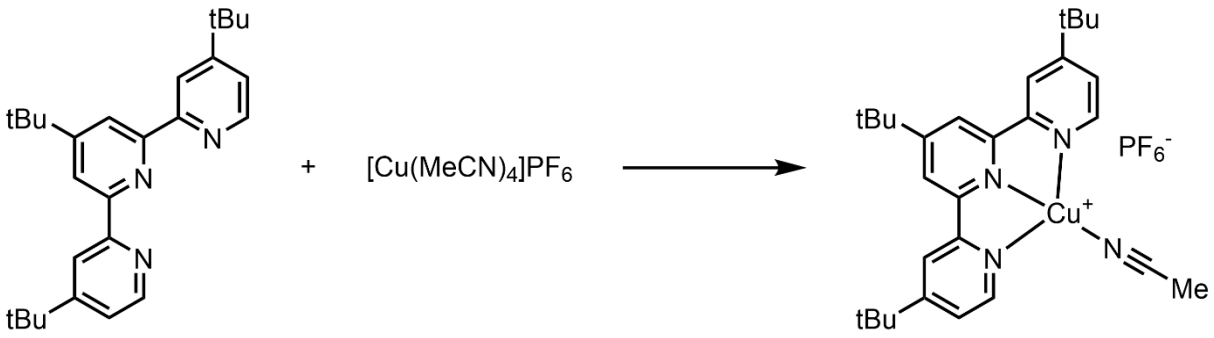

Scheme 65: Synthesis of the Terpyridine-Copper(I) Complex.

An oven-dried Schlenk flask equipped with a magnetic stirring bar is evacuated and refilled with Argon three times. Consequently, 93.2 mg (0.25 mmol) of Tetrakisacetonitrile Copper(I) Hexafluorophosphate and 100.4 mg (0.25 mmol) 4,4′,4″-Tri-tert-butyl-2,2′:6′,2″-terpyridine are added. The solids are then dissolved in 5 ml of dry and degassed Acetonitrile and stirred overnight. The following day, the mixture is filtered under Argon. The solvent is removed under vacuo to obtain a red to brownish powder.

^{1}H NMR (300 MHz, CD3CN) δ = 8.06 (s, 2H), 7.97 (d, J = 6.4 Hz, 4H), 7.32 (d, J = 5.4 Hz, 2H), 1.48 (s, 9H), 1.29 (s, 18H).

^{13}C NMR (75 MHz, CD3CN) δ = 164.52, 163.54, 154.84, 154.52, 149.58, 123.61, 121.98, 121.54, 66.28, 36.66, 36.11, 30.63, 30.45, 15.66.

^{19}F NMR (282 MHz, CD3CN) δ = -71.51, -74.01.

^{31}P NMR (122 MHz, CD3CN) δ = -127.15, -132.97, -138.79, -144.60, -150.42, -150.47, -156.23, -162.05.

MS (ESI-TOF): m/z calcd [M + H]+: 464.2132; found: 464.2133 (without Acetonitrile), m/z calcd [PF_6^-]: 144.9642, found 144.9644.

A.1.3.14. Preparation and Crystallographic Data of Complex CR1 ($C_{80}H_{110}Cu_2F_{12}N_8O_4P_2$)

Firstly 0.01 mmol of the precursor complex are prepared according to the General Procedure for the synthesis of the Terpyridine-Copper(I) complex. To this an equal amount of *tert*-butyl hydroperoxide is added. The mixture is then filtered through a syringe-filter into another Schlenk vessel and cooled in a ice/NaCl bath. To this 2 ml of toluene are added over the course of 2 h using a syringe, taking care to not drop the solvent directly into the solution but let it run down the glass wall. The vessel is then placed at -20 °C until small green crystals formed.

For the crystal structure, please refer to Figure 19.

Table 14: Crystallographic Data for Complex CR1

Empirical Formula	$C_{80}H_{110}Cu_2F_{12}N_8O_4P_2$
Formula Weight	1664.77
Temperature	150(2) K
Wavelength	1.54178 Å
Crystal system	Monoclinic
Space Group	*C*2/*c*
Unit Cell dimensions	a =25.4292(7) Å α = 90°. b = 9.8227(3) Å β = 95.8650(13)°. c = 33.5679(9) Å γ = 90°.
Volume	8340.8(4) Å^3
Z	4
Density (Calculated)	1.326 Mg/m^3
Absorption Coefficient	1.656 mm^{-1}
F(000)	3496
Crystal Size	0.19 x 0.09 x 0.03 mm
Reflections Collected	59093
Independent Refelctions	7372 (R_{int} = 0.0472)
Data / Restraints / Parameters	7372 / 263 / 569
Goodness-of-fit on F^2	1.039
Final R indices [I>2σ(I)]	R_1 = 0.0535, wR_2 = 0.1431
R indices (all data)	R_1 = 0.0593, wR_2 = 0.1487
Largest diff. peak and hole	0.833 and -1.048 e·Å^{-3}

A.1.3.15. Preparation and Crystallographic Data of Complex CR2 ($C_{66}H_{82}CuF_6N_6O_6S_2$)

Crystals of CR2 were obtained from a reaction solution via slow evaporation of the solvent under aerobic conditions.

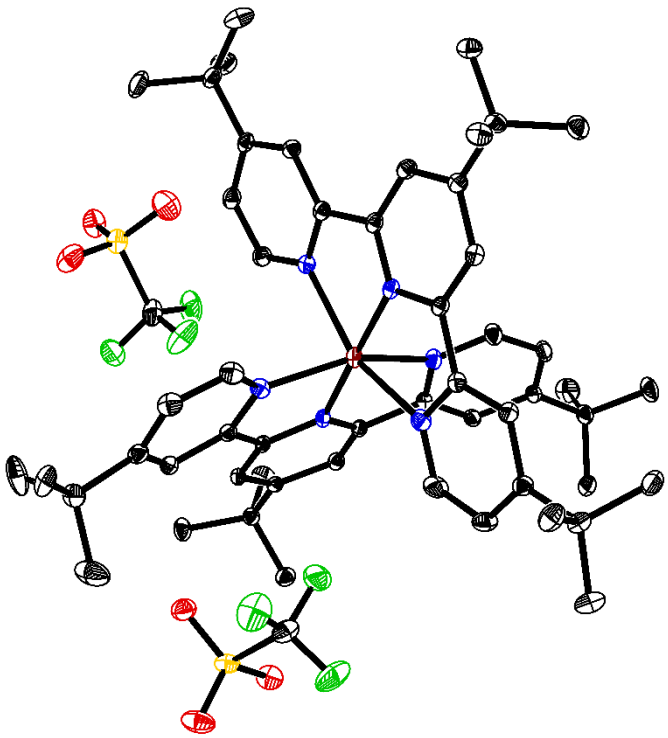

Figure 25: Single Crystal X-Ray Diffraction Crystal Structure of a homoleptic Copper(II) tris-tert-butyl-terpyridine complex (**CR2**). Displacement ellipsoids correspond to a probability level of 30 %. H-atoms and co-crystallized solvents were omitted for clarity.

Table 15: Crystallographic Data for Complex CR2

Empirical Formula	$C_{66}H_{82}CuF_6N_6O_6S_2$
Formula Weight	1303.04
Temperature	150(2) K
Wavelength	0.71073 Å
Crystal system	Monoclinic
Space Group	*P2₁/n*
Unit Cell dimensions	a =14.6085(14) Å α = 90°. b = 19.0953(18) Å β = 105.258(2)°. c = 24.625(2) Å γ = 90°.
Volume	6627.1(11) Å^3
Z	4
Density (Calculated)	1.306 Mg/m^3
Absorption Coefficient	0.464 mm^{-1}
F(000)	2744
Crystal Size	0.45 x 0.11 x 0.07 mm
Reflections Collected	120449
Independent Refelctions	15999 (R_{int} = 0.0485)
Data / Restraints / Parameters	15999 / 34 / 831
Goodness-of-fit on F^2	1.026
Final R indices [I>2σ(I)]	R_1 = 0.0420, wR_2 = 0.1023
R indices (all data)	R_1 = 0.0600, wR_2 = 0.1138
Largest diff. peak and hole	0.705 and -0.767 e·Å^{-3}

A.1.3.16. Preparation and Crystallographic Data for Complex CR3 ($C_{55}H_{48}CuF_{12}N_8P_2$)

Crystals of CR3 were obtained from a reaction solution via slow evaporation of the solvent under aerobic conditions.

For the crystal structure, please refer to Figure 20.

Table 16:Crystallographic Data for Complex CR3

Empirical Formula	$C_{55}H_{48}CuF_{12}N_8P_2$
Formula Weight	1174.49
Temperature	150(2) K
Wavelength	1.54178 Å
Crystal system	Monoclinic
Space Group	*P2₁/n*
Unit Cell dimensions	a =14.5397(5) Å α = 90°. b = 17.3263(6) Å β = 105.1047(15)°. c = 21.3760(8) Å γ = 90°.
Volume	5199.0(3) Å^3
Z	4
Density (Calculated)	1.501 Mg/m^3
Absorption Coefficient	1.967 mm^{-1}
F(000)	2404
Crystal Size	0.420 x 0.110 x 0.090 mm
Reflections Collected	51882
Independent Refelctions	9195 (R_{int} = 0.0322)
Data / Restraints / Parameters	9195 / 0 / 696
Goodness-of-fit on F^2	1.035
Final R indices [I>2σ(I)]	R_1 = 0.0358, wR_2 = 0.1004
R indices (all data)	R_1 = 0.0406, wR_2 = 0.1058
Largest diff. peak and hole	0.325 and -0.443 e·Å^{-3}

A.1.3.17. Preparation and Crystallographic Data for Complex CR4 ($C_{27}H_{35}Br_2CuN_3$)

Crystals of CR4 were obtained from a reaction solution via slow evaporation of the solvent under aerobic conditions.

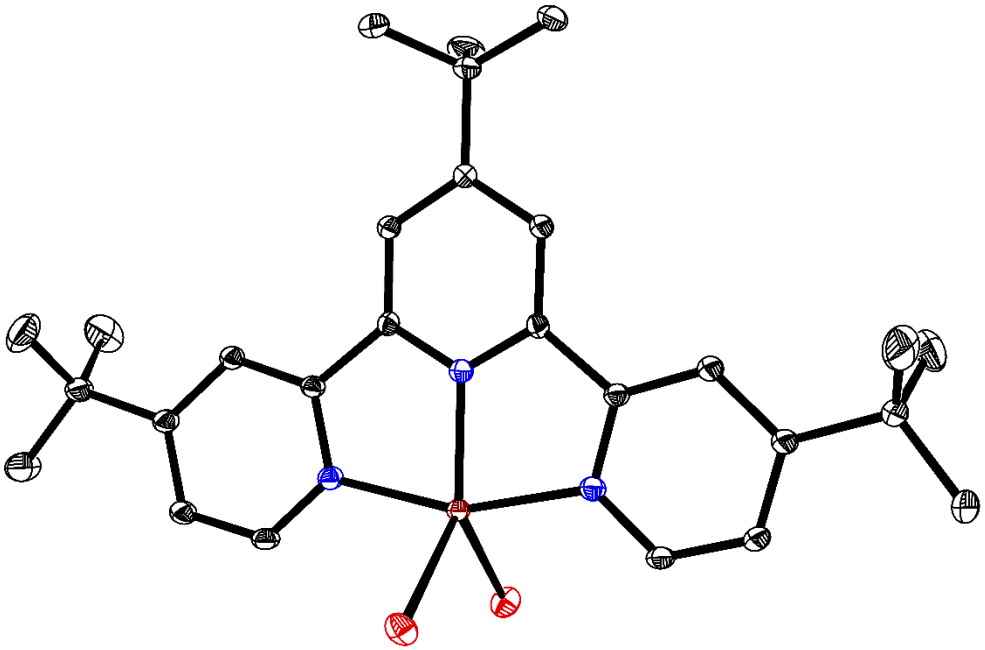

Figure 26: Single Crystal X-Ray Diffraction Crystal Structure of a copper terpyridyl dibromo complex (CR4). Displacement ellipsoids correspond to a probability level of 30 %. H-atoms and co-crystallized solvents were omitted for clarity

Table 17: Crystallographic Data for Complex CR4

Empirical Formula	$C_{27}H_{35}Br_2CuN_3$
Formula Weight	624.94
Temperature	150(2) K
Wavelength	1.54178 Å
Crystal system	Trigonal
Space Group	*P3₂21*
Unit Cell dimensions	a =12.3599(12) Å α = 90°. b = 12.3599(12) Å β = 90°. c = 15.8064(16) Å γ = 90°.
Volume	2091.2(5) Å^3
Z	3
Density (Calculated)	1.489 Mg/m^3
Absorption Coefficient	4.596 mm^{-1}
F(000)	951
Crystal Size	0.21 x 0.21 x 0.08 mm
Reflections Collected	26793
Independent Refelctions	2453 (R_{int} = 0.0249)
Data / Restraints / Parameters	2453 / 3 / 168
Goodness-of-fit on F^2	1.083
Final R indices [I>2σ(I)]	R_1 = 0.0168, wR_2 = 0.0425
R indices (all data)	R_1 = 0.0168, wR_2 = 0.0425
Absolute structure parameter	0.022(4)
Largest diff. peak and hole	0.248 and -0.457 e·Å^{-3}

A.1.3.18. Synthesis of Copper(I)-phenylacetylide

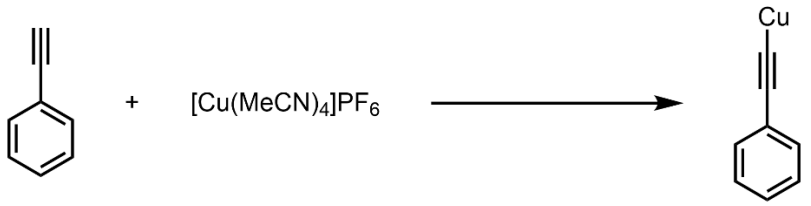

Scheme 66: Synthesis of Copper(I)-phenylacetylide.

The compound is synthesized according to procedures reported in literature.[124] An oven-dried 250 ml Schlenk flask equipped with a magnetic stirring bar is put under vacuum and refilled with oxygen a total amount of three times. To this flask 1.677 g (4.5 mmol) of Tetrakisacetonitrile Copper(I) Hexafluorophosphate and 1.243 g (9.0 mmol) of Potassium carbonate are added. Consequently, the solids are dispensed in 70 ml of dry Dimethyl formamide under Argon. Lastly, 0.5 ml (4.5 mmol) of phenylacetylene are added via syringe while stirring. The suspension is then left stirring over night. On the next day, the bright yellow solid is filtered and washed with 10 % ammonia in water, pure water, ethanol and diethylether. The solid is then dried under vacuum to obtain 518.7 mg (3.15 mmol, 70 %) of the bright yellow powder. Analytics were according to literature.[260]

A.1. Spectra

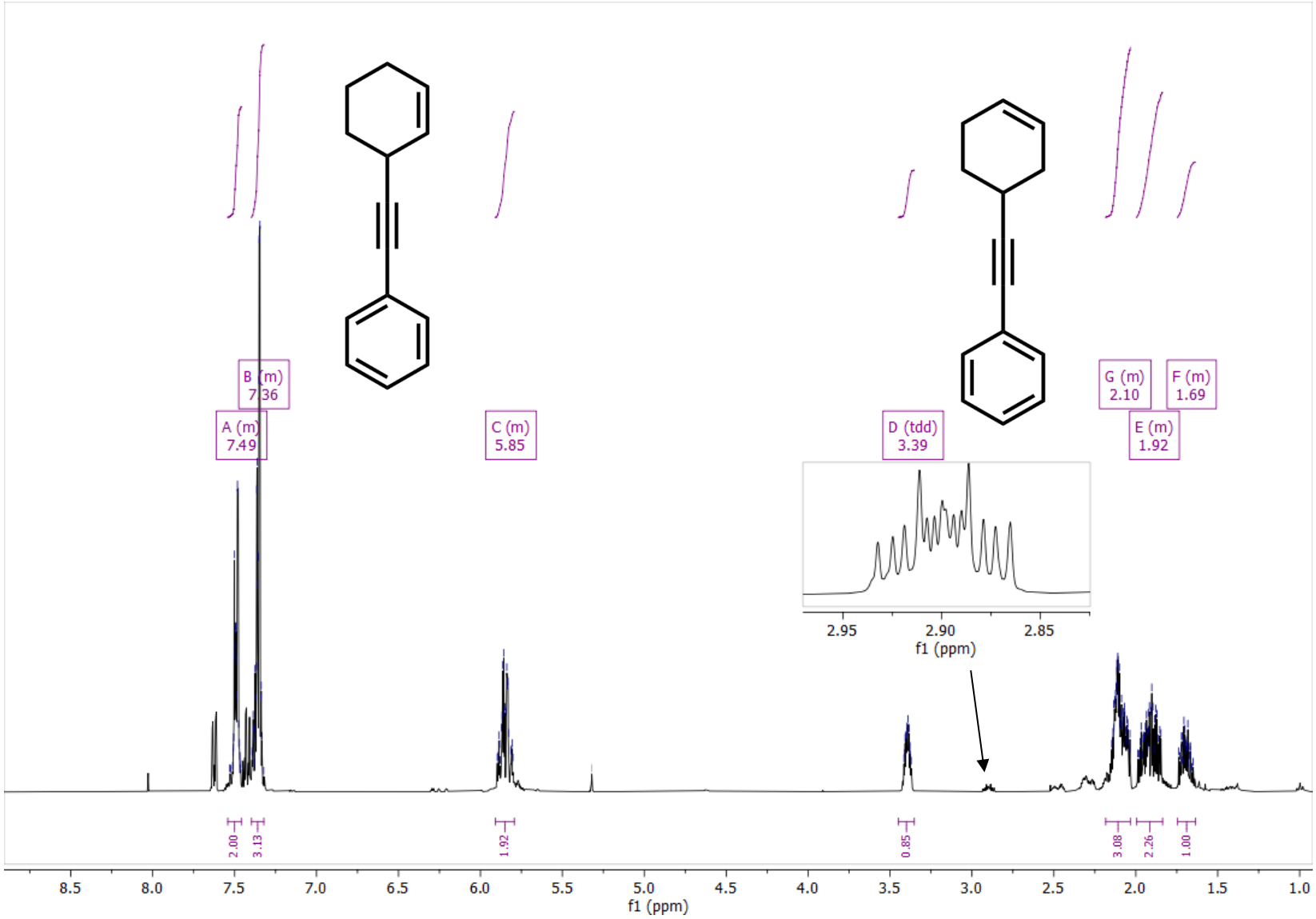

Figure 27: ^{1}H NMR (400 MHz, CD2Cl2) spectrum of (cyclohex-2-en-1-ylethynyl)benzene

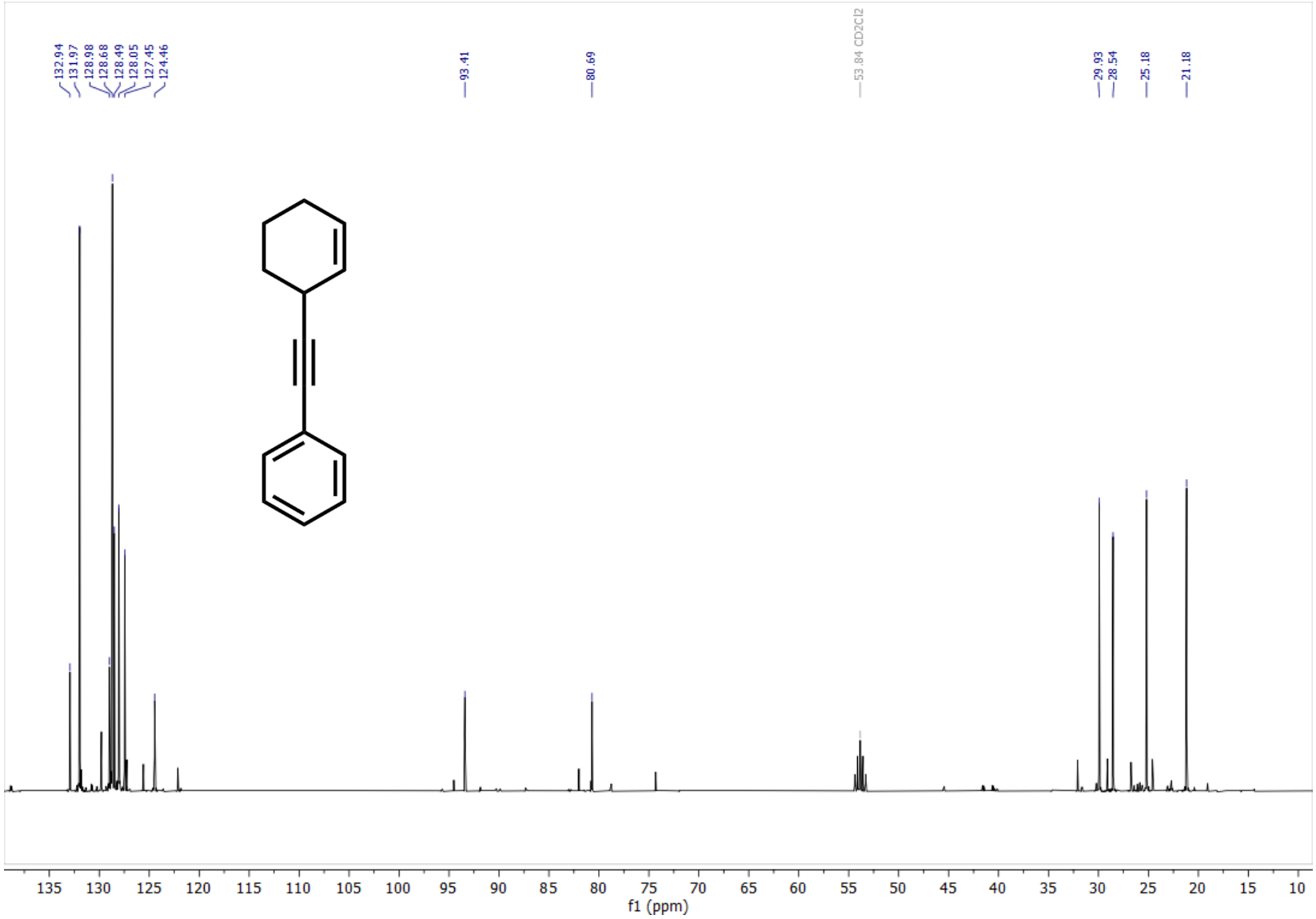

Figure 28: ^{13}C NMR (101 MHz, CD_2Cl_2) spectrum of (cyclohex-2-en-1-ylethynyl)benzene

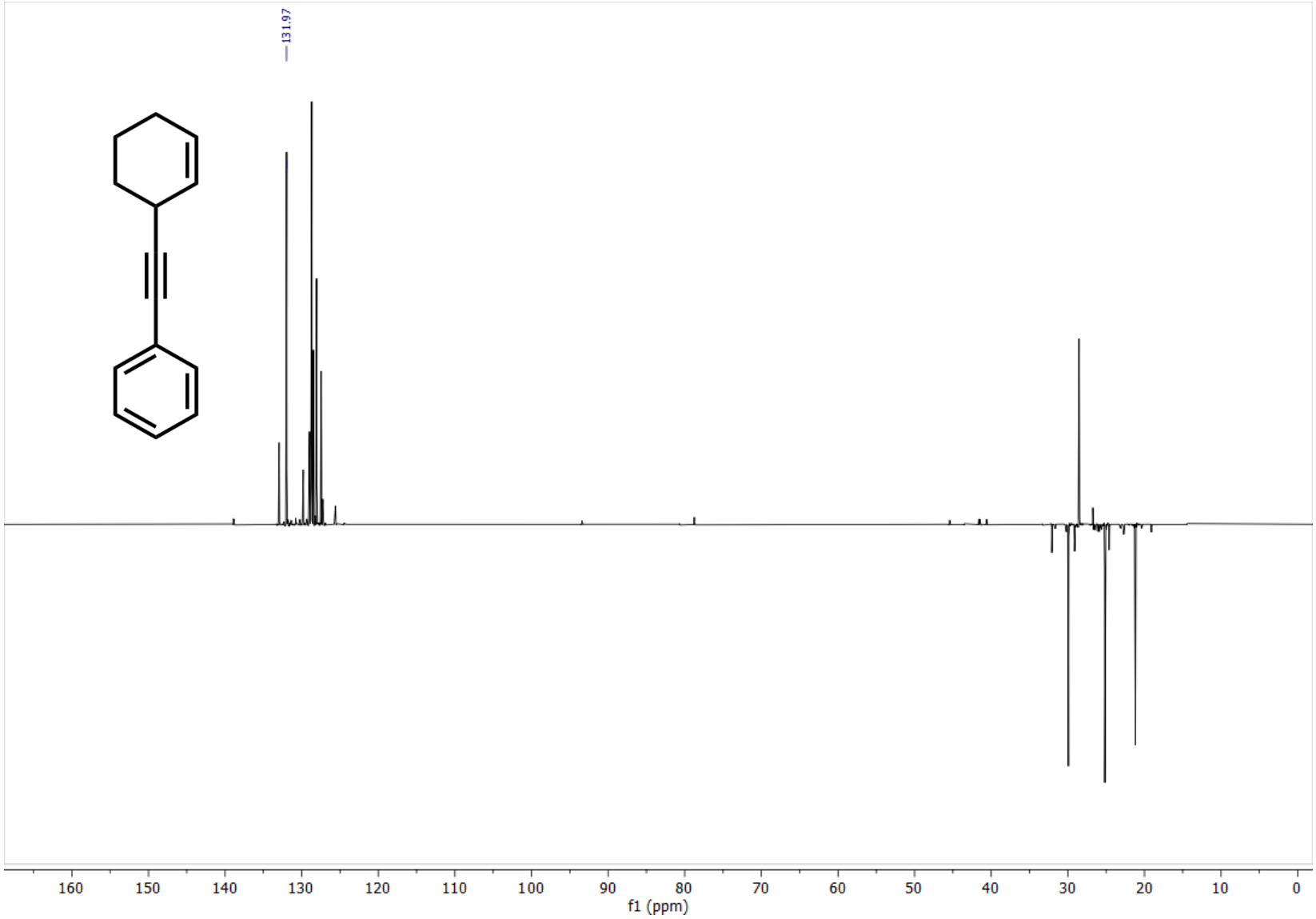

Figure 29: ^{13}C-dept CD2Cl2 spectrum of (cyclohex-2-en-1-ylethynyl)benzene

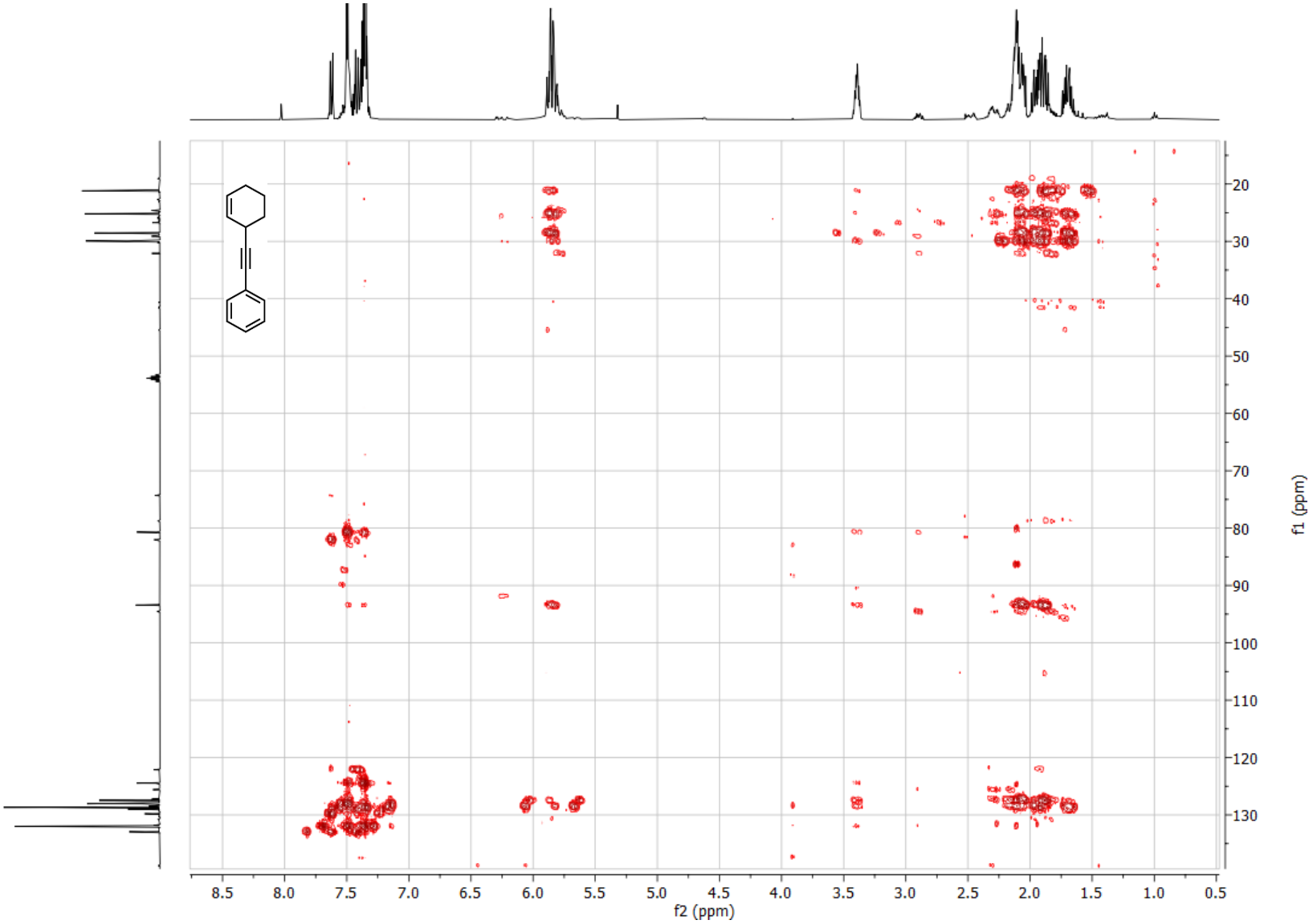

Figure 30: HMBC spectrum of (cyclohex-2-en-1-ylethynyl)benzene

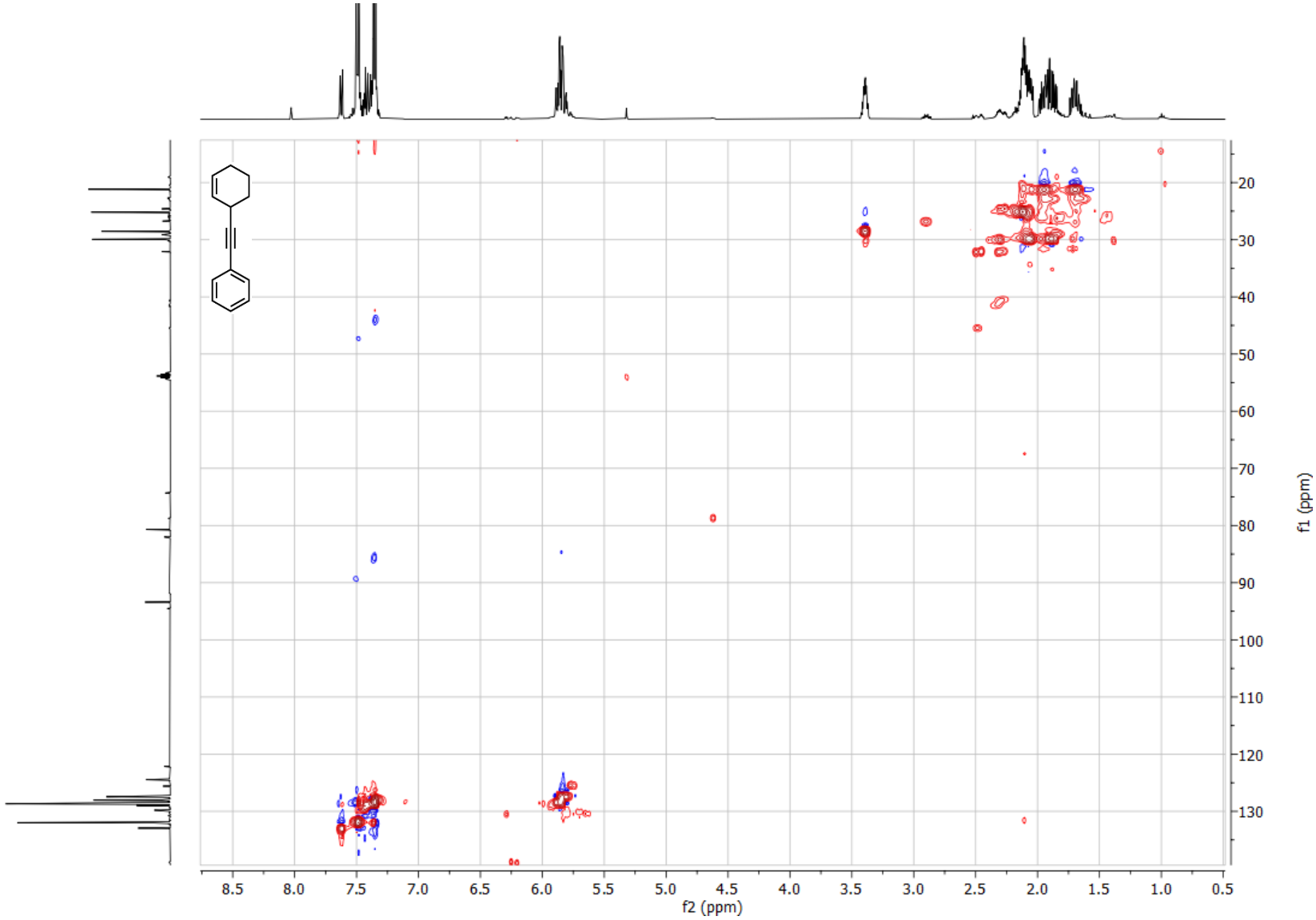

Figure 31: HSQC spectrum of (cyclohex-2-en-1-ylethynyl)benzene

A standard calculation for the yield based on the peak area of the chromatogram obtained from GC-FID measurements is shown below. In this A is referring to the peak area, c to the concentration, m to the increase of the calibration curve and V to the volume.

$$\eta = \frac{\left(\frac{\mathrm{A}(Product)\cdot \mathrm{c}(Standard)}{\mathrm{A}(Standard)\cdot \mathrm{m}(Product)}\right)\cdot V(vial)}{\left(\frac{\mathrm{A}(Product)\cdot \mathrm{c}(Standard)}{\mathrm{A}(Standard)\cdot \mathrm{m}(Product)}\right)+\left(\frac{\mathrm{A}(PA)\cdot \mathrm{c}(Standard)}{\mathrm{A}(Standard)\cdot \mathrm{m}(PA)}\right)+\left(\frac{\mathrm{A}(Glaser)\cdot \mathrm{c}(Standard)}{\mathrm{A}(Standard)\cdot \mathrm{m}(Glaser)}\right)\cdot V(vial)} \qquad (1)$$

$$\eta = \frac{\left(\frac{57.4154\cdot 0.025133807\ \mathrm{mmol}\cdot \mathrm{ml}^{-1}}{366.08017\cdot 0.71716}\right)\cdot 1\ \mathrm{ml}}{\left(\frac{57.4154\cdot 0.025133807\ \mathrm{mmol}\cdot \mathrm{ml}^{-1}}{366.08017\cdot 0.71716}\right)+\left(\frac{16.80847\cdot 0.025133807\ \mathrm{mmol}\cdot \mathrm{ml}^{-1}}{366.08017\cdot 0.83618}\right)+\left(\frac{5.66388\cdot 0.025133807\ \mathrm{mmol}\cdot \mathrm{ml}^{-1}}{366.08017\cdot 0.86822}\right)\cdot 1\ \mathrm{ml}}$$

$$\eta = 0.75$$

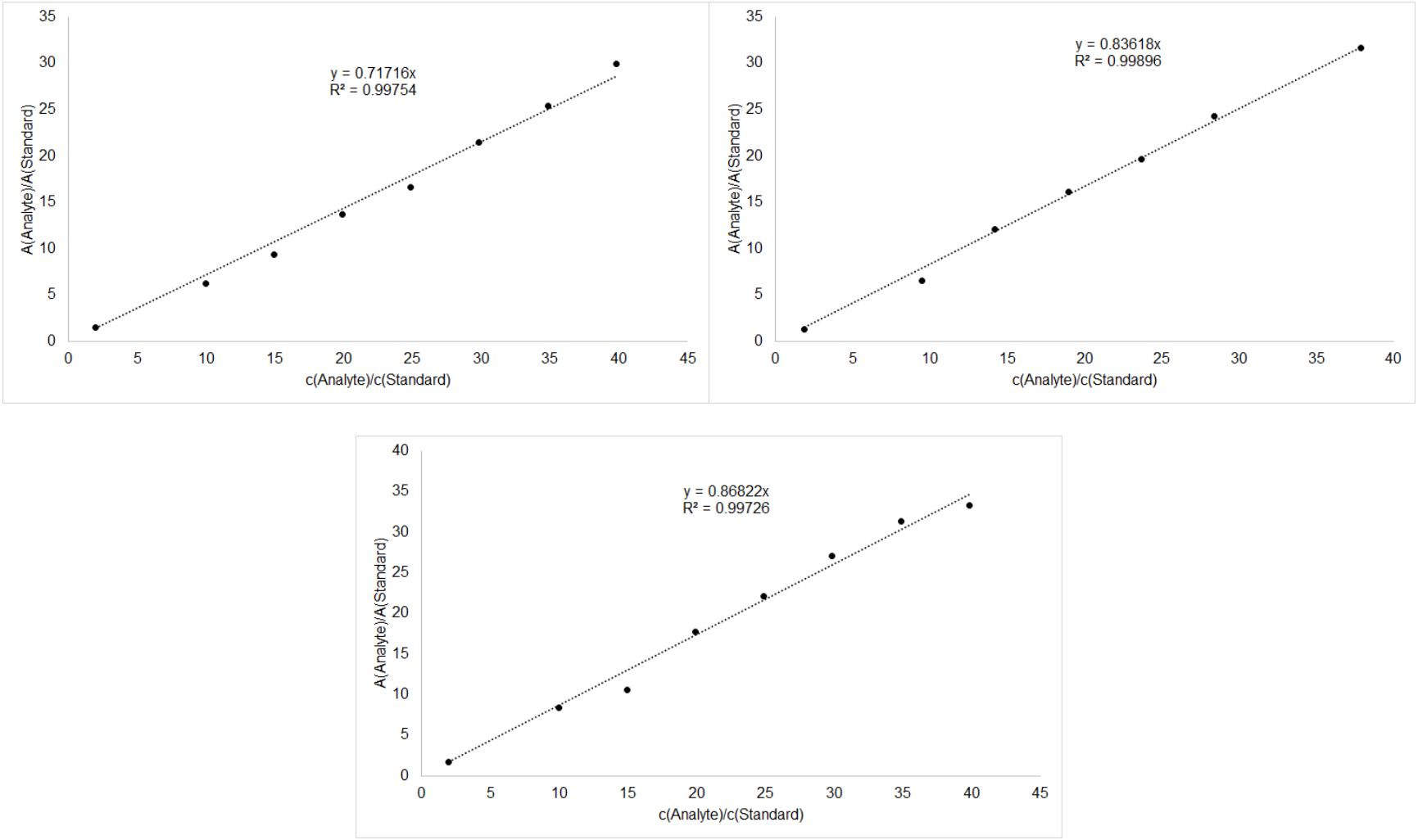

Figure 32: Calibration Curves for (cyclohex-2-en-1-ylethynyl)benzene (up-left), phenylacetylene (up-right) and 1,4-diphenylbutadyine (down-middle).

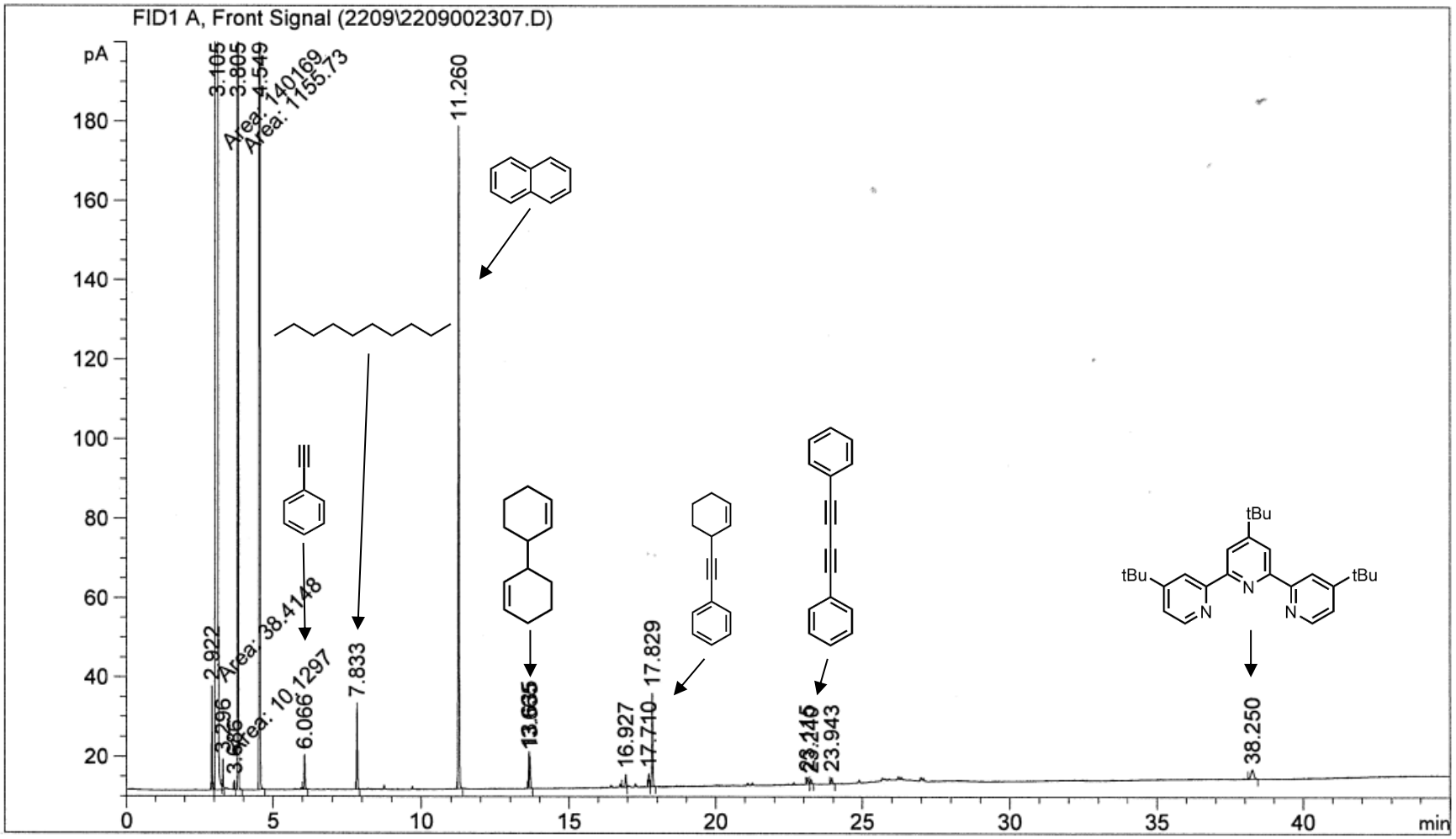

Figure 33: Examplary GC Chromatogramm for a reaction under Standard Conditions. Peaks were assigned via retention time or mass spectrometry.

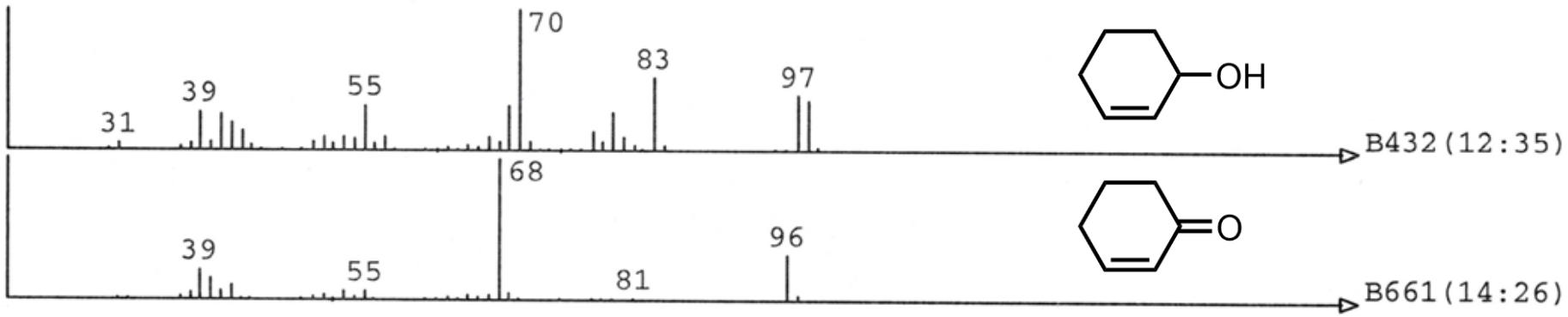

Figure 34: GC/MS of Cyclohex-2-en-1-ol and Cyclohex-2-en-1-one.

The Spectra was confirmed with literature reports.[261]

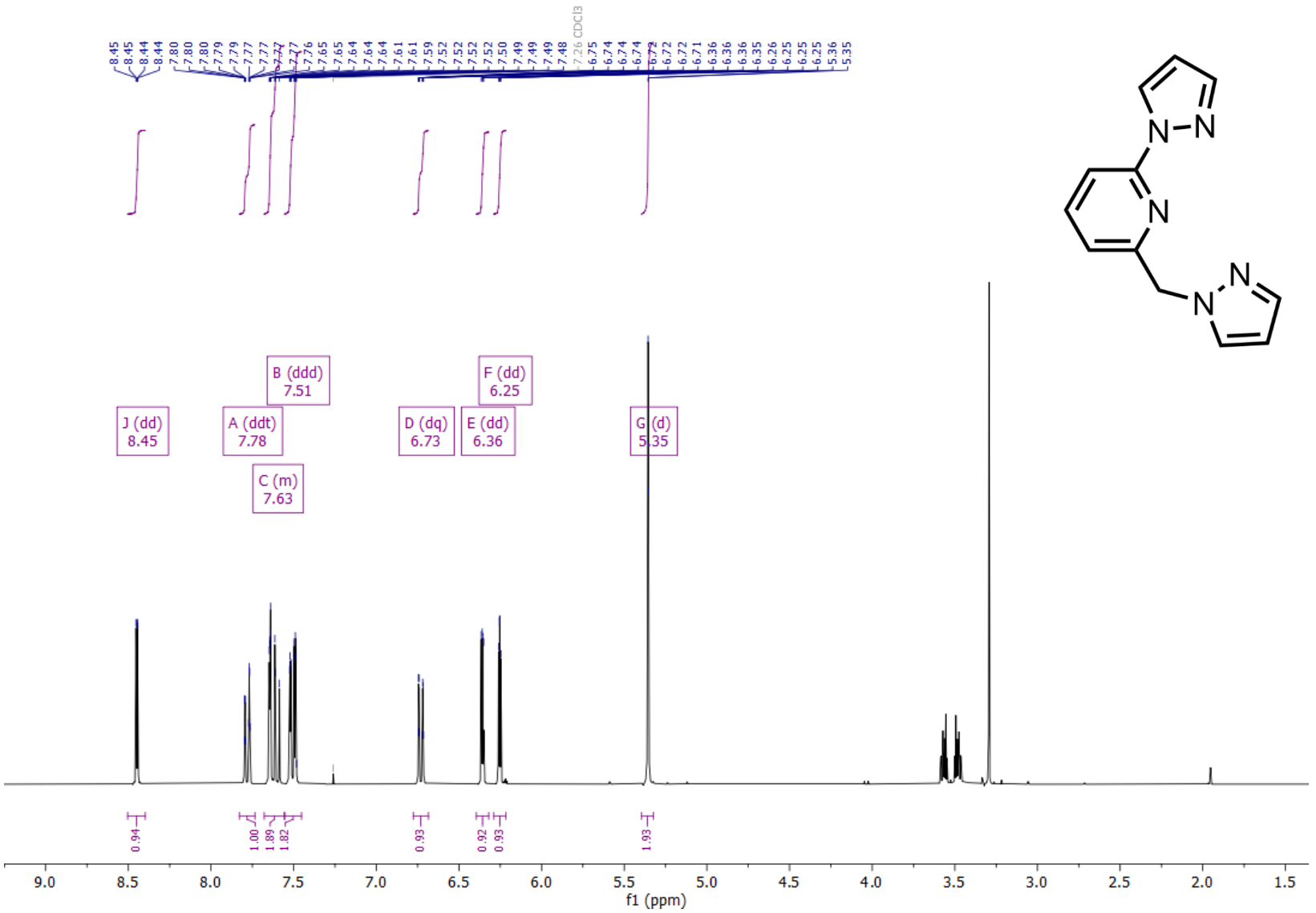

Figure 35: ^{1}H-NMR (300 MHz, CDCl3) spectrum of 2-((1H-pyrazol-1-yl)methyl)-6-(1H-pyrazol-1-yl)pyridine (L8).

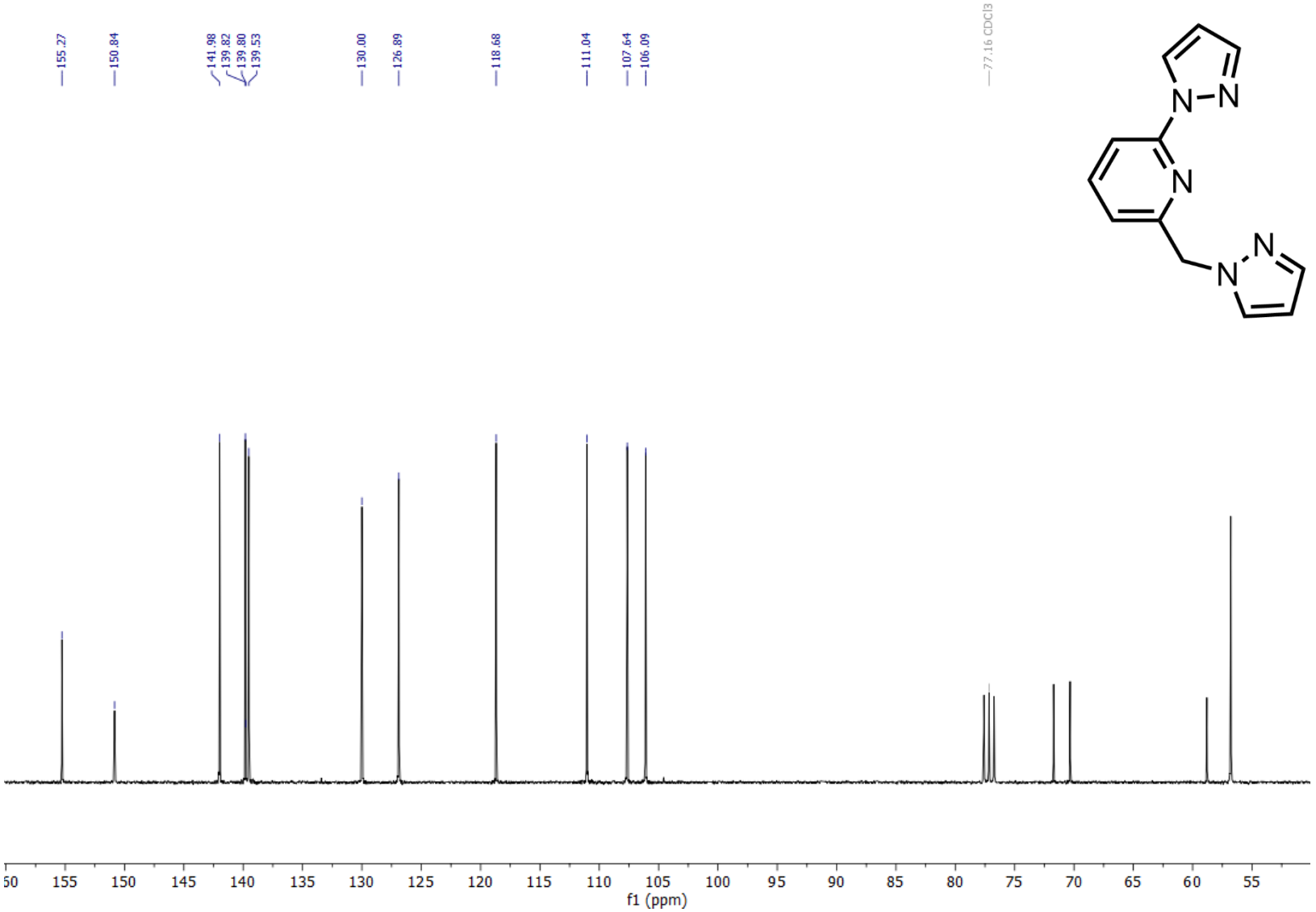

Figure 36: ^{13}C NMR (75 MHz, CDCl3) spectrum of 2-((1H-pyrazol-1-yl)methyl)-6-(1H-pyrazol-1-yl)pyridine (L8).

Figure 37: ^{1}H NMR (300 MHz, CD2Cl2) spectrum of tris(pyridin-2-ylmethyl)amine (L9)

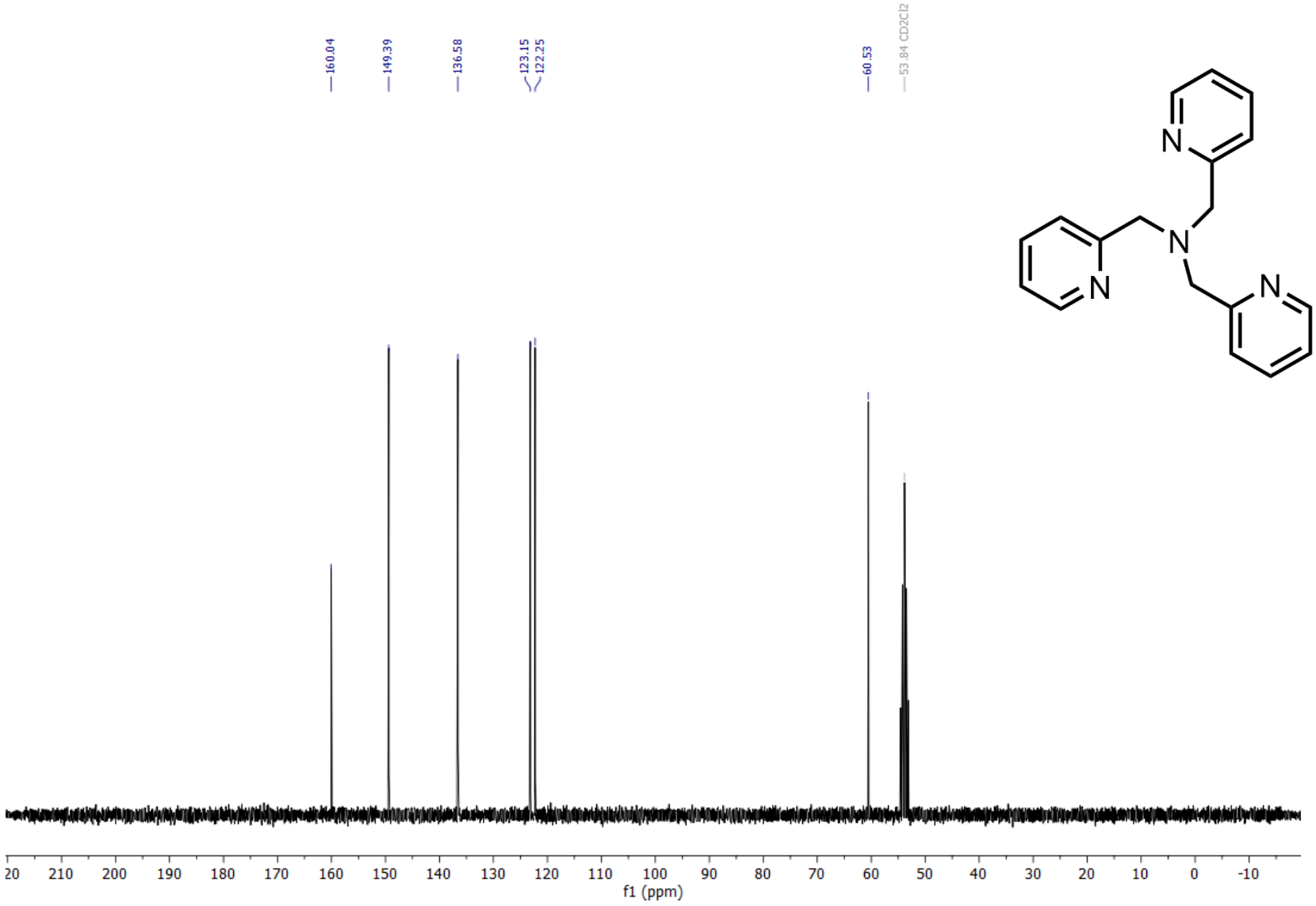

Figure 38: ^{13}C NMR (75 MHz, CD2Cl2) spectrum of tris(pyridin-2-ylmethyl)amine (L9)

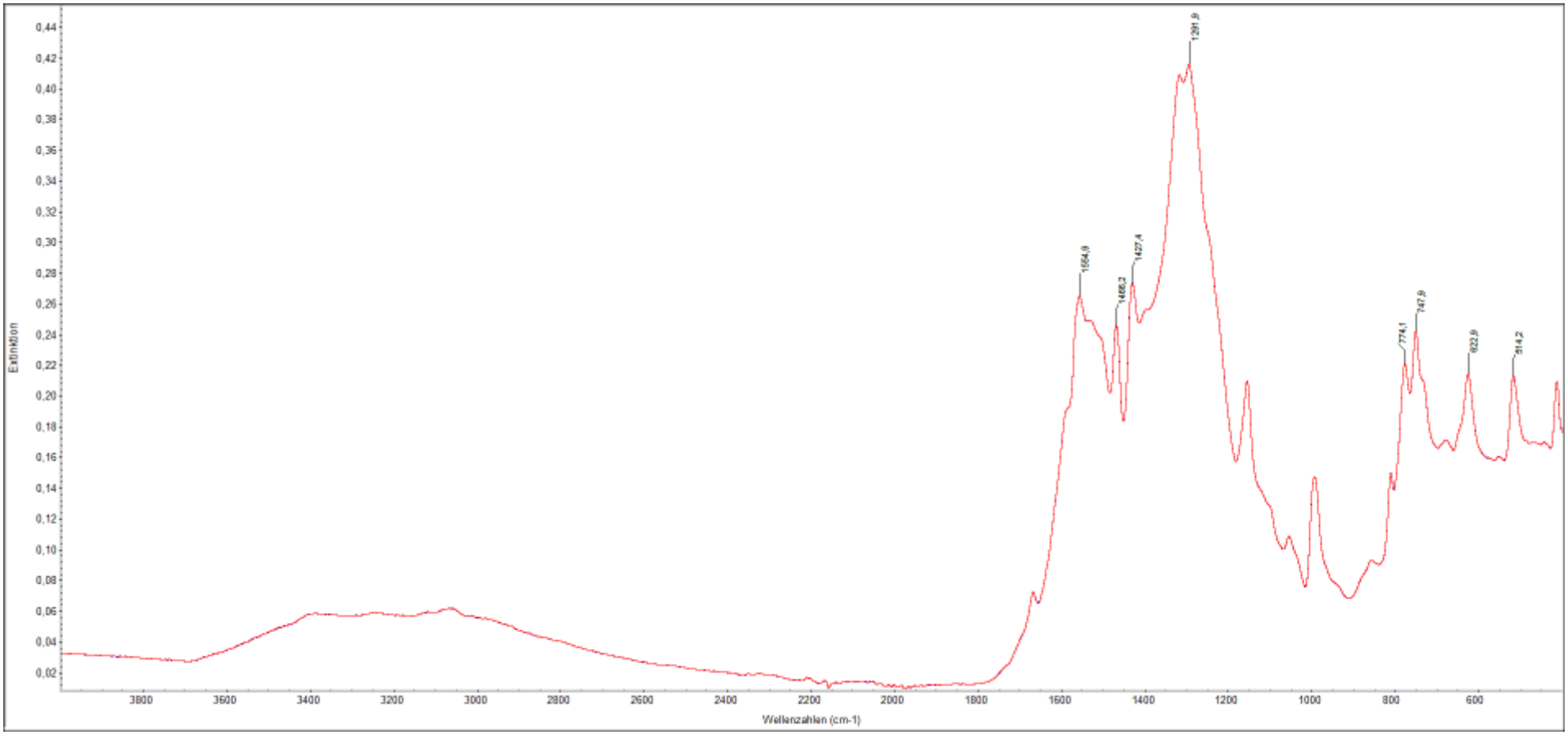

Figure 39: ATR-IR-Spectrum of Ligand **L10**.

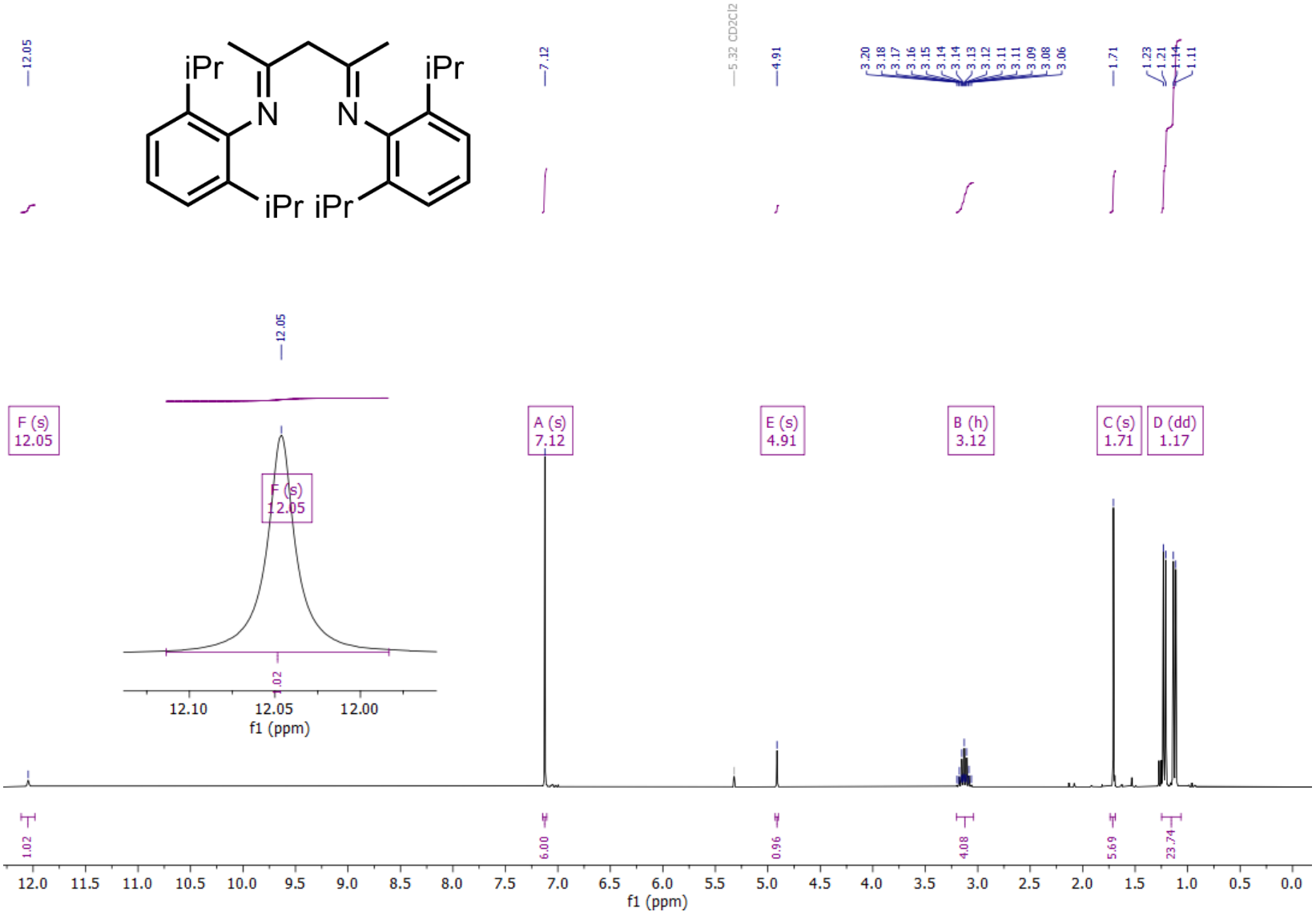

Figure 40: ^{1}H NMR (300 MHz, CD2Cl2) spectrum of (2E,4E)-N2,N4-bis(2,6-diisopropylphenyl)pentane-2,4-diimine

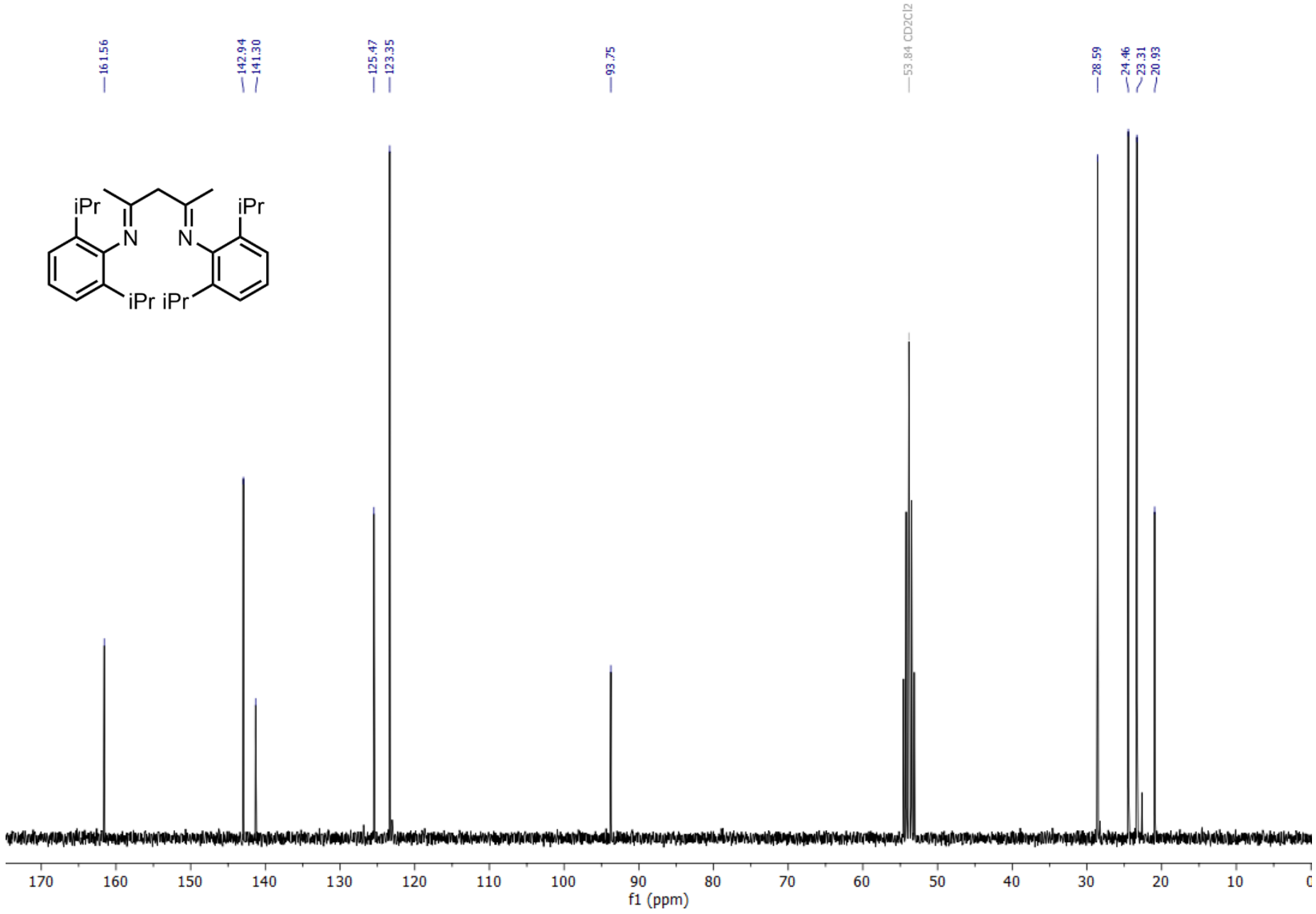

Figure 41: ^{13}C NMR (75 MHz, CD2Cl2) spectrum of (2E,4E)-N2,N4-bis(2,6-diisopropylphenyl)pentane-2,4-diimine

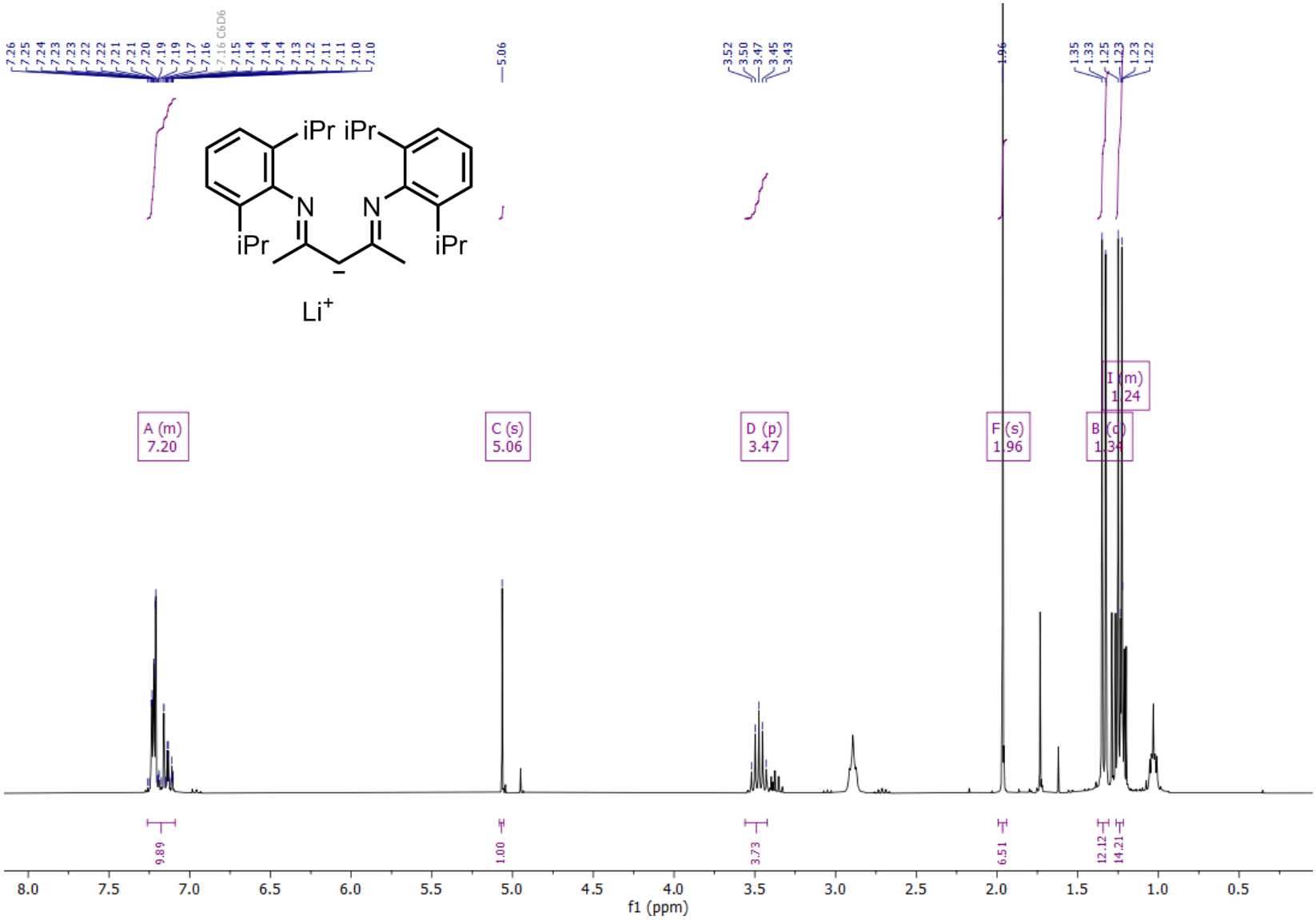

Figure 42: ^{1}H NMR (300 MHz, C6D6) spectrum of lithium (2E,4E)-2,4-bis((2,6-diisopropylphenyl)imino)pentan-3-ide (L12)

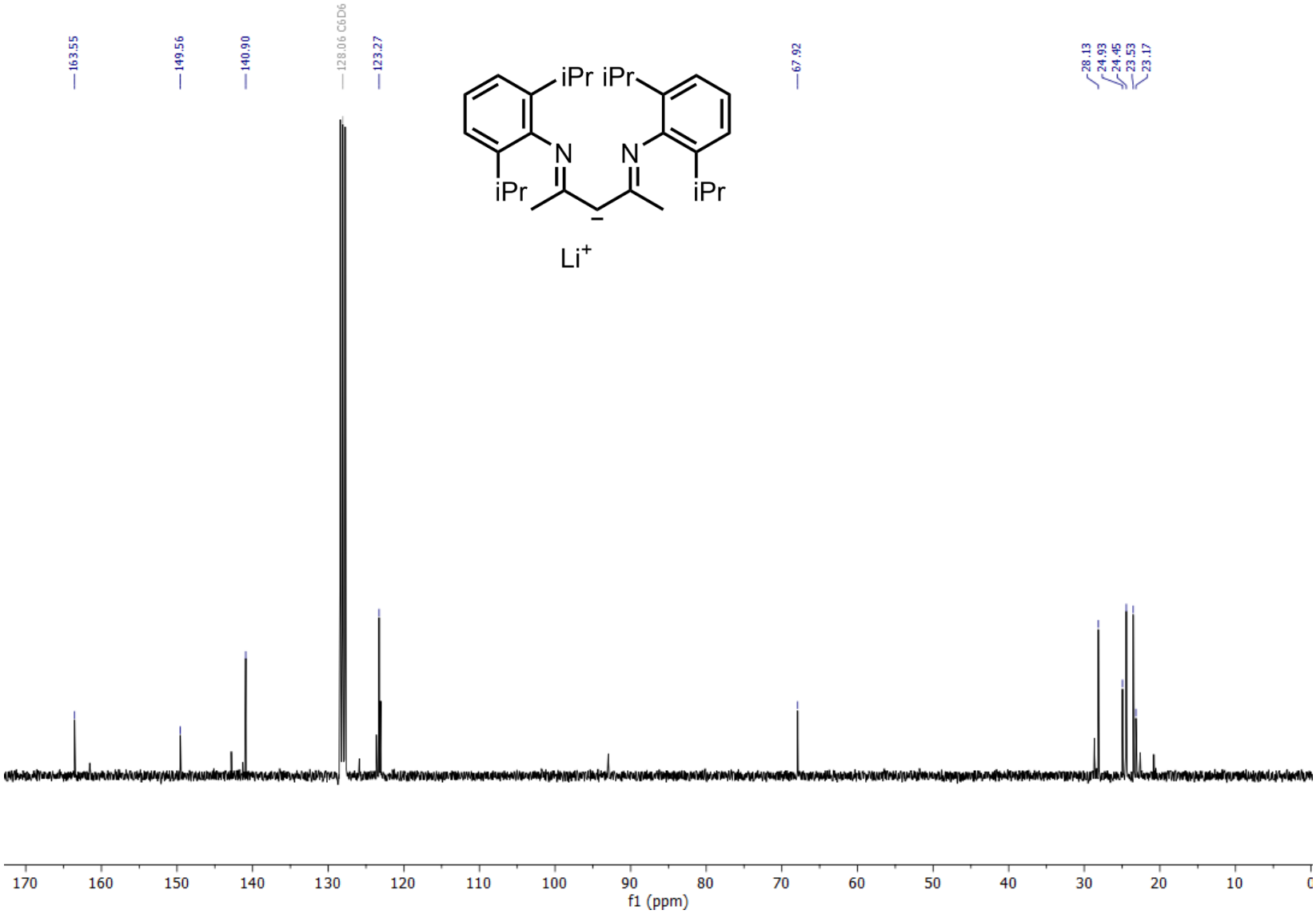

Figure 43: ^{13}C NMR (75 MHz, C6D6) spectrum of lithium (2E,4E)-2,4-bis((2,6-diisopropylphenyl)imino)pentan-3-ide (L12)

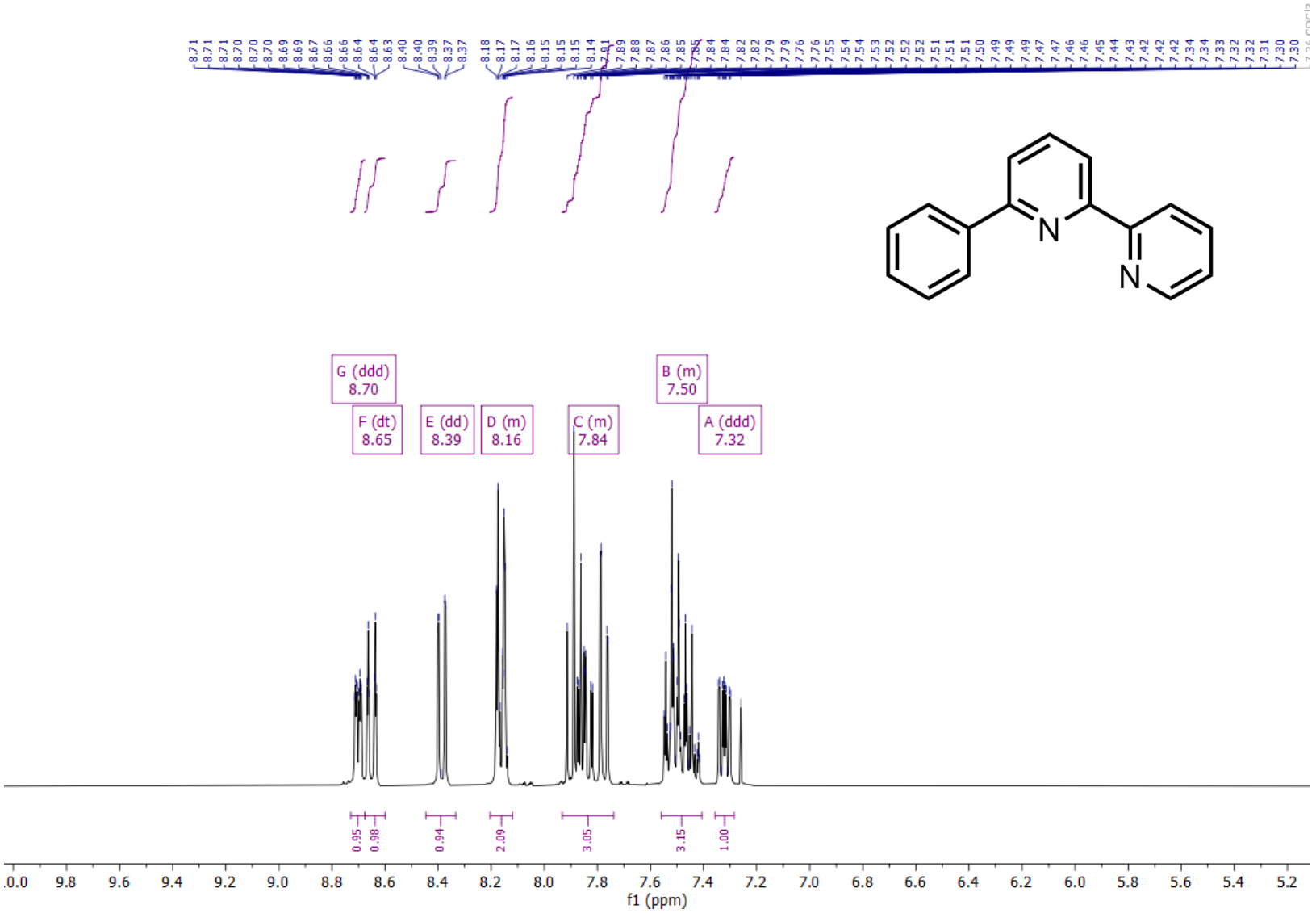

Figure 44: ^{1}H NMR (300 MHz, CDCl3) spectrum of 6-phenyl-2,2'-bipyridine (L13).

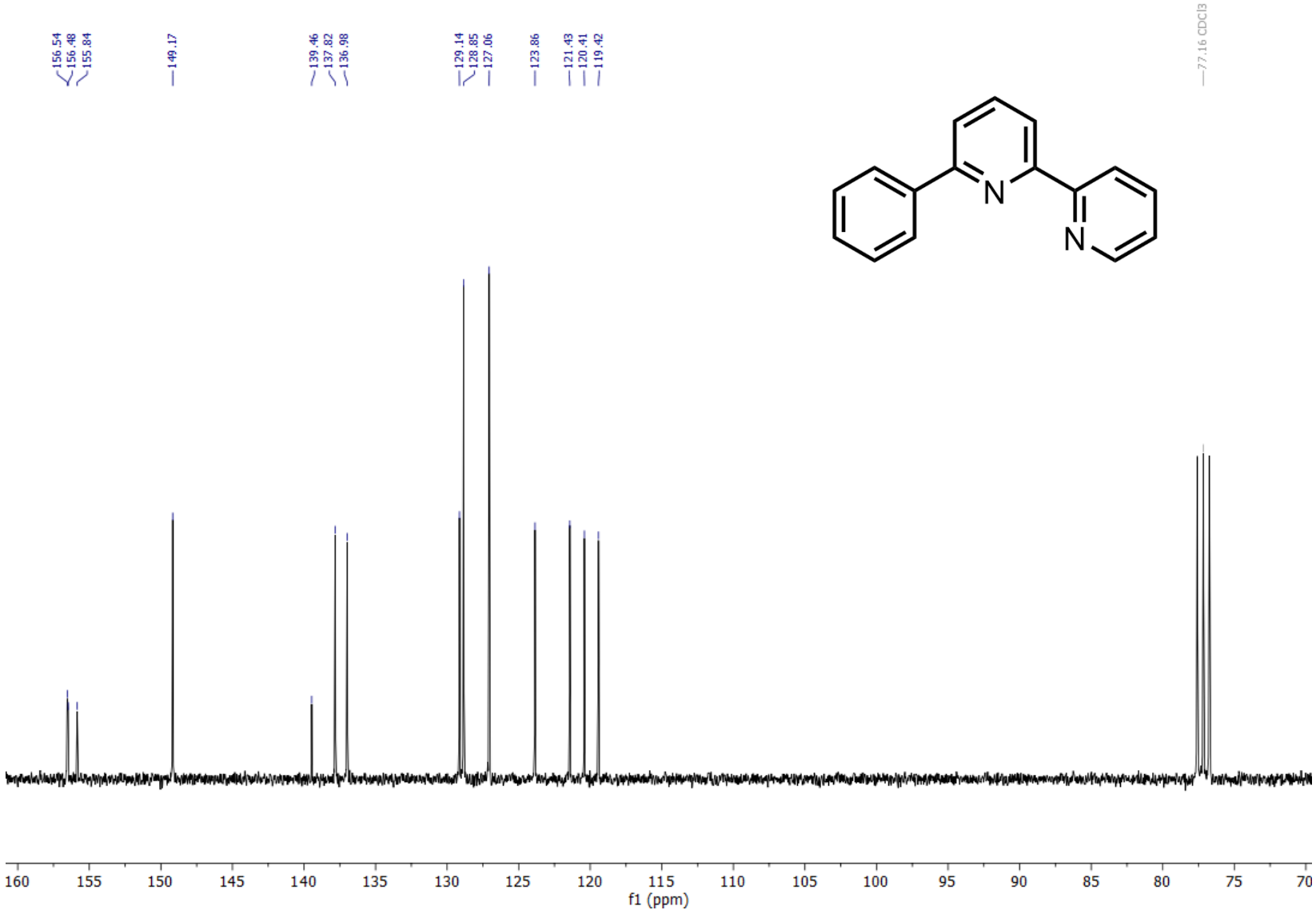

Figure 45: ^{13}C NMR (75 MHz, CDCl3) spectrum of 6-phenyl-2,2'-bipyridine (L13).

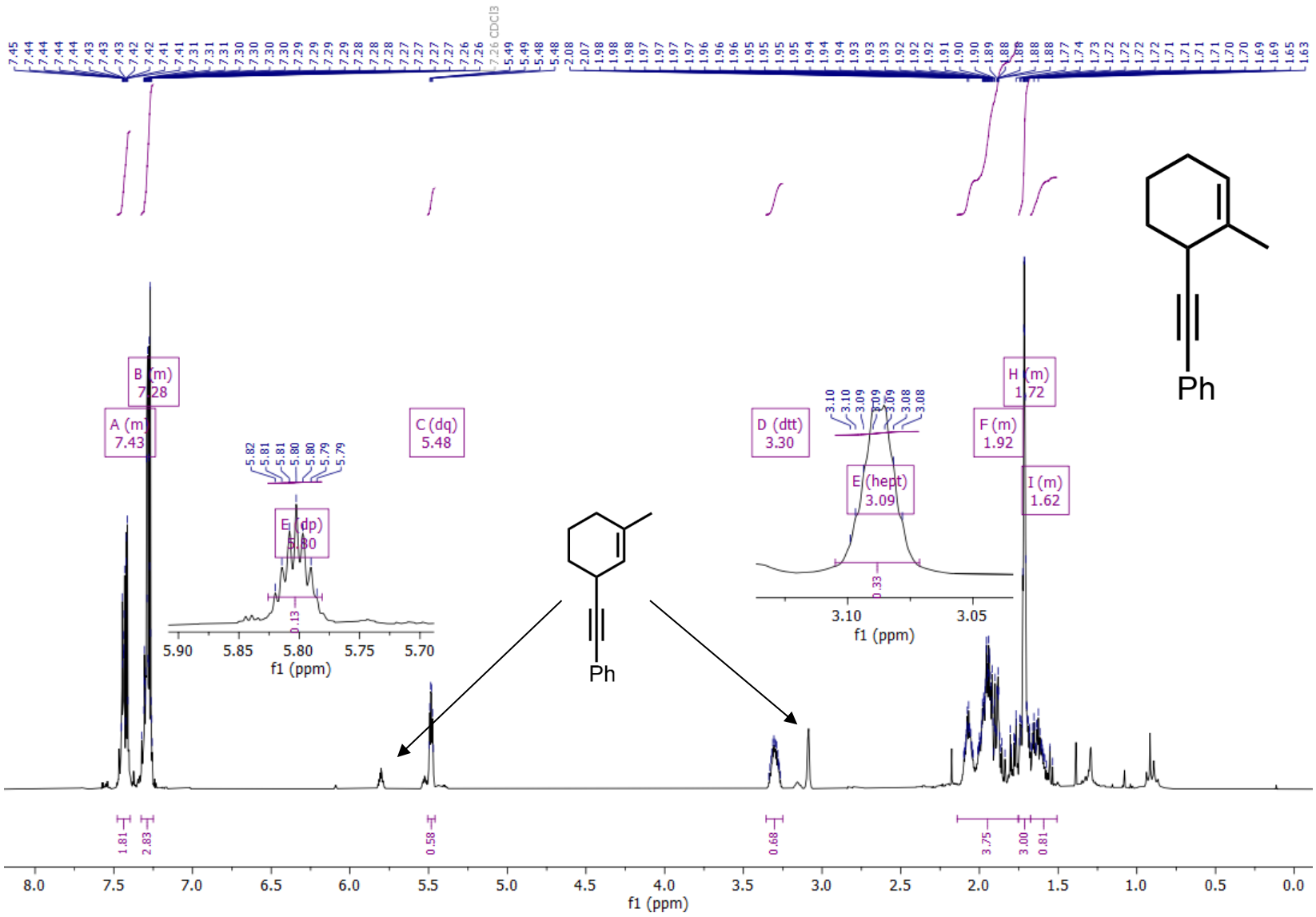

Figure 46: ^{1}H NMR (300 MHz, CDCl3) spectrum of ((2-methylcyclohex-2-en-1-yl)ethynyl)benzene (**A4-1**)

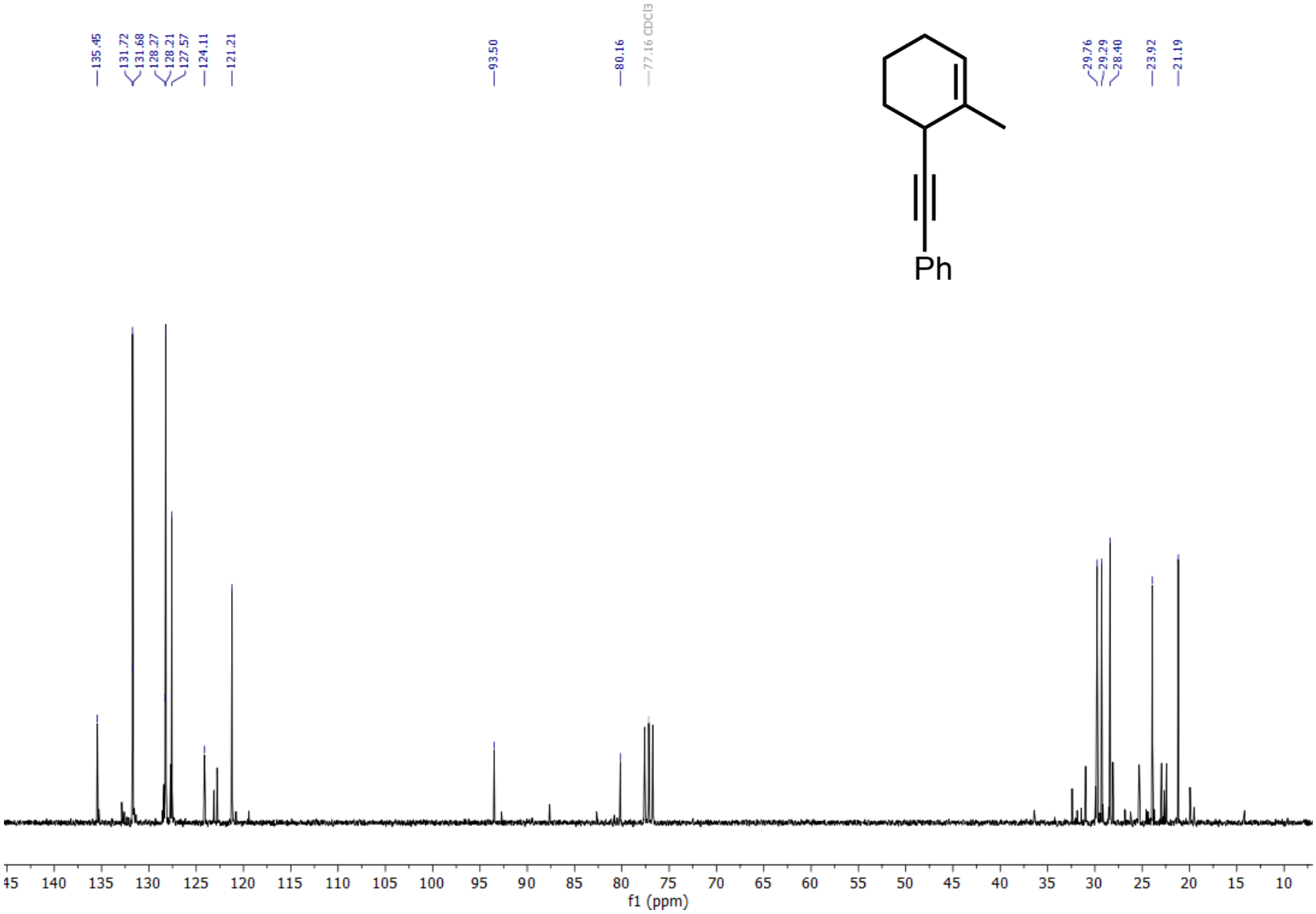

Figure 47: ^{13}C NMR (75 MHz, CDCl3) spectrum of ((2-methylcyclohex-2-en-1-yl)ethynyl)benzene (**A4-1**)

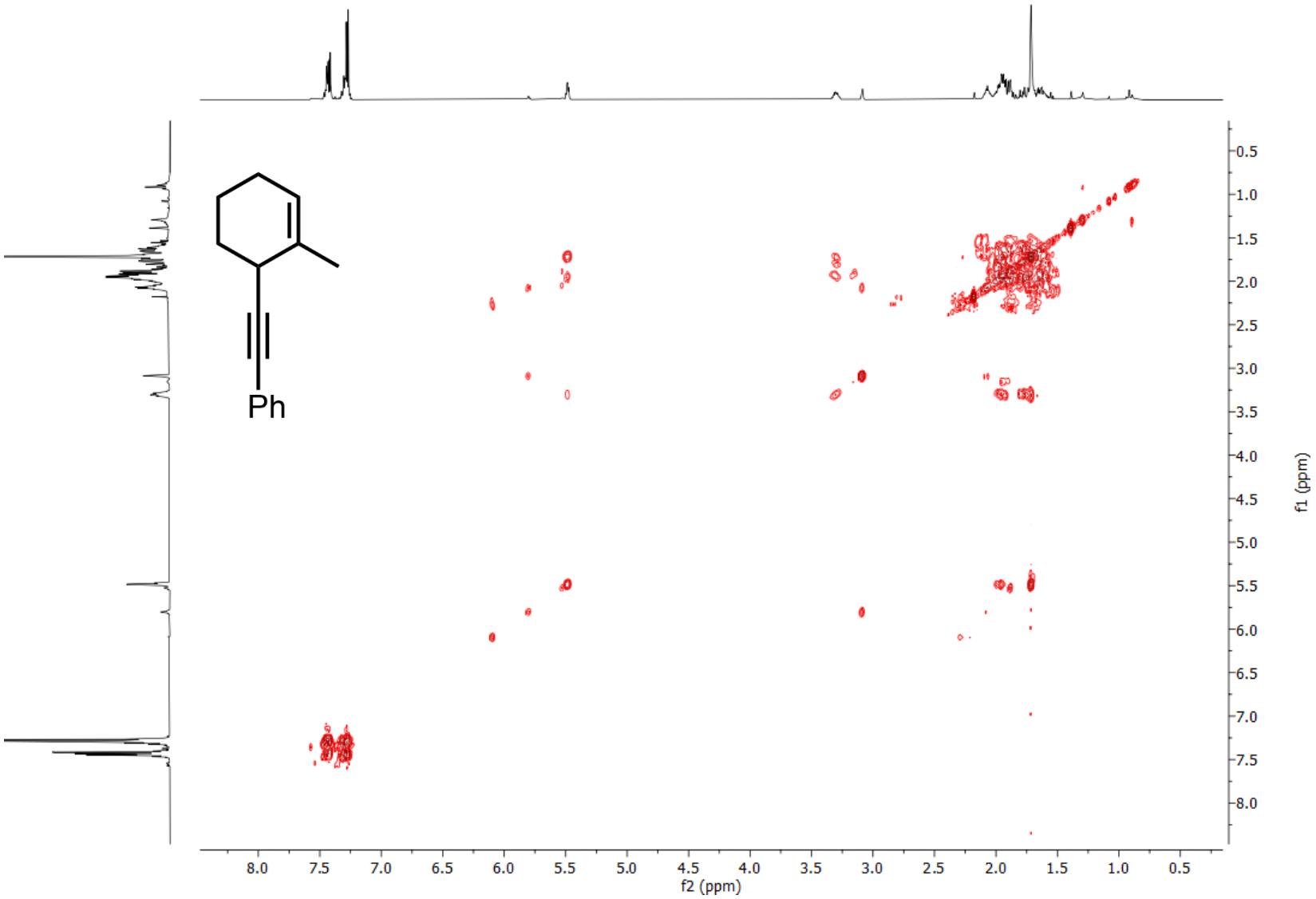

Figure 48: ^{1}H-COSY 45 spectrum of ((2-methylcyclohex-2-en-1-yl)ethynyl)benzene (**A4-1**)

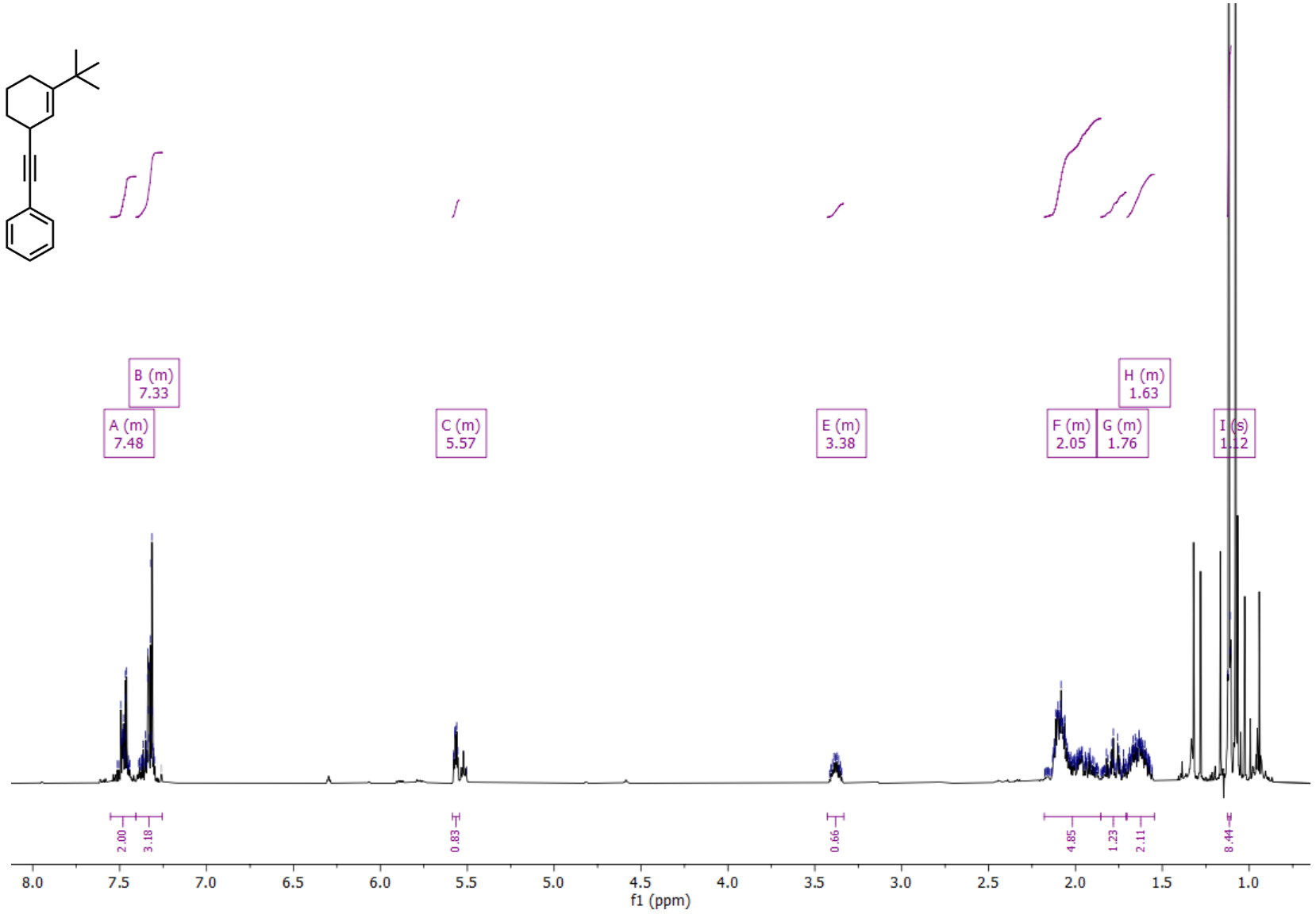

Figure 49: ^{1}H NMR (300 MHz, CDCl3) spectrum of ((3-(tert-butyl)cyclohex-2-en-1-yl)ethynyl)benzene (**A5-1**)

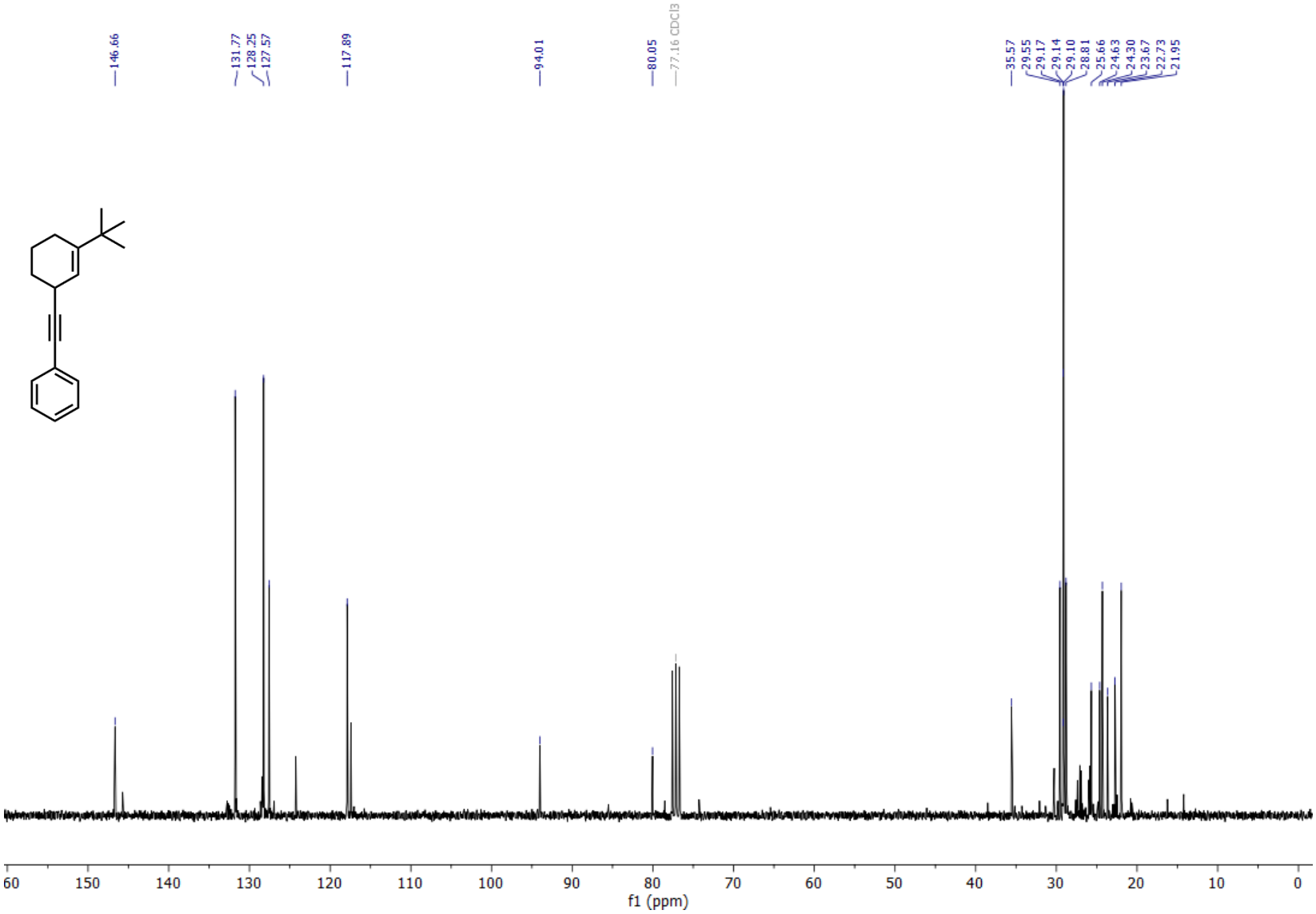

Figure 50: ^{13}C NMR (75 MHz, CDCl3) spectrum of ((3-(tert-butyl)cyclohex-2-en-1-yl)ethynyl)benzene (**A5-1**)

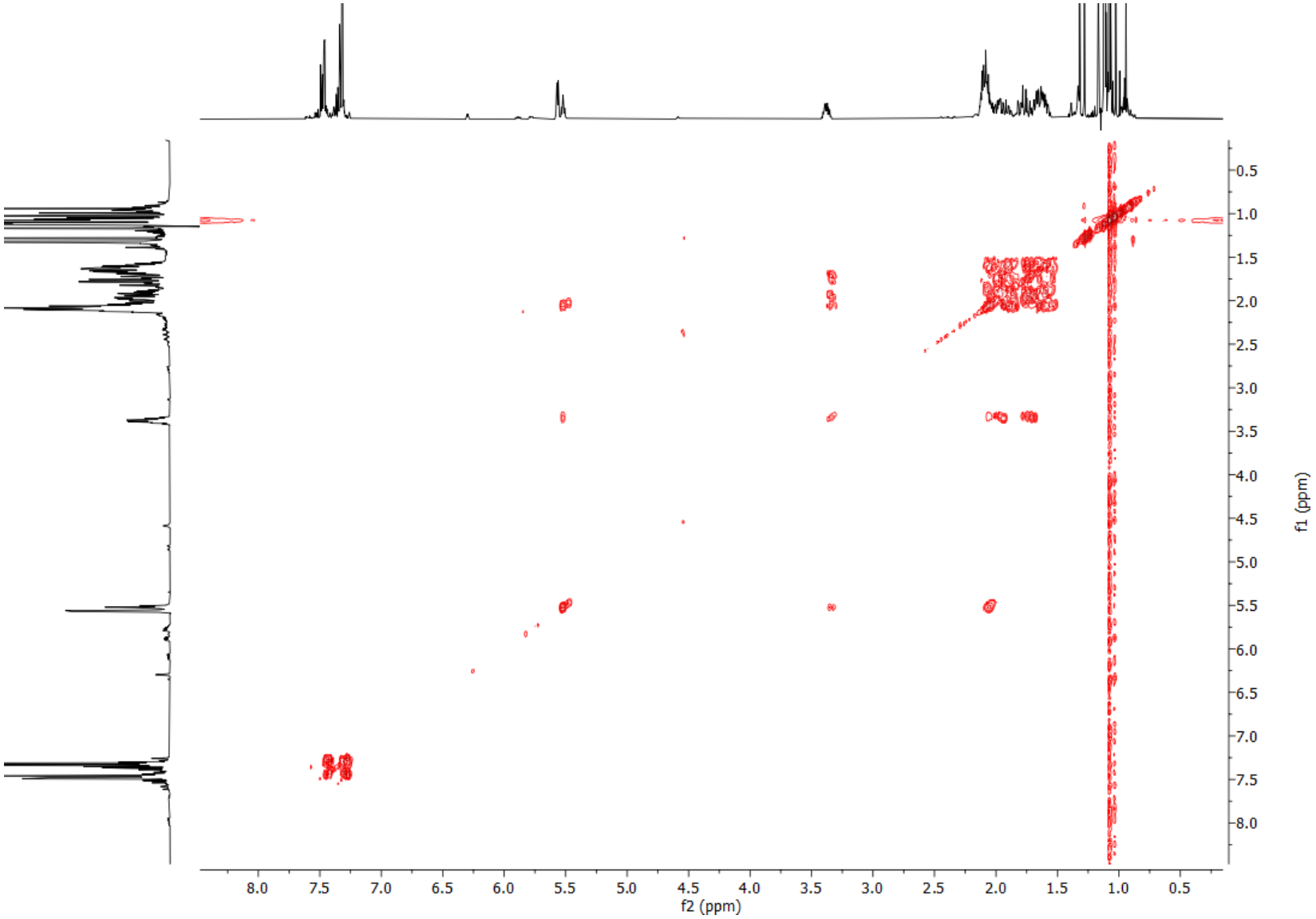

Figure 51: ^{1}H-COSY 45 spectrum of ((3-(tert-butyl)cyclohex-2-en-1-yl)ethynyl)benzene (**A5-1**)

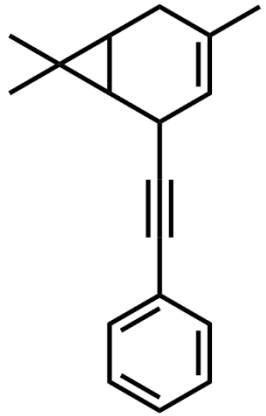

M = 236.16 g/mol

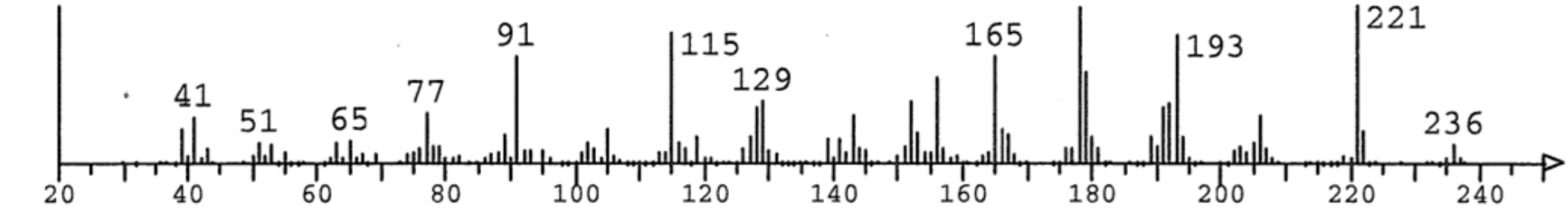

Figure 52: EI-MS of the Reaction Product from the Alkynylation of (+)-3-Caren (**A6**)

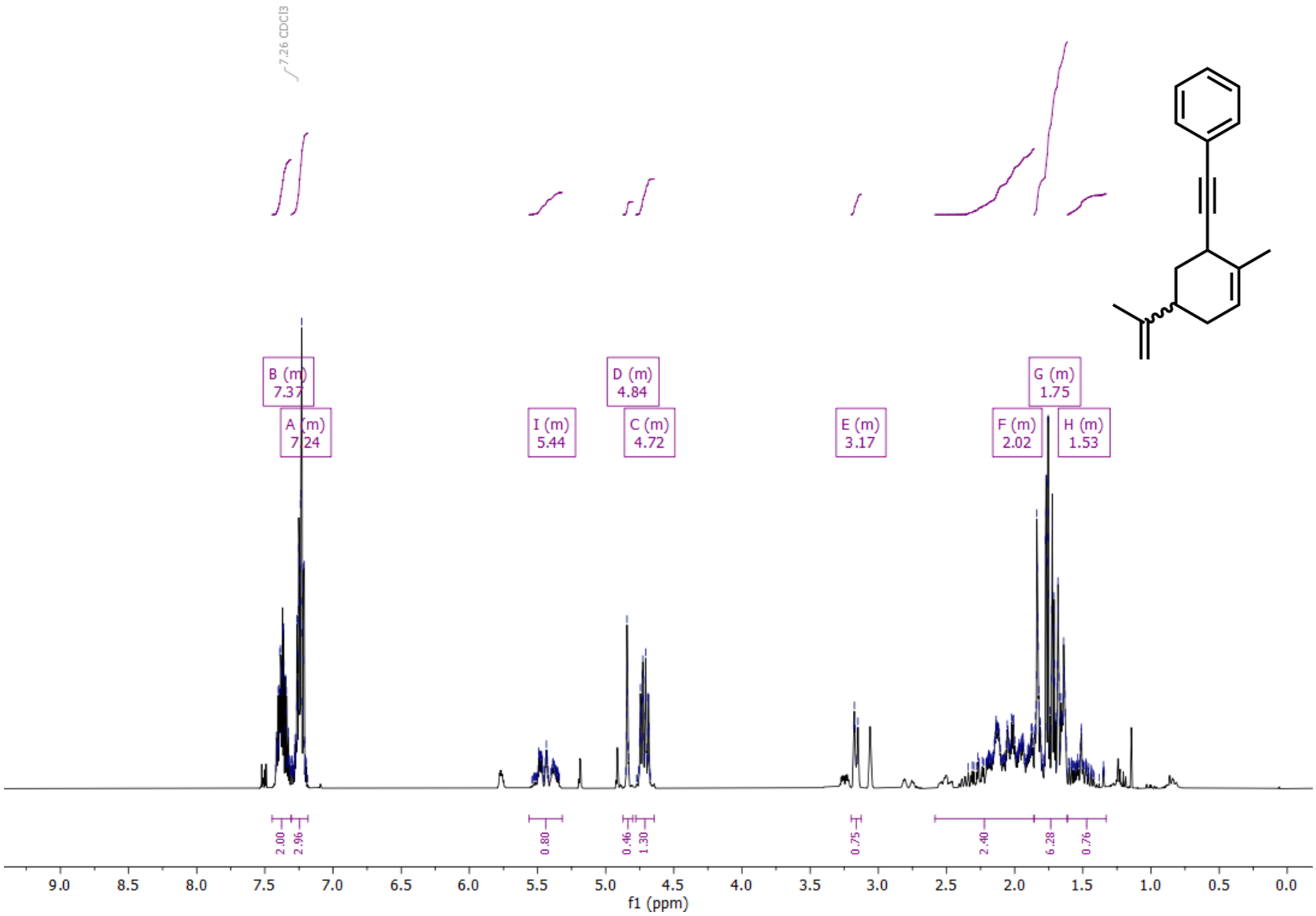

Figure 53: ^{1}H NMR (300 MHz, CDCl3) spectrum of ((2-methyl-5-(prop-1-en-2-yl)cyclohex-2-en-1-yl)ethynyl)benzene (**A7-1**)

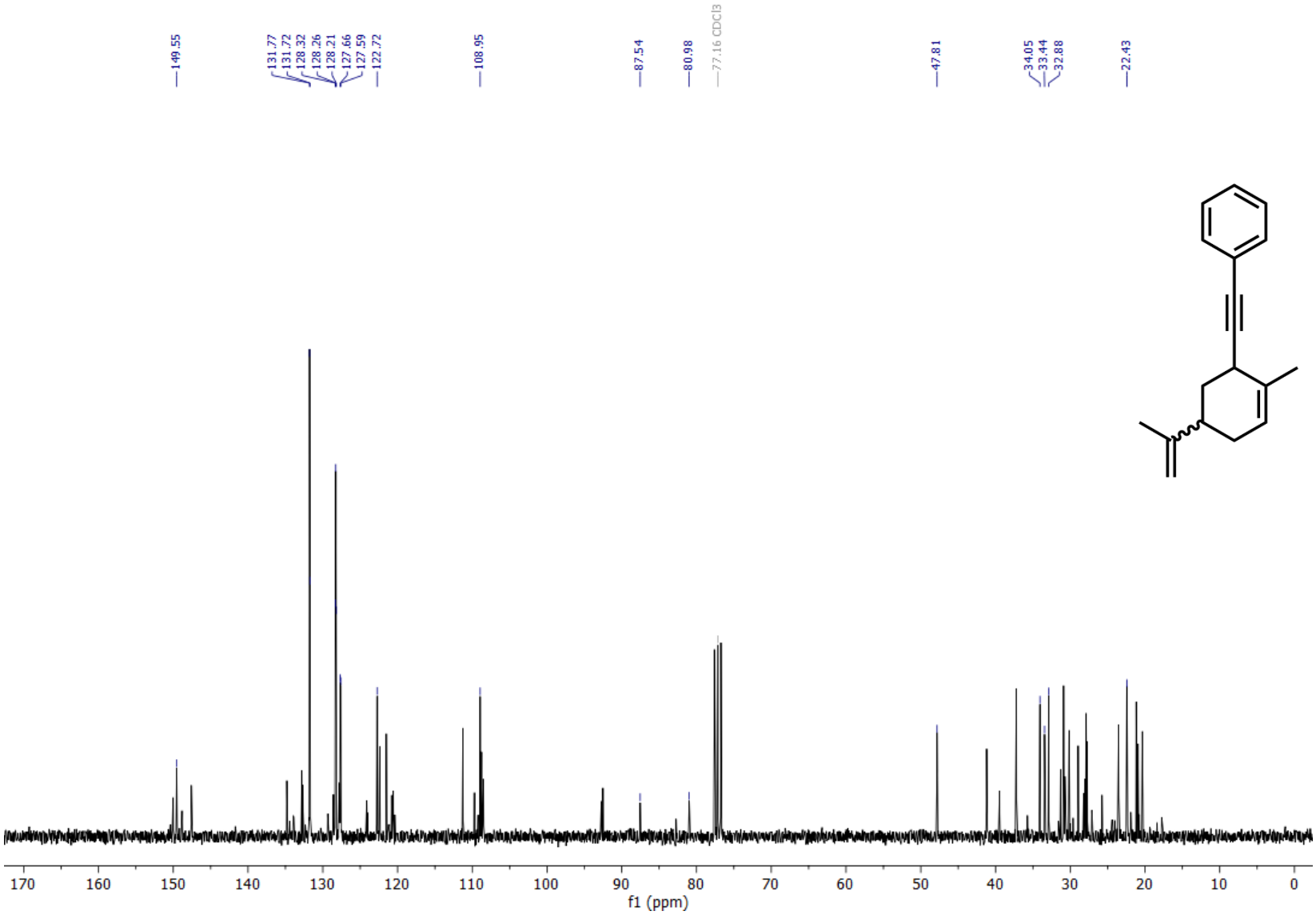

Figure 54: ^{13}C NMR (75 MHz, CDCl3) spectrum of ((2-methyl-5-(prop-1-en-2-yl)cyclohex-2-en-1-yl)ethynyl)benzene (**A7-1**)

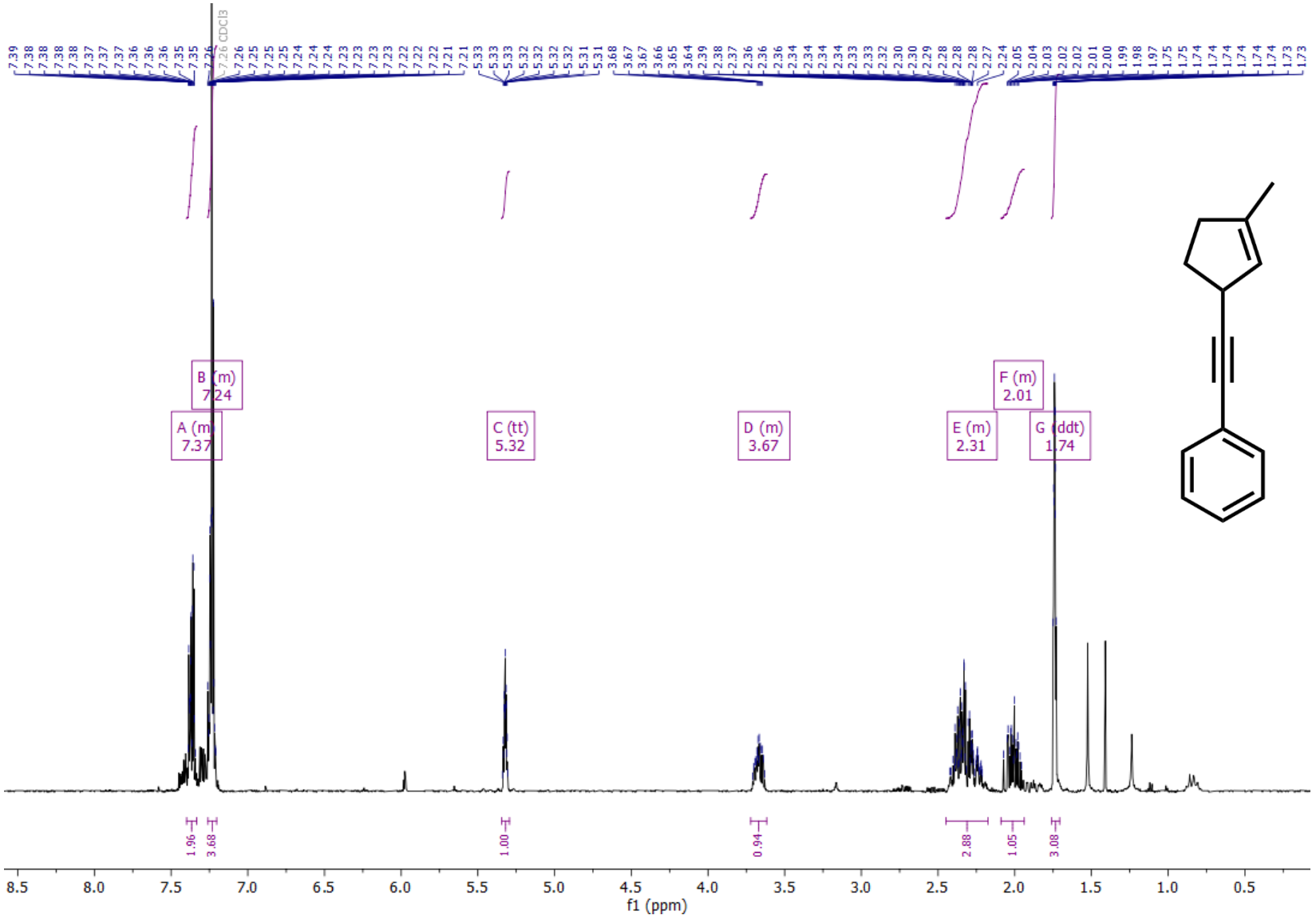

Figure 55: ^{1}H NMR (300 MHz, CDCl3) spectrum of (3-methylcyclopent-2-en-1-yl)ethynyl)benzene (**A8-1**)

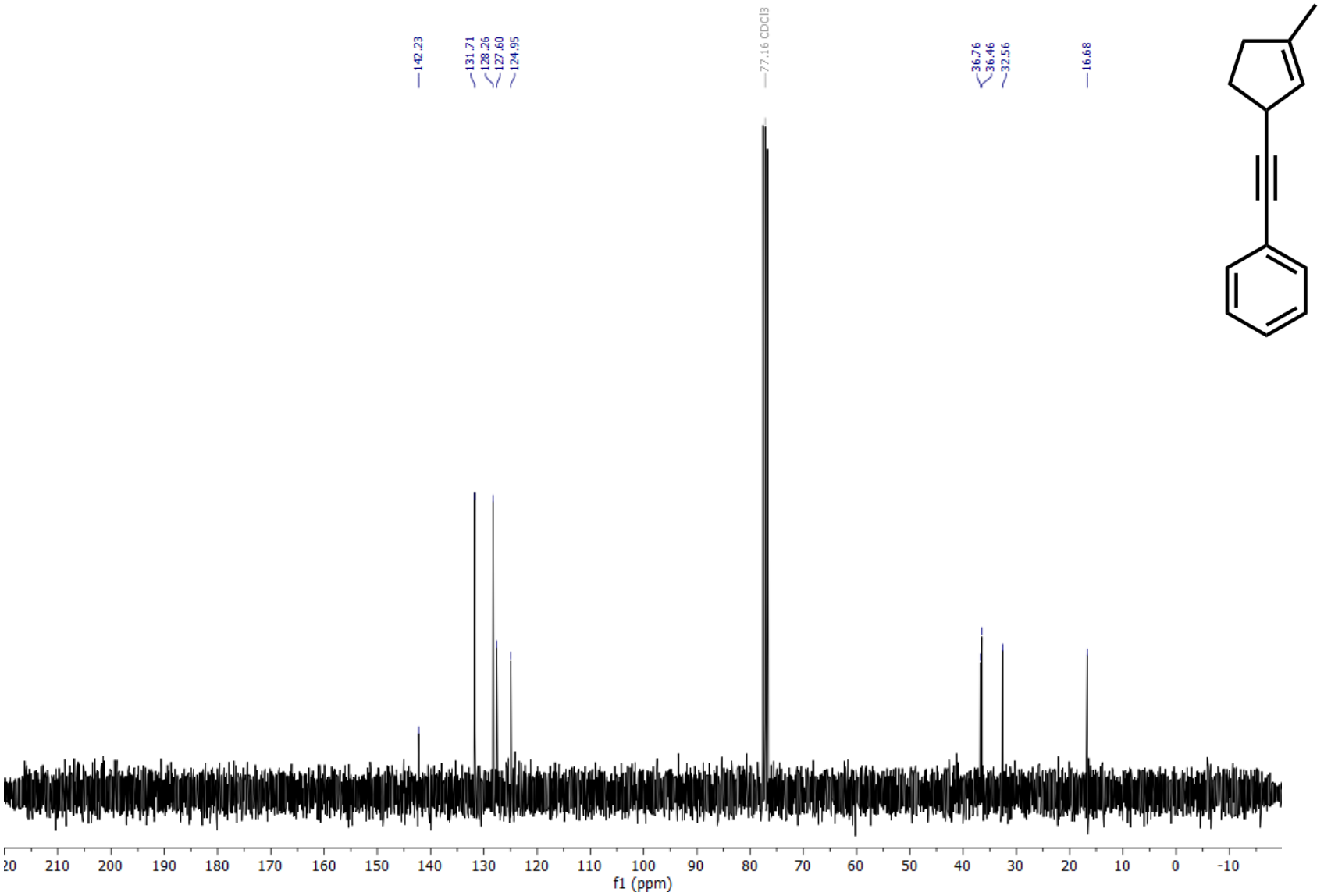

Figure 56: ^{13}C NMR (75 MHz, CDCl3) spectrum of ((3-methylcyclopent-2-en-1-yl)ethynyl)benzene (**A8-1**)

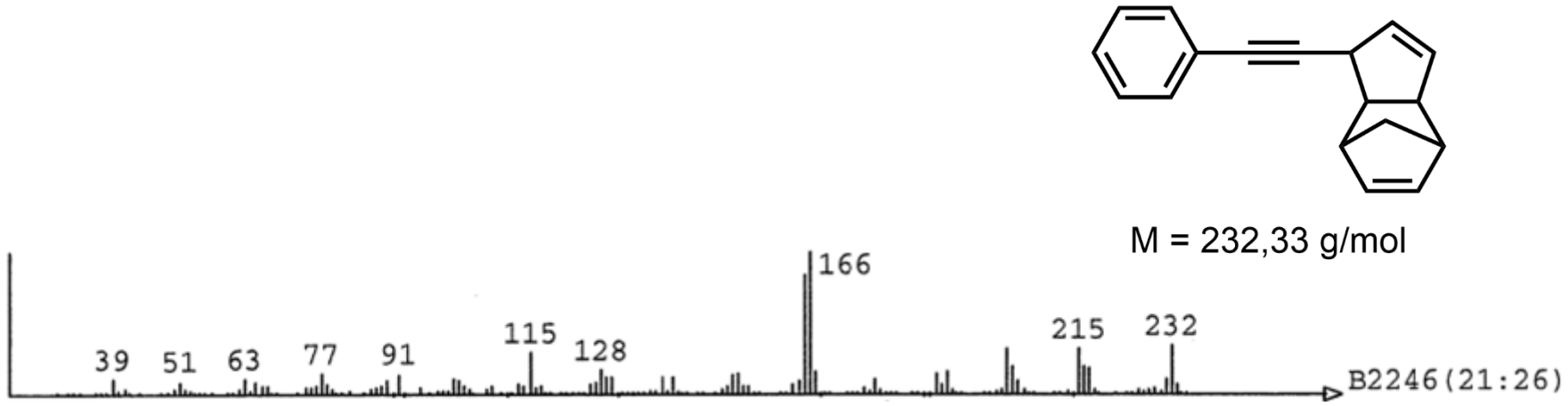

Figure 57: EI-MS of the Reaction Product from the Alkynylation of dicyclopentadiene (**A11**)

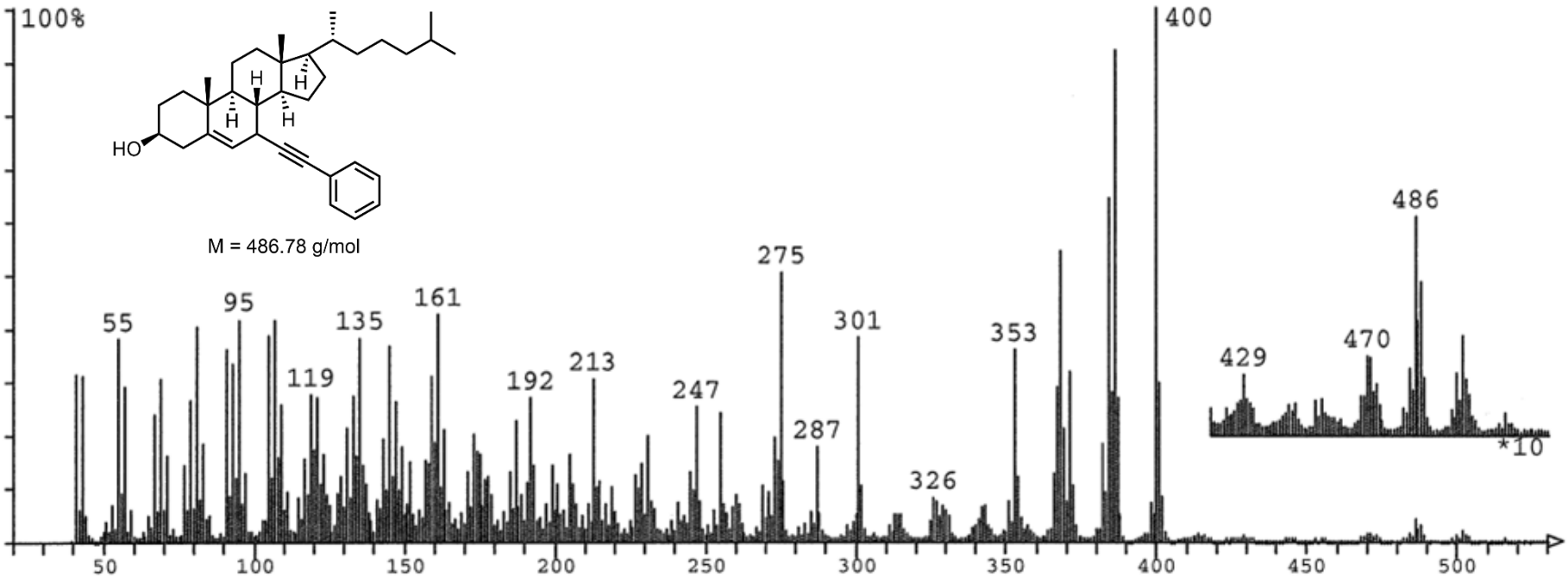

Figure 58: EI-MS of the Reaction Product from the Alkynylation of Cholesterol (**A13**).

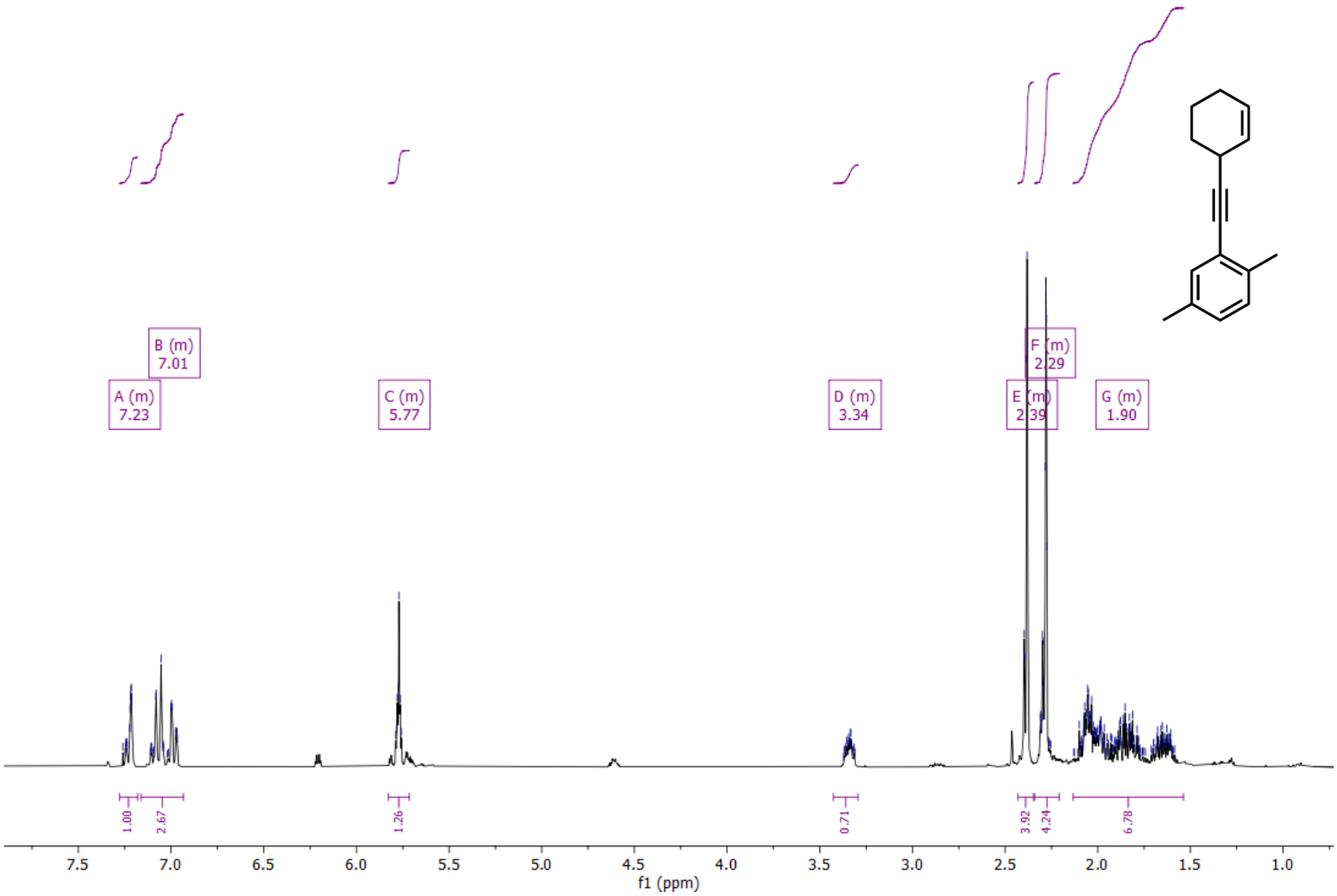

Figure 59: ^{1}H NMR (300 MHz, CDCl3) spectrum of 2-(cyclohex-2-en-1-ylethynyl)-1,4-dimethylbenzene (**B1-1**)

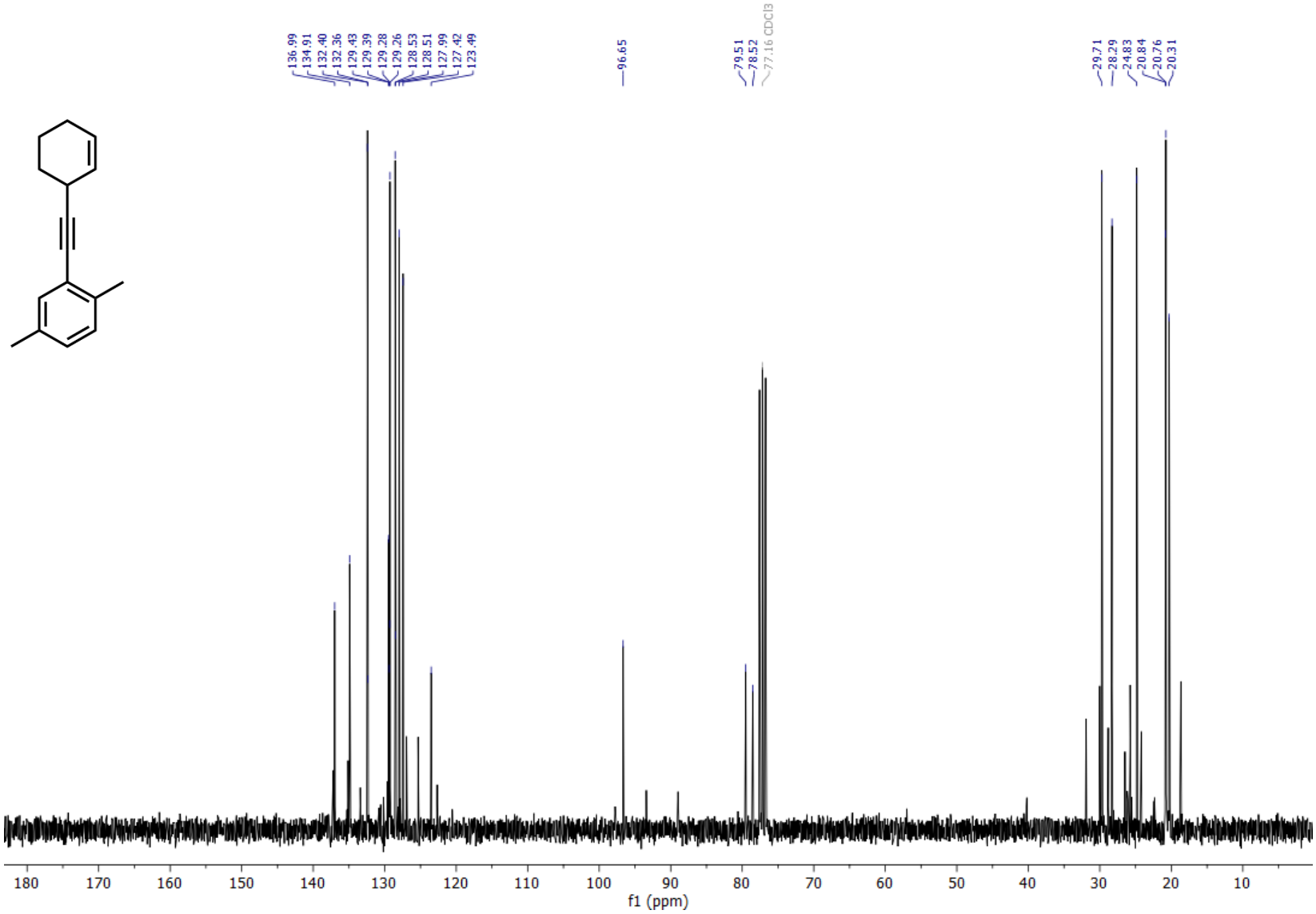

Figure 60: ^{13}C NMR (75 MHz, CDCl3) spectrum of 2-(cyclohex-2-en-1-ylethynyl)-1,4-dimethylbenzene (**B1-1**)

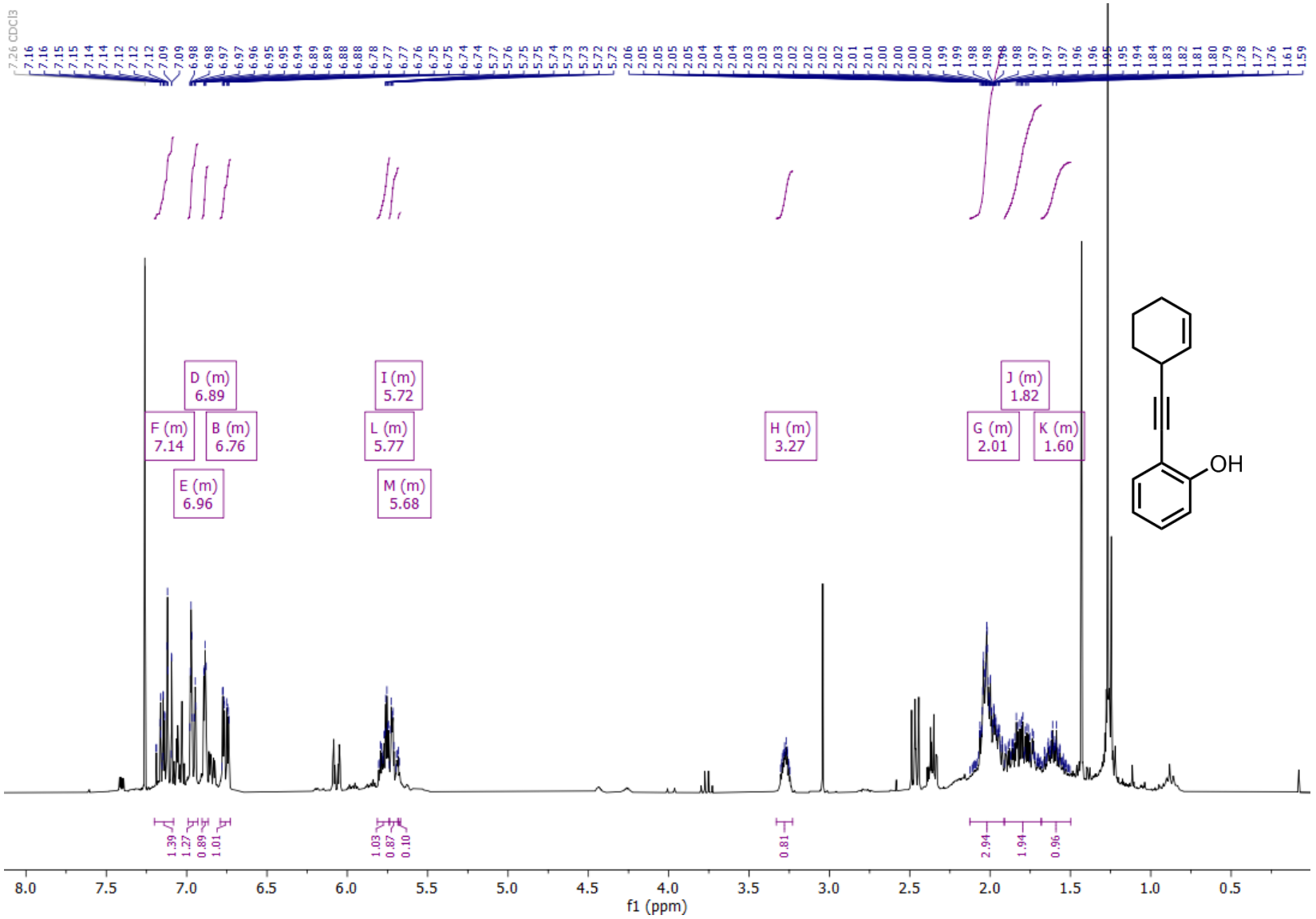

Figure 61: ^{1}H NMR (300 MHz, CDCl3) spectrum of 2-(cyclohex-2-en-1-ylethynyl)phenol (**B2-1**).

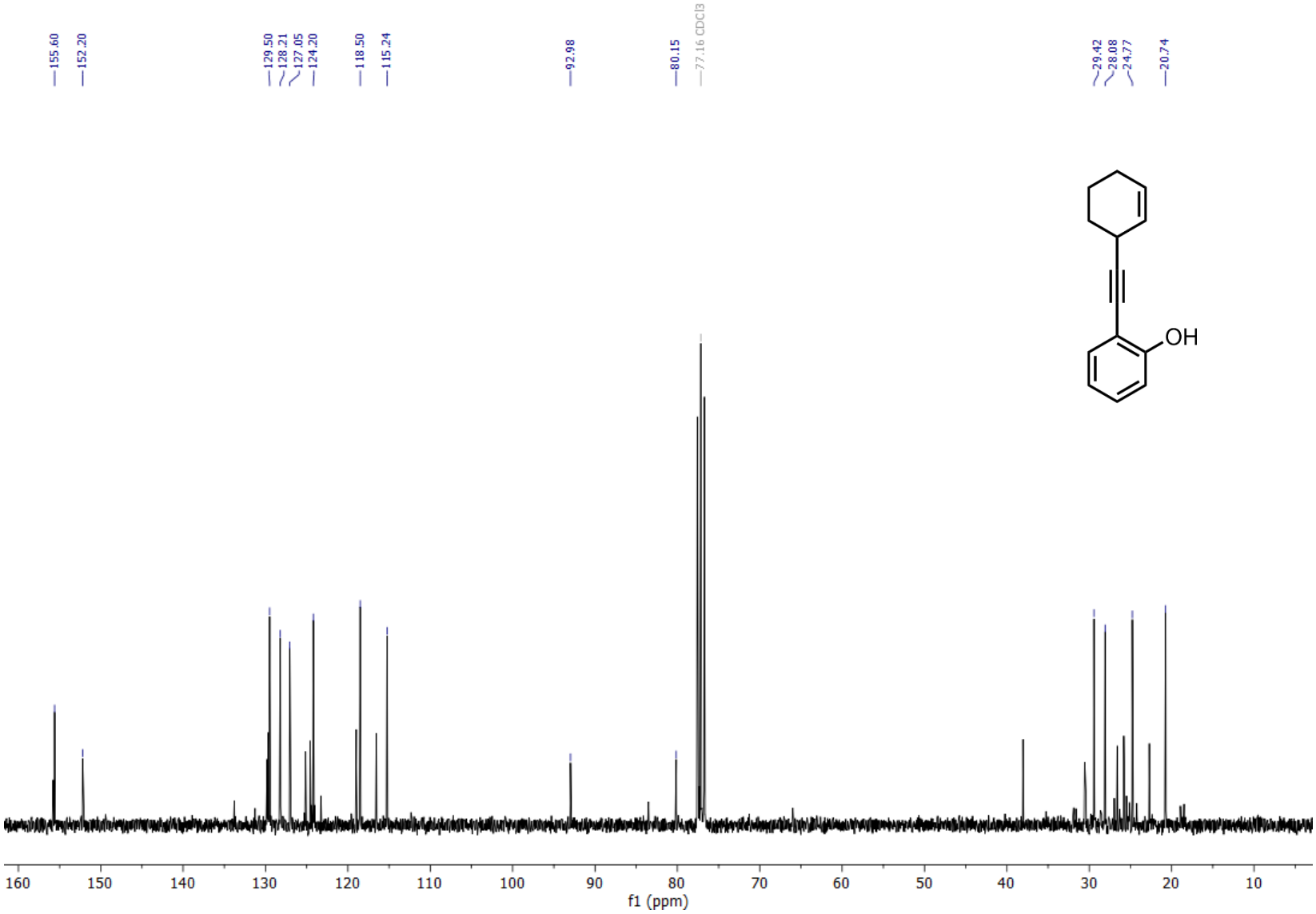

Figure 62: ^{13}C NMR (75 MHz, CDCl3) spectrum of 2-(cyclohex-2-en-1-ylethynyl)phenol (**B2-1**).

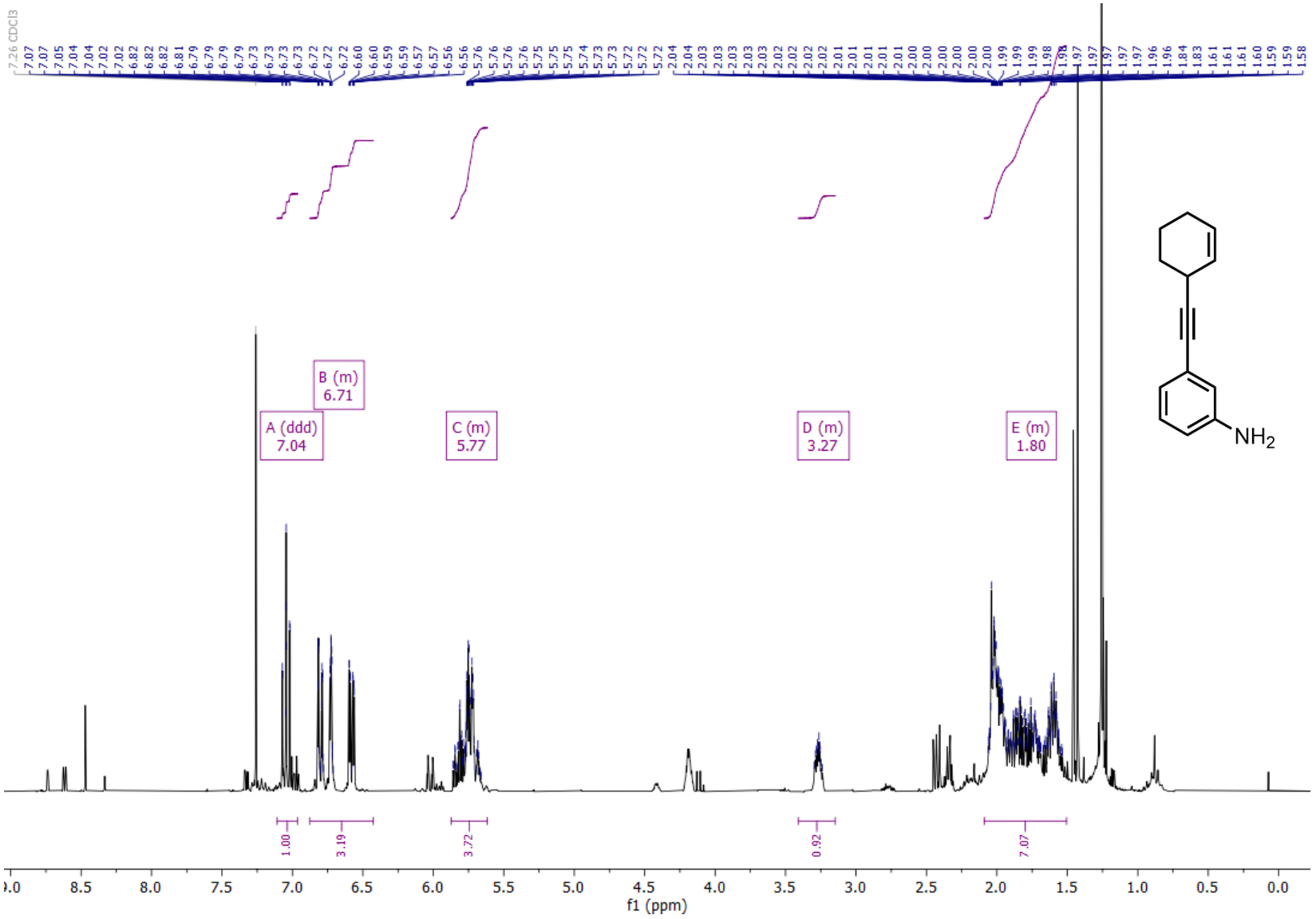

Figure 63: ^{1}H NMR (300 MHz, CDCl3) spectrum of 3-(cyclohex-2-en-1-ylethynyl)aniline (**B3-1**)

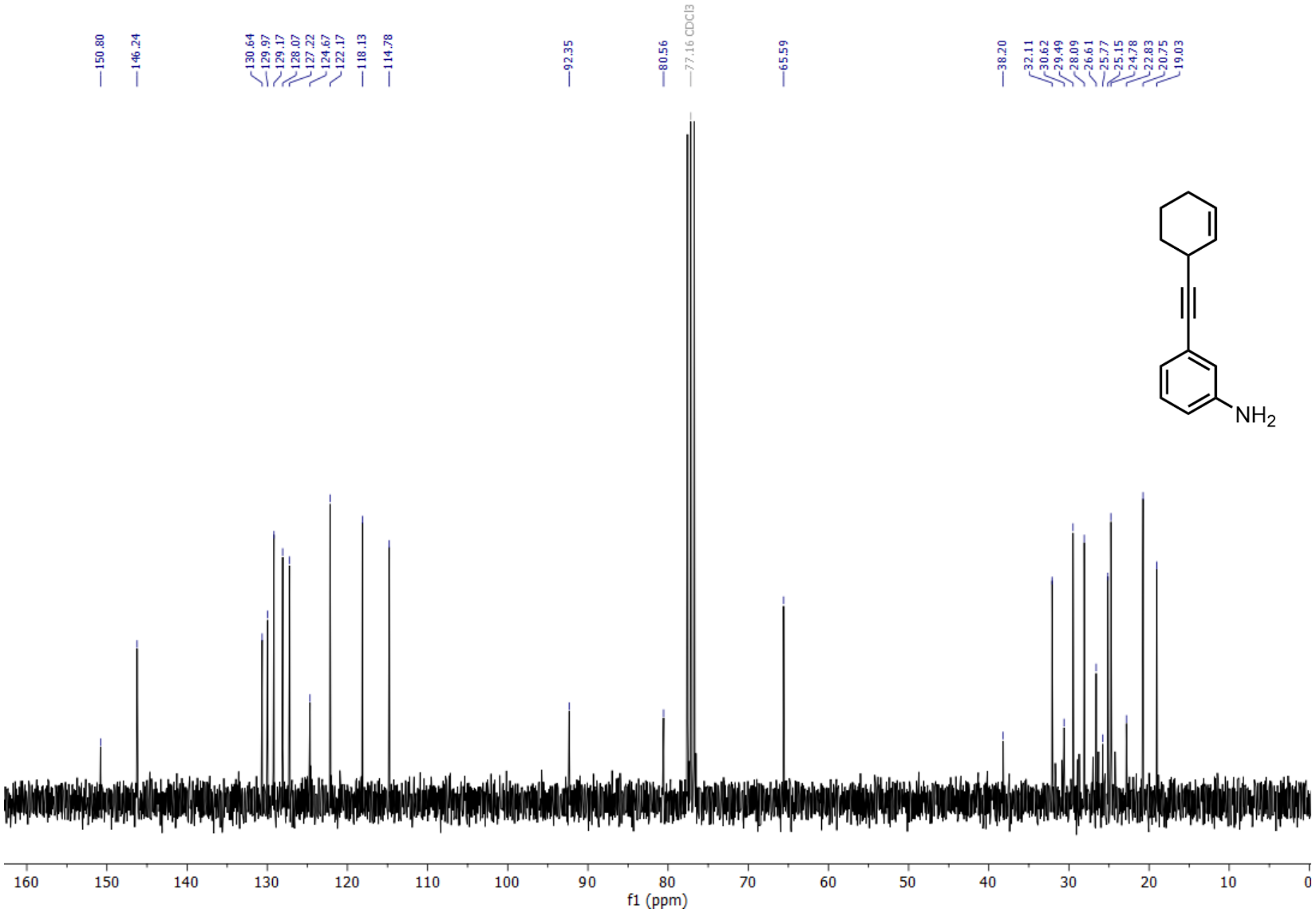

Figure 64: ^{13}C NMR (75 MHz, CDCl3) spectrum of 3-(cyclohex-2-en-1-ylethynyl)aniline (**B3-1**).

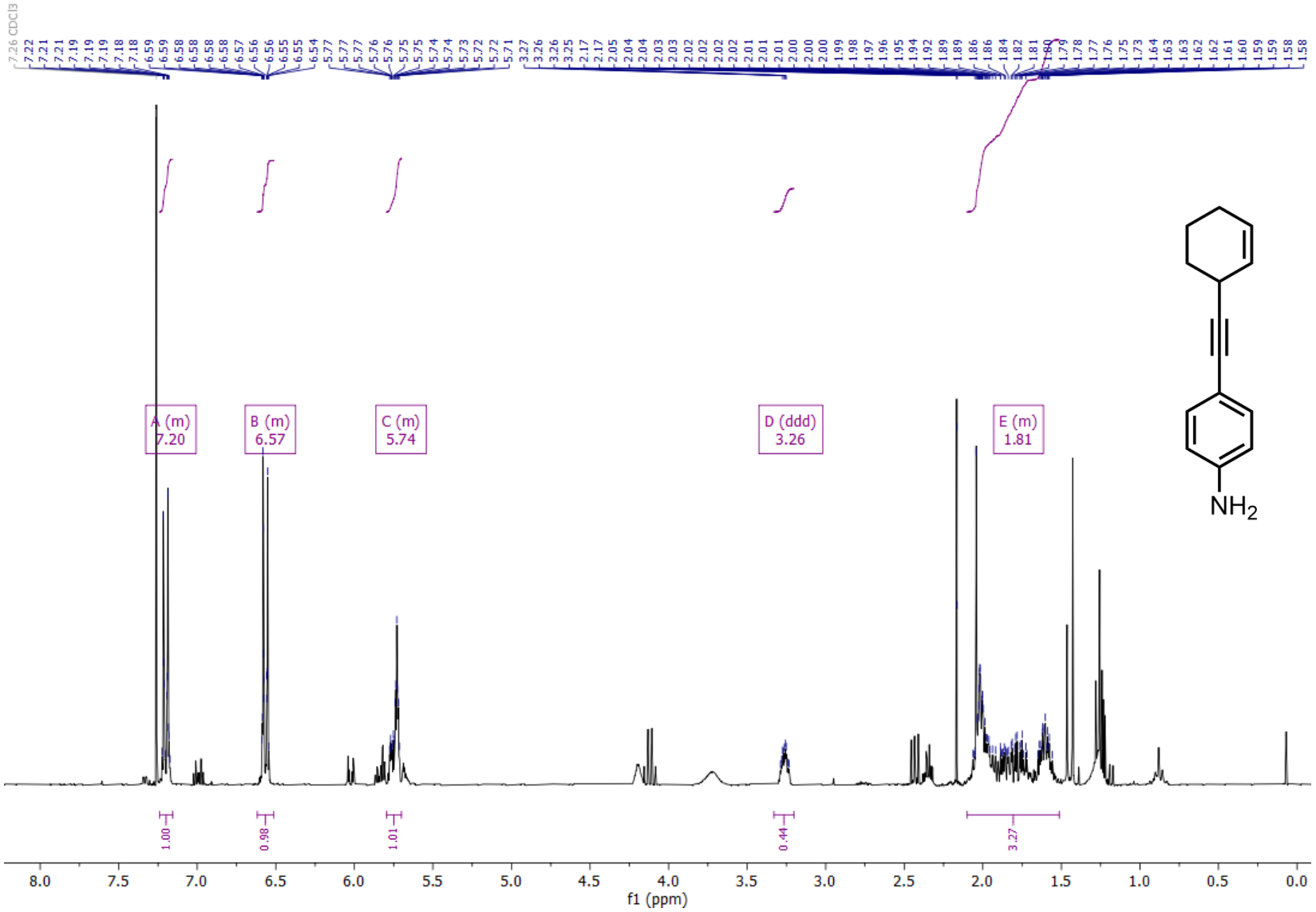

Figure 65: ^{1}H NMR (300 MHz, CDCl3) spectrum of 4-(cyclohex-2-en-1-ylethynyl)aniline (**B4-1**).

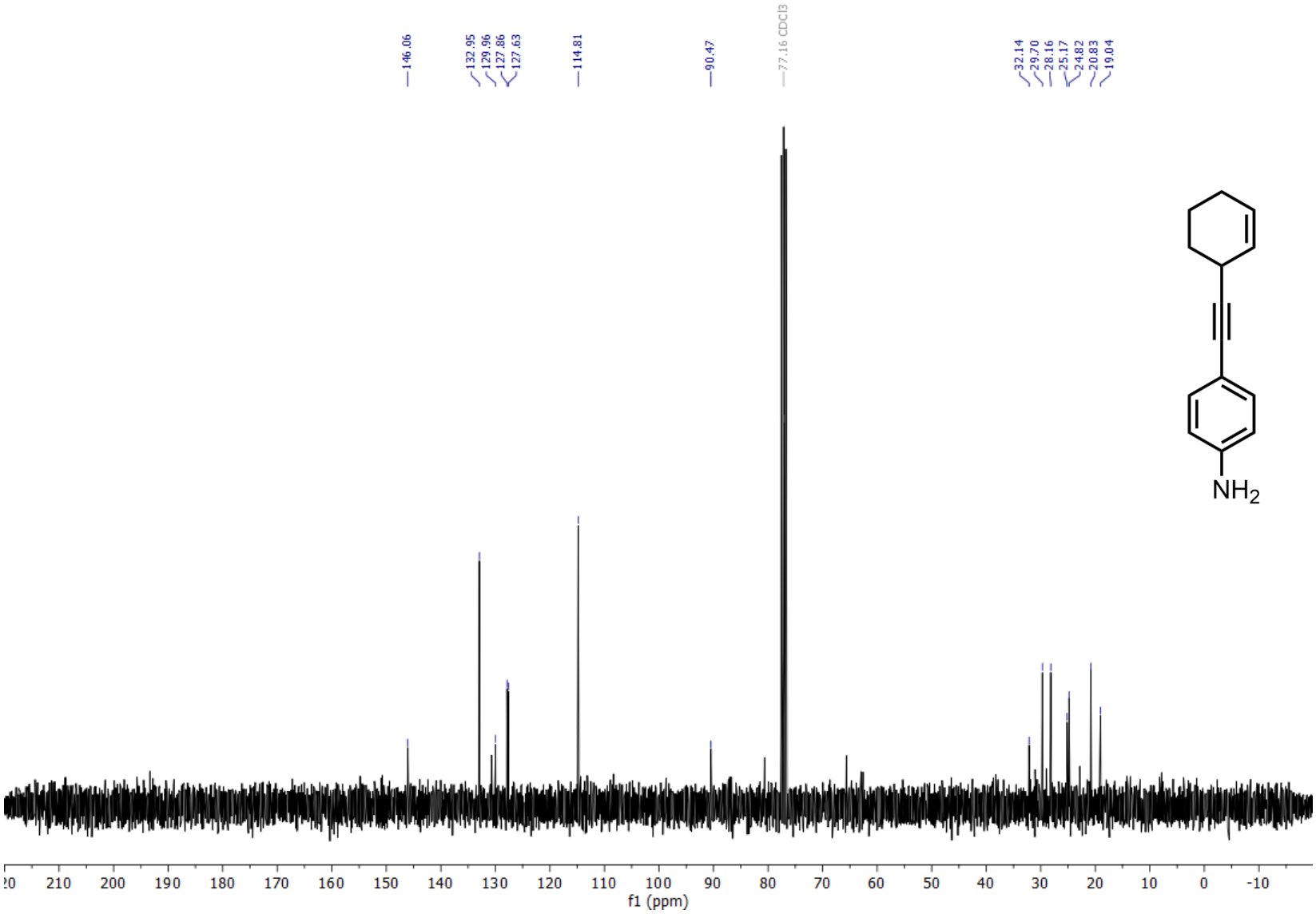

Figure 66: ^{13}C NMR (75 MHz, CDCl3) spectrum of 4-(cyclohex-2-en-1-ylethynyl)aniline (**B4-1**).

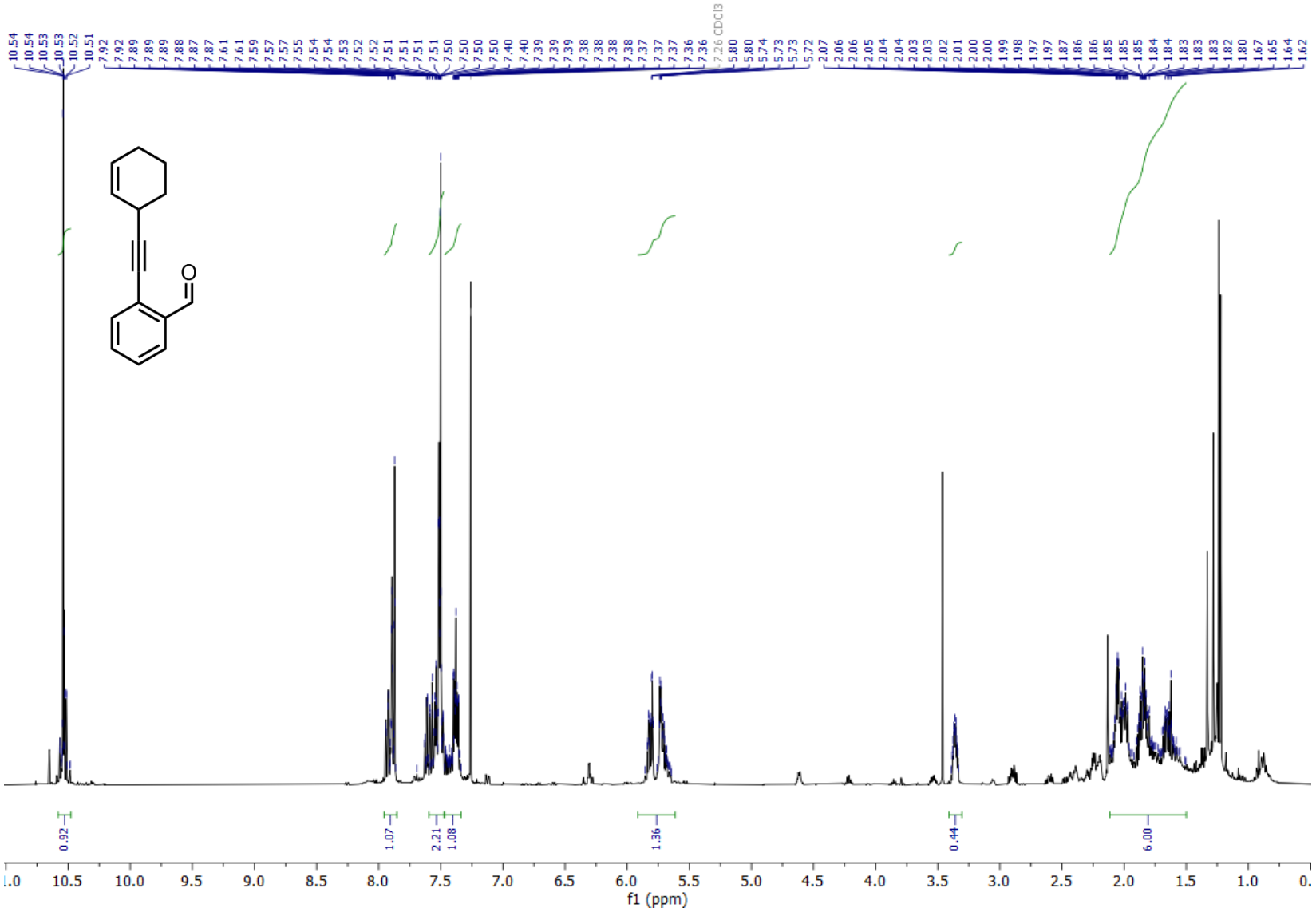

Figure 67: ^{1}H NMR (300 MHz, CDCl3) spectrum of 2-(cyclohex-2-en-1-ylethynyl)benzaldehyde (**B5-1**).

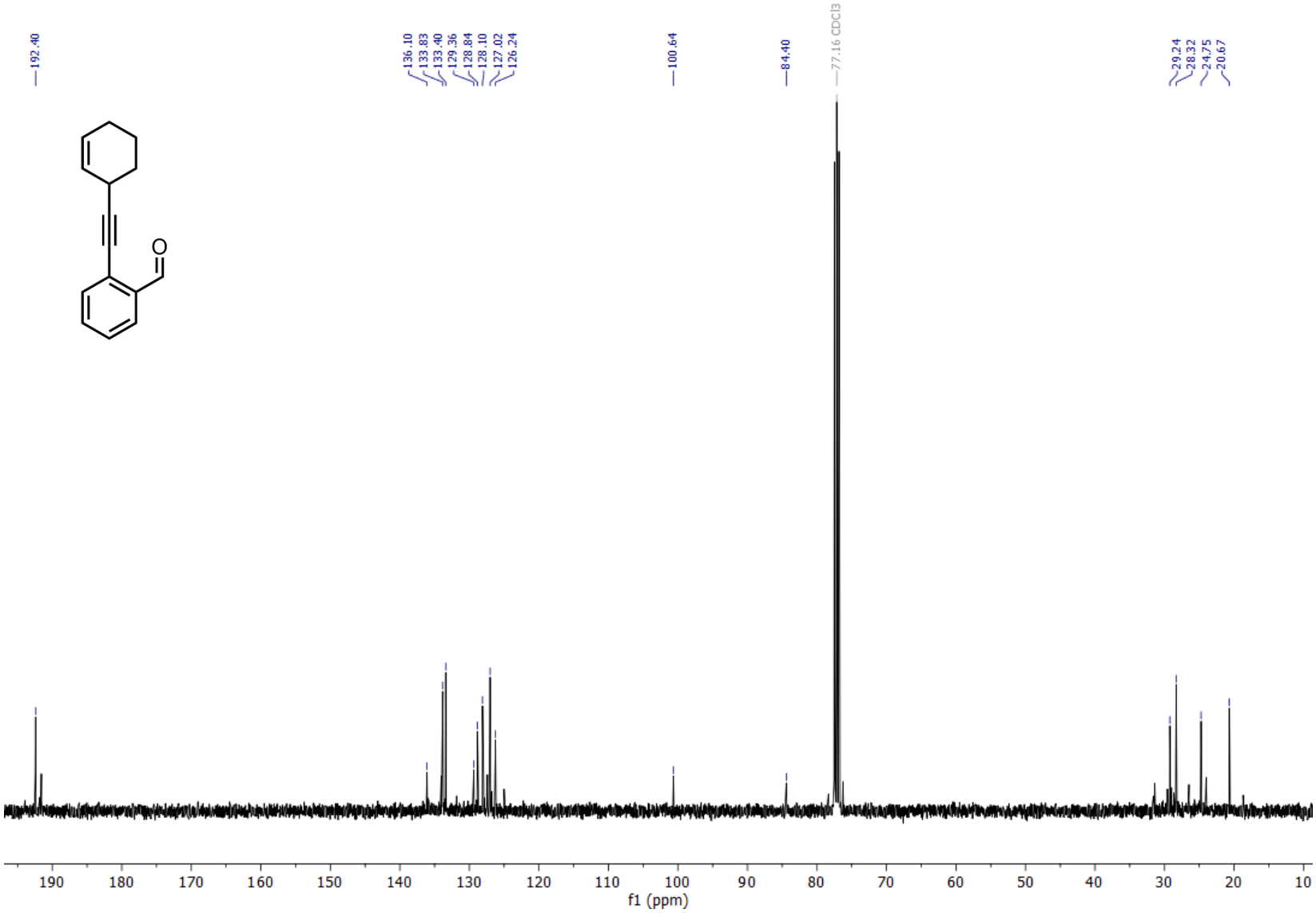

Figure 68: ^{13}C NMR (75 MHz, CDCl3) spectrum of 2-(cyclohex-2-en-1-ylethynyl)benzaldehyde (**B5-1**).

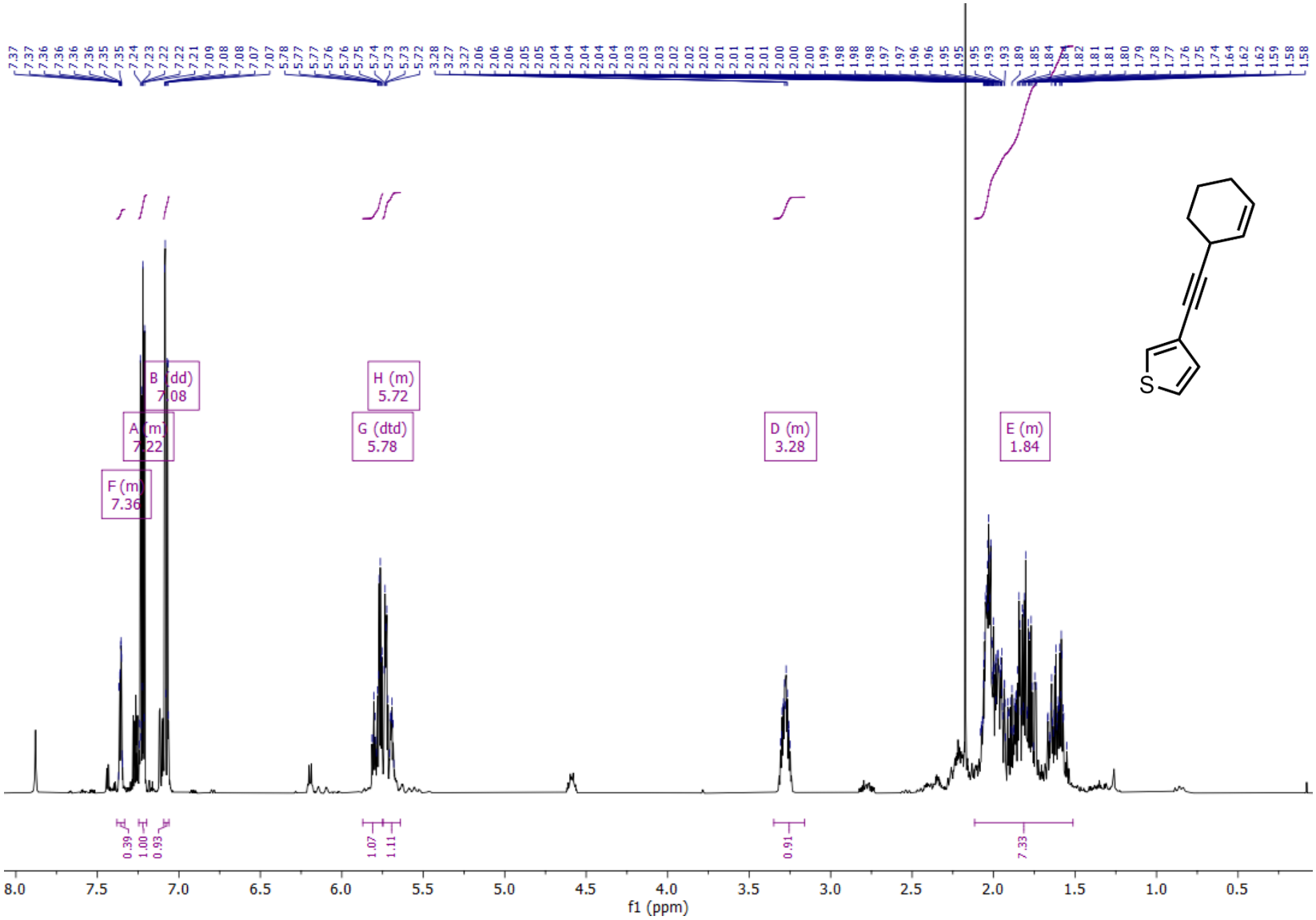

Figure 69: ^{1}H NMR (300 MHz, CDCl3) spectrum of 3-(cyclohex-2-en-1-ylethynyl)thiophene (**B6-1**)

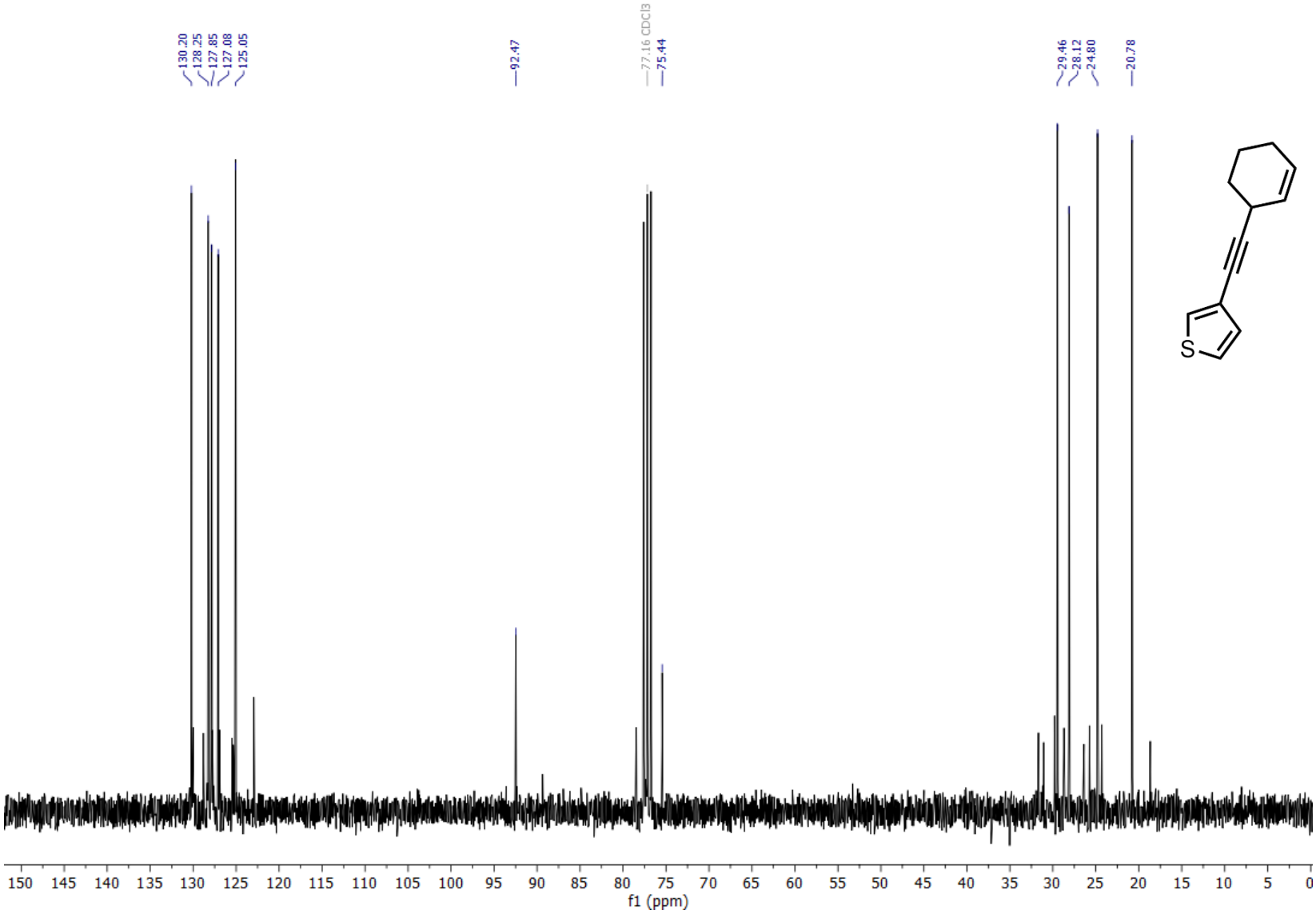

Figure 70: ^{13}C NMR (75 MHz, CDCl3) spectrum of 3-(cyclohex-2-en-1-ylethynyl)thiophene (**B6-1**)

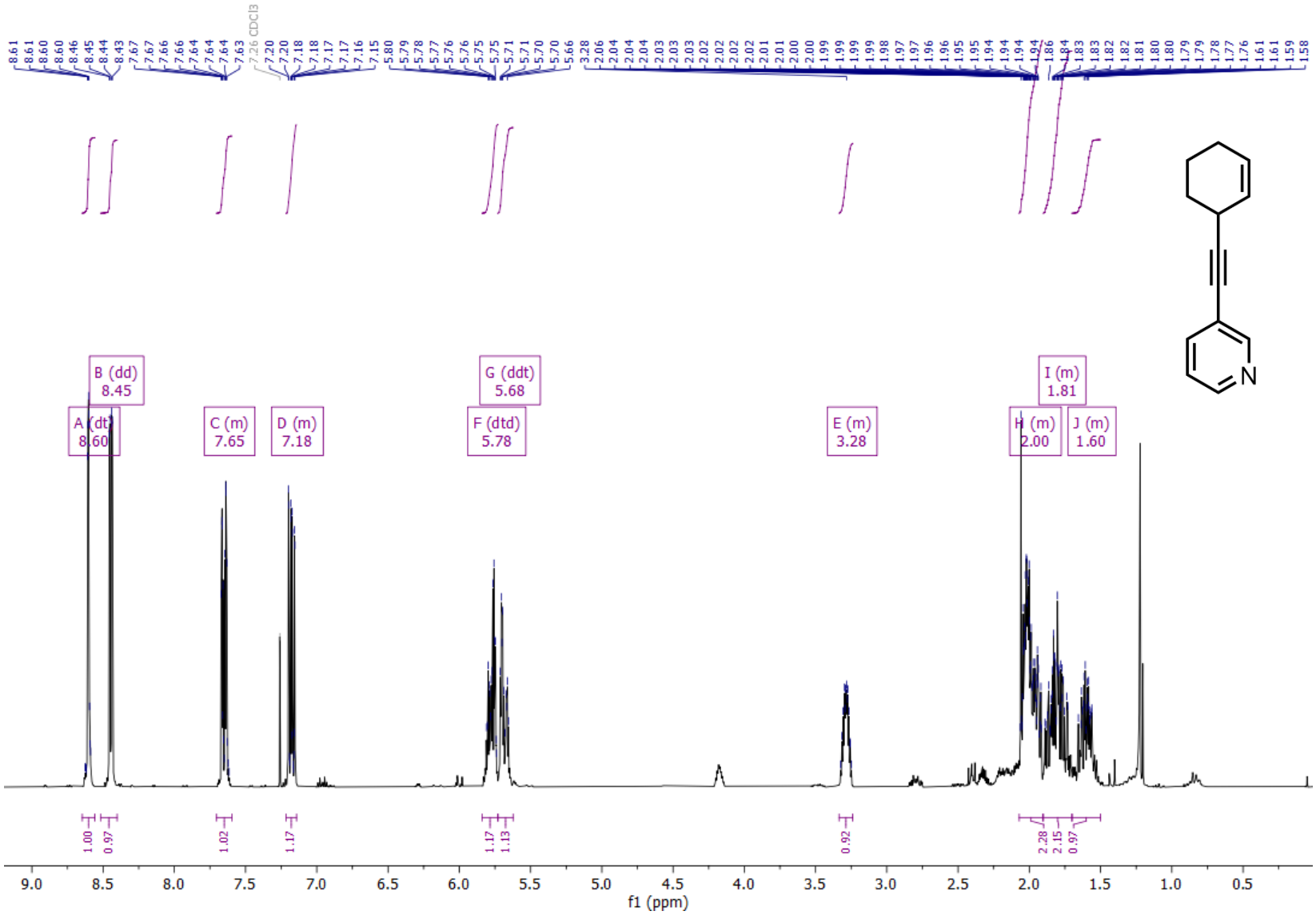

Figure 71: ^{1}H NMR (300 MHz, CDCl3) spectrum of 3-(cyclohex-2-en-1-ylethynyl)pyridine (**B7-1**).

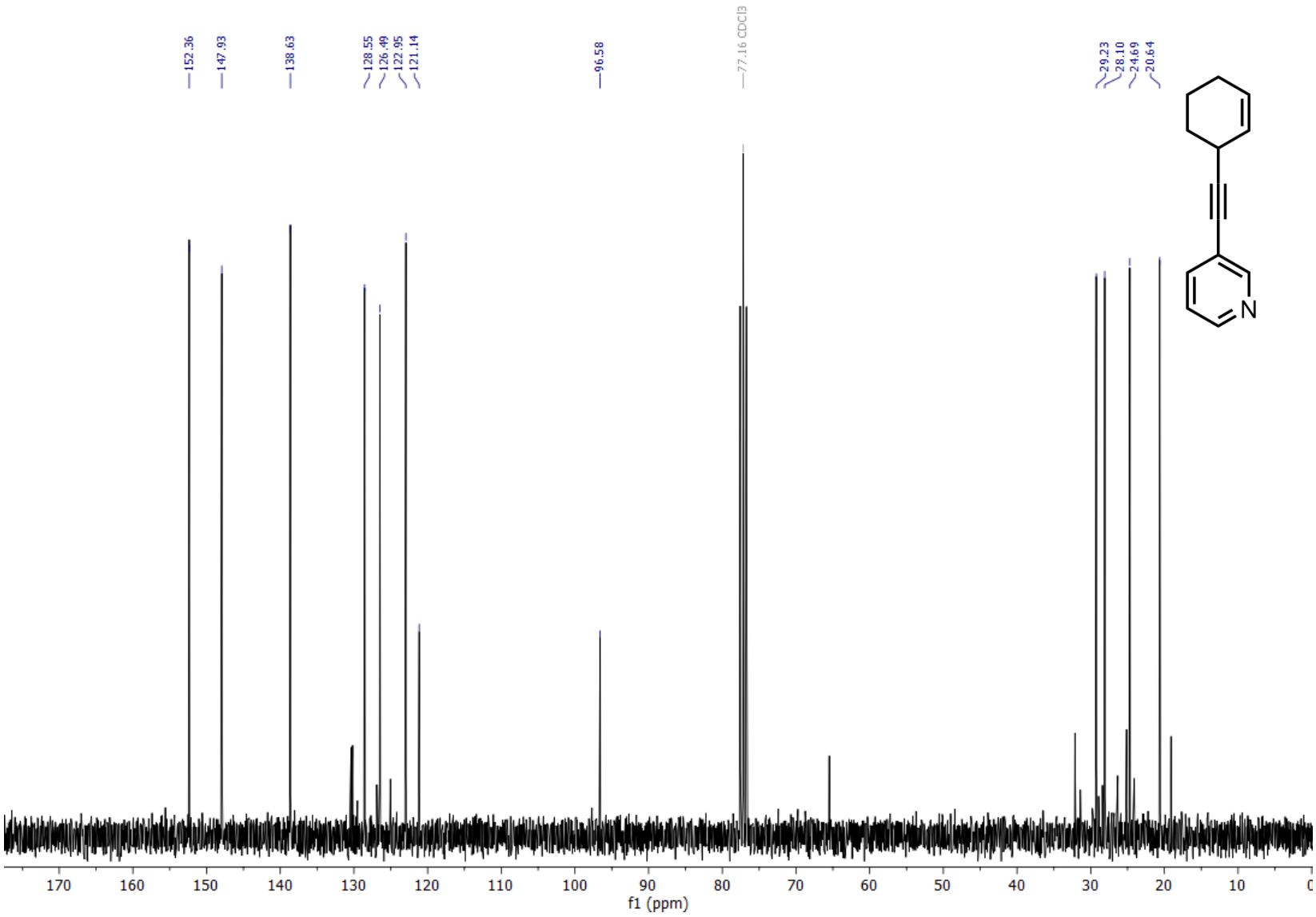

Figure 72: ^{13}C NMR (75 MHz, CDCl3) spectrum of 3-(cyclohex-2-en-1-ylethynyl)pyridine (**B7-1**)

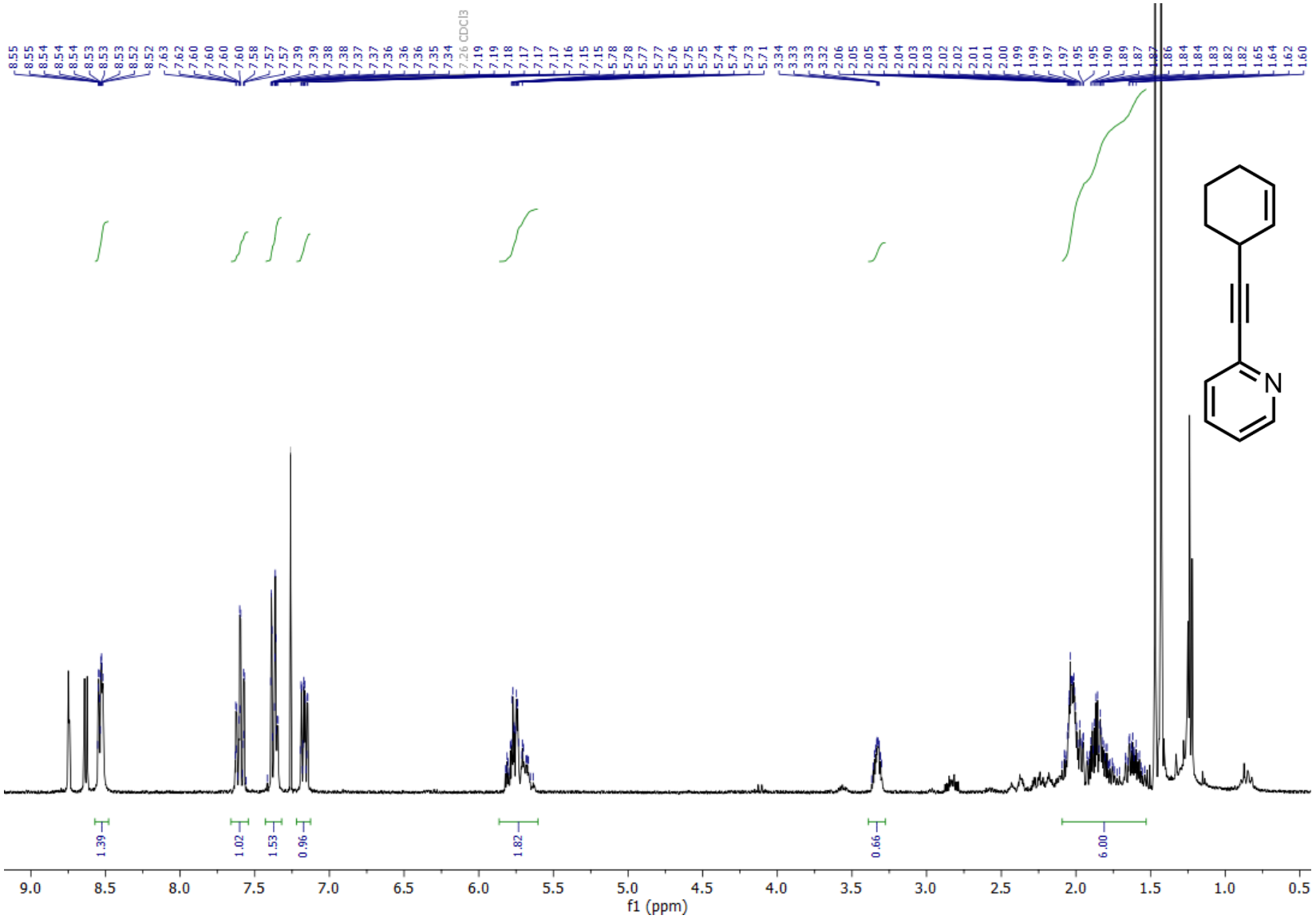

Figure 73: ^{1}H NMR (300 MHz, CDCl3) spectrum of 2-(cyclohex-2-en-1-ylethynyl)pyridine (**B8-1**).

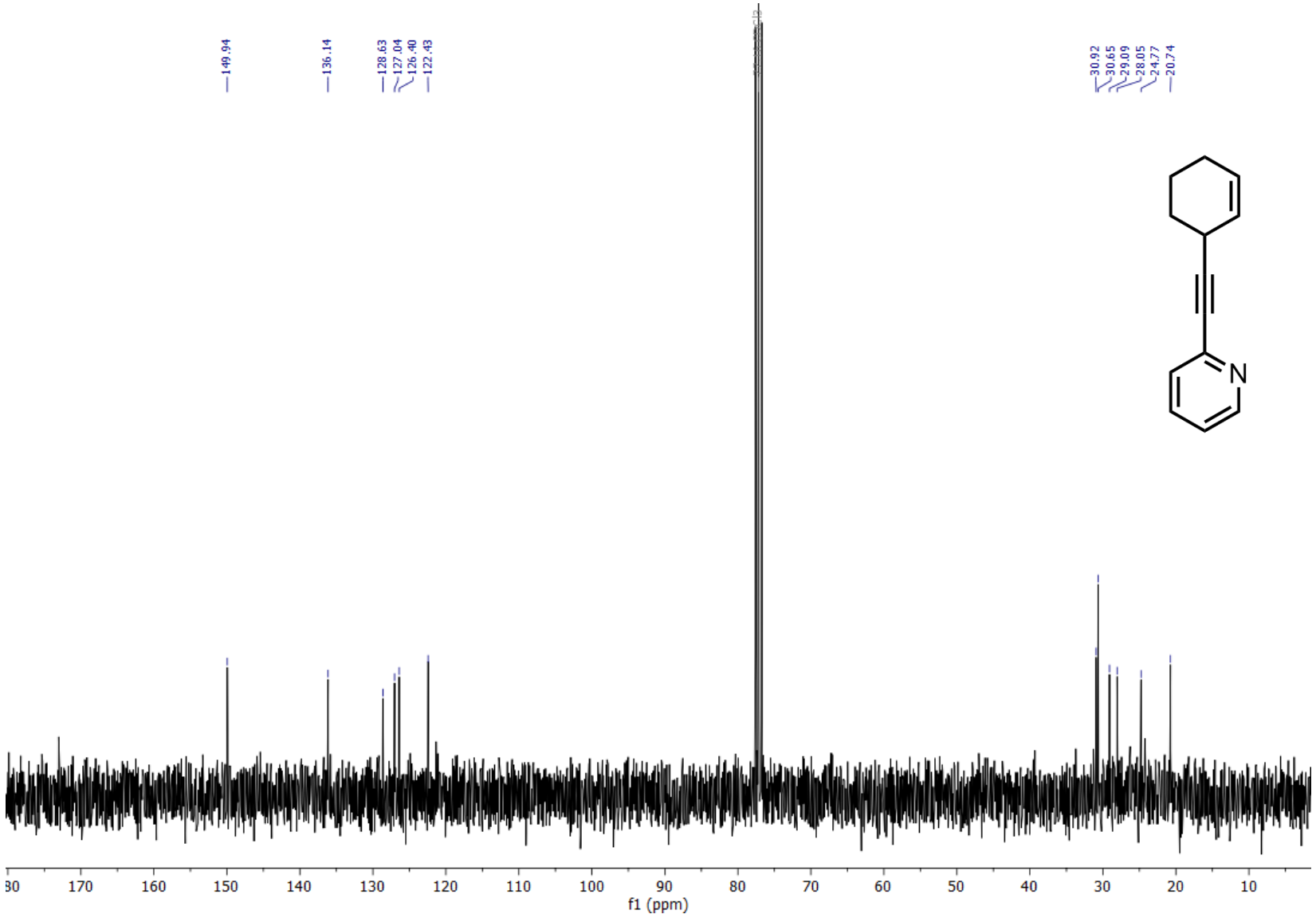

Figure 74: ^{13}C NMR (75 MHz, CDCl3) spectrum of 2-(cyclohex-2-en-1-ylethynyl)pyridine (**B8-1**).

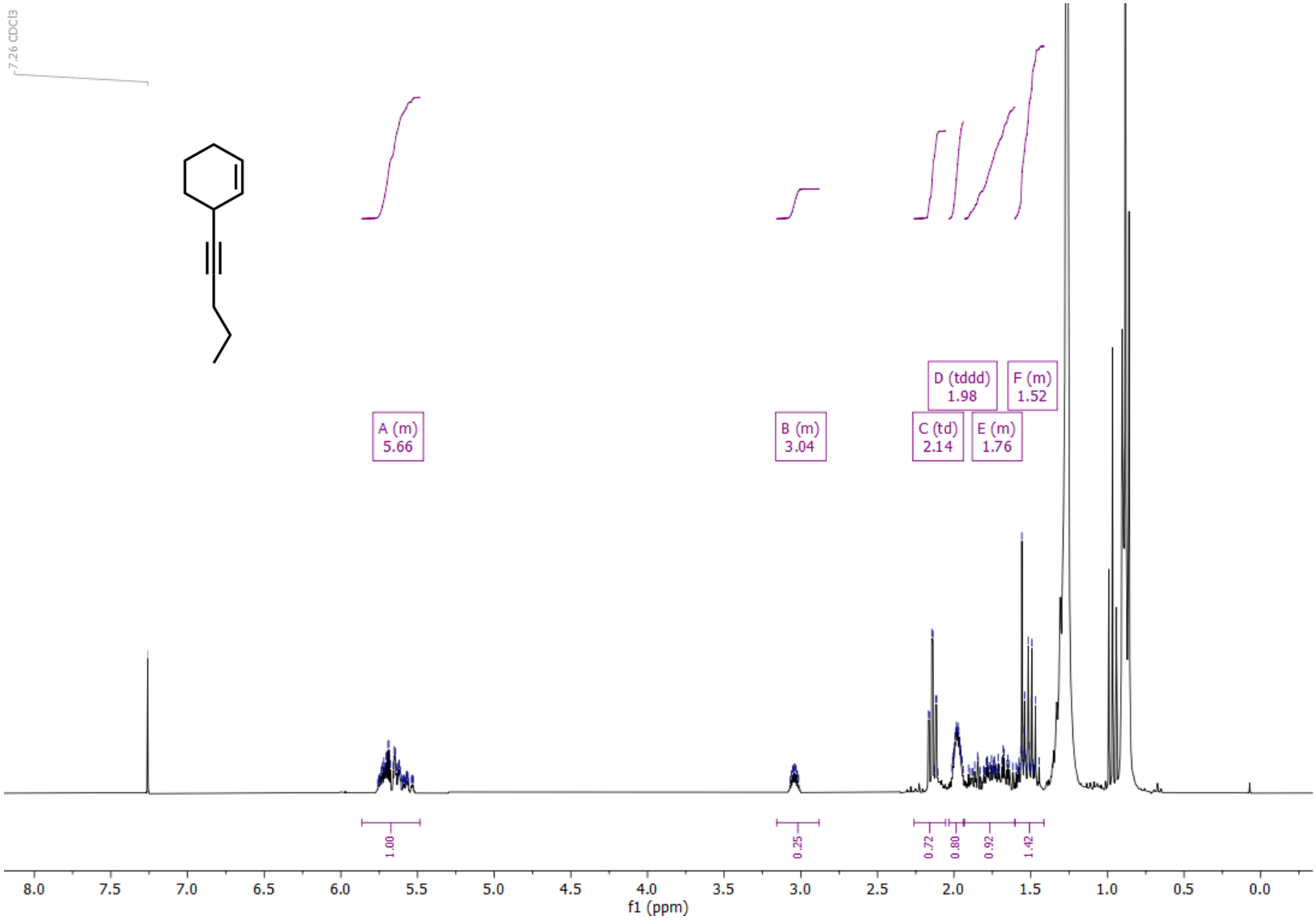

Figure 75: ^{1}H NMR (300 MHz, CDCl3) spectrum of 3-(pent-1-yn-1-yl)cyclohex-1-ene (**B9-1**).

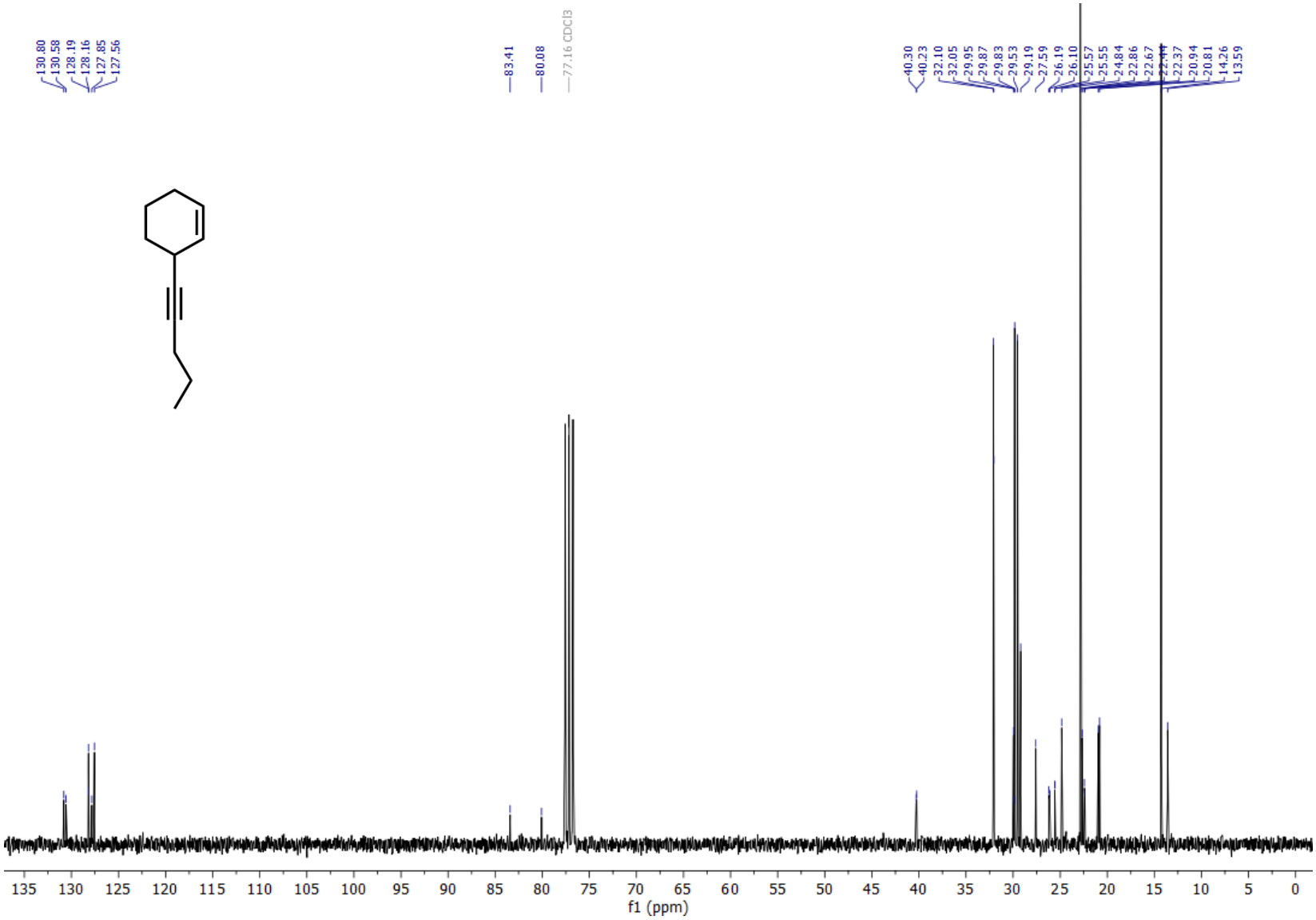

Figure 76: ^{13}C NMR (75 MHz, CDCl3) spectrum 3-(pent-1-yn-1-yl)cyclohex-1-ene (**B9-1**).

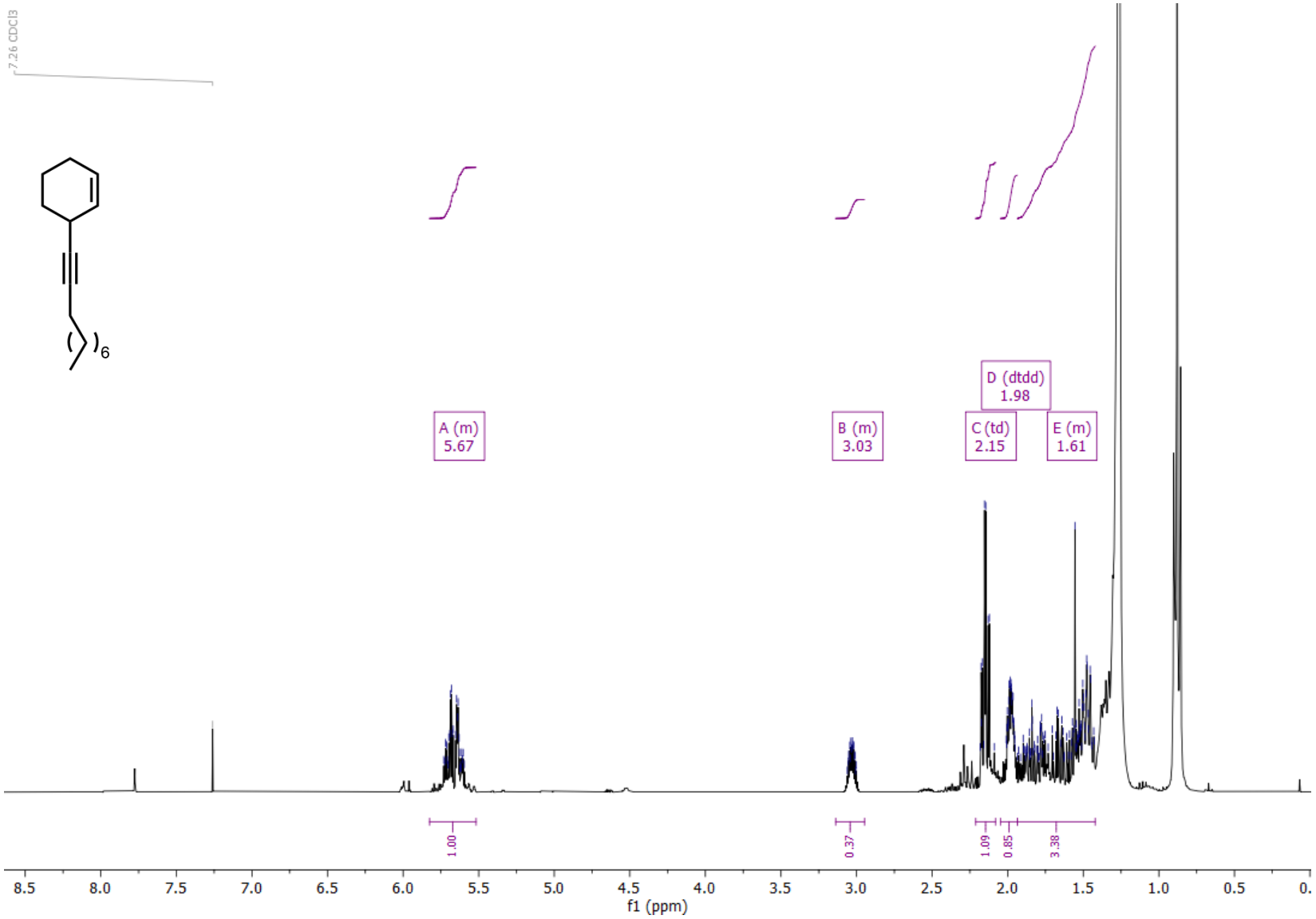

Figure 77: ^{1}H NMR (300 MHz, CDCl3) spectrum of 3-(dec-1-yn-1-yl)cyclohex-1-ene (**B10-1**).

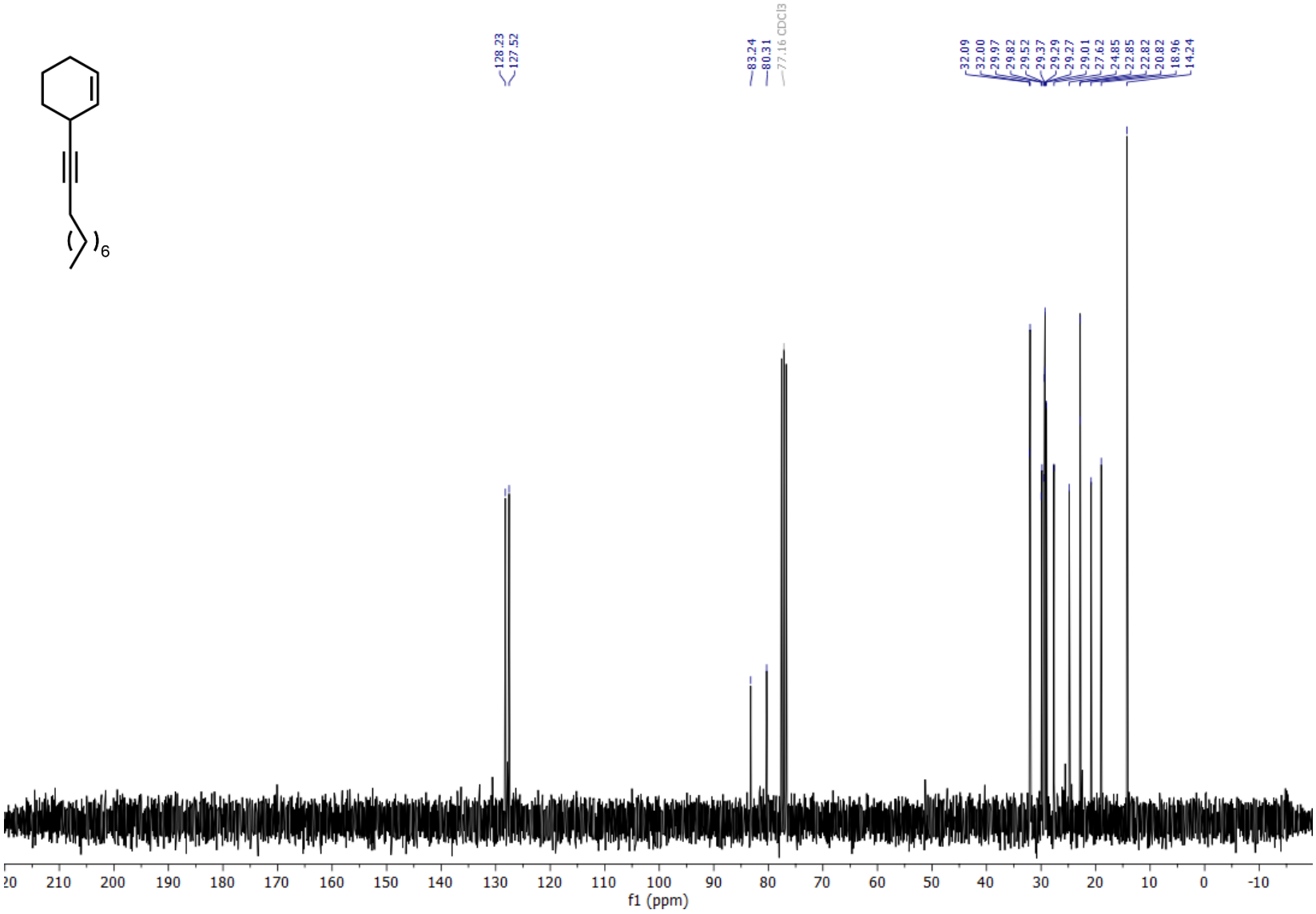

Figure 78: ^{13}C NMR (75 MHz, CDCl3) spectrum 3-(dec -1-yn-1-yl)cyclohex-1-ene (**B10-1**).

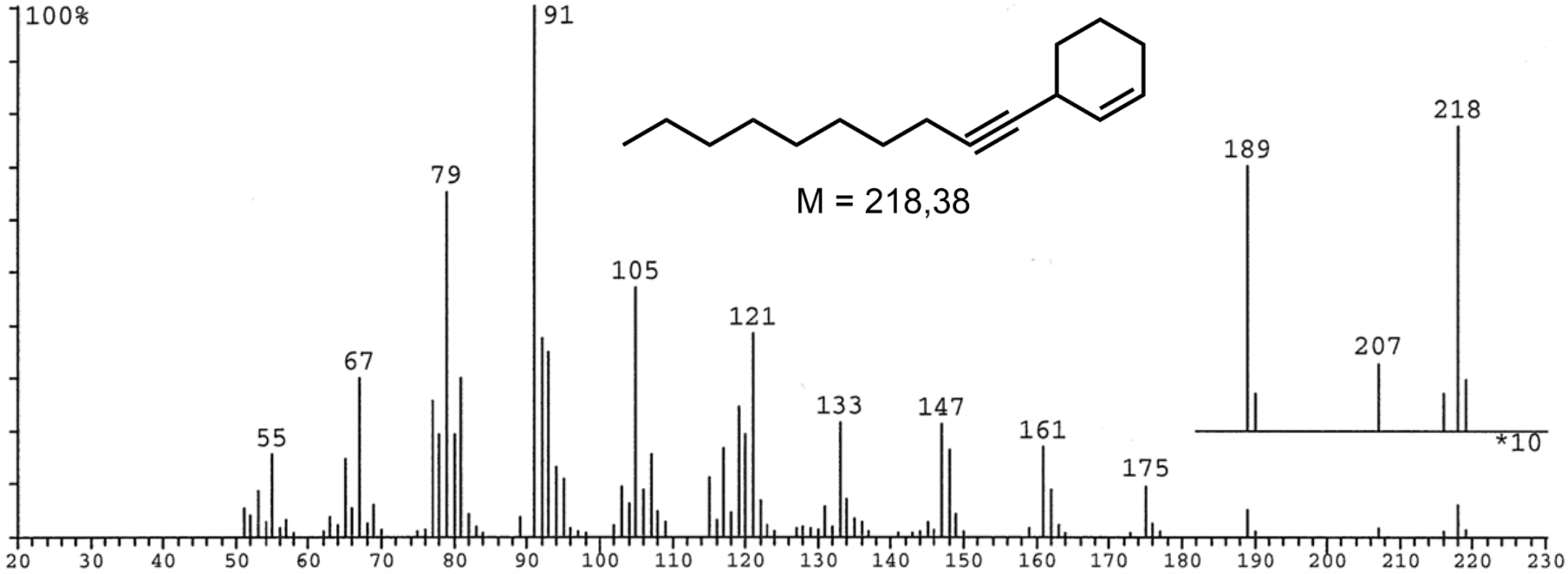

Figure 79: EI-MS of the Reaction Product from the Allylic Alkynylation of dec-1-yne (**B10**)

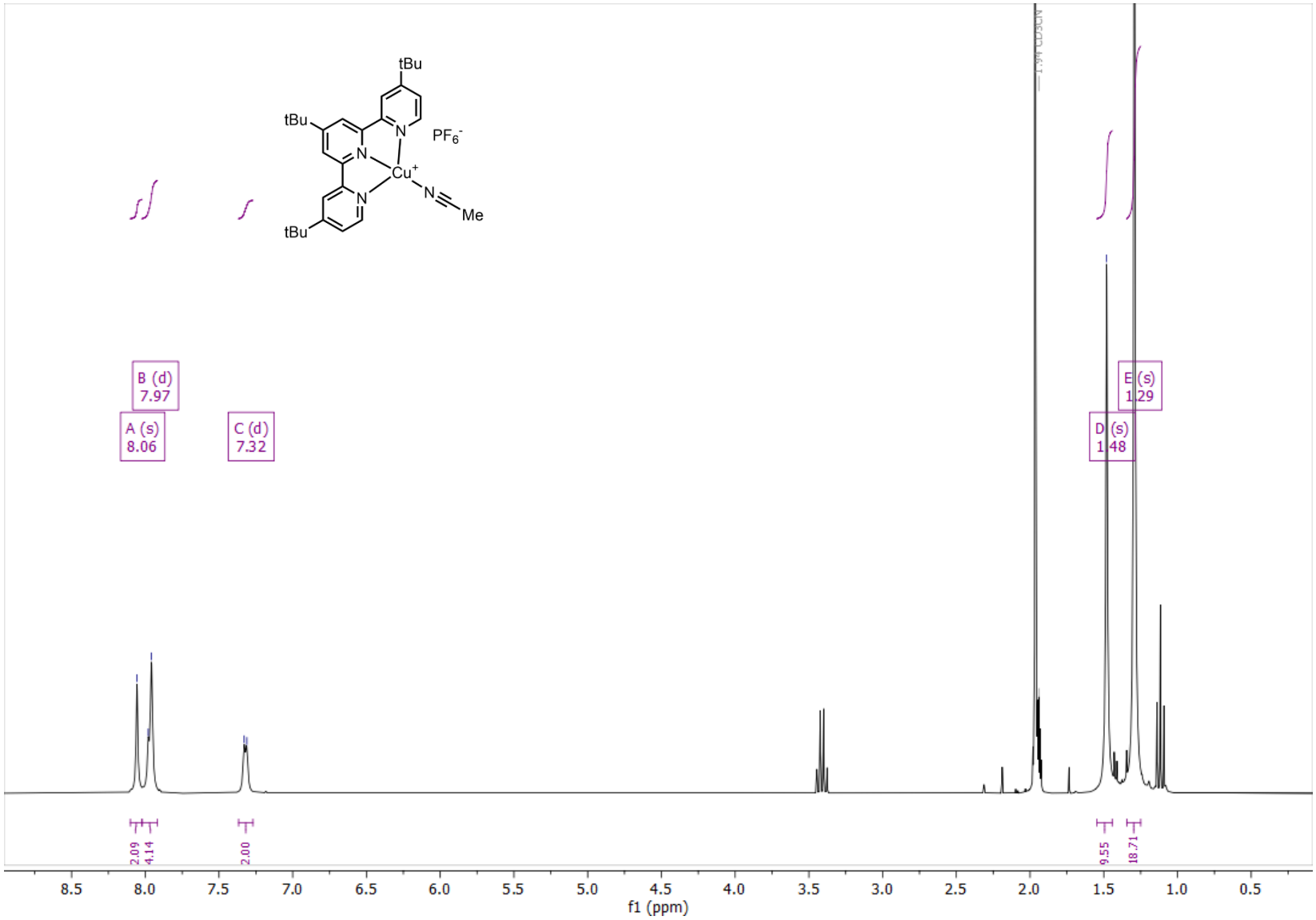

Figure 80: ^{1}H NMR (400 MHz, CD_3CN) spectrum of the terpyridine-copper(I) complex.

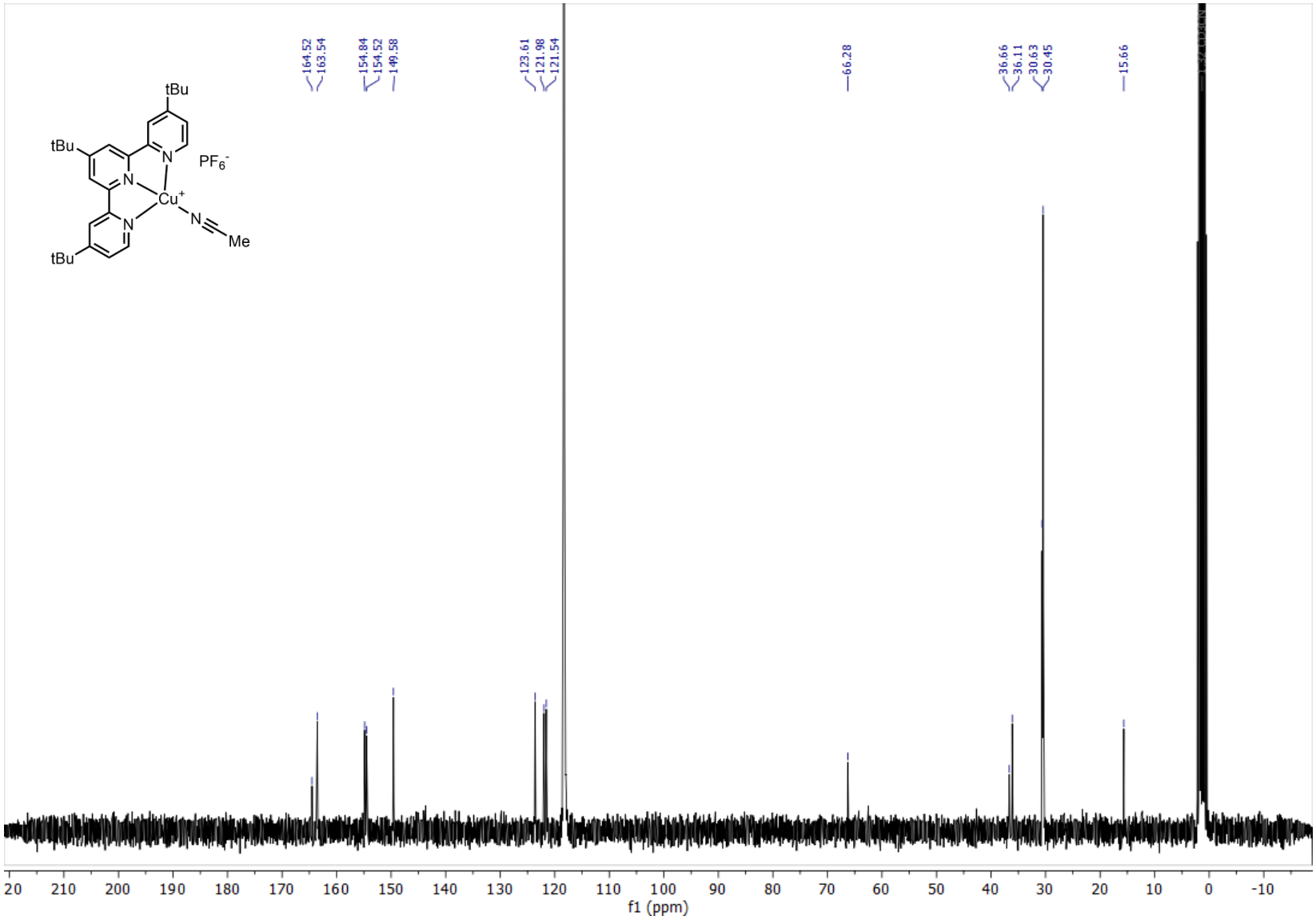

Figure 81: ^{13}C NMR (75 MHz, CD_3CN) spectrum of the terpyridine-copper(I) complex.

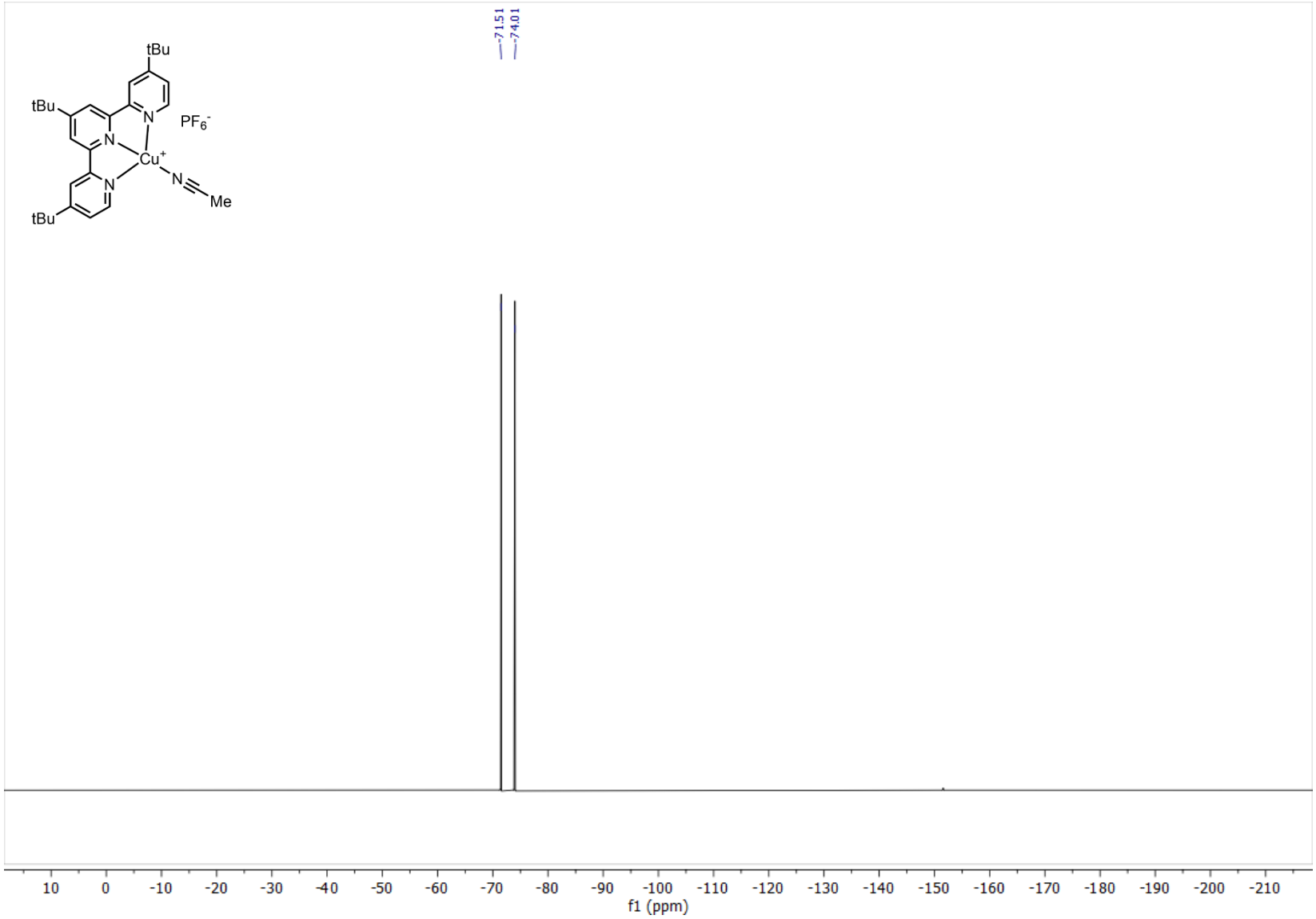

Figure 82: ^{19}F NMR (282 MHz, CD_3CN) spectrum of the terpyridine-copper(I) complex.

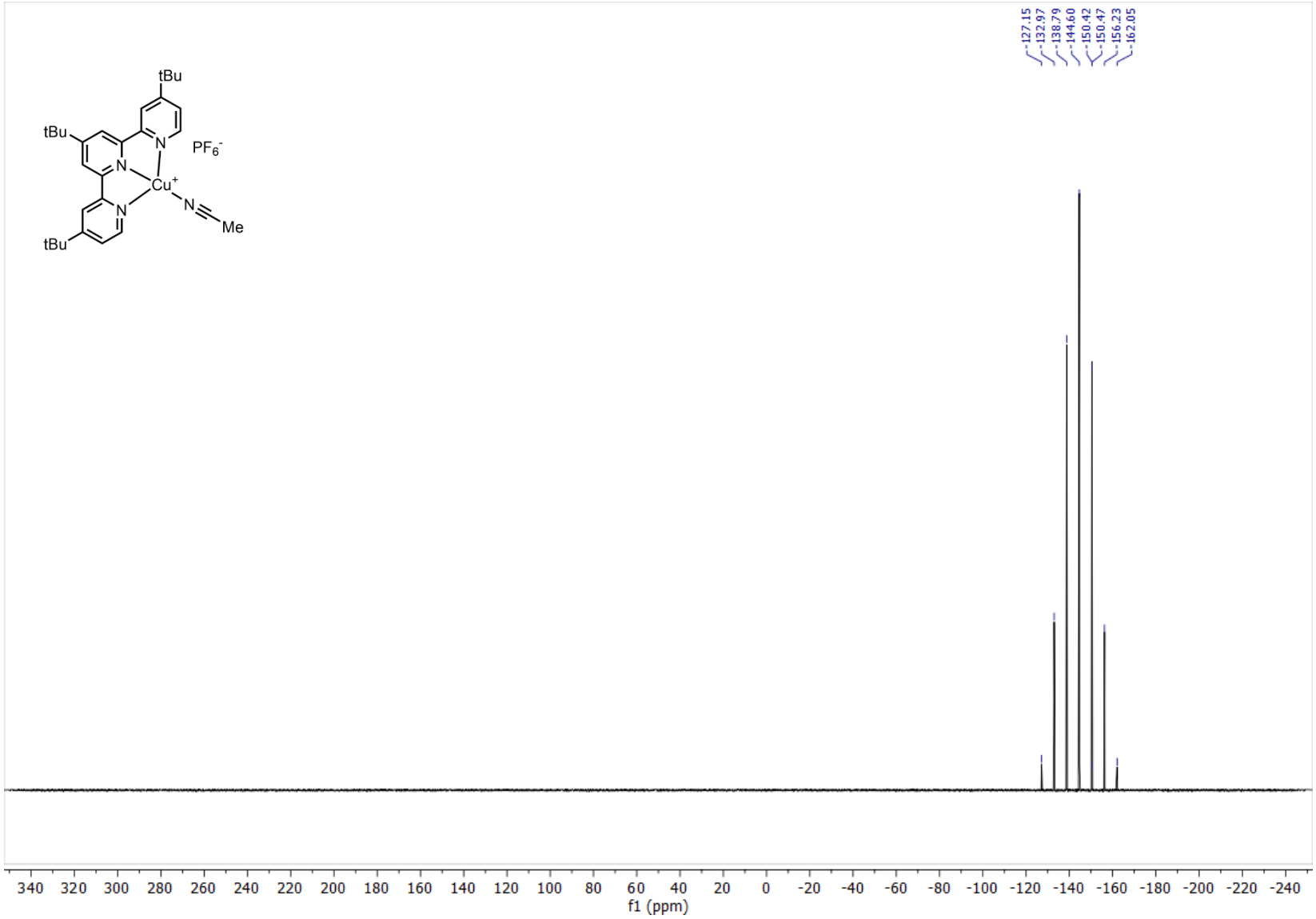

Figure 83: ^{31}P NMR (122 MHz, CD_3CN) spectrum of the terpyridine-copper(I) complex.

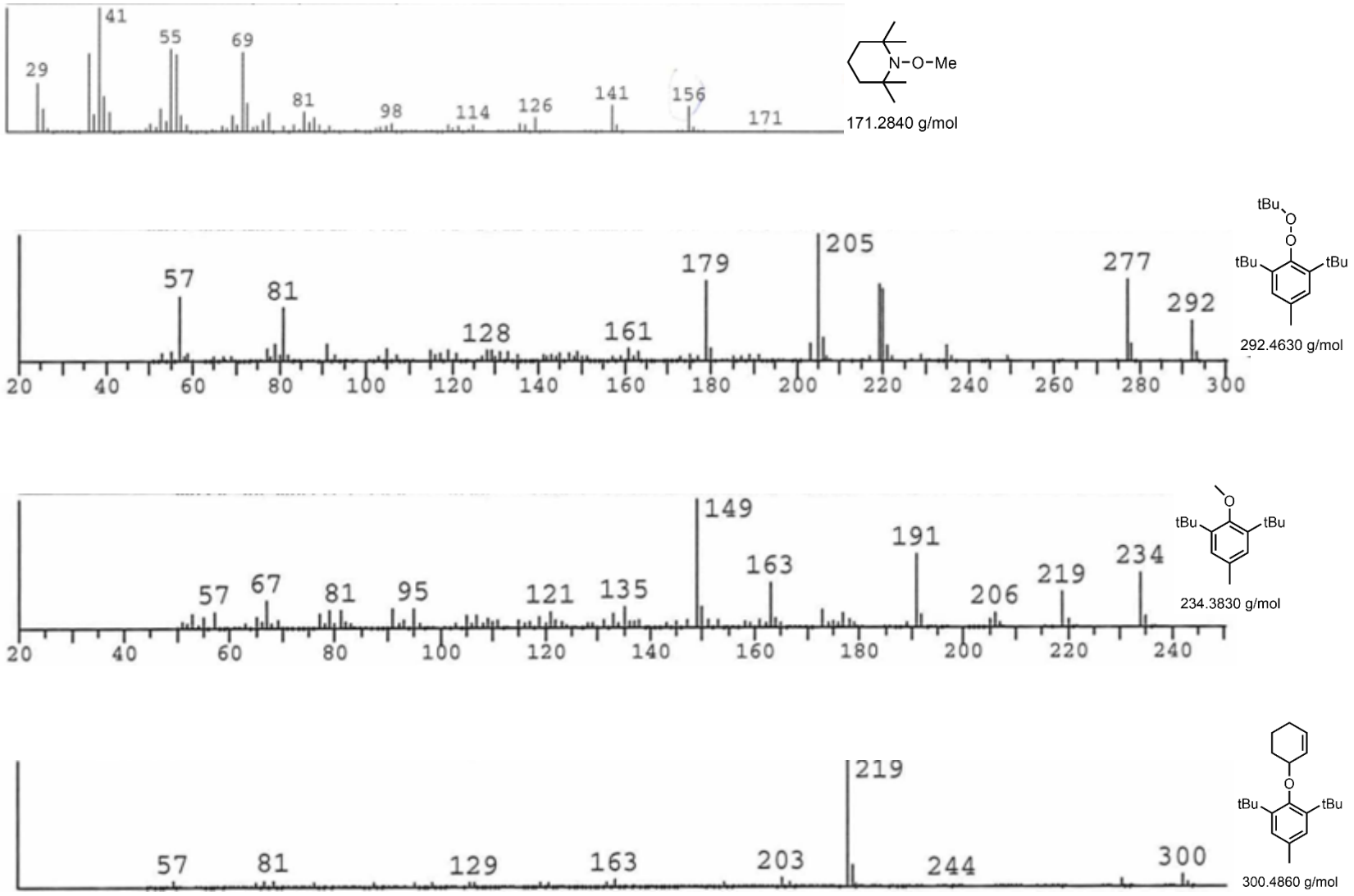

Figure 84: EI-MS of Radical Trapping Intermediates for TEMPO and BHT

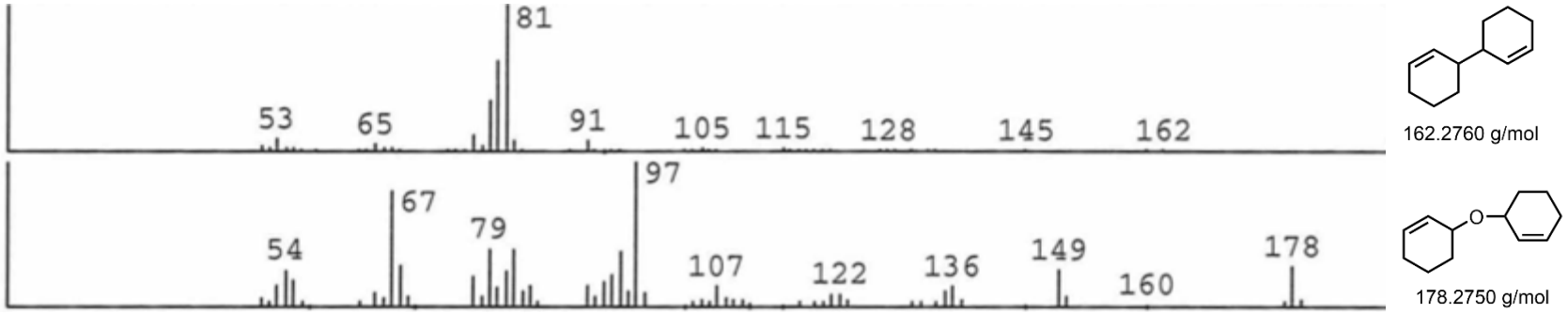

Figure 85: EI-MS of Cyclohexene Coupling Products during Radical Quenching with Ascorbic Acid.

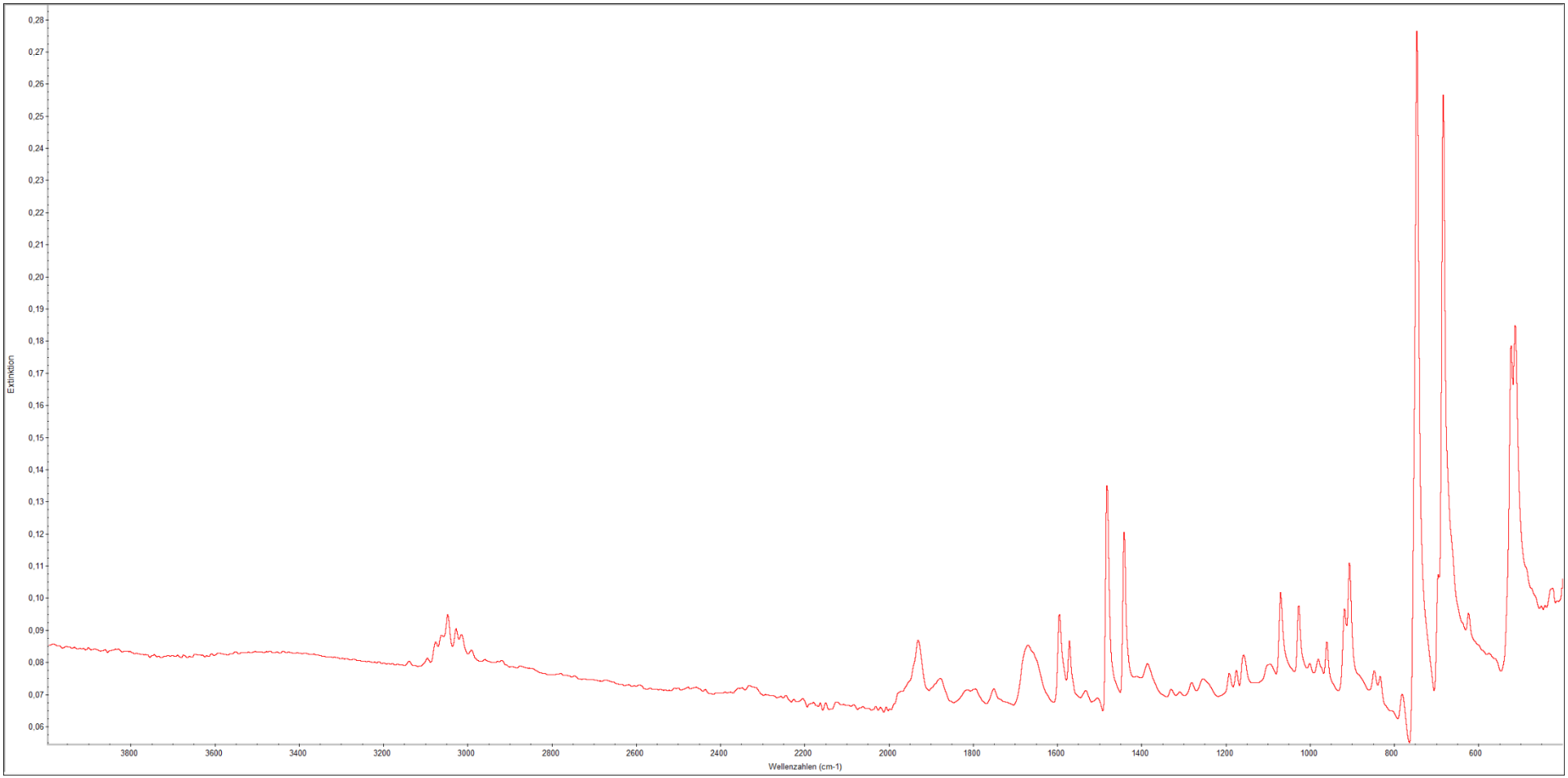

Figure 86: ATR-IR of copper(I) phenylacetylide.

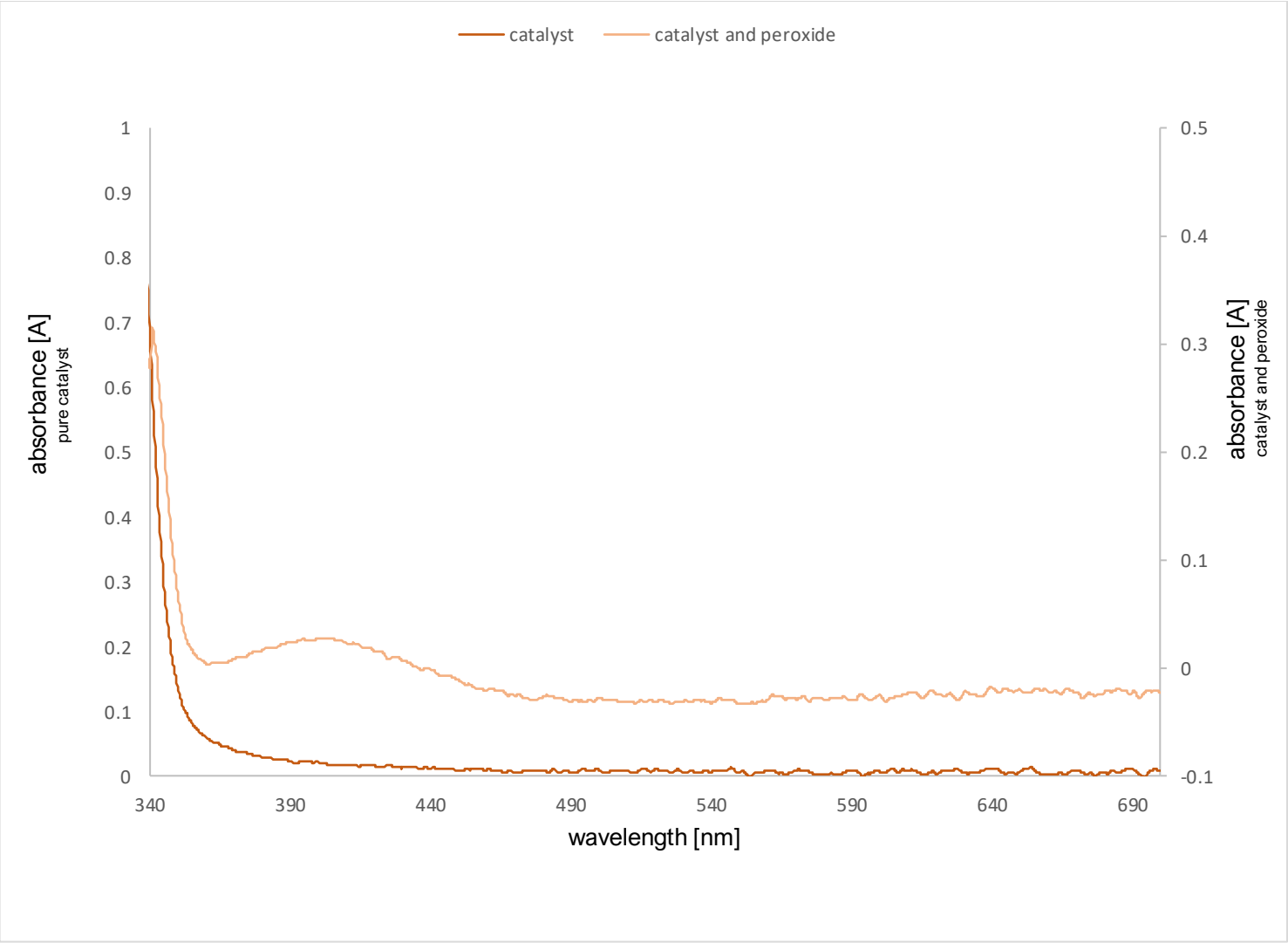

Figure 87: UV-VIS spectra of the copper complex **4** and copper peroxide complex **4B**.